UNIVERSITA' DEGLI STUDI DI PARMA

Dottorato di ricerca in Ingegneria Industriale

Ciclo 23

Nonlinear vibrations of circular cylindrical shells with different boundary conditions and geometric imperfections

Coordinatore:
Chiar.mo Prof. M. Spiga

Tutor:
Chiar.mo Prof. M. Amabili

Dottorando: Ye. Kurylov

CONTENTS

INTRODUCTION

The complex mechanical behaviour of shell structures has been a major concern of structural engineers and scientists for many years. Shell structures can be found e.g. in aircrafts, spacecrafts, rockets, cars, computer CD, DVD, hard-disk, submarines, boats, human body, storage tanks and roof of buildings. In advanced applications these structural components may exhibit a significant nonlinear behaviour that should be taken into consideration and appropriately controlled, and that can be enhanced by fluid-structure interaction and new materials. The increasing need to produce lighter-weight aerospace shell structures and aim to create high-speed underwater vehicles has led to the use of advanced material systems; therefore, appropriate design methods are needed for structures of supercavitating and aerospace vehicles, which nowdays are of the great importance in view of continuing technological development.

SUPERCAVITATING VEHICLES

Cavitation is the appearance of vapour bubbles and pockets inside an initially homogeneous liquid medium. Supercavitation is an extreme version of cavitation in which a single bubble (cavity) envelops the moving object almost completely. The supercavitation also is the natural process inevitably arising at increase of motion velocity of a moving underwater body at constant pressure. Vehicle motion speed is limited to about 35 m/s underwater; therefore, the concept of supercavitating underwater vehicles, allowing drug reduction and underwater speed of 100 m/s and more, has got paramount importance. It is necessary to note that the hydrodynamic drag reduction is important not only for vehicle speed increase, but also for decrease of noises and perturbations in the environmental fluid and for ecological load reduction on water medium as well. Due to this, the supercavitation concept is a useful tool for the following civil and military applications. For example, the Russian navy already deployed a rocket-powered supercavitating torpedo, the Shkval (Squall), that is said to reach a speed of 100 m/s underwater. Mostly of the fundamental research on supercavitating vehicles, necessary to built the Shkval, were first developed at the Hydromechanics Institute of the Ukrainian Academy

of Sciences in Kiev. The Skhval can travel only along a straight trajectory and slowly "processes" around the cavity's circumference and therefore can be considered as a first-generation design.

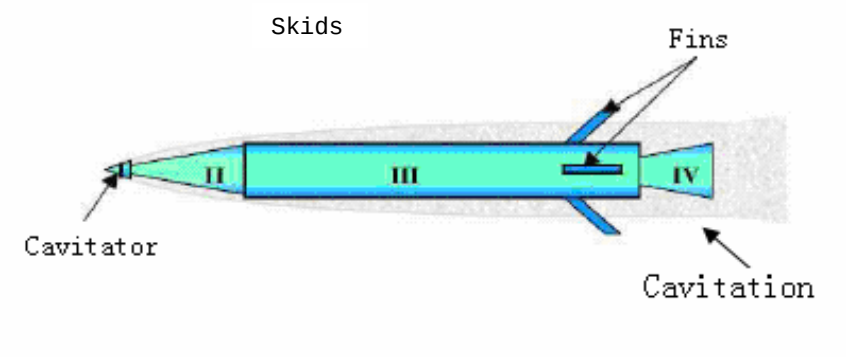

(a)

(b)

Supercavitating vehicle. (a) From Lin et al. 2006; (b) From S. Ashley 2001.

Although extensive efforts have been devoted in the past to the analysis of the fluid dynamic characteristics of supercavitating objects, little research has been dedicated so far to the evaluation of the structural behavior of slender elastic bodies traveling underwater at high speed in supercavitating regimes, and available studies are all linear. Mostly of the studies on guidance, control and stability have considered supercavitating vehicles as rigid bodies, or have addressed the hydrodynamic characteristics of the water/cavity system. Further, the fluid-structure interaction of the elastic shell body of the vehicle with the cavitating fluid and the borders of the cavity must be addressed. In supercavitating underwater vehicles, the interaction between the water and the cavitator nose is particularly important from a structural point of view, as the drag

force increases approximately with the square of the vehicle speed and thus can become very high. The drag force compresses axially the body and may cause its buckling. The buckling condition clearly corresponds to structural failure and therefore has been identified as one of the limiting factors for the operating speed of supercavitating bodies. Buckling stability is a major concern for the structural safety of supercavitating projectiles, which reach velocities of the order of 1500 m/s (i.e. around the sound speed in water). For cylindrical structures such as torpedoes, the value of the critical velocity may approach the limits currently pursued for supercavitating vehicles. Buckling stability hence needs to be addressed in order to assess the structural safety limits of supercavitating vehicles and should be considered in an effort to extend their operating range. In addition, the transient, unsteady nature of the cavitation process and the resulting time-dependent properties of the cavity and of its interactions with the vehicle require investigating the structural behavior of supercavitating vehicles when acted upon time-varying forces. In particular, variations in the velocity of forward motion, oscillations and shape variations of the cavity, and the complex interaction of the propeller forces with the cavity re-entrant jet causes the drag force and the propeller force sustaining the vehicle's motion to be time-dependent. The determination and the analysis of these interactions and the characterization of their dynamic effect are essential in defining the structural stability of supercavitating vehicles. In this analysis is fundamental to take into account geometric imperfections of the shell structure, asymmetry of the compressive load and large-amplitude deformations which give a nonlinear behaviour. The objective of the present research is also to perform really advanced experiments on supercavitating vehicles, measuring the shell response (vibration) due to the fluid-structure interaction and the rocket engine and to develop an active control. Experimental results will be used to improve and validate numerical models. The ground-breaking nature of the research is in the strongly nonlinear nature of the problem, which involves the shell structure, the fluid-structure interaction and the active control.

AEROSPACE VEHICLES

The increasing need to produce lighter-weight aerospace shell structures has led to the use of advanced material systems; therefore, appropriate design methods are needed. For example, the international space station require the Space Shuttle to deliver a large number of payloads; new lighter-weight external fuel tank have been developed to maximize the payload. These “super-light-weight” external tanks, are made of aluminium–lithium alloy. In the design of super-light-weight tanks, the non-linear behaviour of the thin-walled regions of the structure, that experience compressive stresses, must be carefully analyzed. In some applications, such as launchers, the structure can be subjected to an axial time varying load due to a seismic excitation (rockets). Indeed, during the launch the structure is subjected to its own inertia and the payload inertia, the latter one gives a compression load; disturbances arising from rockets action or the external flowing fluid result in an added time varying load.

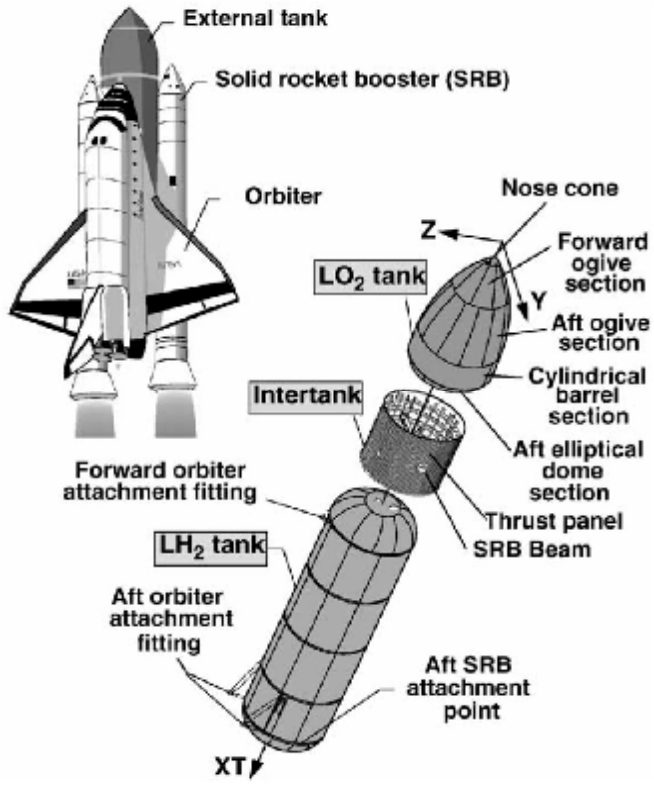

NASA space shuttle with detail of the external tank components. LO_2, liquid oxygen; LH_2, liquid hydrogen. From Nemeth et al. (2002).

Another problem is associated with the sloshing of the liquid fuel in the rocket, which compressibility has been recently found to be not negligible during flight. Experience has taught that the unrestrained free surface of the liquid has an alarming propensity to undergo rather large excursions, for even very small motions of the container, and that one has to adjust very carefully the frequency of the container motion to avoid this sloshing of the liquid. Large oscillations can only be described by using a nonlinear model; considering the liquid compressibility and surface tension in microgravity, it makes the study a challenging problem, especially since the tank must be considered flexible and associated with large-amplitude (i.e. nonlinear) structural vibrations. In the sixties, the Saturn I rocket of the NASA provided a clear example of actual in-flight stability problem arising as a consequence of fuel slosh. In fact, the liquid-sloshing frequencies are often closer to the rigid body control frequencies than to the elastic body frequencies and therefore might ordinarily be a very important problem. However, structural natural frequencies are largely affected (decreased) by the presence of a contained dense fluid (liquid). Moreover, the liquid system is subjected to some degree of control and, hence, the interaction between the elastic structure and the control system become more important. As a consequence of the increased sloshing frequency of some tank shapes and low natural frequencies of structural modes (bulging modes) due to the liquid presence, coupling between the propellant sloshing and elastic modes may result in large dynamic responses.

A complicating aspect is due to large amplitude vibrations that can occur in tanks for space vehicles. In fact, circular cylindrical shells usually show a softening behaviour, decreasing the safety of the system. This nonlinear behaviour is magnified by the presence of a contained liquid. A complication in the problem is given by the presence of the external flowing fluid, which can be responsible of divergence as well as flutter instabilities.

Even though the study of nonlinear vibration of cylindrical shells has a relatively long tradition, several questions still await complete clarification. In some applications, the vibration

response of shells calculated by linear theory is inaccurate. When the vibration amplitude becomes comparable to the shell thickness, a geometrically nonlinear theory should be used for constrained shells (larger amplitudes are possible in the linear regime for free-edge shells).

Two main phenomena have been found by investigators for large-amplitude vibrations of closed (circumferentially complete) circular cylindrical shells forced by harmonic radial excitation: (i) the response-frequency relationship in the vicinity of a resonant frequency is a function of the amplitude of vibration, generally displaying a softening-type behaviour for thin shells, becoming hardening only for very large amplitudes of vibration, and (ii) travelling-wave response occurs close to the peak of the response; amplitude modulation, due to beating very close to the excitation frequency, has also been observed in a narrow region close to exact resonance. For a periodic excitation applied to a circular cylindrical shell, we expect the shell deformation to be a standing wave, symmetrical with respect to the point of application, in the case of small-amplitude vibrations. This symmetrical standing wave is called the *driven mode*. For large-amplitude vibrations, circumferentially travelling waves have been observed in the response of the shell. They can be described as the movement of the nodal lines of the driven mode. The travelling wave appears when a second standing wave (mode), the orientation of which is at $p/(2n)$ (where n is the number of circumferential waves) with respect to the previous one, emerges in addition to the driven mode. This second mode is called the *companion mode*. It has the same modal shape and frequency as the driven mode. The presence of this second mode arises because of the axial symmetry of the shell and is due to nonlinear coupling. It is also of interest to observe that the change (generally reduction) in the frequency of the fundamental (lowest frequency) mode is less than 1 % for many shell geometries when the vibration amplitude is equal to the shell thickness; therefore, this nonlinearity may be considered weak.

Geometric imperfections also play an important role in large-amplitude vibrations of shells and panels. Asymmetric imperfections in closed circular shells split the natural frequencies of driven and companion modes and therefore change significantly their nonlinear interaction

and the traveling wave response. Axisymmetric imperfections outward (with respect with the center of curvature) increase natural frequencies; small axisymmetric imperfections inward (with respect to the center of curvature) decrease natural frequencies.

A literature review of earlier work on the nonlinear vibrations of circular cylindrical shells was given by Evensen (1974). Leissa (1973) also presented a literature review on large-amplitude vibrations of circular cylindrical shells in a section of his classical monograph, *Vibration of Shells*. An extensive review of large-amplitude vibrations of circular cylindrical shells *in vacuo*, and filled with or surrounded by a quiescent fluid, was given by Amabili, Pellicano and Païdoussis (1998) in the Introduction of their paper; see also Païdoussis (2002). Almost at the same time, Kubenko and Koval'chuk (1998) wrote a review paper on research developments on nonlinear vibrations of shells in the former Soviet Union. Recently, the same authors presented another review paper on nonlinear vibrations of shells partially filled with liquids (Kubenko and Koval'chuk 2000a). Specific reviews of work on aeroelasticity of plates and shells were written by Dowell (1970a) and Bismarck-Nasr (1992), including a few nonlinear studies on shells and curved panels. Nonlinear vibrations and dynamics of circular cylindrical shells and panels with and without fluid-structure interaction were reviewed by Amabili and Païdoussis (2003). The problem is also amply discussed by Amabili in his recent monograph (2008).

The literature analysis shows also that in the past several methods were developed for investigating: (i) linear vibrations of complex shells; (ii) nonlinear vibrations of shells having simple shape and boundary conditions. Most of the studies address to vibrations of shells with simply-supported and clamped-clamped boundary conditions, while more complicated boundary conditions, as cantilever (clamped-free) shells are still not investigated, nevertheless their wide application as storage tanks, thermal shields of rockets and engines. Therefore, a contribution toward developing a general framework that allows to study shells with different boundary conditions is welcome. Pellicano (2007) proposed an idea to use orthogonal polynomials instead

of trigonometric functions to expand displacement fields, which allows to satisfy different boundary conditions. The present study is a contribution in this direction introducing a new validated methodology allowing for the application of different boundary conditions at the shell edges without significantly changing the computational technique.

ORGANIZATION OF THE THESIS

The present thesis focuses on nonlinear (finite amplitude) vibrations under harmonic loads of closed (i.e. circumferentially complete) circular cylindrical shells without fluid-structure interaction.

This thesis is structured as follows. Literature review on shells is given in Chapter 1. Studies on nonlinear vibrations of simply supported circular cylindrical shells are reviewed in Chapter 2. Experimental results available in literature for shells with different boundary conditions are presented in Chapter 3. Chapter 4 represents nonlinear vibrations of simply supported shells with polynomial expansion. Nonlinear vibrations of clamped-clamped shell are treated in Chapter 5. Chapter 6 deals with clamped-free circular cylindrical shell, effect of geometric imperfections is also studied. Conclusions resume performed studies.

Generally the thesis is organized in logical and sequential way, according to increase of the problem complexity.

1. LITERATURE REVIEW

1.1. GEOMETRICALLY NONLINEAR SHELL THEORIES

A short overview of some theories for geometrically nonlinear shells will now be given. Figure 1.1 shows a circular cylindrical shell with the co-ordinate system and the displacements of the middle surface.

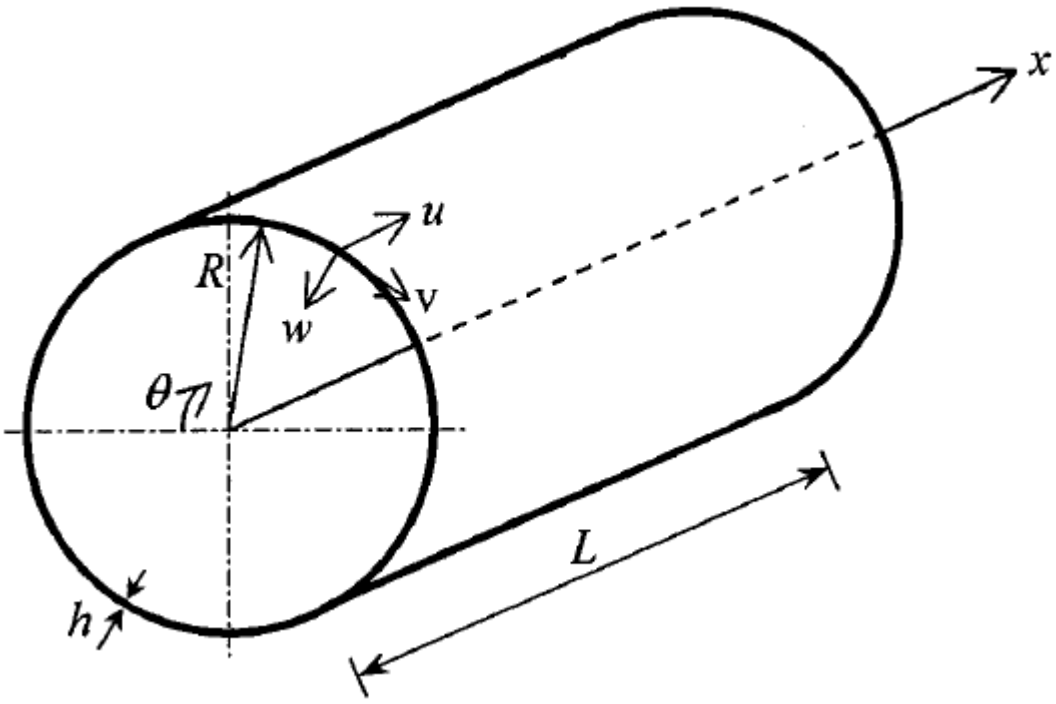

FIGURE 1.1. Shell geometry and coordinate system

Donnell (1934) established the nonlinear theory of circular cylindrical shells under the simplifying shallow-shell hypothesis. Due to its relative simplicity and practical accuracy, this theory has been widely used. The most frequently used form of Donnell's nonlinear shallow-shell theory (also referred as Donnell-Mushtari-Vlasov theory) introduces a stress function in order to combine the three equations of equilibrium involving the shell displacements in the radial, circumferential and axial directions into two equations involving only the radial displacement w and the stress function F:

$$D\nabla^4 w + c\dot{w} + r h\ddot{w} = f + \frac{1}{R}\frac{\partial^2 F}{\partial x^2} + \frac{1}{R^2}\left(\frac{\partial^2 F}{\partial q^2}\frac{\partial^2 w}{\partial x^2} - 2\frac{\partial^2 F}{\partial x \partial q}\frac{\partial^2 w}{\partial x \partial q} + \frac{\partial^2 F}{\partial x^2}\frac{\partial^2 w}{\partial q^2}\right), \quad (1.1)$$

$$\frac{1}{Eh}\nabla^4 F = -\frac{1}{R}\frac{\partial^2 w}{\partial x^2} + \frac{1}{R^2}\left[\left(\frac{\partial^2 w}{\partial x \partial q}\right)^2 - \frac{\partial^2 w}{\partial x^2}\frac{\partial^2 w}{\partial q^2}\right], \quad (1.2)$$

where $D = Eh^3/\left[12(1-n^2)\right]$ is the flexural rigidity, E Young's modulus, n the Poisson ratio, h the shell thickness, R the mean shell radius, r the mass density of the shell, c the damping coefficient, f the radial pressure excitation, and $\nabla^4 = \left[\partial^2/\partial x^2 + \partial^2/(R^2\partial q^2)\right]^2$ is the biharmonic operator. By using Donnell's nonlinear shallow-shell theory, the middle surface strain-displacement relationships are obtained,

$$e_x = \frac{\partial u}{\partial x} + \frac{1}{2}\left(\frac{\partial w}{\partial x}\right)^2, \quad (1.3a)$$

$$e_q = \frac{\partial v}{R\partial q} - \frac{w}{R} + \frac{1}{2}\left(\frac{\partial w}{R\partial q}\right)^2, \quad (1.3b)$$

$$g_{xq} = \frac{\partial u}{R\partial q} + \frac{\partial v}{\partial x} + \frac{\partial w}{\partial x}\frac{\partial w}{R\partial q}. \quad (1.3c)$$

This theory is accurate only for modes of high circumferential wavenumber n; specifically, $1/n^2 << 1$ must be satisfied, so that $n \geq 5$ is required in order to have fairly good accuracy. Donnell's nonlinear shallow-shell equations are obtained by neglecting the in-plane inertia, transverse shear deformation and rotary inertia, giving accurate results only for very thin shells, i.e. $h << R$. Therefore, in-plane displacements are infinitesimal, i.e. $|u| << h$, $|v| << h$, while w is of the order of the shell thickness, $|w| = \mathrm{O}(h)$. The predominant nonlinear terms are retained, but other secondary effects, such as the nonlinearities in curvature strains, are neglected; specifically, the curvature changes are expressed by linear functions of w only.

Von Kármán and Tsien (1941) performed a seminal study on the stability of axially loaded circular cylindrical shells, based on Donnell's nonlinear shallow-shell theory. In their book, Mushtari and Galimov (1957) presented nonlinear theories for moderate and large deformations of thin elastic shells. The nonlinear theory of shallow shells is also discussed in the book of Vorovich (1999).

Sanders (1963) developed a more refined nonlinear theory of shells, expressed in tensorial form; the same equations were obtained by Koiter (1966) around the same period, leading to the designation of these equations as the Sanders-Koiter equations. Later, this theory has been reformulated in lines-of-curvature coordinates, *i.e.* in a form that can be more suitable for applications; see Budiansky (1968). According to the Sanders-Koiter theory, all three displacements are used in the equations of motion. The middle surface strain-displacement relationships in this case are

$$e_x = \frac{\partial u}{\partial x} + \frac{1}{2}\left(\frac{\partial w}{\partial x}\right)^2 + \frac{1}{8}\left(\frac{\partial v}{\partial x} - \frac{\partial u}{R\partial q}\right)^2, \tag{1.4a}$$

$$e_q = \frac{\partial v}{R\partial q} - \frac{w}{R} + \frac{1}{2}\left(\frac{\partial w}{R\partial q} + \frac{v}{R}\right)^2 + \frac{1}{8}\left(\frac{\partial u}{R\partial q} - \frac{\partial v}{\partial x}\right)^2, \tag{1.4b}$$

$$g_{xq} = \frac{\partial u}{R\partial q} + \frac{\partial v}{\partial x} + \frac{\partial w}{\partial x}\left(\frac{\partial w}{R\partial q} + \frac{v}{R}\right). \tag{1.4c}$$

Changes in curvature and torsion are linear according to both the Donnell and the Sanders-Koiter nonlinear theories (Yamaki 1984). The Sanders-Koiter theory gives accurate results for vibration amplitudes significantly larger than the shell thickness for thin shells.

Details on the above-mentioned nonlinear shell theories may be found in Yamaki's (1984) book, with an introduction to another accurate theory, called the modified Flügge nonlinear theory of shells, also referred to as the Flügge-Lur'e-Byrne nonlinear shell theory (Ginsberg 1973). The Flügge-Lur'e-Byrne theory is close to the general large deflection theory of thin shells developed by Novozhilov (1953) and differs only in terms for change in curvature and torsion.

Additional nonlinear shell theories were formulated by Naghdi and Nordgren (1963), using the Kirchhoff hypotheses, and Libai and Simmonds (1988).

1.2. FREE AND FORCED (RADIAL HARMONIC EXCITATION) VIBRATIONS OF SHELLS

The first study on vibrations of circular cylindrical shells is attributed to Reissner (1955), who isolated a single half-wave (lobe) of the vibration mode and analyzed it for simply supported shells; this analysis is therefore only suitable for circular panels. By using Donnell's nonlinear shallow-shell theory for thin-walled shells, Reissner found that the nonlinearity could be either of the hardening or softening type, depending on the geometry of the lobe. Almost at the same time, Grigolyuk (1955) studied large-amplitude free vibrations of circular cylindrical panels simply supported at all four edges. He used the same shell theory as Reissner (1955) and a two-mode expansion for the flexural displacement involving the first and third longitudinal modes. He also developed a single mode approach. Results show a hardening type nonlinearity. Chu (1961) continued with Reissner's work, extending the analysis to closed cylindrical shells. He found that nonlinearity in this case always leads to hardening type characteristics, which, in some cases, can become quite strong.

Cummings (1964) confirmed Reissner's analysis for circular cylindrical panels simply supported at the four edges; he also investigated the transient response to impulsive and step functions, as well as dynamic buckling. Nowinski (1963) confirmed Chu's results for closed circular shells. He used a single-degree-of-freedom expansion for the radial displacement using the linear mode excited, corrected by a uniform displacement that was introduced to satisfy the continuity of the circumferential displacement. All of the above expansions for the description of shell deformation, except for Grigolyuk's, employed a single mode based on the linear analysis of shell vibrations.

Evensen (1963) proved that Nowinski's analysis was not accurate, because it did not maintain a zero transverse deflection at the ends of the shell. Furthermore, Evensen found that

Reissner's and Chu's theories did not satisfy the continuity of in-plane circumferential displacement for closed circular shells. Evensen (1963) noted in his experiments that the nonlinearity of closed shells is of the *softening* type and *weak*, as also observed by Olson (1965). Indeed, Olson (1965) observed a slight nonlinearity of the softening type in the experimental response of a thin seamless shell made of copper; the measured change in resonance frequency was only about 0.75 %, for a vibration amplitude equal to 2.5 times the shell thickness. The shell ends were attached to a ring; this arrangement for the boundary conditions gave some kind of constraint to the axial displacement and rotation. Kaña *et al*. (1966; see also Kaña 1966) also found experimentally a weak softening type response for a thin, simply supported, circular cylindrical shell.

To reconcile this most important discrepancy between theory and experiments, Evensen (1967) (this NASA report contains results obtained around 1964, see also Evensen and Fulton (1967)) used Donnell's nonlinear shallow-shell theory but with a different form for the assumed flexural displacement *w*, involving more modes. Specifically, he included the companion mode in the analysis, as well as an axisymmetric contraction having twice the frequency of the mode excited:

$$\begin{aligned} w = &\left[A_{mn}(t)\cos(nq) + B_{mn}(t)\sin(nq)\right]\sin(mp\,x/L) \\ &+ (n^2/4R)\left[A_{mn}^2(t) + B_{mn}^2(t)\right]\sin^2(mp\,x/L)\,, \end{aligned} \tag{1.5}$$

where n is the circumferential wavenumber, m is the number of axial half-waves, $A_{mn}(t)$ and $B_{mn}(t)$ are two time functions associated to the driven and companion mode, respectively. Evensen's assumed modes are not moment-free at the ends of the shell, as they should be for classical simply supported shells, and the homogeneous solution for the stress function is neglected; however, the continuity of the circumferential displacement is exactly satisfied. Evensen studied the free vibrations and the response to a modal excitation without considering damping and discussed the stability of the response curves. His results are in agreement with Olson's (1965) experiments. Evensen's study is an extension of his very well-known study on

the vibration of rings (1964, 1965, 1966), wherein he proved theoretically and experimentally that thin circular rings display a softening-type nonlinearity. The other classical work on the vibration of circular rings is due to Dowell (1967a) who confirmed Evensen's results and removed the assumption of zero mid-surface circumferential strain. Evensen (1968) also extended his work to infinitely long shells vibrating in a mode in which the generating lines of the cylindrical surface remain straight and parallel, by using the method of harmonic balance and without considering the companion mode. Recently, Evensen (2000) published a paper, originally written in 1968, in which he studied the influence of pressure and axial loading on large-amplitude vibrations of circular cylindrical shells by an approach similar to the one that he used in his previous papers, but neglecting the companion mode; consequently only backbone curves, pertaining to free vibrations, were computed.

It is important to note that, in most studies, the assumed mode shapes (those used by Evensen, for example) are derived in agreement with the experimental observation that, in large-amplitude vibrations, (i) the shell does not spend equal time-intervals deflected outwards and deflected inwards, and (ii) inwards maximum deflections, measured from equilibrium, are larger than outwards ones. However, it is important to say that these differences are very small if compared to the vibration amplitude. Hence, the original idea for mode expansion was to add to asymmetric linear modes an axisymmetric term (mode) giving a contraction to the shell. The axisymmetric term added by Evensen (1966, 1967, 1968, 1974) in equation (1.5) is a squared sine in the axial co-ordinate, the amplitude of which is related to the amplitudes of the linear terms in order to satisfy the continuity of the circumferential displacement. This $\sin^2(mp\,x/L)$ term is therefore always positive (giving contraction) or zero, and it has a frequency of oscillation which is twice the excitation frequency. It was probably first introduced to study buckling of circular cylindrical shells by Russian researchers (see Vol'mir 1956). This term was also used by Agamirov and Vol'mir (1959) to study buckling under dynamic external pressure. The latter paper, in its English translation, inspired Evensen, as he said during his talk at the

ASME Symposium on Nonlinear Dynamics of Shells and Plates (Païdoussis, Amabili and Gonçalves 2000). However, this $\sin^2(mp\,x/L)$ term was used by Agamirov and Vol'mir (1959) and other researchers with *the same* time-dependence as that of the asymmetric term; therefore, the expansion in the form given in equation (1.5) must be attributed to Evensen.

Mayers and Wrenn (1967) analyzed free vibrations of thin, complete circular cylindrical shells. They used both Donnell's nonlinear shallow-shell theory and the Sanders-Koiter nonlinear theory of shells. Their analysis is based on the energy approach and shows that non-periodic (more specifically, quasiperiodic) motion is obtained for free nonlinear vibrations. In their analysis based on Donnell's theory, the same expansion introduced by Evensen, without the companion mode, was initially applied; the backbone curves (pertaining to free vibrations) of Evensen were confirmed almost exactly. A second expansion with an additional degree of freedom was also applied for shells with many axial waves; finally, an expansion with more axisymmetric terms was introduced, but the corresponding backbone curves were not reported. In their analysis based on the Sanders-Koiter theory, an original expansion for the three shell displacements (i.e. radial, circumferential and axial) was used, involving 7 degrees of freedom. However, only one term was used for the flexural displacement, and the axisymmetric radial contraction was neglected; axisymmetric terms were considered for the in-plane displacements. The authors found that the backbone curves for a mode with two circumferential waves predict a hardening-type nonlinearity which increases with shell thickness.

Matsuzaki and Kobayashi (1969a, b) studied theoretically simply supported circular cylindrical shells (1969a), then studied theoretically and experimentally clamped circular cylindrical shells (1969b). Matsuzaki and Kobayashi (1969a) based their analysis on Donnell's nonlinear shallow-shell theory and used the same approach and mode expansion as Evensen (1967), with the opposite sign to the axisymmetric term because they assumed positive deflection outwards. In addition, they discussed the effect of structural damping and studied in detail travelling-wave oscillations. In the paper, considering clamped shells, Matsuzaki and

Kobayashi (1969b) modified the mode expansion in order to satisfy the different boundary conditions and retained both the particular and the homogeneous solutions for the stress function. The analysis found a softening type nonlinearity also for clamped shells, in agreement with their own experimental results. They also found amplitude-modulated response close to resonance and identified it as a beating phenomenon due to frequencies very close to the excitation frequency.

Dowell and Ventres (1968) used a different expansion and approach in order to satisfy exactly the out-of-plane boundary conditions and to satisfy "on the average" the in-plane boundary conditions. They studied shells with restrained in-plane displacement at the ends and obtained the particular and the homogeneous solutions for the stress function. Their interesting approach was followed by Atluri (1972) who found that some terms were missing in one of the equations used by Dowell and Ventres; recently Dowell *et al*. (1998) corrected these omissions. The boundary conditions assumed both by Dowell and Ventres and by Atluri constrain the axial displacement at the shell extremities to be zero, so that they are different from the classical constraints of a simply supported shell (zero axial force at both ends). Atluri (1972) found that the nonlinearity is of the hardening type for a closed circular cylindrical shell, in contrast to what was found in experiments. The axisymmetric term used by Dowell and Ventres and Atluri in their mode expansion is a sine in the axial coordinate (specifically, it is the first axisymmetric mode of linear vibrations) and has an independent time variation, i.e.

$$w = \left[A_{mn}(t)\cos(nq) + B_{mn}(t)\sin(nq)\right]\sin(mp\,x/L) + A_{m0}(t)\sin(mp\,x/L)\,. \qquad (1.6)$$

Their approach was criticized by Evensen (1978a, c) because it gives a hardening type result; he pointed out that satisfaction of continuity of the circumferential displacement "on the average" is not a good enough approximation, in view of its importance in nonlinear vibrations. Dowell (1978) has countered this criticism. Varadan *et al*. (1989) showed that hardening-type results based on the theory of Dowell and Ventres and Atluri are due to the choice of the axisymmetric term. More recently, Amabili *et al*. (1999b, 2000a) showed that at least the first and third axisymmetric modes (axisymmetric modes with an even number of longitudinal half-waves do

not give any contribution) must be included in the mode expansion (for modes with a single longitudinal half-wave), as well as using both the driven and companion modes, to correctly predict the trend of nonlinearity with sufficiently good accuracy:

$$w = \left[A_{1n}(t)\cos(nq) + B_{1n}(t)\sin(nq)\right]\sin(p\,x/L) + A_{10}(t)\sin(p\,x/L) + A_{30}(t)\sin(3p\,x/L)\,. \quad (1.7)$$

If only one term is used, as done by Dowell and Ventres and Atluri, an erroneous hardening-type nonlinearity is obtained. Figure 1.2, taken from Amabili *et al*. (1999b), shows the response of the shell, without companion mode participation, with varying number of axisymmetric modes.

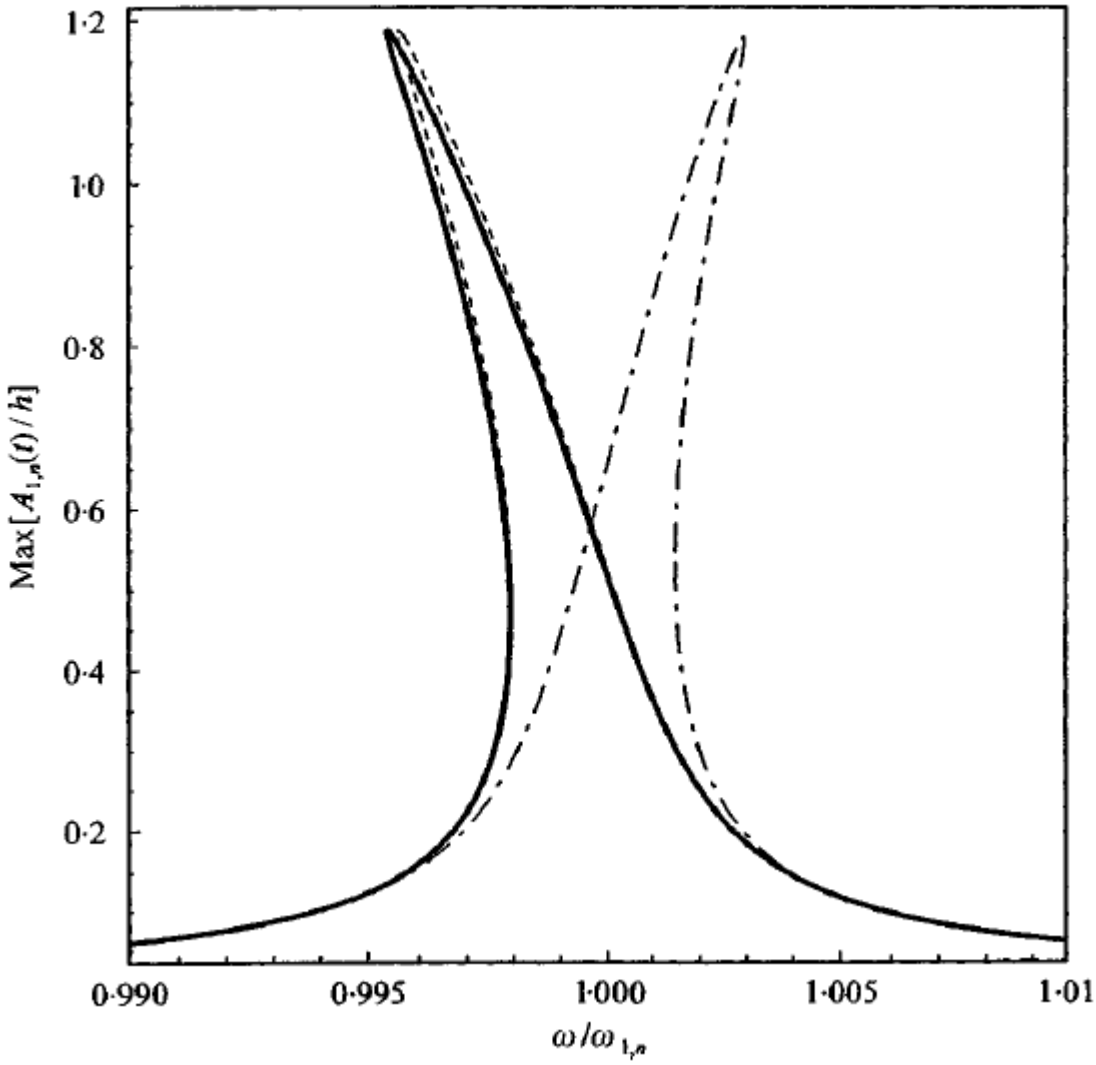

FIGURE 1.2. Frequency response curves for the driven mode without companion mode participation and with one longitudinal half-wave: model with 3 axisymmetric waves (solid line); model with 2 axisymmetric waves (dashed line); model with 1 axisymmetric wave (dashed-dotted line).

Sun and Lu (1968) studied the dynamic behaviour of conical and cylindrical shells under sinusoidal and ramp-type temperature loads. The equations of motion are obtained by starting with strain-displacement relationships that, for cylindrical shells, are those of Donnell's nonlinear shallow-shell theory. All three displacements were used, instead of introducing the stress function F as in equations (1.1) and (1.2). Therefore, the three displacements were expanded by using globally six terms, without considering axisymmetric terms in the radial displacement; these six terms were related together to give a single-degree-of-freedom system with only cubic nonlinearity, and the shell thus exhibited hardening type nonlinearity.

Leissa and Kadi (1971) studied linear and nonlinear free vibrations of shallow shell panels, simply supported at the four edges without in-plane restraints. Panels with two different curvatures in orthogonal directions were studied. This is the first study on the effect of curvature of the generating lines on large-amplitude vibrations of shallow shells. Donnell's nonlinear shallow-shell theory was used in a slightly modified version to take into account the meridional curvature. A single mode expansion of the transverse displacement was used. The Galerkin method was used; the compatibility equation was exactly satisfied, and in-plane boundary conditions were satisfied on the average. Results were obtained by numerical integration and non-simple harmonic oscillations were found. For cylindrical and spherical panels, phase plots show that, during vibrations, inward deflections are larger that outward deflections, as previously found by Reissner (1955) and Cummings (1964); the converse was found for the hyperbolic paraboloid. The analysis shows that for all shells, excluding the hyperbolic paraboloid but including the circular cylindrical panel, a softening nonlinearity is expected, changing to hardening for very large deflections (in particular for vibration amplitude equal to 15 times the shell thickness for a circular cylindrical panel).

El-Zaouk and Dym (1973) investigated free and forced vibrations of closed circular shells having a curvature of the generating lines by using an extended form of Donnell's nonlinear shallow-shell theory to take into account curvature of the generating lines and orthotropy. They

also obtained numerical results for circular cylindrical shells; for this special case, their study is almost identical to Evensen's (1967), but the additional effects of internal pressure and orthotropy are taken into account. Their numerical results showed a softening type nonlinearity, which becomes hardening only for very large displacements, at about 30 times the shell thickness. Stability of the free and forced responses was also investigated.

Ginsberg used a different approach to solve the problem of asymmetric (Ginsberg 1973) and axisymmetric (Ginsberg 1974) large-amplitude vibrations of circular cylindrical shells. In fact, he avoided the assumptions of mode shapes and employed instead an asymptotic analysis to solve the nonlinear boundary conditions for a simply supported shell. The solution is reached by using the energy of the system to obtain the Lagrange equations, which are then solved via the harmonic balance method. Both softening and hardening nonlinearities were found, depending on some system parameters. Moreover, Ginsberg used the more accurate Flügge-Lur'e-Byrne nonlinear shell theory, instead of Donnell's nonlinear shallow-shell theory which was used in all the work discussed in the foregoing (excluding the two papers allowing for curvature of the generating lines). The Flügge-Lur'e-Byrne theory is the same referred as the modified Flügge theory by Yamaki (1984). Ginsberg (1973) studied the damped response to an excitation and its stability, considering both the driven and companion modes.

Chen and Babcock (1975) used the perturbation method to solve the nonlinear equations obtained by Donnell's nonlinear shallow-shell theory, without selecting a particular deflection solution. They solved the classical simply supported case and studied the driven mode response, the companion mode participation, and the appearance of a travelling wave. A damped response to an external excitation was found. The solution involved a sophisticated mode expansion, including boundary layer terms in order to satisfy the boundary conditions. They also presented experimental results in good agreement with their theory, showing a softening nonlinearity. Regions with amplitude-modulated response were also experimentally detected. Based on considerations given by Chen and Babcock (1975), the following interpretation of the companion

mode may be given, as presented by Amabili, Pellicano and Vakakis (2000c). Supposing that the responses of the driven and companion modes have the same frequency of oscillation, i.e. $A_{1,n}(t) = \tilde{A}_{1,n}\cos(w\,t + J_1)$ and $B_{1,n}(t) = \tilde{B}_{1,n}\cos(w\,t + J_2)$, and considering the other generalized coordinates to have smaller amplitude, equations (5-7) can be rearranged as (Amabili *et al*. 2000c)

$$\begin{aligned} w = {} & \left[\tilde{A}_{1,n}\cos(w\,t + J_1) + \tilde{B}_{1,n}\sin(w\,t + J_2)\right]\cos(nq) \\ & + \tilde{B}_{1,n}\sin(nq - w\,t - J_2)\sin(p\,x/L) + O(\tilde{A}_{1,n}^{\,2}, \tilde{B}_{1,n}^{\,2}, \tilde{A}_{1,0}, \tilde{A}_{3,0}\ldots), \end{aligned} \tag{1.8}$$

where $\tilde{A}_{1,n}$ and $\tilde{B}_{1,n}$ are the amplitudes of the driven and companion modes, respectively, and J_1 and J_2 are the phases of the solution. Equation (1.8) gives a wave of amplitude $\tilde{B}_{1,n}$ travelling around the shell with radian frequency $w_T = w/n$, superimposed on a standing wave (globally there is a travelling-wave). Since $q_2 - q_1 \cong p/2$, the amplitude of the resulting standing wave is almost $\tilde{A}_{1,n} - \tilde{B}_{1,n}$. The amplitude and frequency of the travelling wave solution are not affected by the phase relationship between driven and companion modes.

It is important to state that Ginsberg's (1973) numerical results and Chen and Babcock's (1975) numerical and experimental results constitute fundamental contributions to the study of the influence of the companion mode on the nonlinear forced response of circular cylindrical shells. Moreover, in these two studies, a multi-mode approach involving also modes with 2*n* circumferential waves was used. However, Ginsberg (1973) and Chen and Babcock (1975), in order to obtain numerical results, condensed their models to a two-degree-of-freedom one by using a perturbation approach with some truncation error.

Vol'mir *et al*. (1973) studied nonlinear oscillations of simply supported, circular cylindrical panels and plates subjected to an initial deviation from the equilibrium position (response of the panel to initial conditions) by using Donnell's nonlinear shallow-shell theory. Results were calculated by numerical integration of the equations of motion obtained by

Galerkin projection, retaining three or five modes in the expansion. The results reported do not show the trend of nonlinearity but only the time response.

Radwan and Genin (1975) derived nonlinear modal equations by using the Sanders-Koiter nonlinear theory of shells and the Lagrange equations of motion, taking into account imperfections. However, the equations of motion were derived only for perfect, closed shells, simply supported at the ends. The nonlinear coupling between the linear modes, that are the basis for the expansion of the shell displacements, was neglected. As previously observed, this single-mode approach gives the wrong trend of nonlinearity for a closed circular shell. The numerical results give only the coefficients of the Duffing equation, obtained while solving the problem. Radwan and Genin (1976) extended their previous work to include the nonlinear coupling with axisymmetric modes; however, only an approximate coupling was proposed. Most of the numerical results still indicated a hardening type nonlinearity for a closed circular shell; however, a large reduction of the hardening nonlinearity was obtained relative to the case without coupling.

Raju and Rao (1976) employed the Sanders-Koiter theory and used the finite element method to study free vibrations of shells of revolution. They found hardening-type results for a closed circular cylindrical shell, in contradiction with all experiments available. Their paper was discussed by Evensen (1977), Prathap (1978a, b), and then again by Evensen (1978a, b). In particular, Evensen (1977) commented that the authors ignored the physics of the problem: i.e., that thin shells bend more readily than they stretch.

Ueda (1979) studied nonlinear free vibrations of conical shells by using a theory equivalent to Donnell's shallow-shell theory and a finite element approach. Each shell element was reduced to a nonlinear system of two degrees of freedom by using an expansion similar to Evensen's (1967) analysis but without companion mode participation. Numerical results were carried out also for complete circular cylindrical shells and are in good agreement with those obtained by Olson (1965) and Evensen (1967).

Yamaki (1982) performed experiments for large-amplitude vibrations of a clamped shell made of a polyester film. The shell response of the first eight modes is given and the nonlinearity is of softening type for all these modes with a decrease of natural frequencies of 0.6, 0.7, 0.9 and 1.3 % for modes with n = 7, 8, 9 and 10 circumferential waves (and one longitudinal half-wave), respectively, for vibration amplitude equal to the shell thickness (rms amplitude equal to 0.7 times the shell thickness). He also proposed two methods of solution of the problem by using the Donnell's nonlinear shallow-shell theory: one is a Galerkin method and the second is a perturbation approach. No numerical application was performed.

Maewal (1986a, b) studied large-amplitude vibrations of circular cylindrical and axisymmetric shells by using the Sanders-Koiter nonlinear shell theory. The mode expansion used contains the driven and companion modes, axisymmetric modes and terms with twice the number of circumferential waves of the driven modes. However, it seems that axisymmetric modes with three longitudinal half-waves were neglected; as previously discussed, these modes are essential for predicting accurately the trend of nonlinearity. It is strongly believed that the difference between the numerical results of Maewal (1986b) and those obtained by Ginsberg (1973) may be attributed to the exclusion of the axisymmetric modes with three longitudinal half-waves in the analysis. Results were obtained by asymptotic analysis and by a specially-developed finite element method.

Nayfeh and Raouf (1987a, b) studied vibrations of closed shells by using plane-strain theory of shells and a perturbation analysis; thus, their study is suitable for rings but not for supported shells of finite length. They investigated the response when the frequency of the axisymmetric mode is approximately twice that of the asymmetric mode (two-to-one internal resonance). The phenomenon of saturation of the response of the directly excited mode was observed. Raouf and Nayfeh (1990) studied the response of the shell by using the same shell theory previously used by Nayfeh and Raouf (1987a, b), retaining both the driven and companion modes in the expansion, finding amplitude-modulated and chaotic solutions. Only

two degrees of freedom were used in this study; an axisymmetric term and terms with twice the number of circumferential waves of the driven and companion modes were obtained by perturbation analysis and added to the solution without independent degrees of freedom. The method of multiple scales was applied to obtain a perturbation solution from the equations of motion. By using a similar approach, Nayfeh *et al*. (1991) investigated the behaviour of shells, considering the presence of a two-to-one internal resonance between the axisymmetric and asymmetric modes for the problem previously studied by Nayfeh and Raouf (1987a, b).

Gonçalves and Batista (1988) conducted an interesting study on fluid-filled, complete circular cylindrical shells. A mode expansion that can be considered a simple generalisation of Evensen's (1967) was introduced by Varadan *et al*. (1989), along with Donnell's nonlinear shallow-shell theory, in their brief note on shell vibrations. This expansion is the same as that used by Watawala and Nash (1983); as previously observed, it is not moment-free at the ends of the shell. The results were compared with those obtained by using the mode expansion proposed by Dowell and Ventres (1968) and Atluri (1972). Varadan *et al*. (1989) showed that the expansion of Dowell and Ventres and Atluri gives hardening-type results, as previously discussed; the results obtained with the expansion of Watawala and Nash correctly display a softening type nonlinearity.

Koval'chuk and Podchasov (1988) introduced a travelling-wave representation of the radial deflection, in order to allow the nodal lines to travel in the circumferential direction over time. This expansion is exactly the same as that introduced by Kubenko *et al*. (1982) to study free vibrations; however, here forced vibrations were studied. It should be recognized that travelling-wave responses were also obtained in all the other previous work that included the companion mode; however, the expansion used was different.

Andrianov and Kholod (1993) used an analytical solution for shallow cylindrical shells and plates based on Bolotin's asymptotic method, but they obtained results only for a rectangular plate. A modified version of the nonlinear Donnell shallow-shell equations was used. Large-

amplitude vibrations of thin, closed circular cylindrical shells with wafer, stringer or ring stiffening were studied by Andrianov *et al*. (1996) by using the Sanders-Koiter nonlinear shell theory. The solution was obtained by using an asymptotic procedure and boundary layer terms to satisfy the shell boundary conditions. Only the free vibrations (backbone curve) were investigated. The single numerical case investigated showed a softening type nonlinearity.

Chiba (1993a) studied experimentally large-amplitude vibrations of two cantilevered circular cylindrical shells made of polyester sheet. He found that almost all responses display a softening nonlinearity. He observed that for modes with the same axial wavenumber, the weakest degree of softening nonlinearity can be attributed to the mode having the minimum natural frequency. He also found that shorter shells have a larger softening nonlinearity than longer ones. Travelling wave modes were also observed.

Koval'chuk and Lakiza (1995) investigated experimentally forced vibrations of large amplitude in fiberglass shells of revolution. The boundary conditions at the shell bottom simulated a clamped end, while the top end was free (cantilevered shell). One of the tested shells was circular cylindrical. A weak softening nonlinearity was found, excluding the beam-bending mode for which a hardening nonlinearity was measured. Detailed responses for three different excitation levels were obtained for the mode with four circumferential waves (second mode of the shell). Travelling wave response was observed around resonance, as well as the expected weak softening type nonlinearity.

Kobayashi and Leissa (1995) studied free vibrations of doubly curved thick shallow panels; they used the nonlinear first-order shear deformation theory of shells in order to study thick shells. The rectangular boundaries of the panel were assumed to be simply supported at the four edges without in-plane restraints, as previously assumed by Leissa and Kadi (1971). A single mode expansion was used for each of the three displacements and two rotations involved in the theory; in-plane and rotational inertia were neglected. The problem was then reduced to one of a single degree of freedom describing the radial displacement. Numerical results were

obtained for circular cylindrical, spherical and paraboloidal panels. Except for hyperbolic paraboloid shells, a softening behaviour was found, becoming hardening for vibration amplitudes of the order of the shell thickness. However, increasing the radius of curvature, i.e. approaching a flat plate, the behaviour changed and became hardening. The effect of the shell thickness was also investigated.

Thompson and de Souza (1996) studied the phenomenon of escape from a potential well for two-degree-of-freedom systems and used the case of forced vibrations of axially compressed shells as an example. A very complete bifurcation analysis was performed.

Ganapathi and Varadan (1996) used the finite element method to study large-amplitude vibrations of doubly-curved composite shells. Numerical results were given for isotropic circular cylindrical shells. They showed the effect of including the axisymmetric contraction mode with the asymmetric linear modes, confirming the effectiveness of the mode expansions used by many authors, as discussed in the foregoing. Only free vibrations were investigated in the paper, using Novozhilov's theory of shells. A four-node finite element was developed with five degrees of freedom for each node. Ganapathi and Varadan also pointed out problems in the finite element analysis of closed shells that are not present in open shells. The same approach was used to study numerically laminated composite circular cylindrical shells (Ganapathi and Varadan 1995).

Selmane and Lakis (1997a) applied the finite element method to study free vibrations of open and closed orthotropic cylindrical shells. Their method is a hybrid of the classical finite element method and shell theory. They used the refined Sanders-Koiter nonlinear theory of shells. The formulation was initially general but in the end, to simplify the solution, only a single linear mode was retained. As previously discussed, this approximation gives erroneous results for a complete circular shell. In fact, numerical results for free vibrations of the same closed circular cylindrical shell, simply supported at the ends, investigated by Nowinski (1963) and Kanaka Raju and Venkateswara Rao (1976) showed a hardening type nonlinearity. The criticism raised by Evensen (1977) on Nowinski's and Kanaka Raju and Venkateswara Rao's results

should be recalled to explain the hadening type of nonlinearity. Lakis *et al*. (1998) presented a similar solution for closed circular cylindrical shells.

A finite element approach to nonlinear dynamics of shells was developed by Sansour *et al*. (1997, 2002). They implemented a finite shell element based on a specifically developed nonlinear shell theory. In this shell theory, a linear distribution of the transverse normal strains was assumed, giving rise to a quadratic distribution of the displacement field over the shell thickness. They developed a time integration scheme for large numbers of degrees of freedom; in fact, problems can arise in finite element formulations of nonlinear problems with a large number of degrees of freedom due to the instability of integrators. Chaotic behaviour was found for a circular cylindrical panel simply supported on the straight edges, free on the curved edges and loaded by a point excitation having a constant value plus a harmonic component. The constant value of the load was assumed to give three equilibrium points (one unstable) in the static case.

Amabili *et al*. (1998) investigated the nonlinear free and forced vibrations of a simply supported, complete circular cylindrical shell, empty or fluid-filled. Donnell's nonlinear shallow-shell theory was used. The boundary conditions on the radial displacement and the continuity of circumferential displacement were exactly satisfied, while the axial constraint was satisfied on the average. Galerkin projection was used and the mode shape was expanded by using three degrees of freedom; specifically, two asymmetric modes (driven and companion modes), plus an axisymmetric term involving the first and third axisymmetric modes (reduced to a single term by an artificial constraint), were employed. The time dependence of each term of the expansion was general. Different tangential constraints were imposed at the shell ends. An inviscid fluid was considered. Solution was obtained both numerically and by the method of normal forms. Numerical results were obtained for both free and forced vibrations of empty and water-filled shells. Some additions to this paper were given by Amabili *et al*. (1999a). Results showed a softening type nonlinearity and travelling-wave response close to resonance. Numerical results

are in quantitative agreement with those of Evensen (1967), Olson (1965), Chen and Babcock (1975) and Gonçalves and Batista (1988).

In a series of four papers, Amabili, Pellicano and Païdoussis (1999b, c, 2000a, b) studied the nonlinear stability and nonlinear forced vibrations of a simply supported circular cylindrical shell with and without flow by using Donnell's nonlinear shallow-shell theory. The Amabili *et al*. (1999c, 2000a) papers deal with large-amplitude vibrations of empty and fluid-filled circular shells, also investigated by Amabili *et al*. (1998), but use an improved model for the solution expansion. In Amabili et *al*. (1999c) three independent axisymmetric modes with an odd number of longitudinal half-waves were added to the driven and companion modes. Therefore, the model can be considered to be an extension of the three-degree-of-freedom one developed by Amabili *et al*. (1998), in which the artificial kinematic constraint between the first and third axisymmetric modes, previously used to reduce the number of degrees of freedom, was removed. Results showed that the first and third axisymmetric modes are fundamental for predicting accurately the trend of nonlinearity and that the fifth axisymmetric mode only gives a small contribution. Driven modes with one and two longitudinal half-waves were numerically computed. Periodic solutions were obtained by a continuation technique based on the collocation method. Amabili *et al*. (2000a) added, to the expansion of the radial displacement of the shell, modes with twice the number of circumferential waves vis-à-vis the driven mode ($\cos(2nq)$ and $\sin(2nq)$) and up to three longitudinal half-waves, in order to check the convergence of the solution with different expansions. In particular, modes with the terms $\cos(2nq)$ and $\sin(2nq)$ are necessary to predict with accuracy the companion mode response for shells with very small damping. Results for empty and water-filled shells were compared, showing that the contained dense fluid largely enhances the weak softening type nonlinearity of empty shells; a similar conclusion was previously obtained by Gonçalves and Batista (1988). Experiments on a water-filled circular cylindrical shell were also performed and successfully compared to the theoretical results, validating the model developed. Experiments showed a reduction of the resonance frequency by

about 2 % for a vibration amplitude equal to the shell thickness. These experiments are described in detail in Amabili, Garziera and Negri (2002), where additional experimental details and results are given. It is important to note that, in this series of papers (Amabili *et al*. 1999b, c; 2000a, b), the continuity of the circumferential displacements and the boundary conditions for the radial deflection were exactly satisfied.

Pellicano, Amabili and Païdoussis (2002) extended the previous studies on forced vibrations of shells by using a mode expansion where a generic number of modes can be retained. Numerical results with up to 23 modes were obtained and the convergence of the solution discussed. In particular, it is shown that the model developed by Amabili *et al*. (2000a) is close to convergence. In that study a map is also given, for the first time, showing whether the nonlinearity is softening or hardening as a function of the shell geometry. This map is shown in Figure 1.3 and has been computed for steel shells and a mode with 6 circumferential waves and one longitudinal half-wave.

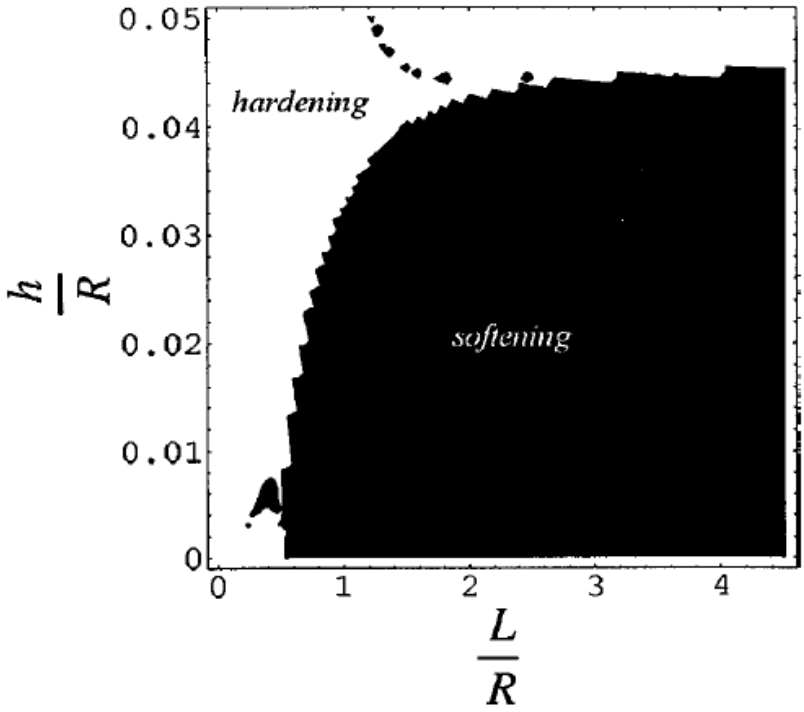

FIGURE 1.3. Map showing the character of nonlinearity versusshell geometry. Circumferentially closed steel shell and mode with 6 circumferential waves and one longitudional half-wave. Black: softening region; white: hardening region.

If the shell is not very short ($L/R > 0.5$) and not thick ($h/R < 0.045$) the nonlinearity is of the softening type, excluding the case of long ($L/R > 5$) thin shells. It is interesting to note that the boundary between softening and hardening regions has been found to be related to internal resonances (i.e. an integer relationship between natural frequencies) between the driven mode and axisymmetric modes.

Large-amplitude (geometrically nonlinear) vibrations of circular cylindrical shells with different boundary conditions and subjected to radial harmonic excitation in the spectral neighbourhood of the lowest resonances have been investigated by Amabili (2003b). In particular, simply supported shells with allowed and constrained axial displacements at the edges have been studied; in both cases the radial and circumferential displacements at the shell edges are constrained. Elastic rotational constraints have been assumed; they allow simulating any condition from simply supported to perfectly clamped, by varying the stiffness of this elastic constraint. The Lagrange equations of motion have been obtained by energy approach, retaining damping through the Rayleigh's dissipation function. Two different nonlinear shell theories, namely Donnell's and Novozhilov's theories, have been used to calculate the elastic strain energy. The formulation is valid also for orthotropic and symmetric cross-ply laminated composite shells; geometric imperfections have been taken into account. The large-amplitude response of circular cylindrical shells to harmonic excitation in the spectral neighbourhood of the lowest natural frequency has been computed for three different boundary conditions. Circular cylindrical shell with restrained axial displacement at the shell edges display stronger softening type nonlinearity than simply supported shells. Both empty and fluid-filled shells have been investigated by using a potential fluid model.

A problem of internal resonance (one-to-one-to-one-to-two) was studied by Amabili, Pellicano and Vakakis (2000c) and Pellicano *et al*. (2000) for a water-filled shell. In these papers, both modal and point excitations were used.

Autoparametric resonances for free flexural vibrations of infinitely long, closed shells were investigated by McRobie *et al*. (1999) and Popov *et al*. (2001) by using the energy formulation previously developed by the same authors (Popov *et al*. 1998a). A simple two-mode expansion, derived from Evensen (1967) but excluding the companion mode, was used. An energy approach was applied to obtain the equations of motion, which were transformed into action-angle co-ordinates and studied by averaging. Dynamics and stability were extensively investigated by using the methods of Hamiltonian dynamics, and chaotic motion was detected. Laing *et al*. (1999) studied the nonlinear vibrations of a circular cylindrical panel under radial point forcing by using the standard Galerkin method, the nonlinear Galerkin method and the post-processed Galerkin method. The system was discretized by the finite-difference method, similarly to the study of Foale *et al*. (1998). The authors conclude that the post-processed Galerkin method is often more efficient than either the standard Galerkin or nonlinear Galerkin methods.

Kubenko and Koval'chuk (2000b) used Donnell's nonlinear shallow-shell theory with Galerkin projection to study nonlinear vibrations of simply supported circular cylindrical shells. Driven and companion modes were included, but axisymmetric terms were neglected, giving a hardening type response. Interaction between two modes with different numbers of circumferential waves was discussed; this kind of interaction arises in correspondence to internal resonances. Results show interesting interactions between these modes. Another study considering the interaction between two modes with different numbers of circumferential waves was developed by Amiro and Prokopenko (1999), who also did not consider axisymmetric terms in the mode expansion.

Yamaguchi and Nagai (1997) studied vibrations of shallow cylindrical panels with a rectangular boundary, simply supported for transverse deflection and with in-plane elastic support at the boundary. The shell was excited by an acceleration having a constant value plus a harmonic component. Donnell's nonlinear shallow-shell theory was utilized with the Galerkin

projection along with a multi-mode expansion of flexural displacement. Initial deflection (imperfection) was taken into account in the theoretical formulation but not in the calculations. The harmonic balance method and direct integration were used. The response of the panel was of the softening type over the whole range of possible stiffness values of the in-plane springs (elastic support), becoming hardening for a vibration amplitude of the order of the shell thickness; in-plane constraints reduce the softening nonlinearity, which turns to hardening for smaller vibration amplitudes. The objective of this study was to investigate regions of chaotic motion; these regions were identified by means of Poincaré maps and Lyapunov exponents. It was found that, when approaching the static instability point (due to the constant acceleration load), chaotic shell behaviour may be observed. In a previous study, Nagai and Yamaguchi (1995) investigated shallow cylindrical panels without in-plane elastic support, via an approach similar to that used by Yamaguchi and Nagai (1997). Also in this case, an accurate investigation of the regions of chaotic motion was performed.

Using a similar approach, Yamaguchi and Nagai (2000) studied oscillations of a circular cylindrical panel, simply supported at the four edges, having an elastic radial spring at the center. The panel was excited by an acceleration with a constant term plus a harmonic component, and regions of chaotic motion were identified. Nagai *et al*. (2001) also studied theoretically and experimentally chaotic vibrations of a simply supported circular cylindrical panel carrying a mass at its center. A single-mode approximation was used by Shin (1997) to study free vibration of doubly-curved, simply supported panels. Backbone curves and response to initial conditions were studied. Free vibrations of doubly-curved, laminated, clamped shallow panels, including circular cylindrical panels, were studied by Abe *et al*. (2000). Both first-order shear deformation theory and classical shell theory (analogous to Donnell's theory) were used. Results obtained neglecting in-plane and rotary inertia are very close to those obtained retaining these effects. Only two modes were considered to interact in the nonlinear analysis. Free vibrations and parametric resonance of complete, simply supported circular cylindrical shells were studied by

Mao and Williams (1998a, b). The shell theory used is similar to Sanders', but the axial inertia is neglected. A single-mode expansion was used without considering axisymmetric contraction. Han *et al*. (1999) studied the axisymmetric motion of circular cylindrical shells under axial compression and radial excitation. A region of chaotic response was detected.

Extensive experiments on large-amplitude vibrations of clamped, circular cylindrical shells were performed by Gunawan (1998). Two almost perfect aluminum shells and two with axisymmetric imperfection were tested. Contact-free acoustic excitation and vibration measurement were used. Mostly of the experiments were performed for the mode with 11 and 9 circumferential waves for perfect and imperfect shells, respectively. These modes were selected in order to have a good frequency separation from other modes and avoid nonlinear interaction among different modes. The effect of axial load on the shell response was investigated. Softening type nonlinearity and traveling wave response were observed for all the shells. Nonstationary responses appeared at relatively large vibration amplitudes.

Mikhlin (2000) studied vibrations of circular cylindrical shells under a radial excitation and an axial static load, using Donnell's nonlinear shallow-shell theory with Galerkin projection and two different two-mode expansions. One included the first circumferential harmonic of the driven mode and the other was derived from Evensen's (1967) expansion; in both cases, the companion mode was not considered. Stability and energy "pumping" from one mode to the other were discussed. Lee and Kim (1999) used a single-mode approach to study nonlinear free vibration of rotating cylindrical shells. The equation of motion shows only a cubic nonlinearity, thus explaining the appearance of hardening nonlinearity. Moussaoui *et al*. (2000) studied free, large-amplitude vibrations of infinitely long, closed circular cylindrical shells, neglecting the motion in the longitudinal direction and assuming that the generating lines of the shell remain straight after deformation. Thus, their model is suitable for rings but it is not adequate for real shells of finite length. The system was discretised by using a multi-mode expansion that excluded all axisymmetric terms, which are fundamental. Therefore, an erroneous hardening

type nonlinearity was obtained. Nayfeh and Rivieccio (2000) used a single-mode expansion of the displacements to study forced vibrations of simply supported, composite, complete circular cylindrical shells. This approach, as previously discussed, is inadequate for predicting the correct trend of nonlinearity; in fact, hardening type results were erroneously obtained and only a cubic nonlinearity was found in the equation of motion. However, due to the simple expansion, the equation of motion was obtained in closed-form.

Jansen (2002) studied forced vibrations of simply supported, circular cylindrical shells under harmonic modal excitation and static axial load. Donnell's shallow-shell theory was used, but the in-plane inertia of axisymmetric modes was taken into account in an approximate way. In-plane boundary conditions were satisfied on the average. A four-degree-of-freedom expansion of the radial displacement was used with Galerkin's method. Numerical results display a softening type response with traveling wave in the vicinity of resonance. The narrow frequency range in which there are amplitude modulations in the response was deeply investigated. In another paper, Jansen (2001) presented a perturbation approach for both the frequency and the shell coordinates. The resulting boundary value problem was numerically approached by using a parallel shooting method. Results are in good agreement with those obtained by the same author (Jansen 2002) via Galerkin's method.

Amabili *et al*. (2003) experimentally studied large-amplitude vibrations of a stainless-steel circular cylindrical panels supported at the four edges. The nonlinear response to harmonic excitation of different magnitude in the neighbourhood of three resonances was investigated. Experiments showed that the curved panel tested exhibited a relatively strong geometric nonlinearity of softening type. In particular, for the fundamental mode, the resonance was reached at a frequency 5 % lower than the natural (linear) frequency, when the vibration amplitude was equal to 0.55 times the shell thickness. This is particularly interesting when these results are compared to the nonlinearity of the fundamental mode of complete (closed around the

circumference), simply supported, circular cylindrical shells of similar length and radius, which display much weaker nonlinearity.

Finite-amplitude vibrations of long shells in beam-bending mode were studied by Hu and Kirmser (1971). Birman and Bert (1987) and Birman and Twinprawate (1988) extended the study to include elastic axial constraints, shells on an elastic foundation, and uniformly distributed static loads. Single-mode and two-mode approximations were used. Results show a softening nonlinearity for long shells without restrained axial displacements at the ends, which becomes hardening for long shells with restrained displacements; other boundary conditions are those of a clamped shell.

Circular cylindrical shells carrying a concentrated mass were investigated by Likhoded (1976). Large-amplitude free vibrations of non-circular cylindrical shells on Pasternak foundations were studied by Paliwal and Bhalla (1993) by using the approach developed by Sinharay and Banerjee (1985, 1986).

Three recent *Letters to the Editor* (Dowell 1998; Amabili *et al*. 1999d; Evensen 1999) indicated that the subject of nonlinear vibrations of shells still needs further analysis, concerning some basic phenomena and experimental results.

A point that was still waiting for an answer was the accuracy of the different nonlinear shell theories available. For this reason, Amabili (2003a) computed the large-amplitude response of perfect and imperfect, simply supported circular cylindrical shells subjected to harmonic excitation in the spectral neighbourhood of the lowest natural frequency, by using five different nonlinear shell theories: (i) Donnell's shallow-shell, (ii) Donnell's with in-plane inertia, (iii) Sanders-Koiter, (iv) Flügge-Lur'e-Byrne and (v) Novozhilov's theories. Except for the first theory, the Lagrange equations of motion were obtained by an energy approach, retaining damping through Rayleigh's dissipation function. The formulation is also valid for orthotropic and symmetric cross-ply laminated composite shells. Both empty and fluid-filled shells were investigated by using a potential fluid model. The effect of radial pressure and axial load was

also studied. Results from the Sanders-Koiter, Flügge-Lur'e-Byrne and Novozhilov's theories were extremely close, for both empty and water-filled shells. For the thin shell numerically investigated by Amabili (2003a), for which $h/R \cong 288$, there is almost no difference among them. Appreciable difference, but not particularly large, was observed between the previous three theories and Donnell's theory with in-plane inertia. On the other hand, Donnell's nonlinear shallow-shell theory turned out to be the least accurate among the five theories compared. It gives excessive softening type nonlinearity for empty shells. However, for water-filled shells, it gives sufficiently precise results, also for quite large vibration amplitude. The different accuracy of the Donnell's nonlinear shallow-shell theory for empty and water-filled shell can easily be explained by the fact that the in-plane inertia, which is neglected in Donnell's nonlinear shallow-shell theory, is much less important for a water-filled shell, which has a large radial inertia due to the liquid, than for an empty shell. Contained liquid, compressive axial loads and external pressure increase the softening type nonlinearity of the shell. A minimum mode expansion necessary to capture the nonlinear response of the shell in the neighbourhood of a resonance was determined and convergence of the solution was numerically investigated.

Geometric imperfections of the shell geometry (e.g. out-of-roundness) were considered in buckling problems since the end of the 1950s; *e.g.*, see Agamirov and Vol'mir (1959), Koiter (1963) and Hutchinson (1965). However, there is no trace of their inclusion in studies of large-amplitude vibrations of shells until the beginning of the '70s. Research on this topic was probably introduced by Vol'mir (1972). Kil'dibekov (1977) studied free vibrations of imperfect, simply supported, complete circular shells under pressure and axial loading by using a simple mode expansion involving two degrees of freedom: the driven mode and an axisymmetric term having the same spatial form of the one introduced by Evensen. Imperfections having the same shape as this expansion were assumed. Donnell's nonlinear shallow-shell theory was used. Softening and hardening nonlinearity were found depending on shell geometry. Results show, in contrast with other studies, that initial imperfections change the linear frequency only in the

presence of an axial load. Koval'chuk and Krasnopol'skaia (1980) studied forced vibrations of closed, simply supported circular cylindrical shells using Donnell's nonlinear shallow-shell theory. The same expansion of the radial displacement introduced by Evensen (1967) was used. Geometric imperfections having the same shape as the driven mode were considered. Both radial and longitudinal (parametric) excitations were examined. Some unstable zones with nonstationary vibrations and travelling waves were detected, due to differences between the driven- and companion-mode natural frequencies, caused by the geometric imperfections. The authors found softening radial responses. Kubenko *et al*. (1982) used a two-mode travelling-wave expansion, taking into account axisymmetric and asymmetric geometric imperfections; the rest of the model for the complete circular shell was similar to those proposed by Koval'chuk and Krasnopol'skaia (1980). Only free vibrations were studied, but the effect of the number of circumferential waves on the nonlinear behaviour was investigated. In particular, the results showed that the nonlinearity is of the softening type and that it increases with the number of circumferential waves. In the studies of Koval'chuk and Krasnopol'skaia (1980) and Kubenko *et al*. (1982) the effect of axisymmetric and asymmetric imperfections was to increase the natural frequency; this is in contrast with results obtained in other studies.

Watawala and Nash (1983) studied the free and forced conservative vibrations of closed circular cylindrical shells using the Donnell's nonlinear shallow-shell theory. Empty and liquid-filled shells with a free-surface and a rigid bottom were studied. A mode expansion that may be considered as a simple generalization of Evensen's (1967) was introduced; therefore, it is not moment-free at the ends of the shell. A single-term was used to describe the shell geometric imperfections. Cases of (i) the circumferential wave pattern of the shell response being the same as that of the imperfection and (ii) the circumferential wave pattern of the response being different from that of the imperfection were analyzed. Numerical results showed softening type nonlinearity. The imperfections lowered the linear frequency of vibrations when the circumferential wave pattern of shell response was the same as that of the imperfection, affecting

the observed nonlinearity. Results for forced vibrations were obtained only for beam-bending modes, for which Donnell's nonlinear shallow-shell theory is not appropriate; these results indicated a hardening type nonlinearity. Hui (1984) studied the influence of imperfections on free vibrations of simply supported circular cylindrical panels; he used Donnell's nonlinear shallow-shell theory and a single-mode expansion; the imperfection was assumed to have the same shape as his single-mode expansion. These imperfections changed the linear vibration frequency (increase or decrease according with the number of circumferential half-waves) and influenced the nonlinearity of the panel.

Jansen (1992) studied large-amplitude vibrations of simply supported, laminated, complete circular cylindrical shells with imperfections. He used Donnell's nonlinear shallow-shell theory and the same mode expansion as Watawala and Nash (1983); the boundary conditions at the shell ends were not fully satisfied. The results showed a softening-type nonlinearity becoming hardening only for very large amplitude of vibrations (generally larger than ten times the shell thickness). Imperfections having the same shape as the asymmetric mode analyzed gave a less pronounced softening behaviour, changing to hardening for smaller amplitudes. Moreover, the linear frequency of the imperfect shell may be considerably lower than the frequency of the perfect shell. In a subsequent study Jansen (2002) developed his model further by using a four-degree-of-freedom expansion. However, numerical results are presented only for a perfect shell. In a third paper by the same author (Jansen 2001), results for composite shells with axisymmetric and asymmetric imperfections are given.

Chia (1987a, b) studied nonlinear free vibrations and postbuckling of symmetrically and asymmetrically laminated circular cylindrical panels with imperfections and different boundary conditions. Donnell's nonlinear shallow-shell theory was used. A single-mode analysis was carried out, and the results showed a hardening nonlinearity. In a subsequent study Chia (1988b) also investigated doubly-curved panels with rectangular base by using a similar shell theory, and a single-mode expansion in all the numerical calculations, for both vibration shape and initial

imperfection. However, in this study, numerical results for circular cylindrical panels and doubly curved shallow shells generally show a softening nonlinearity, which becomes hardening only for very large vibrations, as expected. The equations of motion are obtained by Gakerkin's method and are studied by using the harmonic balance method. Only the backbone curves are given. Iu and Chia (1988a) studied antisymmetrically laminated cross-ply circular cylindrical panels by using the Timoshenko-Mindlin kinematic hypothesis, which is an extension of Donnell's nonlinear shallow-shell theory. Effects of transverse shear deformation, rotary inertia and geometrical imperfections were included in the analysis. The solution was obtained by the harmonic balance method after Galerkin projection. Fu and Chia (1989) extended this analysis to include a multi-mode approach. Iu and Chia (1988b) used Donnell's nonlinear shallow-shell theory to study free vibrations and post-buckling of clamped and simply supported, asymmetrically laminated cross-ply circular cylindrical shells. A multi-mode expansion was used without considering companion mode, as only free vibrations were investigated; radial geometric imperfections were taken into account. The homogeneous solution of the stress function was retained, but the dependence on the axial coordinate was neglected, differently to what was done by Fu and Chia (1989). The equations of motion were obtained by using the Galerkin method and were studied by the harmonic balance method. Three asymmetric and three axisymmetric modes were used in the numerical calculations. Numerical results were compared to those obtained by El-Zaouk and Dym (1973) for a simply supported, glass-epoxy orthotropic circular cylindrical shell, showing some differences. In a later paper, Fu and Chia (1993) included in their model nonuniform boundary conditions around the edges. Softening or hardening type nonlinearity was found, depending on the radius-to-thickness ratio. Only undamped free vibrations and buckling were investigated in all this series of studies.

Elishakoff *et al.* (1987) conducted a nonlinear analysis of small vibrations of an imperfect cylindrical panel around a static equilibrium position. Librescu and Chang (1993) investigated geometrically imperfect, doubly-curved, undamped, laminated composite panels. The nonlinear

theory of shear-deformable shallow panels was used. The nonlinearity was due to finite deformations of the panel due to in-plane loads and imperfections. Only small-amplitude free vibrations superimposed on this finite initial deformation were studied. A single-mode expansion was used to describe the free vibrations and the initial imperfections. The authors found that imperfections of the panels, of the same shape as the mode investigated, lowered the vibration frequency significantly. They also described accurately the post-buckling stability. In fact, curved panels are characterized by an unstable post-buckling behaviour, in the sense that they are subject to a snap-through-type instability. Librescu *et al*. (1996), Librescu and Lin (1997a) and Hause *et al*. (1998) extended this work to include thermomechanical loads and nonlinear elastic foundations (Librescu and Lin 1997b, 1999). Cheikh *et al*. (1996) studied nonlinear vibrations of an infinite circular cylindrical shell with geometric imperfection of the same shape as the mode excited. Plane-strain theory of shells was assumed, which is suitable only for rings (generating lines remain straight and parallel to the shell axis) and a three-degree-of-freedom model, subsequently reduced to a single-degree-of-freedom one, was developed. Results exhibit a hardening type nonlinearity, which is not reasonable for the shell geometry investigated.

Amabili (2003c) included geometric imperfections in the model previously developed by Pellicano *et al*. (2002) and performed in depth experimental investigations on large-amplitude vibrations of an empty and water-filled, simply supported circular cylindrical shell subject to harmonic excitations. The effect of geometric imperfections on natural frequencies was investigated. In particular, it was found that: (i) axisymmetric imperfections do not split the double natural frequencies associated with each couple of asymmetric modes; outward (with respect with the center of curvature) axisymmetric imperfections increase natural frequencies; small inward (with respect with the center of curvature) axisymmetric imperfections decrease natural frequencies; (ii) ovalisation has a small effect on natural frequencies of modes with several circumferential waves and it does not split the double natural frequencies; (iii) imperfections of the same shape as the resonant mode decrease both frequencies, but much more

the frequency of the mode with the same angular orientation; (iv) imperfections with the twice the number of circumferential waves of the resonant mode decrease the frequency of the mode with the same angular orientation and increase the frequency of the other mode; they have a larger effect on natural frequencies than imperfections of the same shape as the resonant mode. The split of the double natural frequencies, which is present in almost all real shells due to manufacturing imperfections, changes the traveling wave response. Good agreement between theoretical and experimental results was obtained. All the modes investigated show a softening type nonlinearity, which is much more accentuated for the water-filled shell, except in a case displaying internal resonance (one-to-one) among modes with different number of circumferential waves. Travelling wave and amplitude-modulated responses were observed in the experiments.

Results for imperfect shells obtained by Donnell's nonlinear shell theory retaining in-plane inertia and Sanders-Koiter nonlinear shell theory are given by Amabili (2003a).

2. NONLINEAR VIBRATIONS OF SIMPLY SUPPORTED CIRCULAR CYLINDRICAL SHELLS

2.1 ELASTIC STRAIN ENERGY OF THE SHELL ACCORDING TO (i) DONNELL, (ii) SANDERS-KOITER, (iii) FLUGGE-LUR'E-BYRNE AND (iv) NOVOZILOV THEORIES

Figure 1.1 of the previous Chapter shows a circular cylindrical shell with the cylindrical coordinate system (O; x, r, q), having the origin O at the centre of one end of the shell. The displacements of an arbitrary point of coordinates (x, q) on the middle surface of the shell are denoted by u, v and w, in the axial, circumferential and radial directions, respectively; w is taken positive outwards. Initial imperfections of the circular cylindrical shell associated with zero initial tension are denoted by radial displacement w_0.

Most of the studies use four strain-displacement relationships for thin shells. They are based on Love's first approximation assumptions: (i) the shell thickness h is small with respect to the radius of curvature R of the middle plane; (ii) strains are small; (iii) transverse normal stress is small; and (iv) the Kirchhoff-Love kinematic hypothesis, in which it is assumed that the normal to the undeformed middle surface remains straight and normal to the midsurface after deformation, and undergoes no thickness stretching. These shell theories are: (i) Donnell's (see Yamaki 1984), (ii) Sanders-Koiter (Yamaki 1984, Budiansky 1968), (iii) Flügge-Lur'e-Byrne (Ginsberg 1973, Yamaki 1984) and (iv) Novozhilov's (Novozhilov 1953) nonlinear shell theories. For all of them, rotary inertia and shear deformations are neglected. According to these shell theories, the strain components e_x, e_q and g_{xq} at an arbitrary point of the shell are related to the middle surface strains $e_{x,0}$, $e_{q,0}$ and $g_{xq,0}$ and to the changes in the curvature and torsion of the middle surface k_x, k_q and k_{xq} by the following three relationships

$$e_x = e_{x,0} + z\,k_x, \tag{2.1a}$$

$$e_q = e_{q,0} + z\,k_q, \tag{2.1b}$$

$$g_{xq} = g_{xq,0} + z\,k_{xq}, \tag{2.1c}$$

where z is the distance of the arbitrary point of the shell from the middle surface.

According to Donnell's nonlinear shell theory, the middle surface strain-displacement relationships and changes in the curvature and torsion are obtained for a circular cylindrical shell

$$e_{x,0} = \frac{\partial u}{\partial x} + \frac{1}{2}\left(\frac{\partial w}{\partial x}\right)^2 + \frac{\partial w}{\partial x}\frac{\partial w_0}{\partial x}, \tag{2.2a}$$

$$e_{q,0} = \frac{\partial v}{R\partial q} + \frac{w}{R} + \frac{1}{2}\left(\frac{\partial w}{R\partial q}\right)^2 + \frac{\partial w}{R\partial q}\frac{\partial w_0}{R\partial q}, \tag{2.2b}$$

$$g_{xq,0} = \frac{\partial u}{R\partial q} + \frac{\partial v}{\partial x} + \frac{\partial w}{\partial x}\frac{\partial w}{R\partial q} + \frac{\partial w}{\partial x}\frac{\partial w_0}{R\partial q} + \frac{\partial w_0}{\partial x}\frac{\partial w}{R\partial q}, \tag{2.2c}$$

$$k_x = -\frac{\partial^2 w}{\partial x^2}, \tag{2.2d}$$

$$k_q = -\frac{\partial^2 w}{R^2\partial q^2}, \tag{2.2e}$$

$$k_{xq} = -2\frac{\partial^2 w}{R\partial x\partial q}. \tag{2.2f}$$

Sanders (1963) developed a more refined nonlinear theory of shells expressed in tensorial form; the same equations were obtained by Koiter (1966) around the same period, leading to the designation of these equations as the Sanders-Koiter equations. The middle surface strain-displacement relationships, changes in the curvature and torsion in this case are (see Yamaki 1984, Budiansky 1968)

$$e_{x,0} = \frac{\partial u}{\partial x} + \frac{1}{2}\left(\frac{\partial w}{\partial x}\right)^2 + \frac{1}{8}\left(\frac{\partial v}{\partial x} - \frac{\partial u}{R\partial q}\right)^2 + \frac{\partial w}{\partial x}\frac{\partial w_0}{\partial x}, \tag{2.3a}$$

$$e_{q,0} = \frac{\partial v}{R\partial q} + \frac{w}{R} + \frac{1}{2}\left(\frac{\partial w}{R\partial q} - \frac{v}{R}\right)^2 + \frac{1}{8}\left(\frac{\partial u}{R\partial q} - \frac{\partial v}{\partial x}\right)^2 + \frac{\partial w_0}{R\partial q}\left(\frac{\partial w}{R\partial q} - \frac{v}{R}\right), \tag{2.3b}$$

$$g_{xq,0} = \frac{\partial u}{R\partial q} + \frac{\partial v}{\partial x} + \frac{\partial w}{\partial x}\left(\frac{\partial w}{R\partial q} - \frac{v}{R}\right) + \frac{\partial w_0}{\partial x}\left(\frac{\partial w}{R\partial q} - \frac{v}{R}\right) + \frac{\partial w}{\partial x}\frac{\partial w_0}{R\partial q}, \tag{2.3c}$$

$$k_x = -\frac{\partial^2 w}{\partial x^2}, \tag{2.3d}$$

$$k_q = \frac{\partial v}{R^2 \partial q} - \frac{\partial^2 w}{R^2 \partial q^2}, \tag{2.3e}$$

$$k_{xq} = -2\frac{\partial^2 w}{R\partial x \partial q} + \frac{1}{2R}\left(3\frac{\partial v}{\partial x} - \frac{\partial u}{R\partial q}\right). \tag{2.3f}$$

Changes in curvature and torsion are linear according to both Donnell's and Sanders-Koiter nonlinear shell theories.

According to Flügge-Lur'e-Byrne nonlinear theory (Ginsberg 1973, Yamaki 1984), the thinness assumption is delayed in the derivations. For this reason, displacements $\tilde{u}$, $\tilde{v}$ and $\tilde{w}$ of points at distance z from the middle surface are introduced; they are related to displacements on the middle surface by the relationships

$$\tilde{u} = u - z\frac{\partial (w + w_0)}{\partial x}, \tag{2.4a}$$

$$\tilde{v} = v - \frac{z}{R}\left(\frac{\partial (w + w_0)}{\partial q} - v\right), \tag{2.4b}$$

$$\tilde{w} = w + w_0. \tag{2.4c}$$

Equations (2.4) are a simplified version of those obtained by Novozhilov (1953). The strain-displacement relationships for a generic point of the shell are

$$e_x = \frac{\partial \tilde{u}}{\partial x} + \frac{1}{2}\left[\left(\frac{\partial \tilde{u}}{\partial x}\right)^2 + \left(\frac{\partial \tilde{v}}{\partial x}\right)^2 + \left(\frac{\partial \tilde{w}}{\partial x}\right)^2\right], \tag{2.5a}$$

$$e_q = \frac{1}{R+z}\left(\frac{\partial \tilde{v}}{\partial q} + \tilde{w}\right) + \frac{1}{2(R+z)^2}\left[\left(\frac{\partial \tilde{u}}{\partial q}\right)^2 + \left(\frac{\partial \tilde{v}}{\partial q} + \tilde{w}\right)^2 + \left(\frac{\partial \tilde{w}}{\partial q} - \tilde{v}\right)^2\right], \tag{2.5b}$$

$$g_{xq} = \frac{\partial \tilde{v}}{\partial x} + \frac{1}{R+z}\frac{\partial \tilde{u}}{\partial q} + \frac{1}{R+z}\left[\frac{\partial \tilde{u}}{\partial x}\frac{\partial \tilde{u}}{\partial q} + \frac{\partial \tilde{v}}{\partial x}\left(\frac{\partial \tilde{v}}{\partial q} + \tilde{w}\right) + \frac{\partial \tilde{w}}{\partial x}\left(\frac{\partial \tilde{w}}{\partial q} - \tilde{v}\right)\right]. \tag{2.5c}$$

The following thinness approximations are now introduced

$$\frac{1}{R+z}=\frac{1}{R}\left[1-\frac{z}{R}+O\left(\left(\frac{z}{R}\right)^2\right)\right], \tag{2.6a}$$

$$\frac{1}{(R+z)^2}=\frac{1}{R^2}\left[1-\frac{2z}{R}+O\left(\left(\frac{z}{R}\right)^2\right)\right], \tag{2.6b}$$

where $O((z/R)^2)$ is a small quantity of order $(z/R)^2$. Equations (2.5) coincide with those obtained by Novozhilov (1953), who did not consider geometric imperfections and neglected z and z^2 at this point of the derivation with respect to R. By introducing equations (2.4) into equations (2.5) and using approximations (2.6), the middle surface strain-displacement relationships, changes in the curvature and torsion are obtained for the Flügge-Lur'e-Byrne nonlinear shell theory (Ginsberg 1973, Yamaki 1984)

$$e_{x,0}=\frac{\partial u}{\partial x}+\frac{1}{2}\left[\left(\frac{\partial u}{\partial x}\right)^2+\left(\frac{\partial v}{\partial x}\right)^2+\left(\frac{\partial w}{\partial x}\right)^2\right]+\frac{\partial w}{\partial x}\frac{\partial w_0}{\partial x}, \tag{2.7a}$$

$$\begin{aligned}e_{q,0}=&\frac{\partial v}{R\partial q}+\frac{w}{R}+\frac{1}{2R^2}\left[\left(\frac{\partial u}{\partial q}\right)^2+\left(\frac{\partial v}{\partial q}+w\right)^2+\left(\frac{\partial w}{\partial q}-v\right)^2\right]\\&+\frac{1}{R^2}\left[\frac{\partial w_0}{\partial q}\left(\frac{\partial w}{\partial q}-v\right)+w_0\left(w+\frac{\partial v}{\partial q}\right)\right],\end{aligned} \tag{2.7b}$$

$$\begin{aligned}g_{xq,0}=&\frac{\partial v}{\partial x}+\frac{\partial u}{R\partial q}+\frac{1}{R}\left[\frac{\partial u}{\partial x}\frac{\partial u}{\partial q}+\frac{\partial v}{\partial x}\left(\frac{\partial v}{\partial q}+w\right)+\frac{\partial w}{\partial x}\left(\frac{\partial w}{\partial q}-v\right)+\frac{\partial w_0}{\partial x}\left(\frac{\partial w}{\partial q}-v\right)\right.\\&\left.+\frac{\partial w}{\partial x}\frac{\partial w_0}{\partial q}+\frac{\partial v}{\partial x}w_0\right].\end{aligned} \tag{2.7c}$$

$$k_x=-\frac{\partial^2 w}{\partial x^2}-\frac{\partial u}{\partial x}\frac{\partial^2(w+w_0)}{\partial x^2}-\frac{\partial v}{\partial x}\frac{\partial^2(w+w_0)}{R\partial x\partial q}+\frac{1}{R}\left(\frac{\partial v}{\partial x}\right)^2, \tag{2.7d}$$

$$\begin{aligned}k_q=&-\frac{\partial^2 w}{R^2\partial q^2}-\frac{w}{R^2}-\frac{(w+w_0)}{R^3}\left(w+\frac{\partial^2 w}{\partial q^2}+\frac{\partial v}{\partial q}\right)-\frac{w}{R^3}\left(w_0+\frac{\partial^2 w_0}{\partial q^2}\right)\\&-\frac{\partial u}{R^2\partial q}\left(\frac{\partial u}{R\partial q}+\frac{\partial^2(w+w_0)}{\partial x\partial q}\right)-\frac{\partial v}{R^3\partial q}\frac{\partial^2(w+w_0)}{\partial q^2},\end{aligned} \tag{2.7e}$$

$$k_{xq} = -2\frac{\partial^2 w}{R\partial x\partial q} + \frac{\partial v}{R\partial x} - \frac{\partial u}{R^2\partial q} - \frac{\partial u}{R\partial x}\left(\frac{\partial u}{R\partial q} + \frac{\partial^2(w+w_0)}{\partial x\partial q}\right) + \frac{\partial v}{R^2\partial x}\left(\frac{\partial v}{\partial q} - \frac{\partial^2(w+w_0)}{\partial q^2}\right) - \frac{\partial^2(w+w_0)}{R^2\partial x\partial q}\left(w + \frac{\partial v}{\partial q}\right) - \frac{\partial^2 w}{R^2\partial x\partial q}w_0 - \frac{\partial^2(w+w_0)}{\partial x^2}\frac{\partial u}{R\partial q} - \frac{\partial v}{\partial x}\frac{\partial^2(w+w_0)}{R^2\partial q^2}. \quad (2.7f)$$

It is important to note that, differently from references (Ginsberg 1973, Yamaki 1984), nonlinear terms in changes in curvature and torsion are retained in equations (2.7d-f). Equations (2.7) have been obtained by neglecting higher order terms in *z*, in order to reduce equations (2.5) to the form given by equations (2.1). Equation (2.7a-c) coincides with those obtained by Novozhilov (1953), excluding geometric imperfections that were not considered by Novozhilov.

According to Novozhilov's nonlinear shell theory, equations (2.4) are replaced by

$$\tilde{u} = u + zq\ , \quad (2.8a)$$

$$\tilde{v} = v + zy\ , \quad (2.8b)$$

$$\tilde{w} = w + w_0 + z\,c\ , \quad (2.8c)$$

where

$$q = -\frac{\partial(w+w_0)}{\partial x}\left(1 + \frac{\partial v}{R\partial q} + \frac{w}{R}\right) + \left(\frac{\partial(w+w_0)}{R\partial q} - \frac{v}{R}\right)\frac{\partial u}{R\partial q} - \frac{\partial w}{\partial x}\frac{w_0}{R}, \quad (2.8d)$$

$$y = -\left(\frac{\partial(w+w_0)}{R\partial q} - \frac{v}{R}\right)\left(1 + \frac{\partial u}{\partial x}\right) + \frac{\partial(w+w_0)}{\partial x}\frac{\partial v}{\partial x}, \quad (2.8e)$$

$$c \cong \frac{\partial u}{\partial x} + \frac{\partial v}{R\partial q} + \frac{w+w_0}{R} + \frac{\partial u}{\partial x}\left(\frac{\partial v}{R\partial q} + \frac{w+w_0}{R}\right) - \frac{\partial u}{R\partial q}\frac{\partial v}{\partial x}. \quad (2.8f)$$

Substituting equations (2.4) and (2.6) into equations (2.5), the following expressions for changes in the curvature and torsion are obtained

$$k_x = -\frac{\partial^2 w}{\partial x^2} + \frac{\partial v}{R\partial x}\left(-\frac{\partial u}{R\partial q} + \frac{\partial v}{\partial x} - \frac{\partial^2(w+w_0)}{\partial x\partial q}\right) + \frac{\partial(w+w_0)}{\partial x}\frac{\partial^2 u}{\partial x^2} + \frac{\partial^2 u}{R\partial x\partial q}\left(-\frac{v}{R} + \frac{\partial(w+w_0)}{R\partial q}\right) + \frac{\partial^2(w+w_0)}{R\partial x\partial q}\frac{\partial u}{R\partial q} - \frac{\partial^2(w+w_0)}{\partial x^2}\left(\frac{w}{R} + \frac{\partial v}{R\partial q} + \frac{\partial u}{\partial x}\right) - \frac{\partial^2 w}{\partial x^2}\frac{w_0}{R}, \quad (2.9a)$$

$$
\begin{aligned}
k_q = &-\frac{\partial^2 w}{R^2 \partial q^2}+\frac{\partial u}{R\partial x}+\frac{\partial v}{R^2\partial q}-\frac{(w+w_0)}{R}\left(\frac{\partial^2 w}{R^2\partial q^2}-\frac{\partial v}{R^2\partial q}-2\frac{\partial u}{R\partial x}\right)-\frac{w}{R}\frac{\partial^2 w_0}{R^2\partial q^2}\\
&-\frac{\partial u}{R^2\partial q}\left(\frac{\partial u}{R\partial q}+\frac{\partial v}{\partial x}+\frac{\partial^2(w+w_0)}{\partial x\partial q}\right)+\frac{\partial v}{R^2\partial q}\left(\frac{\partial v}{R\partial q}+3\frac{\partial u}{\partial x}-\frac{\partial^2(w+w_0)}{R\partial q^2}\right)\\
&+\frac{\partial^2 v}{R^3\partial q^2}\left(\frac{\partial(w+w_0)}{\partial q}-v\right)+\frac{\partial(w+w_0)}{R^2\partial q}\left(-\frac{v}{R}+\frac{\partial w}{R\partial q}\right)-\frac{\partial^2(w+w_0)}{R^2\partial q^2}\frac{\partial u}{R\partial x}\\
&+\frac{\partial w}{R^2\partial q}\frac{\partial w_0}{R\partial q}+\frac{\partial(w+w_0)}{\partial x}\frac{\partial^2 v}{R\partial x\partial q}+\frac{\partial v}{R\partial x}\frac{\partial^2(w+w_0)}{\partial x\partial q},
\end{aligned}
\tag{2.9b}
$$

$$
\begin{aligned}
k_{xq} = &-2\frac{\partial^2 w}{R\partial x\partial q}-\frac{\partial u}{R^2\partial q}+\frac{\partial v}{R\partial x}+\frac{\partial u}{R^2\partial q}\left(-\frac{\partial u}{\partial x}+\frac{\partial^2(w+w_0)}{R\partial q^2}-\frac{\partial v}{R\partial q}\right)\\
&+\frac{\partial^2(w+w_0)}{\partial x^2}\frac{\partial v}{\partial x}-\frac{v}{R^2}\left(\frac{\partial^2 u}{R\partial q^2}+\frac{\partial^2 v}{\partial x\partial q}+\frac{\partial(w+w_0)}{\partial x}\right)+\frac{\partial(w+w_0)}{R^2\partial q}\left(\frac{\partial^2 u}{R\partial q^2}+\frac{\partial w}{\partial x}+\frac{\partial^2 v}{\partial x\partial q}\right)\\
&+\frac{\partial w}{R^2\partial q}\frac{\partial w_0}{\partial x}+\frac{\partial v}{R\partial x}\left(\frac{w+w_0}{R}+2\frac{\partial v}{R\partial q}-\frac{\partial^2(w+w_0)}{R\partial q^2}+2\frac{\partial u}{\partial x}\right)\\
&+\frac{\partial(w+w_0)}{\partial x}\left(\frac{\partial^2 u}{R\partial x\partial q}+\frac{\partial^2 v}{\partial x^2}\right)-2\frac{\partial^2(w+w_0)}{R\partial x\partial q}\left(\frac{w}{R}+\frac{\partial v}{R\partial q}+\frac{\partial u}{\partial x}\right)-2\frac{\partial^2 w}{R^2\partial x\partial q}w_0.
\end{aligned}
\tag{2.9c}
$$

The middle surface strain-displacement relationships are still given by equations (2.7a-c). Equations (2.7a-c) and (2.9a-c) together are an improved version of the Novozhilov's nonlinear shell theory because approximations (2.6) have been used instead of neglecting terms in z and z^2 at this point of the derivation as done by Novozhilov (1953).

The elastic strain energy U_S of a circular cylindrical shell, neglecting s_z as stated by Love's first approximation assumptions, is given by (see Leissa 1973)

$$
U_S = \frac{1}{2}\int_0^{2p}\int_0^{L}\int_{-h/2}^{h/2}\left(s_x e_x + s_q e_q + t_{xq} g_{xq}\right) \mathrm{d}x\, R(1+z/R)\,\mathrm{d}q\,\mathrm{d}z, \tag{2.10}
$$

where h is the shell thickness, R is the shell middle radius, L is the shell length and the stresses s_x, s_q and t_{xq} are related to the strain for homogeneous and isotropic material ($s_z = 0$, case of plane stress) by

$$
s_x = \frac{E}{1-n^2}\left(e_x + n\, e_q\right), \tag{2.11a}
$$

$$
s_q = \frac{E}{1-n^2}\left(e_q + n\, e_x\right), \tag{2.11b}
$$

$$t_{xq} = \frac{E}{2(1+n)} g_{xq}, \tag{2.11c}$$

where E is the Young's modulus and n is the Poisson's ratio. By using equations (2.1, 2.10, 2.11), the following expression is obtained

$$\begin{aligned} U_S = {} & \frac{1}{2}\frac{E\,h}{1-n^2}\int_0^{2p}\int_0^{L}\left(e_{x,0}^2 + e_{q,0}^2 + 2n\,e_{x,0}e_{q,0} + \frac{1-n}{2}g_{xq,0}^2\right)\mathrm{d}x\,R\,\mathrm{d}q \\ & + \frac{1}{2}\frac{E\,h^3}{12(1-n^2)}\int_0^{2p}\int_0^{L}\left(k_x^2 + k_q^2 + 2n\,k_x k_q + \frac{1-n}{2}k_{xq}^2\right)\mathrm{d}x\,R\,\mathrm{d}q \\ & + \frac{1}{2}\frac{E\,h^3}{6R(1-n^2)}\int_0^{2p}\int_0^{L}\left(e_{x,0}k_x + e_{q,0}k_q + n\,e_{x,0}k_q + n\,e_{q,0}k_x + \frac{1-n}{2}g_{xq,0}k_{xq}\right)\mathrm{d}x\,R\,\mathrm{d}q + O(h^4), \end{aligned} \tag{2.12}$$

where $O(h^4)$ is a higher-order term in h and the last term disappears if z/R is neglected with respect to unity in equation (2.10), as it must be done for Donnell's and Sanders-Koiter theories. If this term is neglected, the right-hand side of equation (2.12) can be easily interpreted: the first term is the membrane (also referred to as stretching) energy and the second one is the bending energy. If the last term is retained, membrane and bending energies are coupled.

2.2 BOUNDARY CONDITIONS, MODE EXPANSION, KINETIC ENERGY AND EXTERNAL LOADS

The kinetic energy T_S of a circular cylindrical shell, by neglecting rotary inertia, is given by

$$T_S = \frac{1}{2} r_S\, h \int_0^{2p}\int_0^{L}\left(\dot{u}^2 + \dot{v}^2 + \dot{w}^2\right)\mathrm{d}x\,R\,\mathrm{d}q, \tag{2.13}$$

where r_S is the mass density of the shell. In equation (2.13) the overdot denotes a time derivative.

The virtual work W done by the external forces is written as

$$W = \int_0^{2p}\int_0^{L}\left(q_x u + q_q v + q_r w\right)\mathrm{d}x\,R\,\mathrm{d}q, \tag{2.14}$$

where q_x, q_q and q_r are the distributed forces per unit area acting in axial, circumferential and radial directions, respectively. Initially, only a single harmonic radial force is considered; therefore $q_x = q_q = 0$. The external radial distributed load q_r applied to the shell, due to the radial concentrated force $\hat{f}$, is given by

$$q_r = \hat{f}\, d(Rq - Rq_0)\, d(x - x_0)\cos(w t), \tag{2.15}$$

where w is the excitation frequency, t is the time, d is the Dirac delta function, $\hat{f}$ gives the radial force amplitude positive in z direction, x_0 and q_0 give the axial and angular positions of the point of application of the force, respectively; here, the point excitation is located at $x_0 = L/2$, $q_0 = 0$.

In order to reduce the system to finite dimensions, the middle surface displacements u, v and w are expanded by using approximate functions. The following boundary conditions are imposed at the shell ends, $x = 0, L$:

$$w = w_0 = 0, \tag{2.16a}$$

$$M_x = \frac{E h^3}{12(1-n^2)}\left(k_x + n\, k_q\right) = 0, \tag{2.16b}$$

$$\partial^2 w_0 / \partial x^2 = 0, \tag{2.16c}$$

$$N_x = \frac{E h}{1-n^2}\left(e_{x,0} + n\, e_{q,0}\right) = 0, \tag{2.16d}$$

$$v = 0, \tag{2.16e}$$

where M_x is the bending moment per unit length and N_x is the axial force per unit length; moreover, u, v and w must be continuous in q.

Past studies show that a linear modal base is the simplest choice to discretise the system. In particular, in order to reduce the number of degrees of freedom, it is important to use only the most significant modes. It is necessary to consider, in addition to the asymmetric mode directly driven into vibration by the excitation given in equation (2.15) (driven modes), (i) the orthogonal mode having the same shape and natural frequency but rotated by $p/(2n)$ (companion modes),

(ii) additional asymmetric modes, and (iii) axisymmetric modes. In fact, it has clearly been established that, for large-amplitude shell vibrations, the deformation of the shell involves significant axisymmetric oscillations inwards. According to these considerations, the displacements u, v and w are expanded by using the eigenmodes of the simply supported, empty shell (which are unchanged for the completely filled shell with open ends):

$$u(x,q,t)=\sum_{m=1}^{M_1}\sum_{j=1}^{N}\left[u_{m,j,c}(t)\cos(jq)+u_{m,j,s}(t)\sin(jq)\right]\cos(l_m x)+\sum_{m=1}^{M_2}u_{m,0}(t)\cos(l_m x), \qquad (2.17a)$$

$$v(x,q,t)=\sum_{m=1}^{M_1}\sum_{j=1}^{N}\left[v_{m,j,c}(t)\sin(jq)+v_{m,j,s}(t)\cos(jq)\right]\sin(l_m x)+\sum_{m=1}^{M_2}v_{m,0}(t)\sin(l_m x), \qquad (2.17b)$$

$$w(x,q,t)=\sum_{m=1}^{M_1}\sum_{j=1}^{N}\left[w_{m,j,c}(t)\cos(jq)+w_{m,j,s}(t)\sin(jq)\right]\sin(l_m x)+\sum_{m=1}^{M_2}w_{m,0}(t)\sin(l_m x), \qquad (2.17c)$$

where j is the number of circumferential waves, m is the number of longitudinal half-waves, $l_m = mp/L$ and t is the time; $u_{m,j}(t)$, $v_{m,j}(t)$ and $w_{m,j}(t)$ are the generalized coordinates that are unknown functions of t; the additional subscript c or s indicates if the generalized coordinate is associated to cos or sin function in q except for v, for which the notation is reversed (no additional subscript is used for axisymmetric terms). The integers N, M_1 and M_2 must be selected with care in order to obtain the required accuracy and acceptable dimension of the nonlinear problem.

Excitation in the neighbourhood of resonance of mode with m = 1 longitudinal half-wave and n circumferential waves, indicated as resonant mode (m, n) for simplicity, is considered. The minimum number of degrees of freedom that has been found to be necessary to predict the nonlinear response with good accuracy is 14 (Amabili 2003a). It is observed, for symmetry reasons, that the nonlinear interaction among linear modes of the chosen base involves the asymmetric modes (n > 0) having a given n value (*e.g.* the resonant mode), the asymmetric modes having a multiple of this value of circumferential waves ($k \times n$, where k is an integer), and axisymmetric modes (n = 0); asymmetric modes with different numbers of circumferential waves, that do not satisfy the relationship $k \times n$, have interaction only if their natural frequencies

are very close to relationship 1:1, 1:2 or 1:3 with the frequency of the resonant mode. Only modes with an odd m value of longitudinal half-waves can be considered for symmetry reasons (if geometric imperfections with an even m value are not introduced). In particular, asymmetric modes having up to three longitudinal half-waves ($M_1 = 3$, only odd m values) and modes having n, 2 ´ n, 3 ´ n and 4 ´ n circumferential waves have been considered in the numerical calculations. For axisymmetric modes, up to $M_2 = 9$ has been used (only odd m values).

The minimal expansion used in the numerical calculation (see Section 6) for excitation in the neighbourhood of resonance of mode ($m = 1$, n) is

$$u(x,q,t) = \left[u_{1,n,c}(t)\cos(nq) + u_{1,n,s}(t)\sin(nq)\right]\cos(l_1 x) + \sum_{m=1}^{2} u_{2m-1,0}(t)\cos(l_{2m-1}x), \tag{2.18a}$$

$$\begin{aligned} v(x,q,t) = &\sum_{k=1}^{2}\left[v_{1,kn,c}(t)\sin(knq) + v_{1,kn,s}(t)\cos(knq)\right]\sin(l_1 x) \\ &+\left[v_{3,2n,c}(t)\sin(2nq) + v_{3,2n,s}(t)\cos(2nq)\right]\sin(l_3 x), \end{aligned} \tag{2.18b}$$

$$w(x,q,t) = \left[w_{1,n,c}(t)\cos(nq) + w_{1,n,s}(t)\sin(nq)\right]\sin(l_1 x) + \sum_{m=1}^{2} w_{2m-1,0}(t)\sin(l_{2m-1}x). \tag{2.18c}$$

This expansion has 14 generalized coordinates (degrees of freedom) and guarantees good accuracy (Amabili 2003a).

The point excitation considered in equation (2.15) gives a non-zero contribution only to modes described by a cos function in angular direction, referred to as the driven modes, and to axisymmetric modes. The modes having the shape of the driven modes, but rotated by $p/(2n)$, *i.e.* with form described by sin function in angular direction q, are referred to as the companion mode.

It is extremely interesting to observe that in equations (2.18a) and (2.18c) only the resonant driven and companion modes plus the first and third axisymmetric modes are retained in the minimal expansion. For the circumferential displacement v, no axisymmetric modes are necessary. In fact, the first axisymmetric modes with radial displacement have axial displacement but zero circumferential displacement. However, it is necessary to retain in the

expansion of v terms with $2n$ circumferential waves and 3 longitudinal half-waves. It must be clarified that Donnell's nonlinear shallow-shell theory takes into account in-plane displacements by using the stress function, which has terms having twice the axial and angular wavenumbers of radial.

2.3 TRAVELLING WAVE RESPONSE

The presence of couples of modes having the same shape but different angular orientations, the first one described by $\cos(nq)$ (driven mode for the excitation given by equation (2.15)) and the other by $\sin(nq)$ (companion mode), in the periodic response of the shell leads to the appearance of travelling-wave vibration around the shell in the angular direction. This phenomenon is related to the axial-symmetry of the system and is a fundamental difference *vis-à-vis* linear vibrations.

Away from resonance, the companion mode solution disappears ($u_{m,n,s}(t) = v_{m,n,s}(t) = w_{m,n,s}(t) = 0$) and the generalized coordinates are nearly in phase or in opposite phase. The presence of the companion mode in the shell response leads to the appearance of a travelling wave and to more complex phase-relationships among the generalised coordinates. The mode shapes are represented by equation (2.18). Let us consider for simplicity only radial motion, which is predominant for shells not particularly long. Supposing that the response of the driven and companion modes have the same frequency of oscillation of the excitation, *i.e.* $w_{1,n,c}(t) = \bar{w}_{1,n,c}\cos(w\,t + q_1)$ and $w_{1,n,s}(t) = \bar{w}_{1,n,s}\cos(w\,t + q_2)$, and considering the other coordinates having smaller amplitude, equation (2.18c) can be rearranged as

$$\begin{aligned} w = \Big\{\Big[\bar{w}_{1,n,c}\cos(w\,t + q_1) + \bar{w}_{1,n,s}\sin(w\,t + q_2)\Big]\cos(nq) \\ + \bar{w}_{1,n,s}\sin(nq - w\,t - q_2)\Big\}\sin(p\;x/L) + \mathrm{O}(\bar{w}_{1,n,c}^2, \bar{w}_{1,n,s}^2, \bar{w}_{1,0}, \bar{w}_{3,0}\ldots), \end{aligned} \tag{2.19}$$

where $\bar{w}_{1,n,c}$ and $\bar{w}_{1,n,s}$ are the amplitudes of driven and companion modes, respectively, q_1 and q_2 are the phases and O is a small quantity. Equation (2.19) gives a combined solution consisting

of a standing wave and a travelling wave of amplitude $\bar{w}_{1,n,s}$ and moving in angular direction around the shell with angular velocity *w/n*. The resulting standing wave is given by the sum of the two standing waves, one of amplitude $\bar{w}_{1,n,c}$ and the second of amplitude $\bar{w}_{1,n,s}$, having the same circular frequency *w* and the same shape, but having a phase difference of $q_2 - q_1 - p/2$. When $q_2 - q_1 \cong p/2$, as it is generally observed in calculations and experiments, the amplitude of the resulting standing wave is almost $\bar{w}_{1,n,c} - \bar{w}_{1,n,s}$. In case of zero phase difference, *i.e.* $q_2 - q_1 = 0$, no travelling wave arises.

2.4 RESULTS AVAILABLE IN LITERATURE

Here numerical results available in the literature are shown. Calculations have been performed for a simply supported, empty shell studied by Amabili (2003a), Chen and Babcock (1975), Pellicano, Amabili and Païdoussis (2002), Varadan *et al.* (1989) and Ganapathi and Varadan (1995). Dimensions and material properties are: L = 0.2 m, R = 0.1 m, h = 0.247 mm, E = 71.02 × 10^9 Pa, r = 2796 kg/m^3 and n = 0.31. A harmonic force excitation $\bar{f} = 0.0785$ N and modal damping $z_{1,n} = 0.0005$ are assumed. Only the fundamental mode (n = 6, m = 1) is investigated; it has a natural frequency of 555.9 Hz. The shell response is shown in Figure 2.1, where responses calculated by different authors are compared, namely: Amabili (2003a), who used Donnell's nonlinear shallow-shell theory with a mode expansion involving 36 degrees of freedom; Pellicano, Amabili and Païdoussis (2002), who used Donnell's nonlinear shallow-shell theory with a mode expansion involving 23 degrees of freedom; response calculated by Chen and Babcock (1975), who used the perturbation method to solve the nonlinear equations obtained by Donnell's nonlinear shallow-shell theory; backbone curves (indicating only the resonance, *i.e.* the peak of the response) computed by Varadan, Prathap and Ramani (1989), who used a simple three-mode expansion and Donnell's nonlinear shallow-shell theory, and by Ganapathi and Varadan (1996), who used the finite element method based on Novozhilov's shell theory. Results

of Amabili are more recent and they are intermediate between those obtained by Pellicano, Amabili and Païdoussis (2002) and those obtained by Ganapathi and Varadan (1996) and are close to those of Chen and Babcock (1975). This can be considered a good validation of the model proposed by Amabili (2003a) and described in the sub-section 2.2.

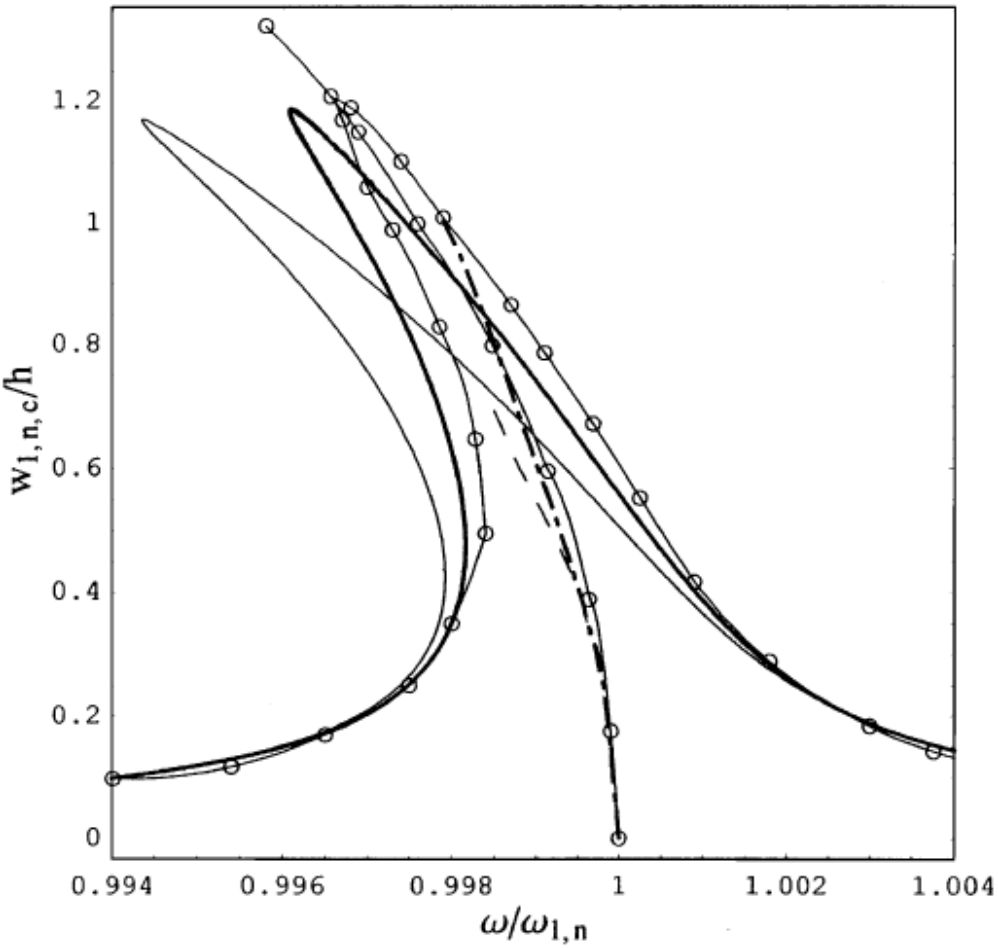

Figure 2.1. Response amplitude - frequency relationship for the fundamental mode of the perfect, empty shell studied by Chen and Babcock (1975); branch "1" only. Only the generalized coordinate $w_{1,n,c}(t)$ is reported. ——, Amabili 2003a (Donnell's theory, Lagrangian approach); ——, backbone curve and shell response from Pellicano *et. all* 2002 (Donnell's nonlinear shallow-shell theory); —○—, backbone curve from Chen and Babcock (1975); – –, results from Varadan *et. all* (1989); —·—, backbone curve from Ganapathi and Varadan (1996).

Amabili (2003a) studied the response of the simply-supported circular cylindrical shell subjected to harmonic point excitation of 2N applied in the middle of the shell in the neighbourhood of the lowest (fundamental) resonance $w_{1,n} = 2p \times 215.3$ rad/s, corresponding to mode (m = 1, n = 5), result is given in Figure 2.2; only the principal (resonant) coordinates, corresponding to driven and companion modes, are shown for brevity. The Flügge-Lur'e-Byrne nonlinear theory of shells has been used in the calculation, with modal damping $z_{1,n} = 0.001$ ($z_{1,n} = z_{1,n,c \text{ or } s}$). All the calculations have been performed by using an expansion involving 16 generalized coordinates, that are the ones given in equations (2.18) with the additional term $\left[u_{1,2n,c}(t)\cos(2nq) + u_{1,2n,s}(t)\sin(2nq)\right]\cos(l_1 x)$ in equation (2.18a).

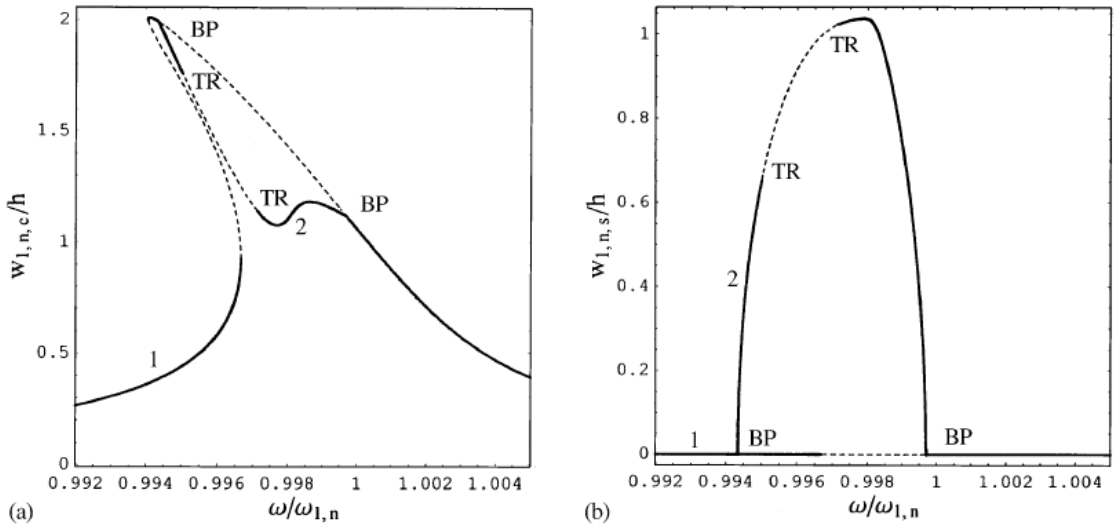

Figure 2.2. Response amplitude - frequency relationship for the fundamental mode of the perfect, empty shell; $V_{1,n} = 0.001$; Flügge-Lur'e-Byrne theory. Only resonant generalized coordinates are reported. (a) Amplitude of $w_{1,n,c}(t)$, driven mode; (b) Amplitude of $w_{1,n,s}(t)$, companion mode. 1, branch "1"; 2, branch "2"; BP, pitchfork bifurcation; TR, Neimark-Sacher bifurcation (Amabili 2003a).

The solution initially presents a single branch "1" with a folding and a typical softening type behaviour and corresponds to a driven mode vibration with zero amplitude of the

companion mode. Branch “1” presents a pitchfork bifurcation around the peak of the response where branch “2” arises and where branch “1” loses stability. Branch “2” is the solution with participation of both driven and companion modes, giving a standing wave plus a travelling wave response around the shell. Branch “2” loses stability at a Neimark-Sacker (torus) bifurcation where amplitude-modulations of the solution arise; modulations end at a second Neimark-Sacker bifurcation. The response between the two Neimark-Sacker bifurcations is quasi-periodic and the Poincaré map shows a limit cycle, as observed by Amabili *et al*. (2000a) by using the Donnell’s shallow-shell theory. Branch “2” ends at a second pitchfork bifurcation where it merges with branch “1” that regains stability. A qualitative similar behaviour has been found in previous studies based on different shell theories and different solution methods; see *e.g*. Chen and Babcock (1975), Amabili *et. all* (1998), Ginsberg (1973).

The response of the shell in the time domain is given in Figures 2.3 and 2.4 for excitation frequency $w / w_{1,n}$ = 0.998 (stable response on branch “2”) and 0.9969 (unstable response on both branches “1” and “2”), respectively. In Figures 2.3(a-c) the generalized coordinates associated with driven, companion and first axisymmetric modes are reported. It is clearly shown that the phase difference between driven and companion modes is $q_2 - q_1 \cong p/2$, giving a travelling wave response. The relative amplitudes among the generalized coordinates $u_{1,n,c/s}$, $v_{1,n,c/s}$ and $w_{1,n,c/s}$ associated with driven and companion modes are almost the same of the one observed for linear free vibrations (eigenvectors of the linear solution). Only very small variations of the relative amplitudes are observed for these modes in the neighbourhood of the resonance. However, this is not true for all the other generalized coordinates. When the excitation has a frequency close to the resonance of mode (*m*=1, *n*), results show that the generalized coordinates associated with driven and companion modes (*m*=1, *n*) have the same frequency of the excitation. The coordinates associated with modes (*m*=1, 2*n*) and (*m*=3, 2*n*) and all the coordinates associated to axisymmetric modes, as shown in Figure 2.3(c), have twice the frequency of the excitation; the coordinates associated with modes (*m*=3, *n*), (*m*=1, 3*n*) and

(*m*=3, 3*n*) have three times the frequency of the excitation. Figure 2.3(c) also shows a negative (inward) axisymmetric oscillation of the shell associated to large-amplitude asymmetric vibration; this is a characteristics of nonlinear vibrations of circular cylindrical shells. Figures 2.4(a, b) show that the response has amplitude-modulations (quasi-periodic) between the two Neimark-Sacher bifurcations, where no stable solution are indicated in Figure 2.2.

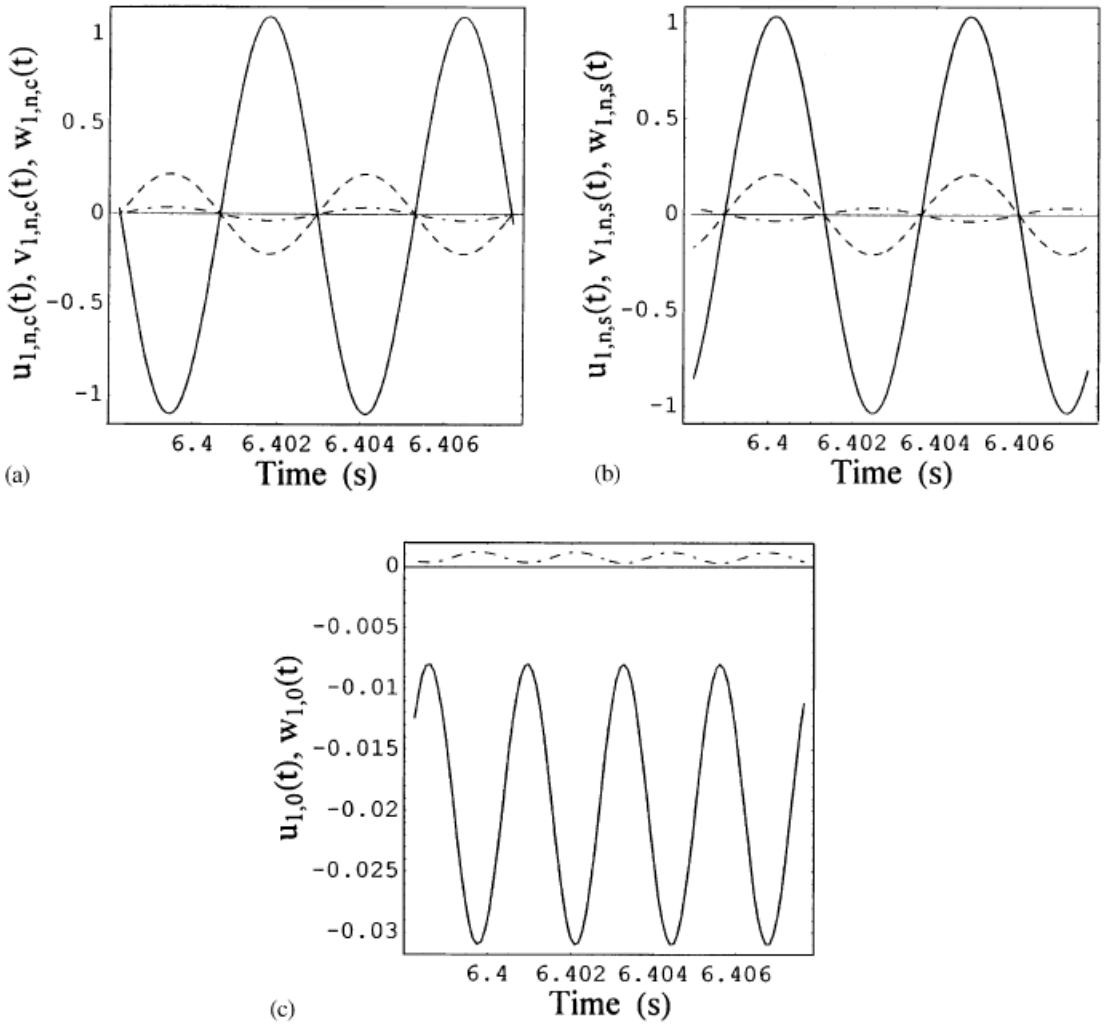

Figure 2.3. Time response of the shell in case of travelling wave response; $w/w_{1,n} = 0.998$; Flügge-Lur'e-Byrne theory. (a) Generalized coordinates associated with the driven mode; ——, $w_{1,n,c}(t)$; – –, $v_{1,n,c}(t)$; – · –, $u_{1,n,c}(t)$. (b) Generalized coordinates associated with the companion mode; ——, $w_{1,n,s}(t)$; – –, $v_{1,n,s}(t)$; – · –, $u_{1,n,s}(t)$. (c) Generalized coordinates associated with the first axisymmetric mode; ——, $w_{1,0}(t)$; – · –, $u_{1,0}(t)$ (Amabili 2003a).

Now that the nonlinear response of the shell in the spectral neighbourhood of the fundamental resonance has been understood, it is interesting to compare results obtained by using the same approach and different shell theories. In Figure 2.5 branch "1" of the solution has been computed with the present Lagrangian approach by using (i) Donnell's, (ii) Sanders-Koiter, (iii) Flügge-Lur'e-Byrne and (iv) Novozhilov's nonlinear shell theories. Results obtained by using Donnell's nonlinear shallow-shell theory, computed by using the mode expansion given by equation (19c) and the approach reported in Amabili *et. all* (1999b,c) and Amabili (2003c), are also given for comparison. For this case, results from Novozhilov's nonlinear theory of shell are practically coincident with those of Flügge-Lur'e-Byrne theory and therefore are not reported in Figure 2.5.

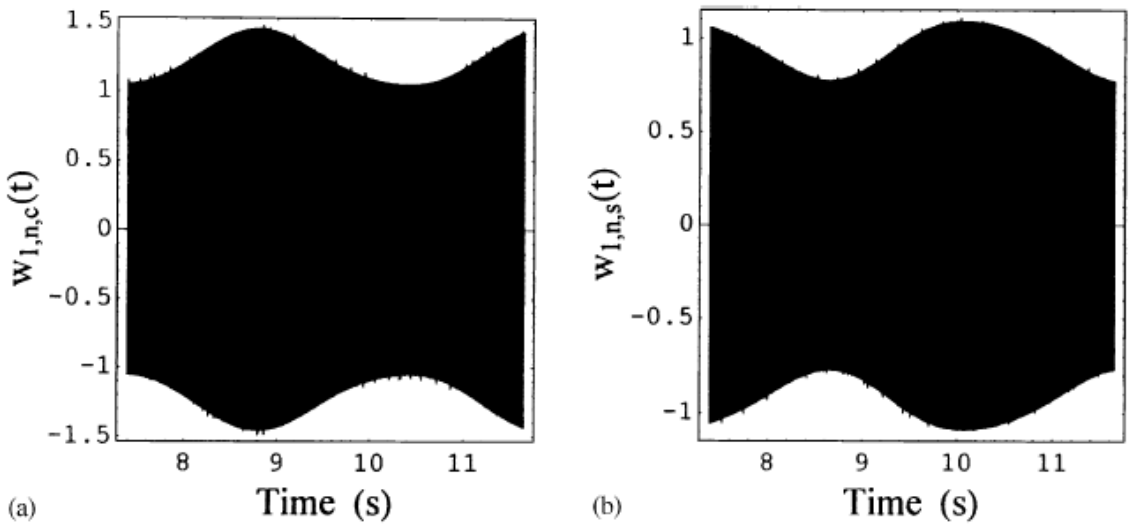

Figure 2.4. Time response of the shell in case of amplitude-modulations (limit cycle); $w/w_{1,n} = 0.9969$; Flügge-Lur'e-Byrne theory. (a) Generalized coordinate $w_{1,n,c}(t)$ associated with the driven mode. (b) Generalized coordinate $w_{1,n,s}(t)$ associated with the companion mode.

Moreover, differences between Flügge-Lur'e-Byrne and Sanders-Koiter theories are absolutely negligible. For practical applications the difference between Flügge-Lur'e-Byrne and Donnell's (present Lagrangian approach) theories can be considered very small as well. However, although all the results obtained by using the present Lagrangian approach are very close to each other,

differences with Donnell's nonlinear shallow-shell theory are quite significant; in particular, an excessive softening nonlinearity is predicted by Donnell's nonlinear shallow-shell theory. In fact, this theory neglects in-plane inertia, which plays a relevant role in axisymmetric modes. In this case, Donnell's nonlinear shallow-shell theory gives a wrong evaluation of the linear natural frequency of the first axisymmetric mode, and it explains the difference with all the other theories. It is interesting to observe that the mode investigated has n = 5 circumferential waves, which is a number almost at the limit of applicability of the Donnell's shallow-shell theory.

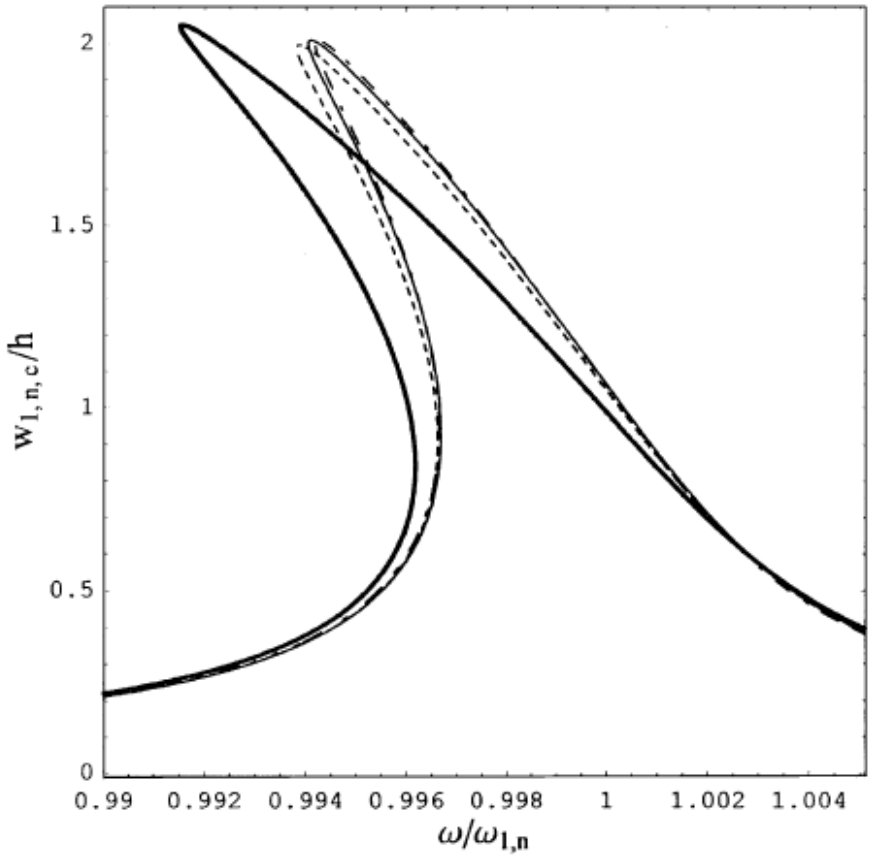

Figure 2.5. Response amplitude - frequency relationship for the fundamental mode of the perfect, empty shell; branch "1" only; $V_{1,n} = 0.001$. Only the generalized coordinate $w_{1,n,c}(t)$ is reported. ——, Donnell's nonlinear shallow-shell theory; – –, Donnell's theory (Lagrangian approach); – · –, Sanders-Koiter theory; ——, Flügge-Lur'e-Byrne theory (coincident with Novozhilov) (Amabili 2003a).

3. EXPERIMENTAL RESULTS AVAILABLE IN LITERATURE

3.1 SIMPLY SUPPORTED SHELLS

3.1.1 EXPERIMENTAL SETUP

Tests have been conducted by Amabili (2003c) on a commercial circular cylindrical shell made of stainless steel and having a longitudinal seam weld. The dimensions and material properties of the shell are: L=520mm, R=149.4mm, h=0.519mm, E=1.98x10^{11}Pa, ρ=7800kg/m^3, ρ_F=1000kg/m^3 and ν=0.3. Two stainless-steel annular plates of external and internal radius of 149.4 and 60mm, respectively, and thickness 0.25mm have been welded to the shell ends to approximate the simply supported boundary condition of the shell. A rubber disk 1 mm thick has been glued to each of these annular end plates (see Fig. 3.1). The tank has been tested empty and completely filled with water. The zero pressure boundary condition is well approximated by the flexible rubber disks at the shell ends. Two small pipe fittings were welded onto one of the end plates in such a position that they do not affect shell vibrations; they are used for filling the specimen with water.

The shell has been suspended horizontally with cables to a box-type frame and has been subjected to (i) burst-random excitation to identify the natural frequencies and perform a modal analysis by measuring the shell response on a grid of points, (ii) harmonic excitation, increasing or decreasing by very small steps the excitation frequency in the spectral neighborhood of the lowest natural frequencies to characterize non-linear responses in presence of large-amplitude vibrations. The excitation has been provided by an electrodynamical exciter (shaker), model LDS V406 with power amplifier LDS PA100E, connected to the shell by a stinger glued in a position close to the middle of the shell, specifically at x=251mm. A piezoelectric force transducer, model B&K 8200, of mass 21g, placed on the shaker and connected to the shell by a stinger, measured the force transmitted. The shell response has been measured by using two accelerometers, model B&K 4393, of mass 2.4g. For all non-linear tests, the two accelerometers have been glued close to the middle of the shell length, specifically at x=264mm, at different

angular positions corresponding to an antinode and a node of the excited driven mode to measure the non-linear response. The time responses have been measured by using the Difa Scadas II front-end connected to a HP c3000 workstation with the software CADA-X of LMS for signal processing and data analysis; the same front-end has been used to generate the excitation signal. The CADA-X closed-loopcontrol has been used to keep constant the value of the excitation force for any excitation frequency, during the measurement of the non-linear response.

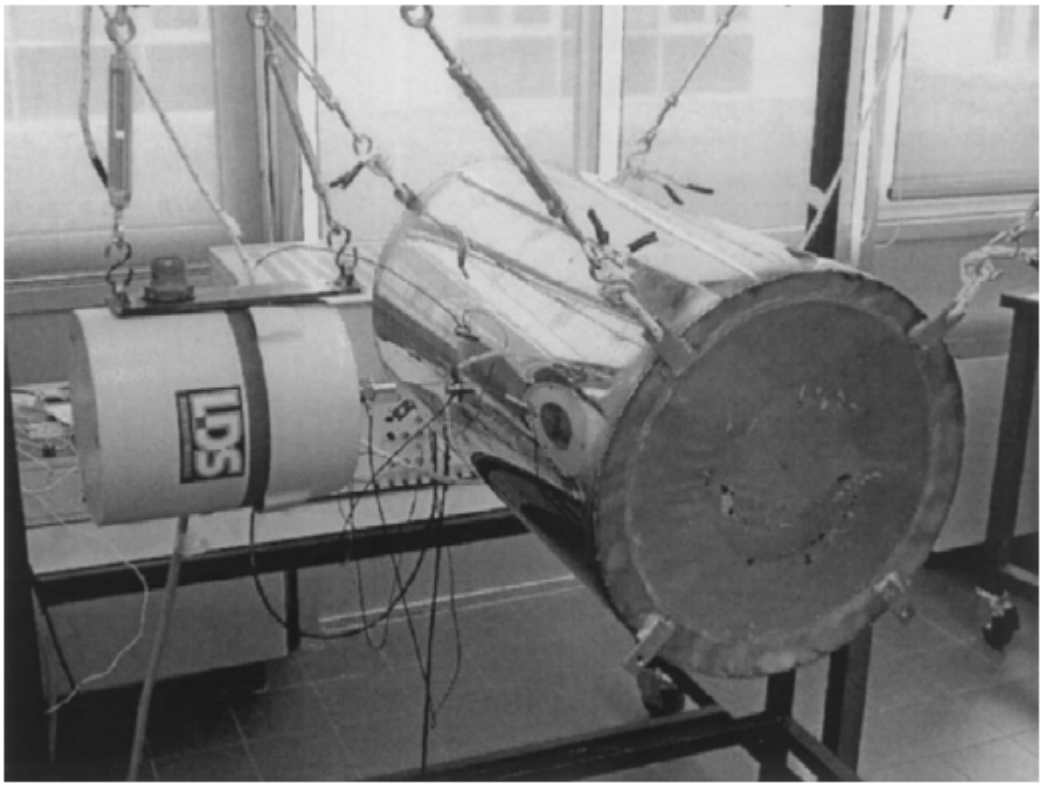

Figure 3.1. Photograph of the experimental setup (Amabili 2003c)

3.1.2 GEOMETRIC IMPERFECTIONS

The shell surface of the tested shell has been measured on a lathe by using a dial gauge on a grid of 100 points, i.e., five equidistant circumferences and 20 positions around each circumference. Moreover, a fine grid of additional 68 points has been measured around the longitudinal weld where small deformations of the shell are present. Fig. 3.2(a) shows the geometry of the measured central circumference with the magnitude of detected imperfection

magnified by a factor 10; in particular, both measured points and their associated Fourier interpolation are given. The origin of the angular co-ordinate O is taken at the excitation point. The geometric imperfections in the central circumference are mainly localized around the weld at θ=63°, as shown in Fig. 3.2(a), with a protuberance of about 0.15mm. Geometric imperfections in the longitudinal direction are plotted in Fig. 3.2(b) at θ=60°, i.e., 3° ahead of the longitudinal welding. Results show that deformations are mainly concentrated at the longitudinal weld and at the shell ends, where the annular end plates have been welded to the shell.

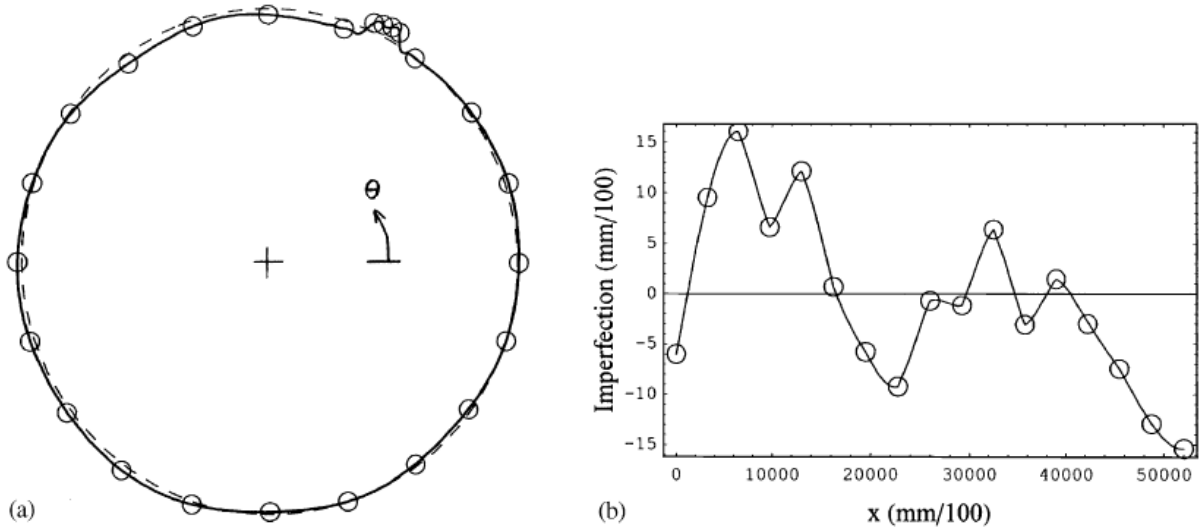

Figure 3.2. Geometric imperfections of the shell surface: (a) central circumference (imperfections magnified l0 times); (b) line at θ= 60°. O, measured point; —, Fourier interpolation; - - -, perfect geometry (Amabili 2003c).

3.1.3 MODAL ANALYSIS (LINEAR RESULTS)

The frequency response functions (FRFs) have been measured between 100 response points and one single excitation point. Both excitation force and measured responses have been in the radial direction. The response points have been located on a grid of five equidistant circumferences and 20 positions around each circumference; this allows for detection of mode shapes with up to 10 circumferential waves. The experimental modal analysis has been performed by using the software CADA-X 3.5b of LMS and burst-random excitation with the following parameters: burst length, 55% for empty shell, 70% for water-filled shell; frequency

resolution 0.15 Hz; 10 averages; uniform windows. The FRFs have been estimated using the H_V technique. The modal parameters have been estimated by using the time domain, least-squares complex exponential technique for the water-filled shell and the frequency domain, direct parameter identification technique for the empty shell. The analysis of the experimental data has been validated by using the modal assurance criterion and the modal phase collinearity.

Due to the axial symmetry of the shell, each asymmetric mode presents two poles in the FRFs associated with orthogonal modes having the same shape but circumferentially rotated by $\pi/(2n)$, i.e., cos(nθ) and sin(nθ) modes. However, due to the small imperfections of the shell, the two frequencies are not coincident but very close. Many of these couple of modes have been experimentally detected in the low-frequency range.

The sum of the measured FRFs is shown in Fig. 3.3 with identification of natural modes.

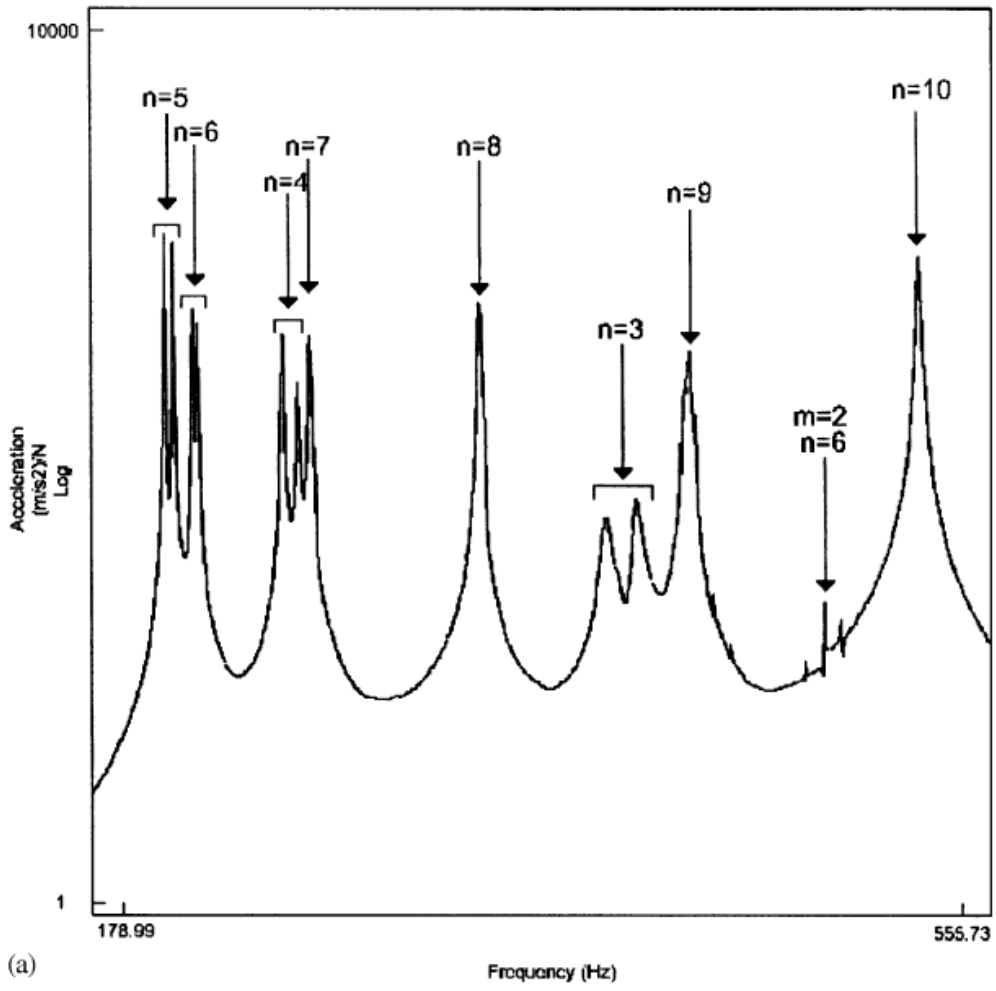

Figure 3.3. Sum of measured FRFs with identification of natural modes (Amabili 2003c).

The measured natural frequencies are presented and compared in Fig. 3.4 to theoretical calculations with the linear Flugge's theory of shells.

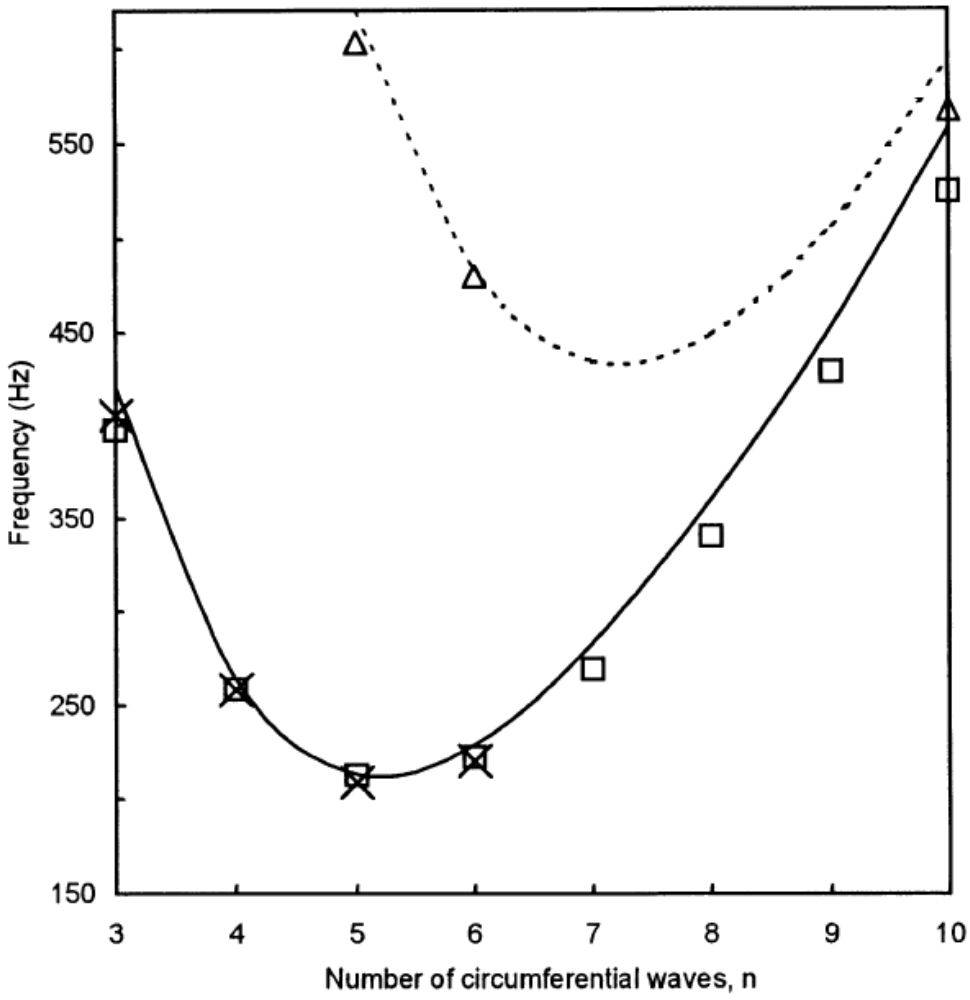

Figure 3.4. Theoretical and experimental natural frequencies. Theoretical results: —, *m*=1; ---, *m*=2. Experimental results: □, *m*=1; x , *m*=1, 2nd mode; Δ, *m*=2 (Amabili 2003c).

In Fig. 3.5 eighth experimental mode shapes with one longitudinal half-wave (m=l) and different number of circumferential waves *n* are shown. The dashed line represents the 2nd mode, when a couple of modes has been detected. The fundamental mode is (n=5, *m*=l). Theoretical and experimental results are in good agreement both in natural frequencies and mode shapes. This assures that the experimental boundary conditions approximate simple supports with good accuracy.

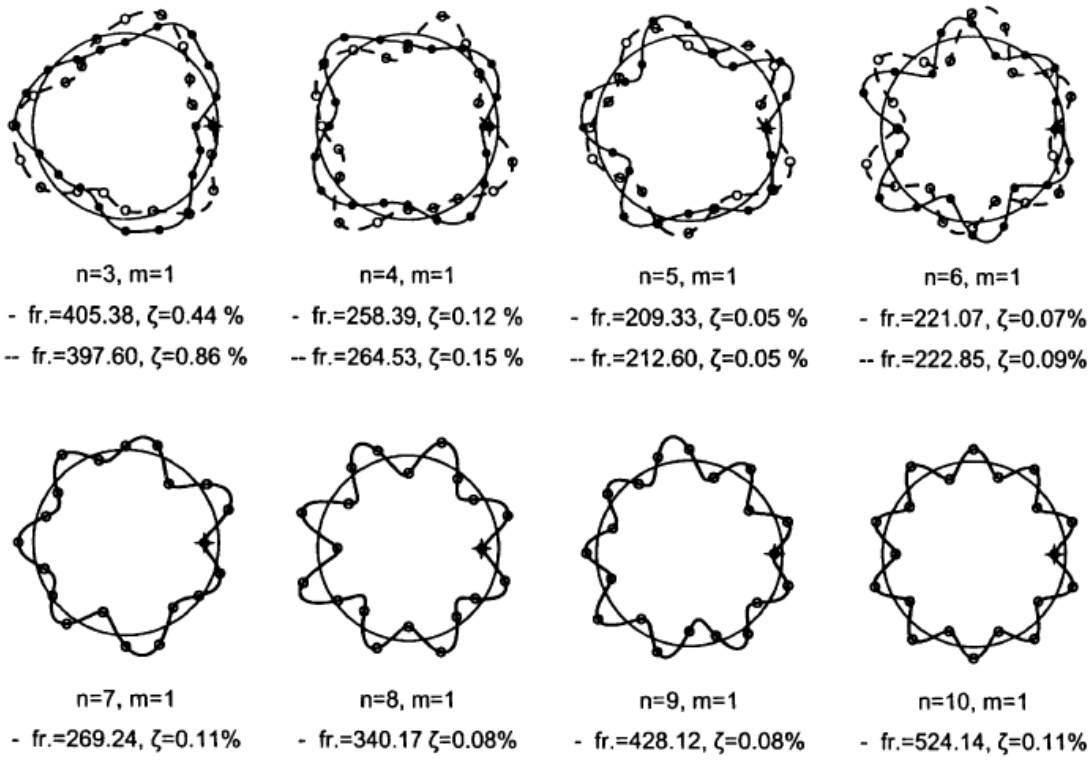

Figure 3.5. Experimental modes. O , ● measured points; —,---- interpolating lines from Fourier analysis; + driving point (Amabili 2003c).

3.1.4 COMPARISON OF EXPERIMENTAL AND THEORETICAL RESULTS

The measured accelerations have been converted to displacements, dividing by the excitation circular frequency squared, and have been plotted in Fig. 3.6 together with the theoretical responses for the case with a force level of 0.75N; normalization of frequency with respect to $\omega_{1,n}$=212.6x2π has been performed. When comparing filtered experimental results to theoretical results only co-ordinates $A_{1,n}(t)$ and $B_{1,n}(t)$ must be considered because the others, which have higher frequency, are eliminated by the filter. The theoretical curves have been computed by including the geometric imperfection, which had the value needed to reproduce the frequency difference between the two modes (n=5, m=1); this value was not too far from the geometric imperfection with 10 circumferential waves measured on the central circumference. The modal damping used to calculate the theoretical curves have been identified by matching the

maximum value of the measured response. The agreement between the theoretical curves and the experimental results is particularly good.

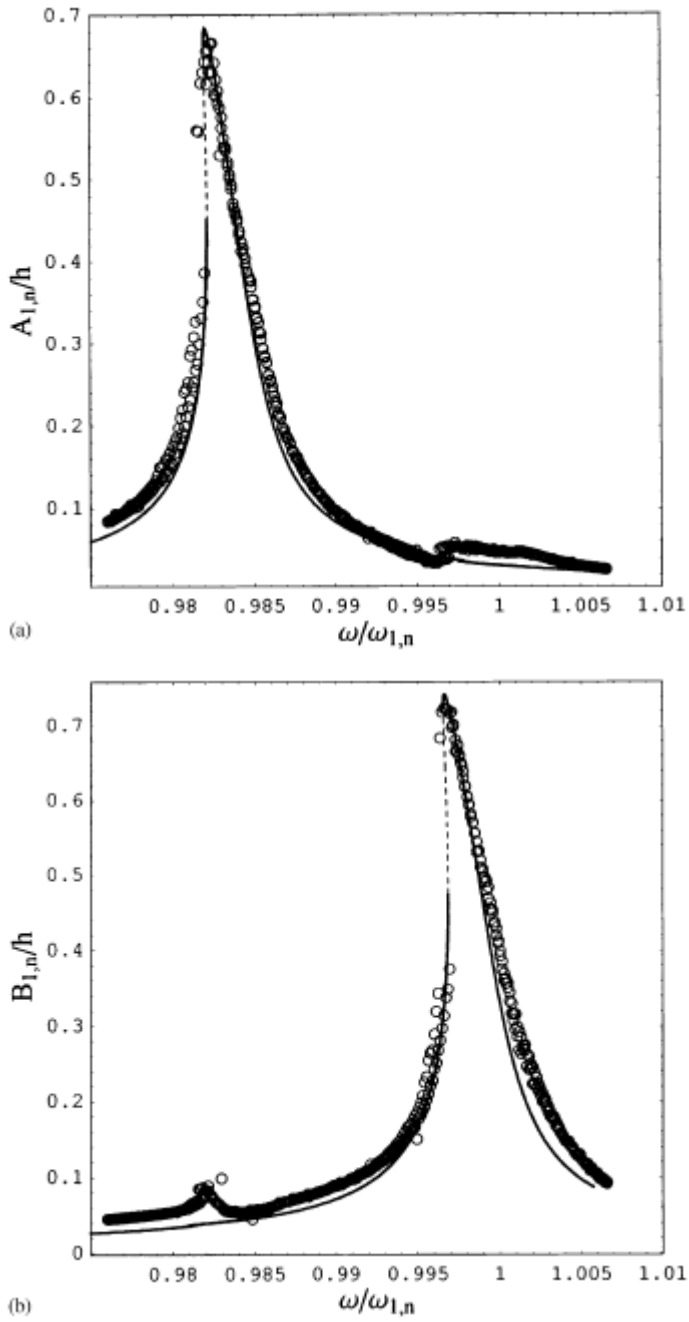

Figure 3.6. Response amplitude–frequency relationship for the fundamental mode; force 0.75 ○,experimental data; ——, stable theoretical solutions; – – –, unstable theoretical solutions: (a) displacement/h from the 1st accelerometer; (b) displacement/h from the 2nd accelerometer. (Amabili 2003c).

3.2 CLAMPED-FREE SHELLS

These experimental studies were carried out by Chiba (1993a) on the non-linear hydroelastic vibrations of a cantilever circular cylindrical tank. They present results for an empty tank. In the studies, two polyester test cylinders were used with radius R=240mm, thickness h=0.254mm, and length L=480 and 160mm (L/R = 2.0 and 2/3, respectively). The non-linearity of the response of the flexible wall was investigated. It was found that the degree of non-linearity depends on the vibration mode, i.e. on the circumferential wave number and the axial wave number of the shell, as well as on the length of the tank. Travelling responses were observed in which a response with circumferential wave number N moved around in a circumferential direction.

3.2.1 TEST TANK

Test cylinders with radius R=240mm were made of polyester sheet with thickness h=0.254mm by lap-jointing along the longitudinal seam and bonding an acrylic end plate with thickness 14mm along one edge for a clamped-free tank. The lengths of the tanks L were chosen so that the aspect ratios L/R were 2/3 and 2.0. The thickness ratio was R/h = 945. The material properties of the polyester sheet are: E = 4.65×10^9 Pa (in-roll) and E = 6.96×10^9 Pa (out-of-roll), r = 1400 kg/m^3 and n = 0.38.

At a lap-jointed seam of the shell, each side end of the wall was cut into a triangular cross section to decrease the influence of the seam in the circumferential direction, and bonded in the longitudinal direction with two-component epoxy adhesive. The width of the seam was 8-9 mm. At the lower end of the shell, a silicone-type adhesive was used to bond the shell wall and the end plate, and the clamped end of the wall was firmly fixed by an outer ring made of brass which was 8mm wide and 1.5mm thick. The capacity of the cylinders was tested by filling them with water. The strength of the seam and the clamped boundary at the bottom were checked and the results were satisfactory.

3.2.2 TEST EQUIPMENT

A schematic diagram of the test set-up filled with liquid is shown in Fig. 1. In the figure, a signal from an exciter control (1) is sent to a pair of exciters (2 and 2') which are placed face to face with the tank (3) between them. The signal then passes through two phase regulators (4 and 4') and two amplifiers (5 and 5'). The test tank is excited by either in-phase or out-of-phase excitation, which means that the natural mode is excited with either an even or an odd circumferential wave number. With this technique one can excite each natural mode separately, and this is an effective method for a vibration system in which natural frequencies are as closely distributed as they are in a cylindrical tank system (Chiba *et. all* 1985).

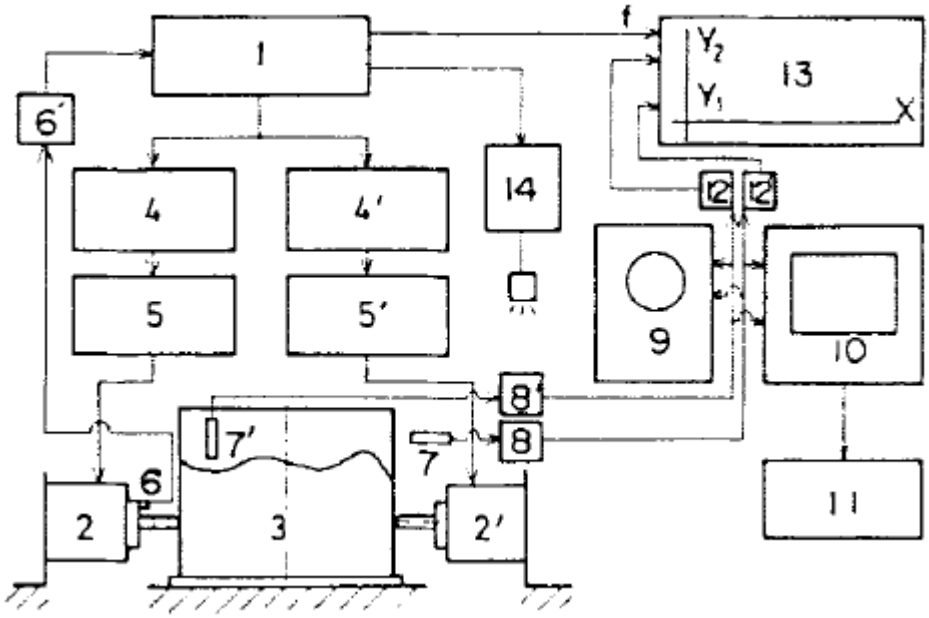

Figure 3.7. Schematic diagram of the test set-up: (1) exciter control, B & K 1050; (2,2′) exciters, B & K 4808; (3) test tank; (4,4′) level phase controllers, B & K 5899; (5, 5′) power amplifier, B & K 2712; (6) accelerometer, B & K 4393; (7) optical sensor probe, ELTROTEC FAR-P-A1; (7') optical sensor probe, ELTROTEC FAR-P-A3; (8,8') optical sensor, ELTROTEC CLS-K-10; (9) oscilloscope, PHILIPS PM 3234; (10) FFT analyzer, SCHLUMBERGER SI 1220; (11) *X*-*Y* plotter. H.P. 7475A; (12,12′) AC-DC converter, PHILIPS PM 5171; (13) *X*-*Y* recorder, PHILIPS PM 8132; (14) stroboscope, B & K 4913 (Chiba 1993a).

In order to excite the tank wall with a constant harmonic displacement amplitude, the output of an accelerometer (6), which measures the displacement of the exciter head, is fed back to the exciter control.

The responses of the tank wall and the liquid free surface are measured by the optical sensors (7) and (7'), respectively. Each sensor probe can be moved along the tank wall and the liquid free surface in both the circumferential and the longitudinal or radial directions. The output of the two amplifiers (8 and 8') can be monitored by an oscilloscope (9), and the frequency components of these signals are analyzed by an FFT analyzer (10). The output of the analyzer is recorded on a plotter (11). Further, rms values of each response can be obtained by using two AC-DC converters (12 and 12'), and the frequency response curves are recorded on an X-Y recorder (13). The stroboscope (14) is a powerful instrument for recognition of the travelling responses observed in the experiment. The experimental layout is shown in Fig. 3.8.

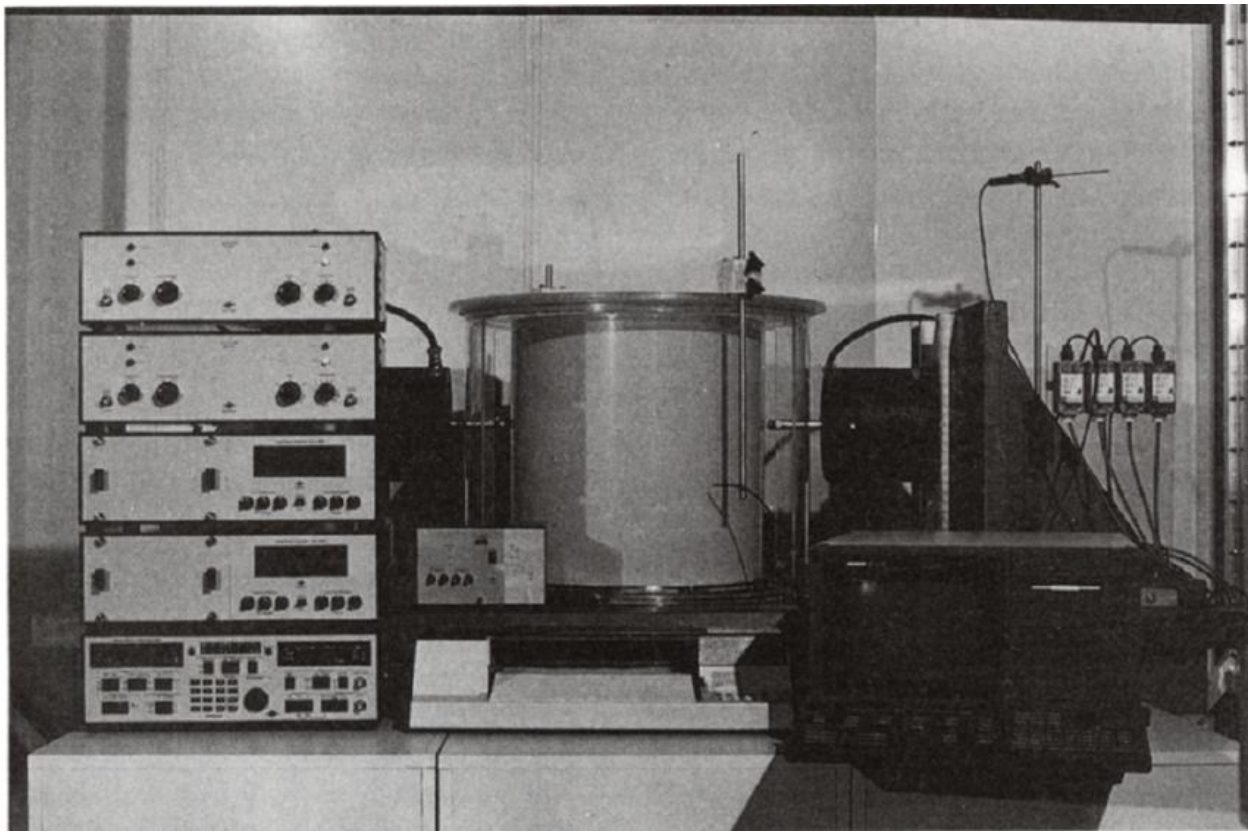

Figure 3.8. Overall view of the test set-up (Chiba 1993a).

3.2.3 TEST PROCEDURE

In the experiment, the frequency response curves of a liquid free surface or a flexible wall under a constant sinusoidal displacement excitation were measured to determine the coupled natural frequencies and to investigate the non-linearity of the system. The location of the excitation point in the longitudinal direction of the tank was located at 110mm (x/L=0.23) for the test tank with L=480mm, and at 35mm (x/L=0.22) for the test tank with L=160mm. The contacting force between an exciter rod and a flexible wall was kept small and almost constant at each liquid height level by changing the distance between the flexible wall and the exciter.

The excitation frequency was swept down at a rate of 0.02 Hz when measuring only the response of the wall. When measuring both the wall and the liquid free surface responses, the excitation frequency was swept down at a rate of 0.015 Hz.

3.2.4 TEST RESULTS

Before proceeding to the investigation of the non-linearity of the shell wall response, it was important to check the linear natural frequencies of the test tanks used in the experiment and compare these with the analytical results (Chiba *et. all* 1984). The analysis is based on the Donnell equation, and both the axisymmetric deformation of the wall due to the static pressure and the liquid free surface conditions are taken into consideration. The precision of the analysis had been shown to be excellent by comparing it with the corresponding experimental results (Chiba *et. all* 1985).

The linear natural frequencies measured in the experiment for the test tanks with L=480 and 160 mm are shown with the theoretical results in Fig. 3.9(a) and (b), respectively. In the figure, the numerical results calculated using two kinds of Young's modulus, i.e. the in-roll and out-of-roll directions are shown by solid and dotted lines respectively. These figures show good agreement with theoretical results in which

Young's modulus for the in-roll direction was used, and experimental results on the linear natural frequency.

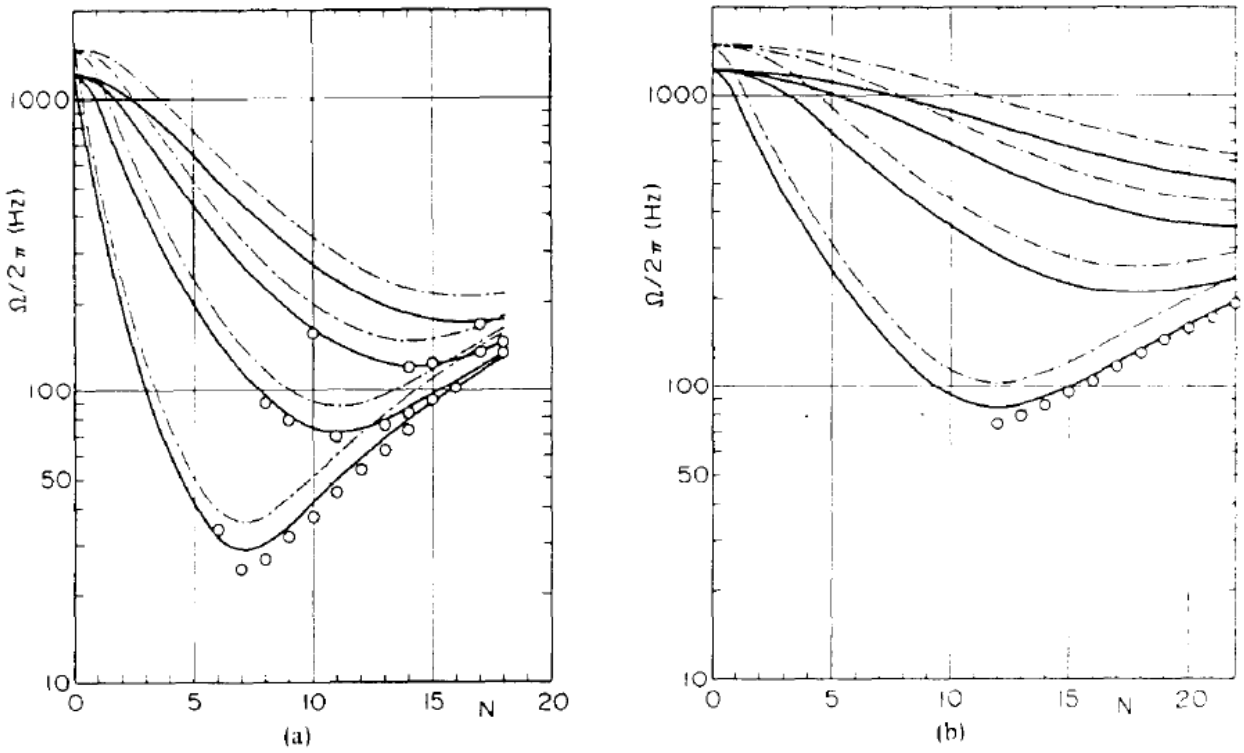

Figure 3.9. Linear natural frequency: (−·−) numerical results; (○) experimental results. (a) L=480mm, (b) L=160mm (Chiba 1993a).

The non-linearity of the response, i.e. the amplitude dependency of the natural frequency, was studied by measuring the frequency response curves of the wall with different excitation amplitudes, and measuring backbone curves by following each peak of the response. For example, the frequency response curves measured at $\xi=x/L=0.95$ of the $(m,N)=(1,7)$ mode of the tank with L=480mm are shown in Fig. 3.10(a). In this case, the excitation amplitude Δ_ε =0.0125, 0.025, 0.05, 0.1, 0.2, 0.4, 0.6…1.2 mm, and the excitation frequency was swept down at a constant rate of 0.02 Hz. An approximate backbone curve is obtained from the frequency response curves by following each peak of the response, and is presented in Fig. 3.10(b). In the figure, the abscissa is the normalized excitation frequency with respect to a small amplitude linear natural frequency $\Omega 2\pi$ while the ordinate is the rms value of the normalized amplitude with

shell thickness *h*. Hereafter, the measured backbone curves are represented in this form to make it easy to see the non-linearity of the response. From the figure, one can see that the response has a softening non-linearity, i.e. the natural frequency decreases with increasing vibration amplitude.

To study the non-linearity of the response, the measuring point must be suitably selected on the object surface. If the measuring point is near the node of the vibration mode, the measured amplitude is not the maximum amplitude of the vibration mode and the backbone curve obtained has an overlooked non-linearity rather than the real one. Therefore, in the experiment, the measuring point was selected at the point of maximum displacement of the mode in the circumferential and axial directions of the shell.

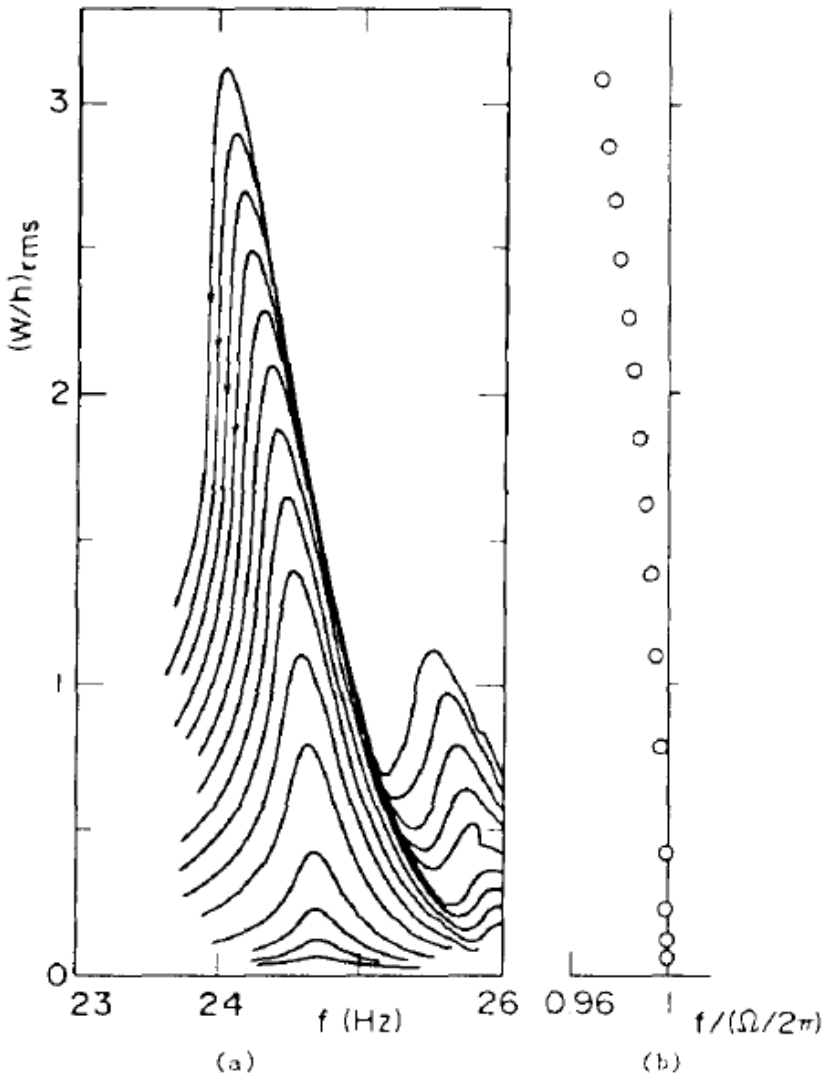

Figure 3.10. (a) Frequency response curves and (b) backbone curve. *L*=480 mm; (1.7) mode (Chiba 1993a).

The backbone curves of some vibration modes for the empty tanks with L=480 and 160 mm are shown in Fig. 3.11(a) and (b), respectively. In Fig. 3.11(a), the results for the axial mode up to m=3 are presented, while in Fig. 3.11(b) only the results with m=1 are shown in order to demonstrate the effect of the length of the shell. In Fig. 3.11(a) the results for m=1 are shown in two curves, i.e. (1,8), (1,9), (1,10), (1,11) and (1,12) modes. From these figures, it can be seen that almost all responses have a softening non-linearity except one mode with (1,12) for the tank with L=480 mm, which has a hardening non-linearity.

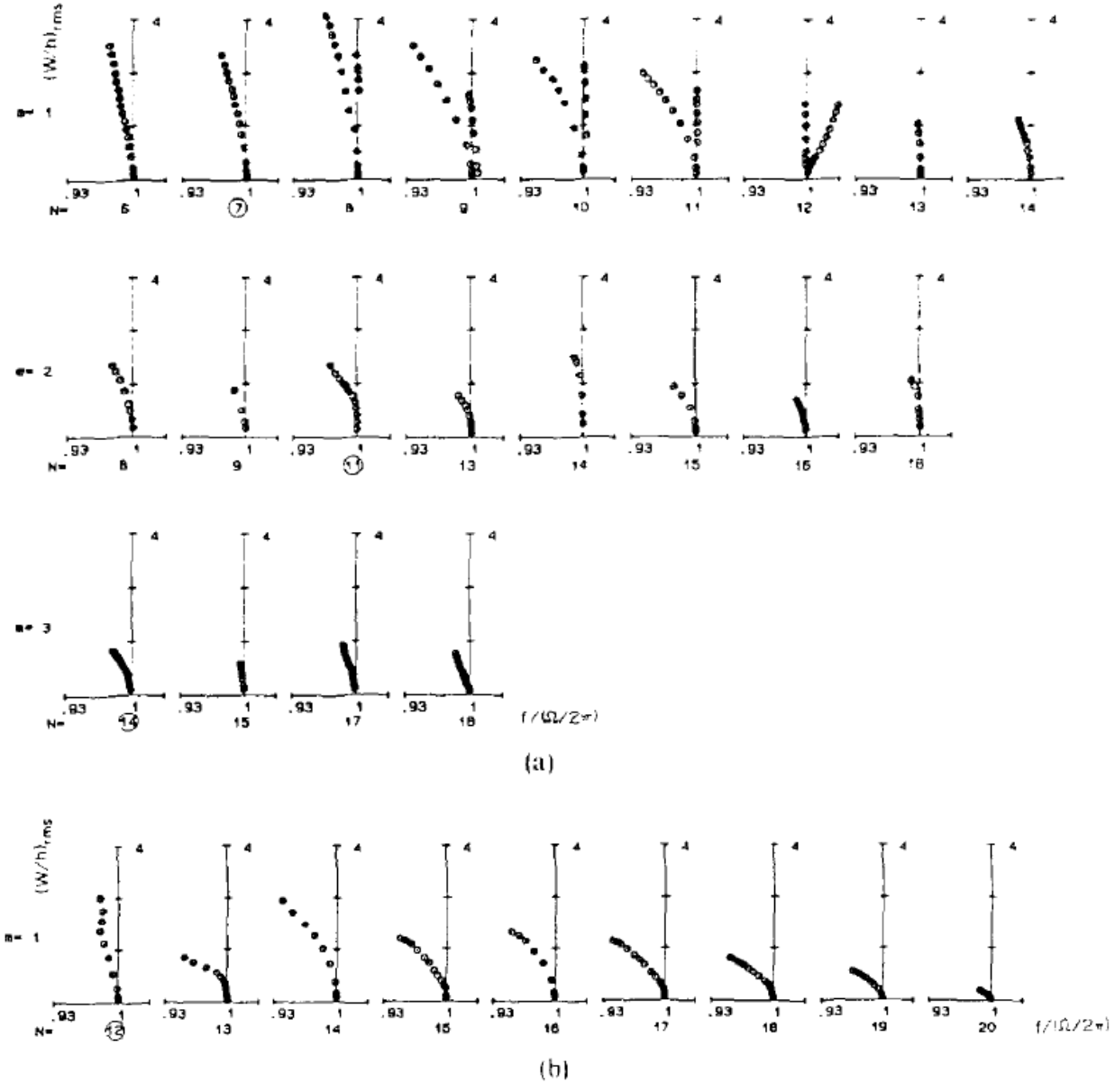

Figure 3.11. Backbone curves: (a) L=480 mm; (b) L=160 mm (Chiba 1993a).

In general, the following results were obtained:

(a) In modes with the same axial wave number m, the response of the mode with the circumferential wave number N, which corresponds to the minimum natural frequency of the same order of m and is marked with a circle in the figure, has the weakest degree of softening non-linearity. With an increase or decrease of the circumferential wave number N from $\bar{N}$, the degree of softening non-linearity increases and the response amplitude decreases.

(b) The maximum amplitude has a tendency to decrease with an increase in the axial wave number m.

(c) The shorter tank has a larger softening non-linearity than the taller one, which means that if one measures the natural frequency of the short tank, one has to choose the excitation amplitude with great care.

4. NONLINEAR VIBRATIONS OF SIMPLY SUPPORTED SHELLS WITH POLYNOMIAL EXPANSIONS

The main goal of the present study is developing of a general framework that allows studying circular shells with different boundary conditions. As for any new approach it strongly required to validate it with results available in literature. Previous Chapter shows that several efficient methods were developed in the past for investigating nonlinear vibrations of circular cylindrical shells with simply supported boundary conditions. Results, available in literature for simply supported shells, show good validation and convergence and it looks logical to start investigations with this well-studied boundary conditions.

4.1 LINEAR VIBRATIONS: MODAL ANALYSIS

In order to carry out a linear vibration analysis, in the present section, linear Sanders–Koiter (2.3) theory is considered.

The best basis for expanding displacement fields is the eigenfunction basis, but only for special boundary conditions such basis can be found analytically; generally, eigenfunctions must be evaluated numerically.

In order to attack the general problem of circular cylindrical shell vibration, displacement fields are expanded by means of a double series: deformation in the circumferential direction is presented by harmonic functions, (a) Chebyshev polynomials are considered in the axial direction.

Let us now consider natural modes of vibration, i.e. a synchronous motion:

$$\begin{aligned} u(h,q,t) &= U(h,q)\,f(t), \\ v(h,q,t) &= V(h,q)\,f(t), \\ w(h,q,t) &= W(h,q)\,f(t), \end{aligned} \tag{4.1}$$

where $U(h,q)$, $V(h,q)$ and $W(h,q)$ represent the mode shape and $f(t)$ is an harmonic function.

Now the modal shape is expanded in a double series in terms of Chebyshev polynomials $T_m^*(h)$ and harmonic functions:

$$U(h,q) = \sum_{m=0}^{M_U} \sum_{n=0}^{N} U_{m,n} T_m^*(h) \cos(nq), \tag{4.2a}$$

$$V(h,q) = \sum_{m=0}^{M_V} \sum_{n=0}^{N} V_{m,n} T_m^*(h) \sin(nq), \tag{4.2b}$$

$$W(h,q) = \sum_{m=0}^{M_W} \sum_{n=0}^{N} W_{m,n} T_m^*(h) \cos(nq), \tag{4.2c}$$

where $T_m^*(h) = T_m(2h-1)$ and $T_m(\cdot)$ is the m-*th* order Chebyshev polynomial of the first kind. The transformation of coordinates from h to $2h$-1 is necessary since Chebyshev polynomials are defined between –1 and 1, while $T_m^*(h)$ has been introduced in order to be defined between 0 and 1. In equations (4.2a-c) $U_{m,n}$, $V_{m,n}$ and $W_{m,n}$ are unknown coefficients.

For the case of (b) ordinary power polynomials instead of equations (4.2) one will have the following expressions:

$$U(h,q) = \sum_{m=0}^{M_U} \sum_{n=0}^{N} U_{m,n} h^m \cos(nq), \tag{4.3a}$$

$$V(h,q) = \sum_{m=0}^{M_V} \sum_{n=0}^{N} V_{m,n} h^m \sin(nq), \tag{4.3b}$$

$$W(h,q) = \sum_{m=0}^{M_W} \sum_{n=0}^{N} W_{m,n} h^m \cos(nq) \tag{4.3c}$$

4.1.1 BOUNDARY CONDITIONS

In case of polynomials, boundary conditions are satisfied by applying constraints to the unknown coefficients in expansions (4.2) or (4.3). Some of the coefficients $U_{m,n}$, $V_{m,n}$ and $W_{m,n}$ can be suitably chosen in order to satisfy boundary conditions.

For the simply supported shell the following boundary conditions are imposed:

$$w=0,\ v=0,\quad M_{\mathrm{x}}=0,\ N_{\mathrm{x}}=0 \qquad \text{at} \quad h=0,1. \tag{4.4a-d}$$

Initially, the expansion with Chebyshev polynomial is investigated. Equations (4.4a,b) give

$$W(h,q)=\sum_{\mathrm{m}=0}^{M_{\mathrm{W}}}\sum_{\mathrm{n}=0}^{N} W_{\mathrm{m,n}}T_{\mathrm{m}}^{*}(h)\cos(nq)=0 \qquad \text{for} \quad h=0,1. \tag{4.5a}$$

$$V(h,q)=\sum_{\mathrm{m}=0}^{M_{\mathrm{V}}}\sum_{\mathrm{n}=0}^{N} V_{\mathrm{m,n}}T_{\mathrm{m}}^{*}(h)\sin(nq)=0 \qquad \text{for} \quad h=0,1. \tag{4.5b}$$

Then, by using Eqs. (4.5a,b), equations (4.4c,d) are reduced to

$$\frac{\partial^2 W(h,q)}{\partial h^2}=\sum_{\mathrm{m}=0}^{M_{\mathrm{W}}}\sum_{\mathrm{n}=0}^{N} W_{\mathrm{m,n}}\frac{\partial^2 T_{\mathrm{m}}^{*}(h)}{\partial h^2}\cos(nq)=0 \qquad \text{for} \qquad h=0,1. \tag{4.5c}$$

$$\frac{\partial U(h,q)}{\partial h}=\sum_{\mathrm{m}=0}^{M_{\mathrm{U}}}\sum_{\mathrm{n}=0}^{N} U_{\mathrm{m,n}}\frac{\partial T_{\mathrm{m}}^{*}(h)}{\partial h}\cos(nq)=0 \qquad \text{for} \quad h=0,1. \tag{4.5d}$$

In Eq. (4.5d) nonlinear terms have been neglected. In fact, since the Rayleigh-Ritz method is used to find the solution, just geometric boundary condition has to be exactly satisfied.

Such conditions are valid for any q and n, therefore Eqs. (4.5a-d) are modified as follows:

$$\sum_{\mathrm{m}=0}^{M_{\mathrm{W}}} W_{\mathrm{m,n}}T_{\mathrm{m}}^{*}(h)=0, \qquad \sum_{\mathrm{m}=0}^{M_{\mathrm{V}}} V_{\mathrm{m,n}}T_{\mathrm{m}}^{*}(h)=0,$$

$$\sum_{\mathrm{m}=0}^{M_{\mathrm{W}}} W_{\mathrm{m,n}}\frac{\partial^2 T_{\mathrm{m}}^{*}(h)}{\partial h^2}=0, \qquad \sum_{\mathrm{m}=0}^{M_{\mathrm{U}}} U_{\mathrm{m,n}}\frac{\partial T_{\mathrm{m}}^{*}(h)}{\partial h}=0, \quad \text{for} \quad n=0,1... \quad \text{at}\, h=0,1. \tag{4.6}$$

For the expansion using power polynomials, the boundary conditions are satisfied in a similar way. Specifically, for power polynomials equations (4.4a-d) become

$$\sum_{\mathrm{m}=0}^{M_{\mathrm{W}}} W_{\mathrm{m,n}}h^{\mathrm{m}}=0, \qquad \sum_{\mathrm{m}=0}^{M_{\mathrm{V}}} V_{\mathrm{m,n}}h^{\mathrm{m}}=0,$$

$$\sum_{\mathrm{m}=0}^{M_{\mathrm{W}}} W_{\mathrm{m,n}}\frac{\partial^2 (h^{\mathrm{m}})}{\partial h^2}=0, \qquad \sum_{\mathrm{m}=0}^{M_{\mathrm{U}}} U_{\mathrm{m,n}}\frac{\partial (h^{\mathrm{m}})}{\partial h}=0, \quad \text{for} \quad n=0,1... \quad \text{at}\, h=0,1. \tag{4.7}$$

The linear algebraic system (4.6) or (4.7) is solved in terms of the coefficients $U_{1,n}, U_{2,n}, V_{0,n}, V_{1,n}, W_{0,n}, W_{1,n}, W_{2,n}, W_{3,n}$ for $n = 0,1,\ldots$. Therefore the expansions of *u*, *v* and *w* can be obtained in terms of remaining unknown coefficients.

4.1.2 EIGENVALUE PROBLEM

Expressions (4.1) and (4.2) or (4.3) are inserted into the expressions of kinetic and potential energies; in particular, the nonlinear terms are neglected in the potential energy. Then a set of ordinary differential equations is obtained by using the Lagrange equations. These equations can be immediately decoupled in the variable *q*.

An intermediate step is the reordering of variables. A vector **q** containing all variables is built; this vector has a different structure according to the shell boundary conditions (Pellicano 2007). Specifically, for simply supported edges:

$$\mathbf{q} = \left(U_{0,0}, U_{3,0}, \ldots, U_{0,1}, U_{3,1}, \ldots, V_{2,0}, V_{3,0}, \ldots, V_{2,1}, V_{3,1}, \ldots, W_{4,0}, W_{5,0}, \ldots, W_{4,1}, W_{5,1}, \ldots\right) f(t) \tag{4.8}$$

The number of variables needed to describe a mode with *n* nodal diameters is $M_T = M_U + M_V + M_W - 5$.

Lagrange equations for free vibrations are

$$\frac{d}{dt}\left(\frac{\partial L}{\partial \dot{q}_i}\right) - \frac{\partial L}{\partial q_i} = 0, \qquad i = 1, 2, \ldots, N_{\max}, \tag{4.9}$$

where $L = T_s - U_s$ and $N_{\max} = M_T \times (N+1)$. Assuming harmonic motion, $f(t) = e^{jwt}$, one obtains

$$\left(-w^2\mathbf{M} + \mathbf{K}\right)\mathbf{q} = \mathbf{0}, \tag{4.10}$$

which is the classical eigenvalue problem in nonstandard form; it gives natural frequencies and mode shapes.

The mode shape corresponding to the *j*-th mode is given by equations (4.2) or (4.3), where $U_{m,n}, V_{m,n}, W_{m,n}$ are substituted with $U_{m,n}^{(j)}, V_{m,n}^{(j)}, W_{m,n}^{(j)}$, which are the components of the *j*-th

eigenvector obtained from equation (4.10) and the vector function $\mathbf{U}^{(j)}(h)=\left(U^{(j)}(h),V^{(j)}(h),W^{(j)}(h)\right)^{T}$ is the *j*-th eigenfunction vector of the original problem.

Mode shapes are normalized by $U^{(j)}(h)/\max\left(U^{(j)}(h)\right)$, $V^{(j)}(h)/\max\left(V^{(j)}(h)\right)$ and $W^{(j)}(h)/\max\left(W^{(j)}(h)\right)$ for any h.

One should mention that for accurate numerical calculations, a very high numerical accuracy is required in calculating the eigenvectors (mode shapes) and all the coefficients to be introduced in the matrices. Sample of program for solving boundary conditions and eigenvalue problem for simply supported shell should be found in Appendix A.

4.2 NONLINEAR VIBRATIONS

In the nonlinear analysis, the full nonlinear expression of the potential shell energy, containing terms up to fourth order, is considered. Displacement fields $u(h,q,t)$, $v(h,q,t)$ and $w(h,q,t)$ are expanded by using the linear mode shapes obtained in the previous linear analysis:

$$u(h,q,t)=\sum_{j=1}^{M}\sum_{n=0}^{N}U^{(j)}(h)\left[u_{j,n,c}(t)\cos(nq)+u_{j,n,s}(t)\sin(nq)\right],$$

$$v(h,q,t)=\sum_{j=1}^{M}\sum_{n=0}^{N}V^{(j)}(h)\left[v_{j,n,c}(t)\sin(nq)+v_{j,n,s}(t)\cos(nq)\right], \qquad (4.11)$$

$$w(h,q,t)=\sum_{j=1}^{M}\sum_{n=0}^{N}W^{(j)}(h)\left[w_{j,n,c}(t)\cos(nq)+w_{j,n,s}(t)\sin(nq)\right],$$

where the total number of degrees of freedom in the nonlinear analysis is $2M\times N+M$, which is generally much smaller than N_{max} used in the linear analysis. In equations (4.11) both sin and cos mode shapes in q are introduced since a circular cylindrical shell is axisymmetric; therefore, both families of modes are participating in the shell response.

Expansions (4.11) satisfy the boundary conditions and the normalized mode shapes $U^{(j)}(h)$, $V^{(j)}(h)$, $W^{(j)}(h)$ are known functions, evaluated in the previous linear analysis, and are

expressed in terms of polynomials. In equation (4.11) the generalized coordinates $u_{j,n,c/s}(t)$, $v_{j,n,c/s}(t)$, $w_{j,n,c/s}(t)$ are obviously no more harmonic functions. Using expansion (4.11) one can select suitable shapes for each displacement field separately, improving convergence and reducing number of degrees of freedom. It is interesting to note that, due to the normalization, the generalized coordinates represent the maximum amplitude of vibration since $\max\left(U^{(j)}(h)\right)$, $\max\left(V^{(j)}(h)\right)$ and $\max\left(W^{(j)}(h)\right)$ after normalization are one.

Expansion (4.11) is inserted in the expressions giving strain and kinetic energies, virtual work and damping.

Only a radial harmonic concentrated force is assumed to act on the shell. The external radial distributed load q_r applied to the shell, due to the radial concentrated force f, is given by

$$q_r = f\, d(Rq - Rq_0)\, d(x - x_0)\cos(w\,t), \tag{4.12}$$

where w is the excitation frequency, t is the time, d is the Dirac delta function, f gives the radial force amplitude positive in z direction, x_0 and q_0 give the axial and angular positions of the point of application of the force, respectively; here, the point excitation is assumed to be located at $x_0 = L/2$, $q_0 = 0$; as a consequence of this excitation, the generalized coordinates with subscript c are directly excited (driven modes) and those with subscript s are not directly excited (companion modes).

The following notation is introduced for brevity

$$\mathbf{p} = \left\{u_{j,n,c}, u_{j,n,s}, v_{j,n,c}, v_{j,n,s}, w_{j,n,c}, w_{j,n,s}\right\}^{T},\ j = 1, \mathbf{K}\, M \ \text{ and } \ n = 0, \mathbf{K}\, N\,. \tag{4.13}$$

The generic element of the time-dependent vector $\mathbf{p}$ is referred to as p_i; the dimension of $\mathbf{p}$ is dofs, which is the number of degrees of freedom used in the mode expansion.

The generalized forces Q_j are obtained by differentiation of the Rayleigh's dissipation function and of the virtual work done by external forces

$$Q_i = -\frac{\partial F}{\partial p_i} + \frac{\partial W}{\partial p_i}\,. \tag{4.14}$$

The Lagrange equations of motion for the fluid-filled shell are

$$\frac{\mathrm{d}}{\mathrm{d}t}\left(\frac{\partial T}{\partial \dot{p}_{\mathrm{i}}}\right)-\frac{\partial T}{\partial p_{\mathrm{i}}}+\frac{\partial U}{\partial p_{\mathrm{i}}}=Q_{\mathrm{i}}\,,\quad i=1,\mathbf{K}\,\mathrm{dofs}\,, \tag{4.15}$$

where $\partial T/\partial p_{\mathrm{i}}=0$. These second-order equations have very long expressions containing quadratic and cubic nonlinear terms.

The very complicated term giving quadratic and cubic nonlinearities can be written in the form

$$\frac{\partial U}{\partial p_{\mathrm{i}}}=\sum_{\mathrm{k}=1}^{\mathrm{dofs}} p_{\mathrm{k}}\, f_{\mathrm{k,i}}+\sum_{\mathrm{j,k}=1}^{\mathrm{dofs}} p_{\mathrm{j}}\, p_{\mathrm{k}}\, f_{\mathrm{j,k,i}}+\sum_{\mathrm{j,k,l}=1}^{\mathrm{dofs}} p_{\mathrm{j}}\, p_{\mathrm{k}}\, p_{\mathrm{l}}\, f_{\mathrm{j,k,l,i}}\,, \tag{4.16}$$

where coefficients f have long expressions that include also geometric imperfections.

The set of ordinary nonlinear differential equations (3.16) is studied by using numerical continuation methods and bifurcation analysis.

4.3 NUMERICAL RESULTS

The equations of motion have been obtained by using the *Mathematica* computer software (Wolfram, 1999) in order to perform analytical surface integrals of trigonometric and Chebyshev functions. The generic Lagrange equation *j* is divided by the modal mass associated with $\ddot{p}_{\mathrm{j}}$ and then is transformed in two first-order equations. A non-dimensionalization of variables is also performed for computational convenience: the frequencies are non-dimensionalized dividing by the natural frequency of the resonant mode and the vibration amplitudes are divided by the shell thickness *h*. The resulting 2×dofs equations are studied by using the software AUTO (Doedel *et. all,* 1998) for continuation and bifurcation analysis of nonlinear ordinary differential equations. The software AUTO is capable of continuation of the solution, bifurcation analysis and branch switching by using the pseudo-arclength continuation method. In particular, the shell response under harmonic excitation has been studied by using an analysis in two steps: (i) first the excitation frequency has been fixed far enough from resonance

and the magnitude of the excitation has been used as bifurcation parameter; the solution has been started at zero force where the solution is the trivial undisturbed configuration of the shell and has been continued up to reach the desired force magnitude; (ii) when the desired magnitude of excitation has been reached, the solution has been continued by using the excitation frequency as bifurcation parameter.

4.3.1 SIMPLY SUPPORTED SHELL: CHEBYSHEV POLYNOMIAL VERSUS TRIGONOMETRIC EXPANSIONS

A test case of a simply supported circular cylindrical shell is analyzed. Calculations have been performed for a shell having the following dimensions and material properties: L = 0.2 m, R = 0.1 m, h = 0.247 mm, $E = 71.02 \times 10^9$ Pa, r = 2796 kg/m^3 and n = 0.31, which corresponds to a case studied by several authors (see Chapter 2). The mode investigated is (m=1, n=6) which has one longitudinal half-wave and 6 circumferential waves.

Chebyshev polynomials of 15th power were used to obtain mode shapes of the problem (linear vibration study). Such high power was chosen to obtain axisymmertrical modes with relatively high number of axial half-waves m; specifically mode (m=7, n=0) and higher. But since contribution of these modes is small, in farther analysis only modes up to (5,0) are taken into consideration. Therefore polynomials of 9th power can be used to save computational time. If one has no aim to study influence of higher modes (both – axisymmertrical and asymmetrical), even polynomials of the 7th power give accurate results. Natural frequencies of some modes (important modes in the nonlinear model) obtained by using polynomials of different power are compared in Table 4.1. The agreement is excellent (only for the 7th power polynomials, higher modes have 1 percent difference with the exact frequency).

The mode shapes for the three cases presented in Table 4.1 (7th, 9th and 15th power of polynomials) also perfectly coincide with the exact solution (shapes are perfect sin and cos), but,

in order to obtain higher axisymmertrical modes, it is necessary to use polynomials of power 15th.

Mode (m, n)	(1,n)	(1,2n)	(3,2n)	(3,n)	(1,0)
7th power Chebyshev polynomial	553.33	882.22	1439.66	3061.19	7784.15
9th power Chebyshev polynomial	553.33	882.22	1455.67	3040.78	7784.15
15th power Chebyshev polynomial	553.33	882.22	1555.56	3040.66	7784.15
Exact with trigonometric function	553.37	882.26	1455.69	3040.69	7784.15

Table 4.1. Comparison of natural frequencies (Hz) for simply supported shell obtained by using Chebyshev polynomials; present theory (polynomials of different power) versus exact results obtained with trigonometric functions.

Figure 4.1 shows the frequency-response curve (computed by using the model with 28 degrees of freedom) of the driven mode $w_{1,6,c}$; companion mode participation is not active. Specifically, the following modes are used in the model:

$$\begin{aligned} &w\text{: } (1,n),\ (1,2n),\ (1,0),\ (3,0),\ (5,0);\\ &u\text{: } (1,n),\ (1,2n),\ (3,2n),\ (1,0),\ (3,0),\ (5,0);\\ &v\text{: } (1,n),\ (1,2n),\ (1,3n),\ (1,4n),\ (3,2n),\ (3,4n). \end{aligned} \tag{4.17}$$

In expansion (4.17) each asymmetric mode (i.e. mode with second integer number different from zero) must be counted twice to obtain the number of degrees of freedom since both cos (driven) and sin (companion) modes are used.

The present results (continuous thick line) are compared to those obtained analytically by Amabili (2003a), Chen and Babcock (1975), Pellicano et al. (2002), Ganapathi and Varadan (1996) (only free vibration curve, also named backbone curve), Varadan et al. (1989) (only free vibration curve). The amplitude of the external modal excitation is $f = 0.0785$ N and the modal damping ratio is $z_{1,6} = 0.0005$. The linear circular frequency of the driven and companion modes is $w_{1,6} = 2p \times 553.33$ rad/s. Figure 2 shows reasonably good agreement between the present results and those available in the literature.

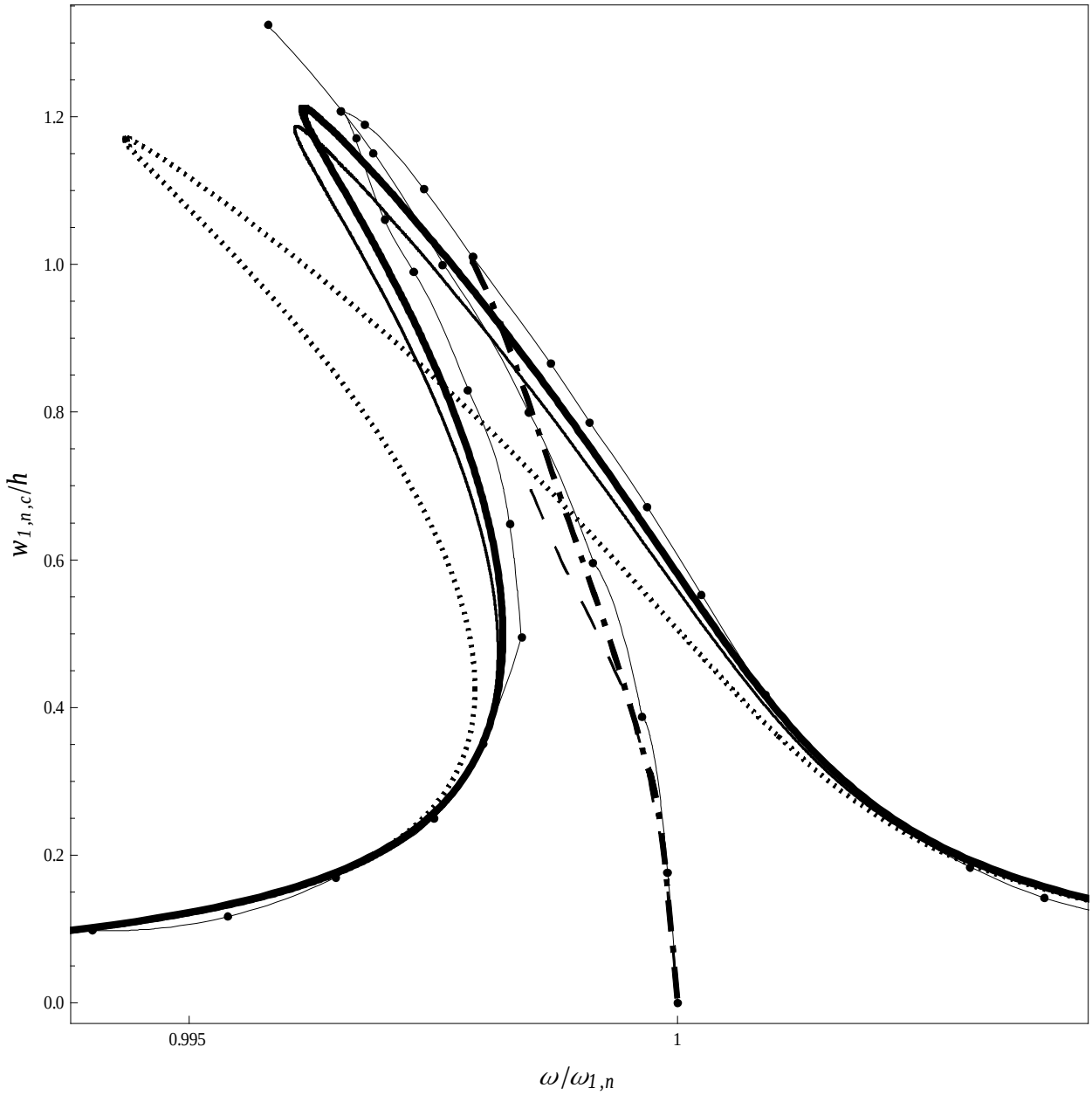

Figure 4.1 Frequency-response curve for simply supported shell (only branch 1 without companion mode participation is shown). ▬▬, 28 dofs, present model with Chebyshev polynomial expansion; ——, response computed by Amabili (2003a); –•–, backbone curve (free vibration) and forced response, from Pellicano et *al*. (2002); ·····, response computed by Chen and Babcock (1975); –·–, backbone curve from Varadan et al. (1989); – –, backbone curve from Ganapathi and Varadan (1986).

In order to investigate the convergence of the expansion given in equation (4.17), the 28 dofs response is compared with reduced models; the comparison is shown in Figure 4.2.

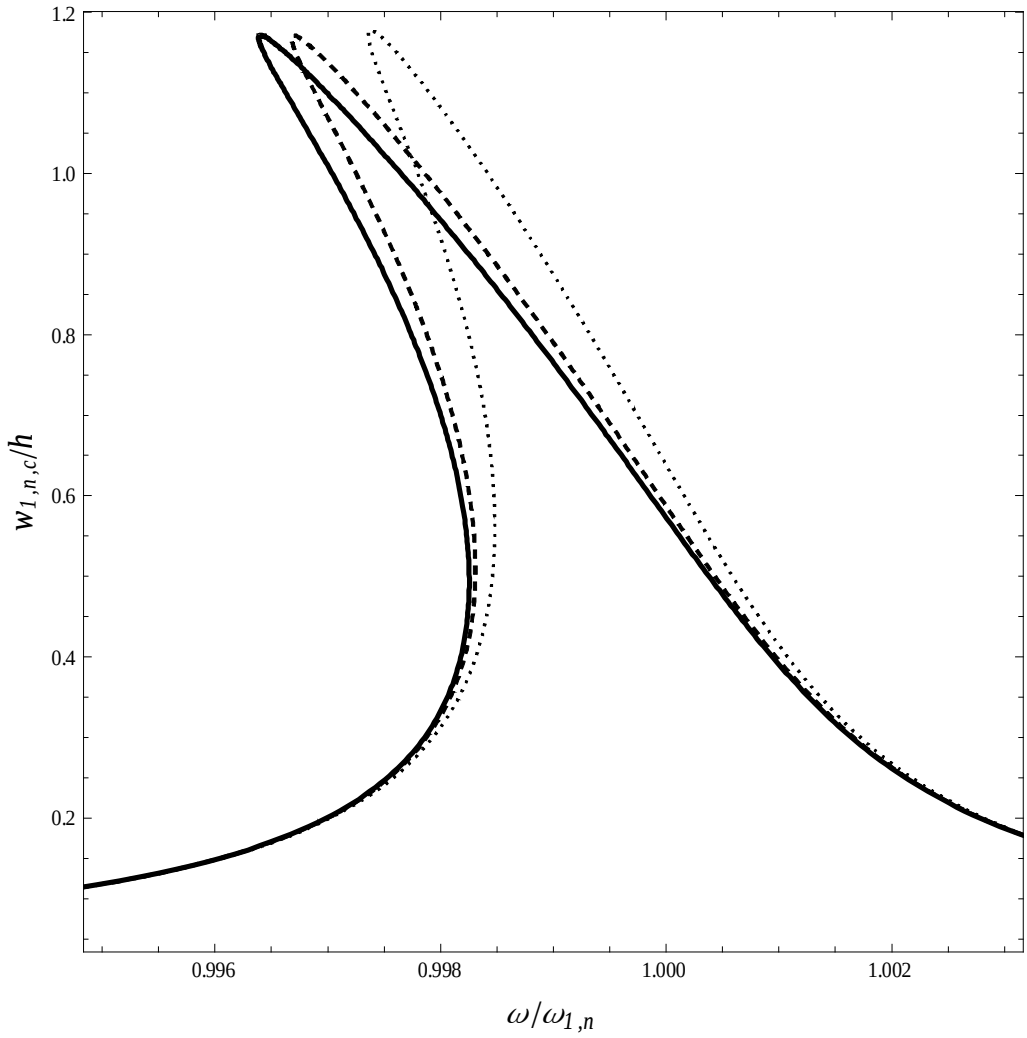

Figure 4.2. Frequency-response curve for simply supported shell (only branch 1 without companion mode participation is shown). Full 28 dofs model compared to reduced models. ——, 28 dofs, present model with Chebyshev polynomial expansion; – –, model excluding mode u(3,2n); ·····, model excluding u(3,2n) and v(1,3n).

Reduction of the model was performed step by step (with trials that exclude specific modes), and only the most significant cases, for which influence of the mode is high, are shown in the figure. In Figure 4.2, the bold line shows the full model in equation (4.17); the dashed line represents the same model excluding mode $u(3,2n)$; the dotted line excludes modes $u(3,2n)$ and $v(1,3n)$. Specifically the two modes $u(3,2n)$ and $v(1,3n)$ give a contribution increasing the softening type nonlinearity, but their influence is not large; in fact, it can be expected that modes with $3n$ and $4n$ circumferential waves do not contribute significantly (the system is softening so

modes with 3n circumferential waves play a smaller role than 2n modes); a similar consideration can be applied to modes with 3 axial half-waves (excluding axisymmetric modes that has to reach high axial wavenumber for convergence of the solution).

One also should note that mode having 2n circumferential waves $w(1,2n)$ plays a significant role in the softening behavior of the shell. The model missing that mode (not shown in the figure) shows strongly hardening behavior.

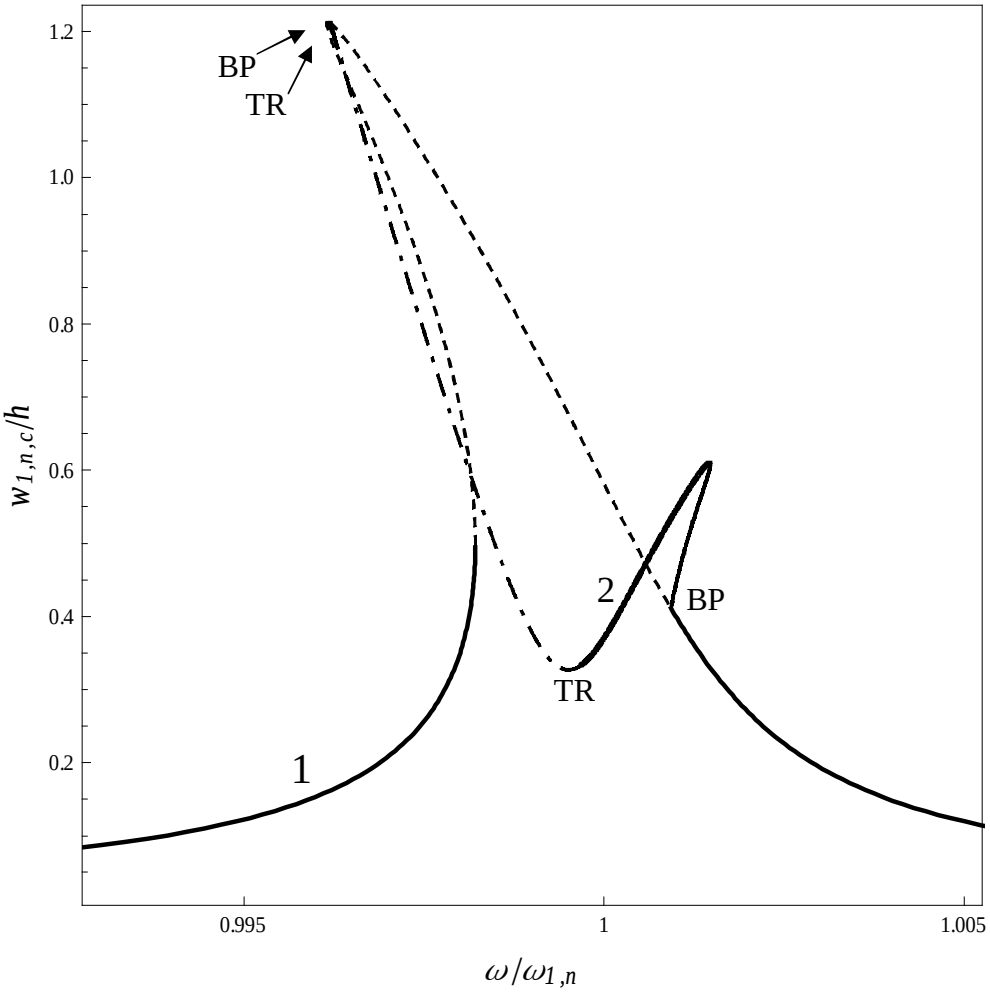

(a)

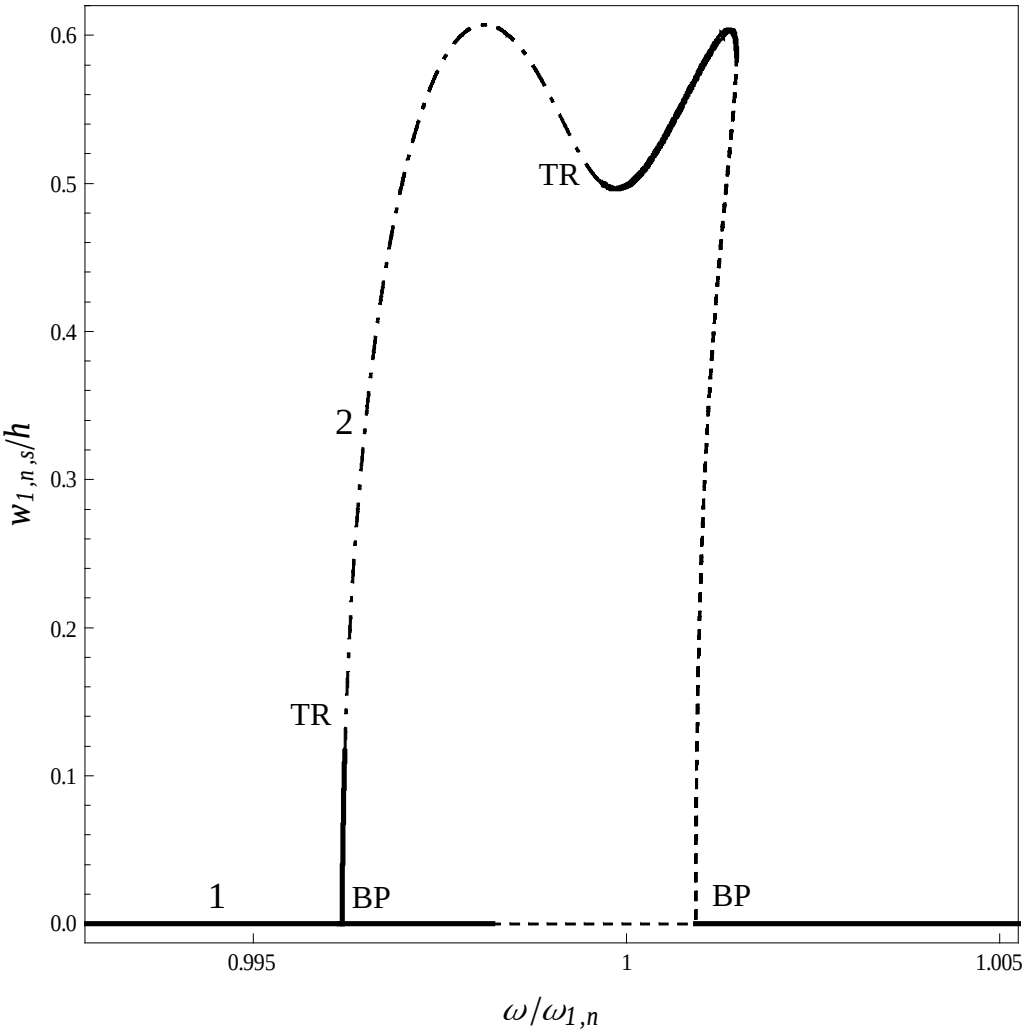

(b)

Figure 4.3. Frequency-response curve for simply supported shell with companion mode participation; 28 dofs model with Chebyshev polynomial expansion. —, stable periodic solution; −·−, stable quasi-periodic solution; – –, unstable solutions; BP, pitchfork bifurcation; TR, Neimark-Sacker bifurcation; 1, branch 1; 2, branch 2. (a) Generalized coordinate $w_{1,n,c}$; (b) generalized coordinate $w_{1,n,s}$.

Figure 4.3 shows the frequency-response relationship with companion mode participation (i.e. the actual response of the shell) for the model in equation (4.17). The main branch 1 in Figure 4.3 corresponds to vibration with zero amplitude of the companion mode $w_{1,6,s}$. This branch has pitchfork bifurcations (BP) at $w/w_{1,6}$ = 0. 99619 and at 1.00092, where branch 2

appears. This new branch corresponds to participation of both $w_{1,6,c}$ and $w_{1,6,s}$, giving a traveling-wave response moving around the shell; the phase shift between the two coordinates is almost $\pi/2$. The companion mode presents a node at the location of the excitation force and therefore it is not directly excited; its amplitude is different from zero only for large-amplitude vibrations, due to nonlinear coupling. The appearance of branch 2 is related to the 1:1 internal resonance of $w_{1,6,c}$ and $w_{1,6,s}$, which is due to the axial symmetry of the circular cylindrical shell. This branch appears for sufficiently large excitation, and it can be observed for vibration amplitude of the order of at least 1/10 of the shell thickness.

Branch 2 undergoes two Neimark-Sacker (torus) bifurcations (TR in the figure) at $w/w_{1,6}$ = 0. 99623 and 0.99675. Amplitude-modulated (quasi-periodic) response is indicated in Figure 4.3 on branch 2 for 99623 < $w/w_{1,6}$ < 0.99675, that is, bracketed by the two Neimark-Sacker bifurcations.

4.3.2 POWER POLYNOMIAL VERSUS CHEBYSHEV POLYNOMIAL AND TRIGONOMETRIC EXPANSIONS FOR SIMPLY SUPPORTED SHELL

The mode expansion in equation (4.17) is used for both power and Chebyshev polynomials and for trigonometric functions. To have perfect comparison, power polynomials of the same power of Chebyshev polynomials were used. Calculations show that high powers (higher than 9^{th} power) are not applicable for ordinary power polynomials, since increasing power mass and stiffness matrixes become very badly conditioned even using extremely high precision during calculations in Mathematica software. Polynomials of 9^{th} power give acceptable mode shapes (perfect sin and cos) and frequencies but do not allow considering axisymmetric modes higher than (5,0). Natural frequencies of some modes (important modes in the nonlinear model) are presented for comparison in Table 4.2; the agreement with the exact solution is excellent.

Mode (m, n)	(1,n)	(1,$2n$)	(3,$2n$)	(3,n)	(1,0)
9th power polynomial	553.33	882.22	1455.67	3040.78	7784.15
Exact with trigonometric function	553.37	882.26	1455.69	3040.69	7784.15

Table 4.2. Comparison of natural frequencies (Hz) for simply supported shell obtained by using power polynomials; present theory (polynomials of different power) versus exact results obtained with trigonometric functions.

Figure 4.4 compares the shell response for the three different types of expansions: Chebyshev polynomials, power polynomials and trigonometric functions. Results are very close each other.

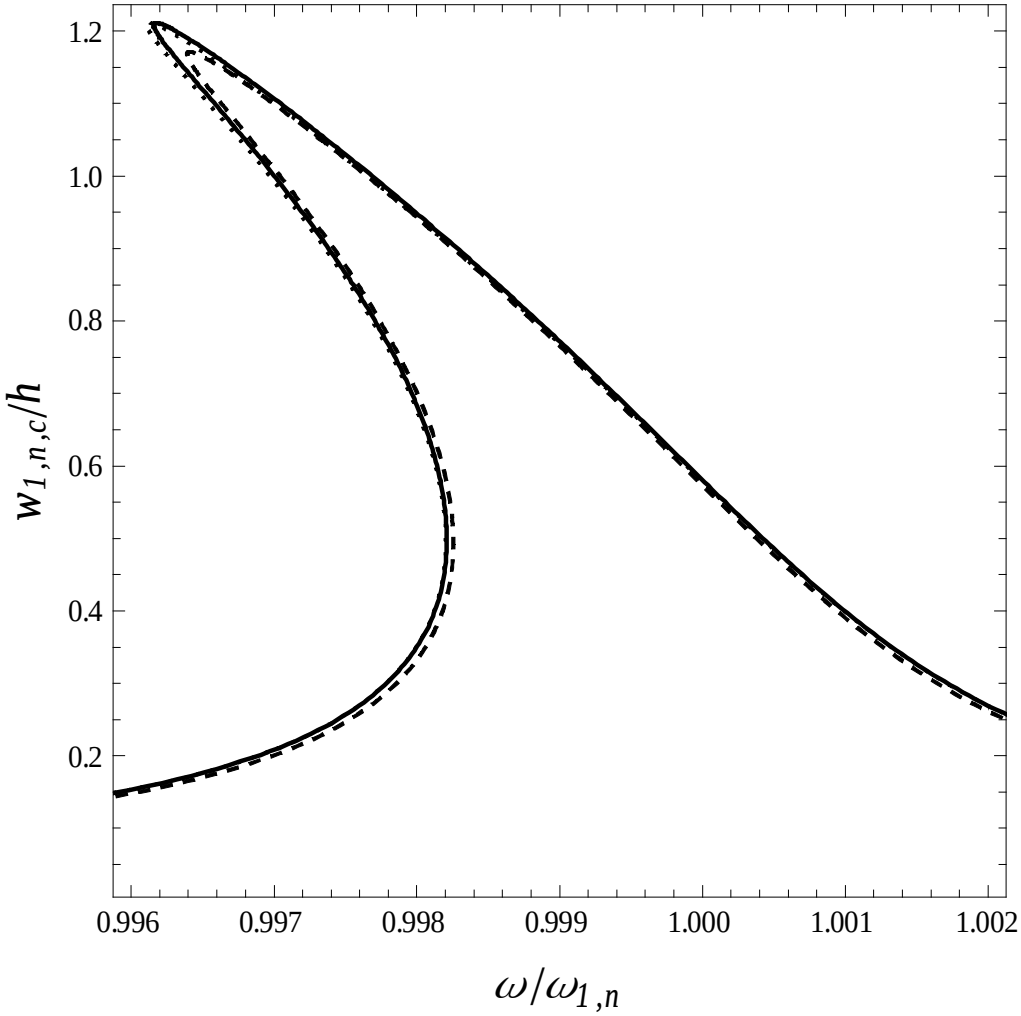

Figure 4.4. Frequency-response curve for the simply supported shell obtained by using Chebyshev polynomials (——, solid line), ordinary power polynomials (·····, dotted line) compared to results obtained by Amabili (2003a) with trigonometric functions (– –, dashed line).

5. NONLINEAR VIBRATIONS OF CLAMPED-CLAMPED SHELLS WITH POLYNOMIAL EXPANSIONS

5.1 LINEAR ANALYSIS

In order to carry out a linear vibration analysis, in the present section, linear Sanders–Koiter (2.3) theory is considered.

The best basis for expanding displacement fields is the eigenfunction basis, but only for special boundary conditions such basis can be found analytically; generally, eigenfunctions must be evaluated numerically.

Formally procedure of linear analysis for clamped-clamped shells is the same as described in the previous Chapter for the simply supported shells. The modal shape is expanded in a double series in terms of Chebyshev polynomials $T_m^*(h)$ and harmonic functions (4.2) or (4.3) in the case of ordinary power polynomials.

5.1.1 BOUNDARY CONDITIONS

In case of polynomials, boundary conditions are satisfied by applying constraints to the unknown coefficients in expansions (4.2) or (4.3). Some of the coefficients $U_{\mathrm{m,n}}$, $V_{\mathrm{m,n}}$ and $W_{\mathrm{m,n}}$ can be suitably chosen in order to satisfy boundary conditions.

For the clamped-clamped shell the following boundary conditions are imposed:

$$w = 0, \qquad \frac{\partial w}{\partial h} = 0, \qquad v = 0, \qquad u = 0, \qquad \text{at } h = 0,1. \tag{5.1a-d}$$

For the case of Chebyshev polynomials equations (5.1a-d) give

$$W(h,q) = \sum_{\mathrm{m}=0}^{M_{\mathrm{w}}} \sum_{\mathrm{n}=0}^{N} W_{\mathrm{m,n}} T_{\mathrm{m}}^*(h) \cos(nq) = 0 \qquad \text{for} \quad h = 0,1. \tag{5.2a}$$

$$\frac{\partial W(h,q)}{\partial h} = \sum_{\mathrm{m}=0}^{M_{\mathrm{w}}} \sum_{\mathrm{n}=0}^{N} W_{\mathrm{m,n}} \frac{\partial T_{\mathrm{m}}^*(h)}{\partial h} \cos(nq) = 0 \qquad \text{for} \qquad h = 0,1. \tag{5.2b}$$

$$V(h,q)=\sum_{m=0}^{M_V}\sum_{n=0}^{N}V_{m,n}T_m^*(h)\sin(nq)=0 \qquad \text{for} \quad h=0,1 \tag{5.2c}$$

$$U(h,q)=\sum_{m=0}^{M_U}\sum_{n=0}^{N}U_{m,n}T_m^*(h)\cos(nq)=0 \qquad \text{for} \quad h=0,1. \tag{5.2d}$$

Such conditions are valid for any q and n, therefore Eqs. (5.2a-d) are modified as follows:

$$\sum_{m=0}^{M_W}W_{m,n}T_m^*(h)=0, \qquad \sum_{m=0}^{M_V}V_{m,n}T_m^*(h)=0,$$

$$\sum_{m=0}^{M_W}W_{m,n}\frac{\partial T_m^*(h)}{\partial h}=0, \qquad \sum_{m=0}^{M_U}U_{m,n}T_m^*(h)=0, \quad \text{for} \quad n=0,1... \quad \text{at } h=0,1. \tag{5.3}$$

For the expansion using power polynomials, the boundary conditions are satisfied in a similar way. Specifically, for power polynomials equations (5.1a-d) become

$$\sum_{m=0}^{M_W}W_{m,n}h^m=0, \qquad \sum_{m=0}^{M_V}V_{m,n}h^m=0,$$

$$\sum_{m=0}^{M_W}W_{m,n}\frac{\partial(h^m)}{\partial h}=0, \qquad \sum_{m=0}^{M_U}U_{m,n}h^m=0, \quad \text{for} \quad n=0,1... \quad \text{at } h=0,1. \tag{5.4}$$

The linear algebraic system (5.3) or (5.4) is solved in terms of the coefficients $U_{0,n},U_{1,n},V_{0,n},V_{1,n},W_{0,n},W_{1,n},W_{2,n},W_{3,n}$ for $n=0,1...$. Therefore the expansions of u, v and w can be obtained in terms of remaining unknown coefficients.

5.1.2 EIGENVALUE PROBLEM

Expressions (4.1) and (4.2) or (4.3) are inserted into the expressions of kinetic and potential energies; in particular, the nonlinear terms are neglected in the potential energy. Then a set of ordinary differential equations is obtained by using the Lagrange equations. These equations can be immediately decoupled in the variable q.

An intermediate step is the reordering of variables. A vector **q** containing all variables is built; this vector has a different structure according to the shell boundary conditions (Pellicano 2007). Specifically, for clamped-clamped edges:

$$\mathbf{q} = \left(U_{2,0}, U_{3,0}, ..., U_{2,1}, U_{3,1}, ..., V_{2,0}, V_{3,0}, ..., V_{2,1}, V_{3,1}, ..., W_{4,0}, W_{5,0}, ..., W_{4,1}, W_{5,1}, ...\right) f(t) \tag{5.5}$$

The number of variables needed to describe a mode with *n* nodal diameters is $M_T = M_U + M_V + M_W - 5$.

Lagrange equations for free vibrations are

$$\frac{d}{dt}\left(\frac{\partial L}{\partial \dot{q}_i}\right) - \frac{\partial L}{\partial q_i} = 0, \qquad i = 1, 2, ..., N_{\max}, \tag{5.6}$$

where $L = T_s - U_s$ and $N_{\max} = M_T \times (N+1)$. Assuming harmonic motion, $f(t) = e^{jwt}$, one obtains

$$\left(-w^2\mathbf{M} + \mathbf{K}\right)\mathbf{q} = \mathbf{0}, \tag{5.7}$$

which is the classical eigenvalue problem in nonstandard form; it gives natural frequencies and mode shapes.

The mode shape corresponding to the *j*-th mode is given by equations (4.2) or (4.3), where $U_{m,n}, V_{m,n}, W_{m,n}$ are substituted with $U^{(j)}_{m,n}, V^{(j)}_{m,n}, W^{(j)}_{m,n}$, which are the components of the *j*-th eigenvector obtained from equation (5.7) and the vector function $\mathbf{U}^{(j)}(h) = \left(U^{(j)}(h), V^{(j)}(h), W^{(j)}(h)\right)^T$ is the *j*-th eigenfunction vector of the original problem.

Mode shapes are normalized by $U^{(j)}(h) / \max\left(U^{(j)}(h)\right)$, $V^{(j)}(h) / \max\left(V^{(j)}(h)\right)$ and $W^{(j)}(h) / \max\left(W^{(j)}(h)\right)$ for any *h*.

One should mention that for accurate numerical calculations, a very high numerical accuracy is required in calculating the eigenvectors (mode shapes) and all the coefficients to be introduced in the matrices.

5.2 NUMERICAL RESULTS

Nonlinear analysis is described in the previous Chapter, Subsection 4.2.

The equations of motion have been obtained by using the *Mathematica* computer software (Wolfram, 1999) in order to perform analytical surface integrals of trigonometric and Chebyshev functions. The generic Lagrange equation *j* is divided by the modal mass associated with $\mathbf{f}_j$ and then is transformed in two first-order equations. A non-dimensionalization of variables is also performed for computational convenience: the frequencies are non-dimensionalized dividing by the natural frequency of the resonant mode and the vibration amplitudes are divided by the shell thickness *h*. The resulting 2×dofs equations are studied by using the software AUTO (Doedel *et. all,* 1998) for continuation and bifurcation analysis of nonlinear ordinary differential equations. The software AUTO is capable of continuation of the solution, bifurcation analysis and branch switching by using the pseudo-arclength continuation method. In particular, the shell response under harmonic excitation has been studied by using an analysis in two steps: (i) first the excitation frequency has been fixed far enough from resonance and the magnitude of the excitation has been used as bifurcation parameter; the solution has been started at zero force where the solution is the trivial undisturbed configuration of the shell and has been continued up to reach the desired force magnitude; (ii) when the desired magnitude of excitation has been reached, the solution has been continued by using the excitation frequency as bifurcation parameter.

Calculations have been performed for a shell having the following dimensions and material properties: L = 520 mm, R = 149.4 mm, h = 0.519 mm, $E = 1.98 \times 10^{11}$ Pa, r = 7800 kg/m^3 and n = 0.3. The mode investigated is (m=1, n=6).

Similarly to the case of simply supported shell, Chebyshev polynomials of 15th power have been used to obtain mode shapes. Since, as it will be shown, contribution of higher modes is significant, the power of polynomials cannot be reduced for the case of clamped shell.

The response of the circular cylindrical shell subjected to harmonic point excitation of 3N applied at the middle of the shell in the spectral neighbourhood of the lowest (fundamental) resonance $w_{1,n} = 2p \times 313.7$ rad/s, corresponding to mode (m = 1, n = 6), is given in Figure 5.1;

eight generalized coordinates are shown, just a selection of some of the most interesting coordinates, in order to show their contribution to the global response of the shell. All the calculations reported in this section, if not diversely specified, have been performed by using an expansion involving 30 generalized coordinates (with companion modes), namely:

$$\begin{aligned} &w\text{: (1,n), (1,2n), (3,2n), (1,0), (3,0), (5,0), (7,0), (9,0), (11,0);} \\ &u\text{: (1,n), (1,2n), (3,2n), (1,0), (3,0), (5,0), (7,0), (9,0), (11,0);} \\ &v\text{: (1,n), (1,2n), (3,2n).} \end{aligned} \tag{5.8}$$

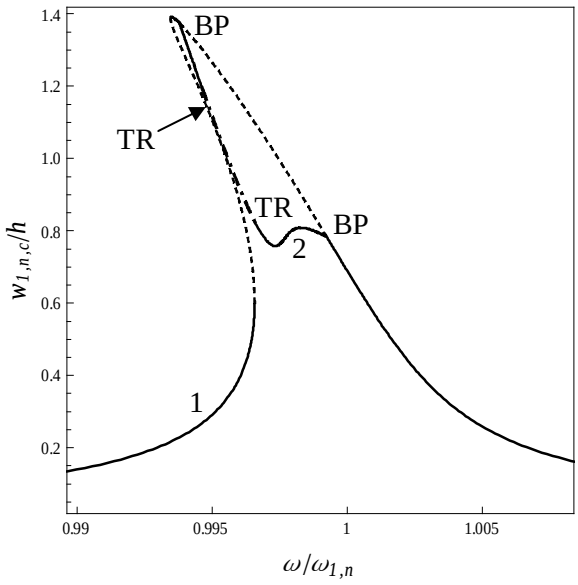

(a)

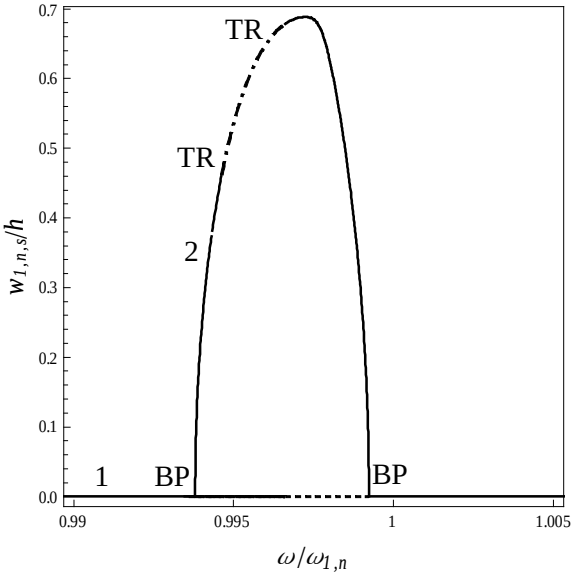

(b)

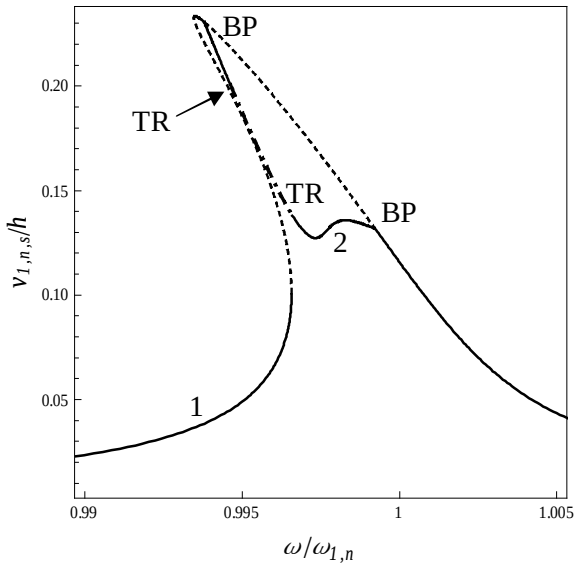

(c)

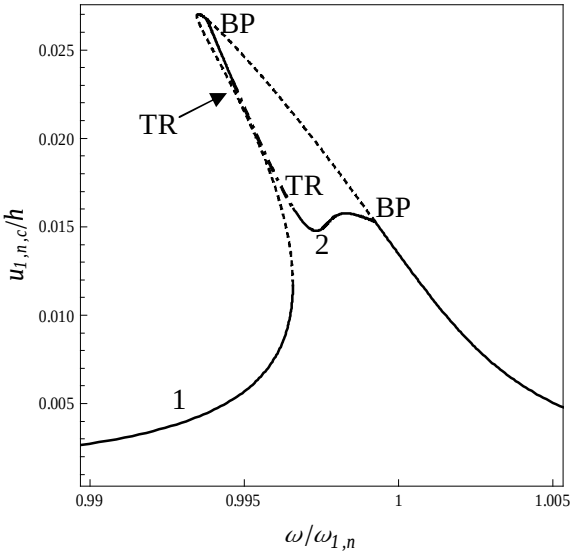

(d)

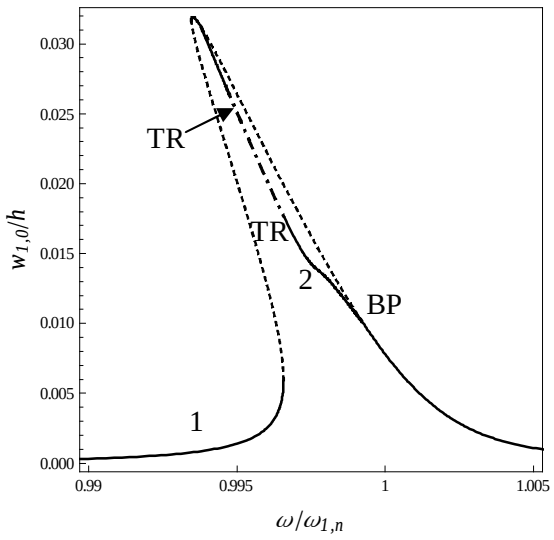

(e)

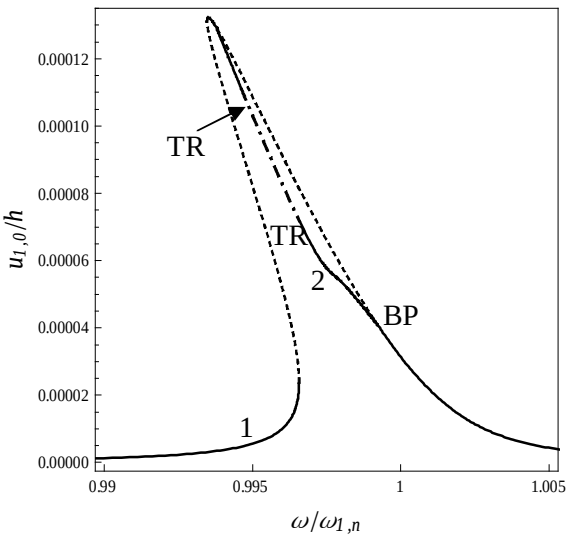

(f)

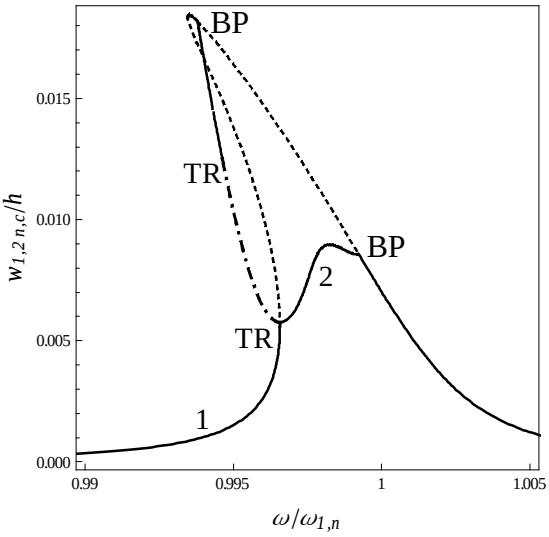

(g)

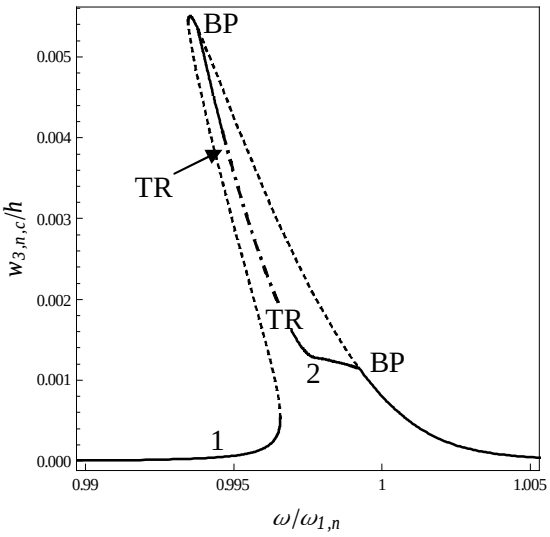

(h)

Figure 5.1. Frequency-response curve for clamped shell with companion mode participation; 30 dofs model with Chebyshev polynomial expansion. —, stable periodic solution; −·−, stable quasi-periodic solution; – –, unstable solutions; BP, pitchfork bifurcation; TR, Neimark-Sacker bifurcation; 1, branch 1; 2, branch 2. (a) Generalized coordinate $w_{1,n,c}$; (b) generalized coordinate $w_{1,n,s}$; (c) generalized coordinate $v_{1,n,s}$; (d) generalized coordinate $u_{1,n,c}$; (e) generalized coordinate $w_{1,0}$; (f) generalized coordinate $u_{1,0}$; (g) generalized coordinate $w_{1,2n,c}$; (h) generalized coordinate $w_{3,n,c}$.

The main coordinates in Figure 5.1 are the driven and companion resonant modes, given in Figures 5.1(a) and (b), respectively. The solution initially presents a single branch 1 with one folding and the typical softening type behaviour; this branch corresponds to driven mode vibration with zero amplitude of the companion mode. Branch 1 presents a pitchfork bifurcation around the peak of the response where branch 2 arises and branch 1 loses stability. Branch 2 is the solution with participation of both driven and companion modes, giving a standing wave plus a travelling wave response around the shell. Branch 2 loses stability at a Neimark-Sacker (torus) bifurcation where amplitude-modulations of the solution arise; modulations end at a second Neimark-Sacker bifurcation. Branch 2 ends at a second pitchfork bifurcation where it merges with branch 1 that regains stability. Figures 5.1(c) and (d) show the response of in-plane coordinates; Figures 5.1(e) and (f) present axisymmetric coordinates; finally Figures 5.1(g) and (h) show the generalized coordinates $w_{1,2n,c}$ and $w_{3,n,c}$, respectively.

In order to investigate the convergence of expansion (5.8), the 30 dofs response is compared with reduced models; comparison is shown in Figure 5.2 The bold line presents the full model given in equation (5.8), dotted line presents the same model excluding modes $u(3,0)$ and $w(3,0)$, dashed line excludes modes $u(7,0)$ and $w(7,0)$. Modes $u(5,0)$ and $w(5,0)$ have no significant effect on response of the shell (not shown in the figure). This result shows that the 30 dofs model can be reduced to the size of the simply supported model without a significant reduction of accuracy.

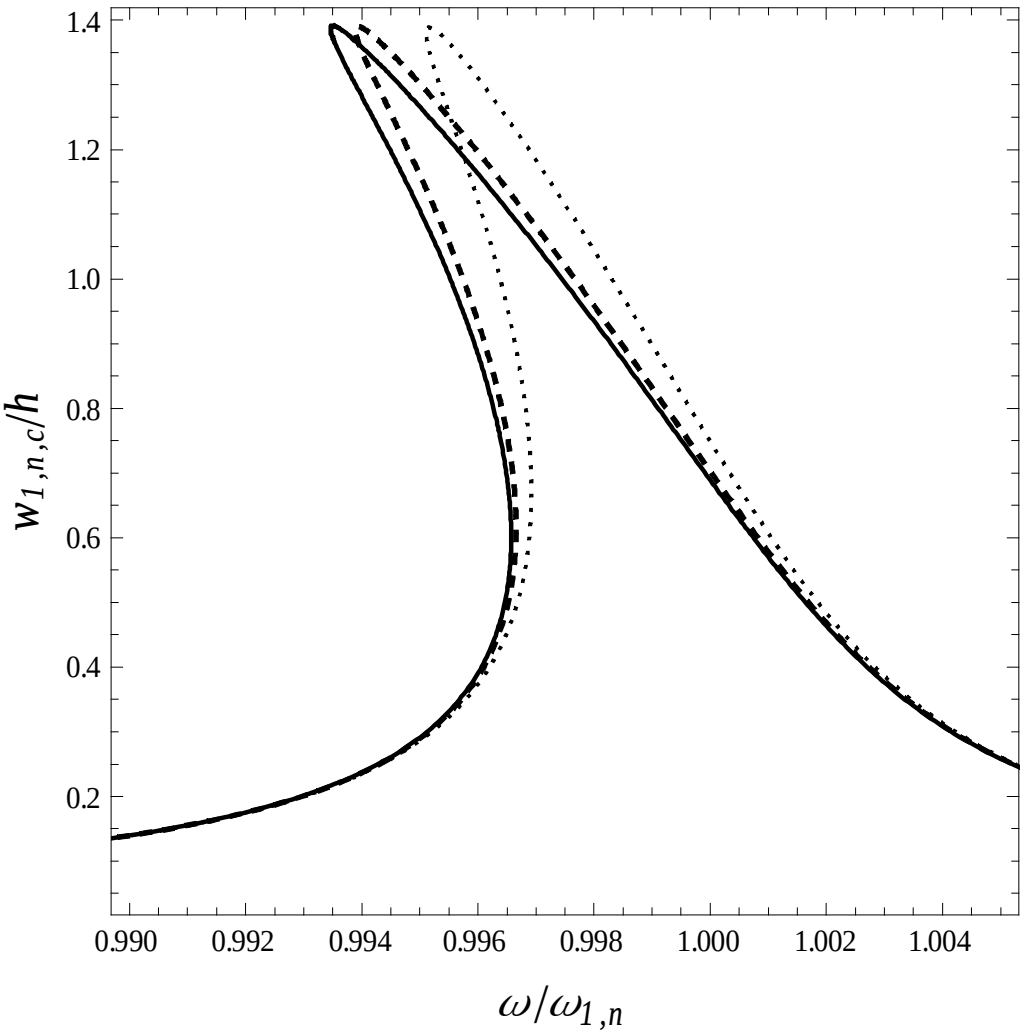

Figure 5.2. Frequency-response curve for the clamped shell (without companion modes participation); Full model comparing with reduced models. ——, 30 dofs, present model with Chebyshev polynomial expansion; – –, model excluding modes $u(7,0)$ and $w(7,0)$; ·····, model excluding $u(3,0)$ and $w(3,0)$.

A farther investigation of the convergence has been performed. In fact, higher order axisymmetrical modes (namely, $u(9,0)$ and $w(9,0)$) are strictly required in expansion since absence of these modes changes the shell response from softening type to strongly hardening; this is shown in Figure 5.3.

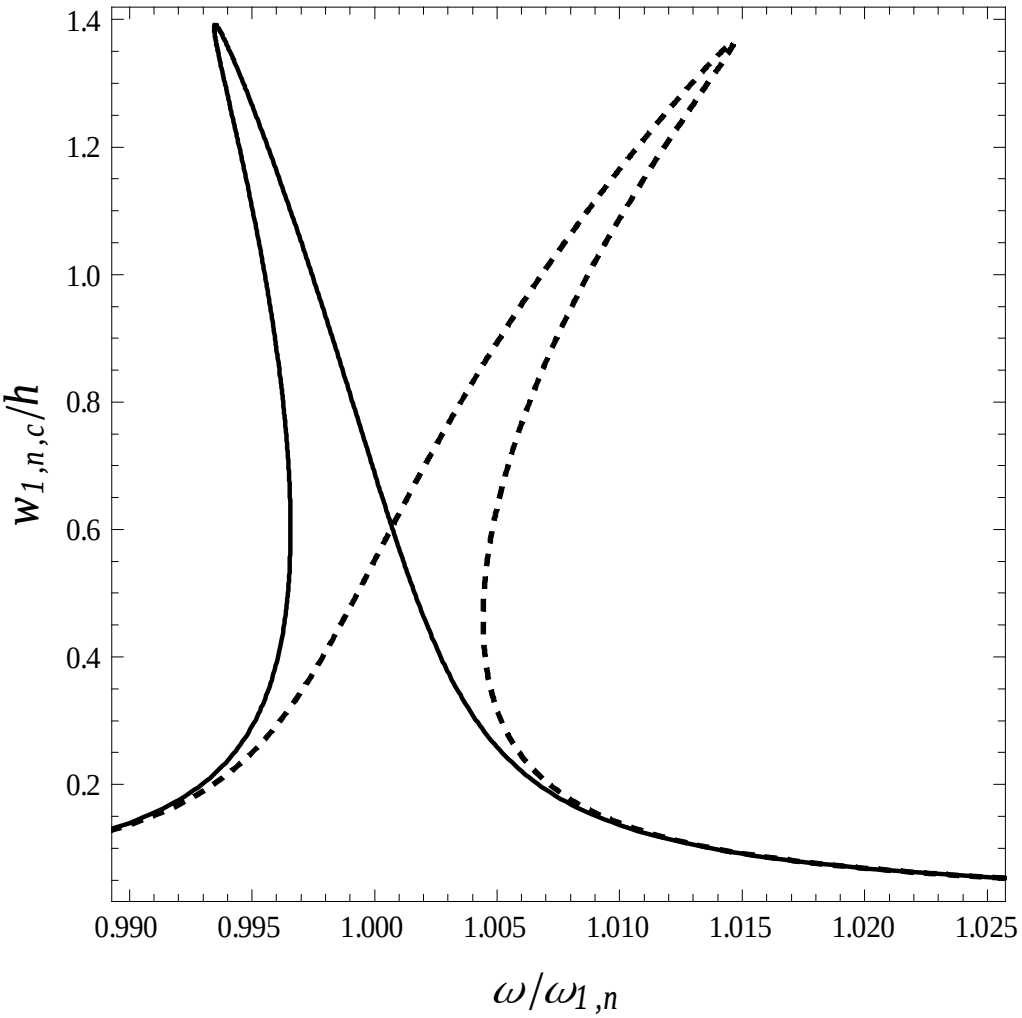

Figure 5.3. Frequency-response curve for the clamped shell (without companion modes participation); Full model comparing with reduced models. ——, 30 dofs, present model with Chebyshev polynomial expansion; – –, model excluding modes $u(9,0)$ and $w(9,0)$.

The present results are also compared in Figure 5.4 to those obtained by Amabili (2003a) using Donnell's nonlinear theory and trigonometric functions in the expansions. The agreement between these two results is quite good.

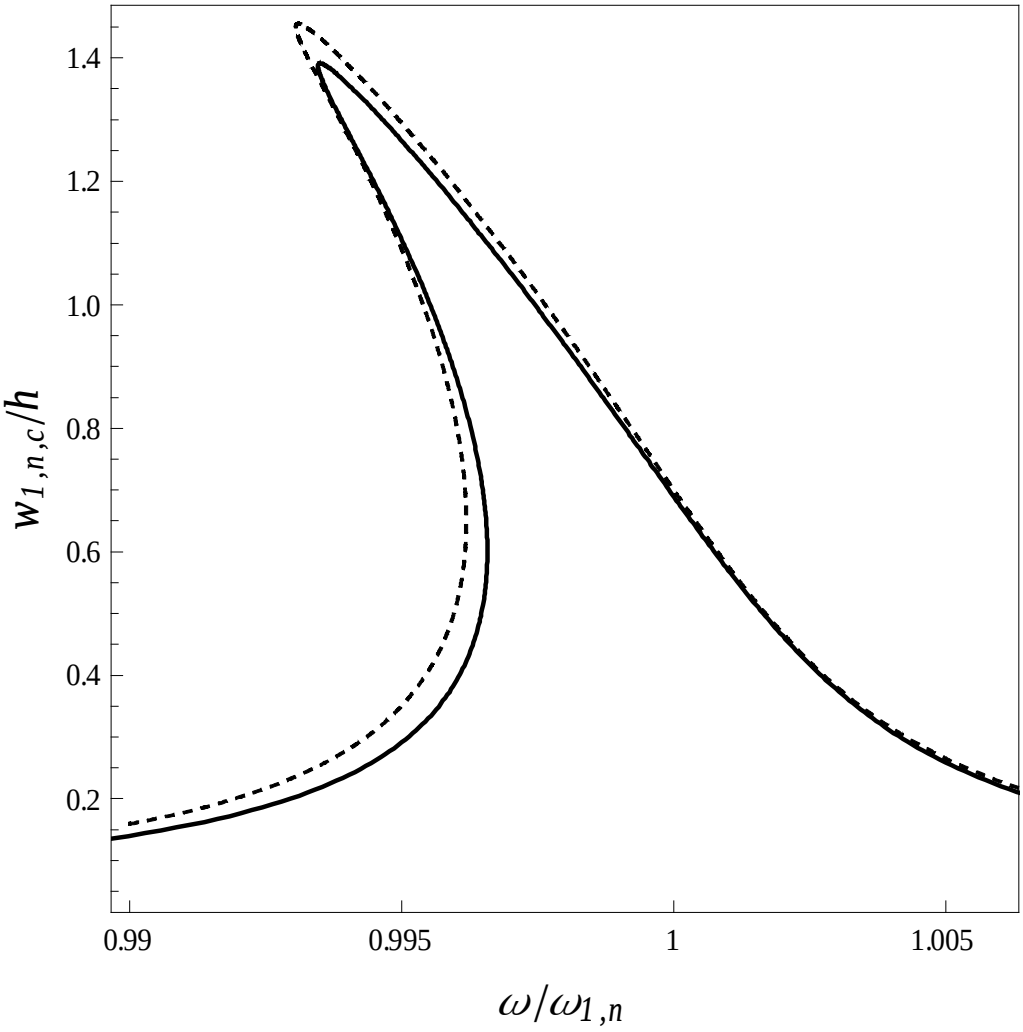

Figure 5.4. Frequency-response curve for the clamped shell obtained by using Chebyshev polynomial expansions (30 dofs) compared with results obtained by Amabili (2003a) with trigonometric functions. ——, 30 dofs, present model with Chebyshev polynomial expansion; – –, results from Amabili (2003a).

6. NONLINEAR VIBRATIONS OF CLAMPED-FREE CIRCULAR CYLINDRICAL SHELLS

6.1 DISCRETIZATION AND BOUNDARY CONDITIONS

Figure 6.1 shows a circular cylindrical shell having radius R, length L and thickness h; a cylindrical coordinate system ($O; x, r, q$) is considered in order to take advantage of the axial symmetry of the structure; the origin is placed at the centre of the clamped end of the shell. The displacements of arbitrary point on the middle surface are: axial $u(x, q, t)$, circumferential $v(x, q, t)$ and radial $w(x, q, t)$. Geometric imperfections are considered in the theory by means of initial radial displacements $w_0(x, q)$ associated to zero initial stress.

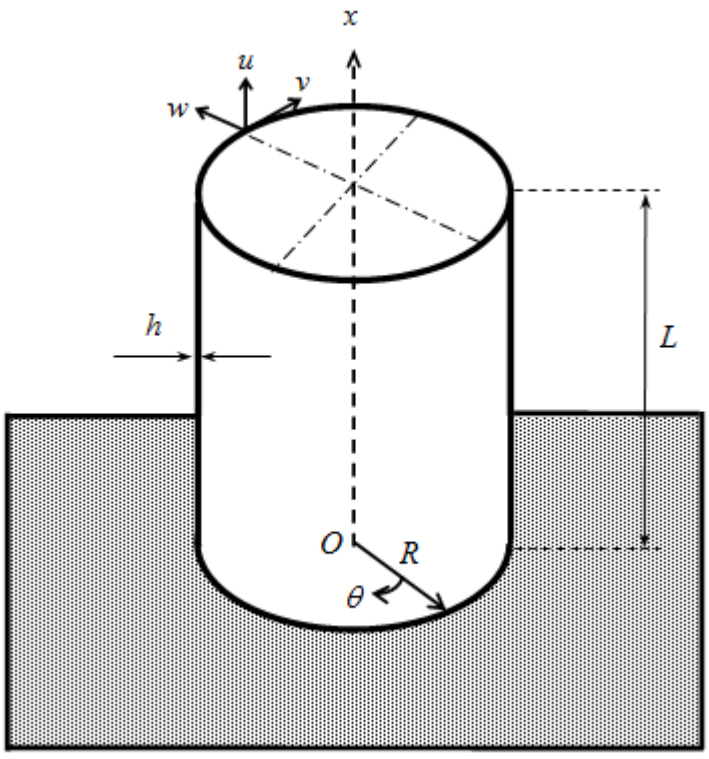

Figure 6.1. Clamped-free circular cylindrical shell: coordinate system and dimensions.

In order to study vibrations of circular cylindrical shell, displacement fields are expanded by means of a double series: the deformation in the circumferential direction is expanded by harmonic functions due to the periodicity of the structure, which is closed on itself, while

Chebyshev polynomials are used for displacements in the axial direction. In particular, the axial coordinate x is rewritten by using the nondimensional variable $h = x/L$, where L is the shell length. This transformation gives, e.g., $\partial / \partial x = (1/L)\partial / \partial h$.

Limiting to a linear analysis at the beginning, let us consider a natural mode of vibration, i.e. a synchronous vibration:

$$\begin{aligned} u(h,q,t) &= U(h,q)\, f(t), \\ v(h,q,t) &= V(h,q)\, f(t), \\ w(h,q,t) &= W(h,q)\, f(t), \end{aligned} \tag{6.1}$$

where functions $U(h,q)$, $V(h,q)$ and $W(h,q)$ represent the mode shape, while $f(t)$ is the time function, which is the same for all the displacements.

As it was mentioned, in order to satisfy boundary conditions, the modal shape is expanded in a double series in terms of harmonic functions and Chebyshev polynomials $T_m^*(h)$:

$$\begin{aligned} U(h,q) &= \sum_{m=0}^{M_U}\sum_{n=0}^{N} U_{m,n,d} T_m^*(h)\cos(nq), \\ V(h,q) &= \sum_{m=0}^{M_V}\sum_{n=0}^{N} V_{m,n,d} T_m^*(h)\sin(nq), \\ W(h,q) &= \sum_{m=0}^{M_W}\sum_{n=0}^{N} W_{m,n,d} T_m^*(h)\cos(nq), \end{aligned} \tag{6.2}$$

where $T_m^*(h) = T_m(2h-1)$ and T_m is the m-*th* order Chebyshev polynomial of the first kind and n is the number of circumferential waves of the mode shape. The transformation of coordinates from h to $2h$-1 is necessary since Chebyshev polynomials are defined between –1 and 1, while $T_{\mathrm{m}}^*(h)$ has been introduced in order to be defined between 0 and 1. In equations (6.2) $U_{m,n,d}$, $V_{m,n,d}$ and $W_{m,n,d}$ are unknown coefficients depending on the integer index m and n; the last subscript d stays for driven mode.

Due to the symmetry of the structure, a second mode, identical to the first one but rotated by $\pi/2n$, is always associated to the one represented by equation (6.2) for any $n \neq 0$. This can be represented by

$$\begin{aligned} U(h,q) &= \sum_{m=0}^{M_U}\sum_{n=1}^{N} U_{m,n,c}T_m^*(h)\sin(nq), \\ V(h,q) &= \sum_{m=0}^{M_V}\sum_{n=1}^{N} V_{m,n,c}T_m^*(h)\cos(nq), \\ W(h,q) &= \sum_{m=0}^{M_W}\sum_{n=1}^{N} W_{m,n,c}T_m^*(h)\sin(nq), \end{aligned} \tag{6.3}$$

where the subscript c indicates companion mode.

If the mode in equation (6.2) is the one directly excited by the external excitation, this is referred as the driven mode. Then, the second mode described by equation (6.3) is referred to as the companion.

Boundary conditions are considered by applying constraints to the free coefficients of expansions (6.2) or (6.3). Some of the coefficients $U_{m,n,d}, V_{m,n,d}, W_{m,n,d}$ (or $U_{m,n,c}, V_{m,n,c}, W_{m,n,c}$) can be suitably chosen in order to satisfy the boundary conditions.

For the clamped-free (clamped at $x = 0$) shell the following boundary conditions are imposed (Koiter, 1963):

$$u = v = w = \frac{\partial w}{\partial x} = 0, \quad \text{at} \quad x = 0, \tag{6.4a}$$

$$N_x = N_{xq} + \frac{M_{xq}}{R} = M_x = Q_x + \frac{\partial M_{xq}}{R\partial q} = 0, \quad \text{at} \quad x = L, \tag{6.4b}$$

where N_x, N_{xq}, M_x, M_{xq}, Q_x are the normal force per unit length in axial direction, shear force per unit length, bending moment per unit length in axial direction, torsion moment per unit length and force normal to the shell per unit length, respectively. It can be observed that boundary conditions (6.4a) are of geometric type, while natural boundary conditions are applied at the free edge of the shell, at $x = L$ (i.e. $h = 1$).

In fact, since the Rayleigh-Ritz method is used to find the solution, just geometric boundary condition has to be exactly satisfied; it means that conditions (6.4b) do not have to be satisfied by the expansion since they will be satisfied by minimization of the system energy. Equation (6.4a) can be rewritten in the following form:

$$U(h,q)=\sum_{m=0}^{M_U}\sum_{n=0}^{N}U_{m,n,d}T_m^*(h)\cos(nq)=0,\quad \text{at}\quad h=0, \tag{6.5a}$$

$$V(h,q)=\sum_{m=0}^{M_V}\sum_{n=0}^{N}V_{m,n,d}T_m^*(h)\sin(nq)=0,\quad \text{at}\quad h=0, \tag{6.5b}$$

$$W(h,q)=\sum_{m=0}^{M_W}\sum_{n=0}^{N}W_{m,n,d}T_m^*(h)\cos(nq)=0,\quad \text{at}\quad h=0, \tag{6.5c}$$

$$\frac{\partial W(h,q)}{\partial h}=\sum_{m=0}^{M_W}\sum_{n=0}^{N}W_{m,n,d}\frac{\partial T_{\mathrm{m}}^*(h)}{\partial h}\cos(nq)=0,\quad \text{at}\quad h=0. \tag{6.5d}$$

Equations (6.5a-d) are valid for any q and n; therefore they are simplified into:

$$\begin{aligned}&\sum_{m=0}^{M_U}U_{m,n,d}T_{\mathrm{m}}^*(h)=0, \qquad \sum_{m=0}^{M_V}V_{m,n,d}T_m^*(h)=0,\\ &\sum_{m=0}^{M_W}W_{m,n,d}T_m^*(h)=0, \qquad \sum_{m=0}^{M_W}W_{m,n,d}\frac{\partial T_m^*(h)}{\partial h}=0,\end{aligned} \quad \text{for } n=0,1... \quad \text{at} \quad h=0. \tag{6.6a-d}$$

This linear algebraic system is solved in terms of the coefficients $U_{0,n,d},V_{0,n,d},W_{0,n,d},W_{1,n,d}$, for $n=0,1...$; these coefficients can be obtained exactly in terms of the remaining ones.

6.2 LINEAR VIBRATIONS

The linear analysis is obtained by using Sanders–Koiter shell theory (see Chapter 2), in which only linear terms in the strain-displacement relationships are retained. Since the shell with clamped-free edges does not present a simple closed-form solution, the solution is obtained solving numerically an eigenvalue problem.

Equations (6.1) and (6.2) or (6.3) are inserted into the expressions of kinetic and potential energies (see Chapter 2); in particular, the nonlinear terms are neglected. Then a set of ordinary differential equations is obtained by using the Lagrange equations. These equations can be immediately decoupled in the variable *q*.

An intermediate step is the reordering of variables. A vector **q** containing all variables is built:

$$\mathbf{q} = [U_{1,0}, U_{2,0}, ..., U_{1,n,d}, U_{2,n,d}, ..., V_{1,0}, V_{2,0}, ..., V_{1,n,d}, V_{2,n,d}, ..., W_{2,0}, W_{3,0}, ..., W_{2,n,d}, W_{3,n,d}, ...] f(t). \tag{6.7}$$

The dimension of the vector **q** is N_{max}. In equation (6.7), both axisymmetric and asymmetric terms are included; for axisymmetric terms the subscript *d* (or *c* in case of companion mode, which gives exactly the same frequency of the driven mode) is omitted since there is a single mode instead of the couple of driven and companion modes. For asymmetric terms, just driven modes can be considered. In fact, companion modes have exactly the same frequency and mode shapes, just exchanging sin and cos functions, as shown by comparing equations (6.2) and (6.3).

The number of variables needed to describe a mode with any number of circumferential waves (after decoupling in *q*) is $M_T = M_U + M_V + M_W - 1$.

The Lagrange equations for free vibrations are

$$\frac{\mathrm{d}}{\mathrm{d}t}\left(\frac{\partial L}{\partial \dot{q}_i}\right) - \frac{\partial L}{\partial q_i} = 0, \quad i = 1, 2, ..., N_{max}, \tag{6.8}$$

where $N_{max} = M_T \times (N+1)$ and $L = T_s - U_s$, being T_S the kinetic energy and U_S the potential energy of the shell, which are given in Appendix A. In these energy expressions, only linear strain-displacement relationship have to used, being the nonlinear relationships used later in the nonlinear analysis.. Using (6.7) and assuming harmonic motion, $f(t) = e^{jwt}$ with *j* being the imaginary unit and *w* the vibration frequency, one obtains

$$\left(-w^2\mathbf{M}+\mathbf{K}\right)\mathbf{q}=\mathbf{0},$$

(6.9)

which is the classical eigenvalue problem in nonstandard form; it gives natural frequencies *w* and mode shapes **q**. In equation (6.9) **M** is the mass matrix, obtained from $\mathrm{d}/\mathrm{d}t\left(\partial L/\partial \dot{q}_{\mathrm{i}}\right)$, and **K** is the stiffness matrix, obtained from $\partial L/\partial q_{\mathrm{i}}$.

The mode shape corresponding to the *j*-th mode is given by equations (6.5), where the coefficients $U_{m,n,d}, V_{m,n,d}, W_{m,n,d}$ are substituted with $U_{m,n}^{(j)}, V_{m,n}^{(j)}, W_{m,n}^{(j)}$, which are the components of the *j*-th eigenvector obtained from equation (6.9). Then, the following functions of the longitudinal variable *h* are introduced

$$\begin{aligned} U^{(j)}(h) &= \sum_{m=0}^{M_U}\sum_{n=0}^{N} U_{m,n}^{(j)} T_m^*(h), \\ V^{(j)}(h) &= \sum_{m=0}^{M_V}\sum_{n=0}^{N} V_{m,n}^{(j)} T_m^*(h), \\ W^{(j)}(h) &= \sum_{m=0}^{M_W}\sum_{n=0}^{N} W_{m,n}^{(j)} T_m^*(h), \end{aligned} \tag{6.10}$$

The vector function $\mathbf{U}^{(\mathrm{j})}(h)=\left(U^{(\mathrm{j})}(h), V^{(\mathrm{j})}(h), W^{(\mathrm{j})}(h)\right)^{\mathrm{T}}$ is the *j*-th eigenfunction vector of the original problem.

Mode shapes are normalized in order to have unit maximum displacement by $U^{(\mathrm{j})}(h)/\max\left(U^{(\mathrm{j})}(h)\right)$, $V^{(\mathrm{j})}(h)/\max\left(V^{(\mathrm{j})}(h)\right)$ and $W^{(\mathrm{j})}(h)/\max\left(W^{(\mathrm{j})}(h)\right)$ for any *h*. For simplicity, the normalized mode shapes will be indicated with $U^{(\mathrm{j})}(h)$, $V^{(\mathrm{j})}(h)$, $W^{(\mathrm{j})}(h)$ in the following part of the paper.

It should be mentioned that, for accurate numerical calculations, a very high numerical accuracy is required in calculating the eigenvectors (mode shapes) and all the coefficients to be introduced in the matrices.

6.3 NONLINEAR RESULTS

Nonlinear analysis is described in the Chapter 4.

The equations of motion have been obtained by using the *Mathematica* 6 computer software (Wolfram, 1999) in order to perform analytical surface integrals of trigonometric and Chebyshev functions. The set of ordinary nonlinear differential equations is studied by using numerical continuation methods and bifurcation analysis. The Lagrange equations are rewritten in vectorial notation and pre-multiplied by the inverse of the mass matrix in order to decouple them. Then, each equation is transformed in two first-order equations. A non-dimensionalization of variables is also performed for computational convenience: the frequencies are non-dimensionalized dividing by the natural frequency of the resonant mode and the vibration amplitudes are divided by the shell thickness h. The resulting 2×dofs equations are studied by using the software AUTO (Doedel *et. all,* 1998) for continuation and bifurcation analysis of nonlinear ordinary differential equations. The software AUTO is capable of continuation of the solution, bifurcation analysis and branch switching by using arclength continuation and collocation methods. In particular, the shell response under harmonic excitation has been studied by using a numerical continuation analysis in two steps: (i) first the excitation frequency has been fixed far enough from resonance and the magnitude of the excitation has been used as bifurcation parameter; the solution has been started at zero force where the solution is the trivial undisturbed configuration of the shell and has been continued up to reach the desired force magnitude; (ii) when the desired magnitude of excitation has been reached, the solution has been continued by using the excitation frequency as bifurcation parameter. The detected pitchfork bifurcations are then followed and Neimark-Sacher bifurcations are detected on the bifurcated branch of the solution.

6.3.1 PERFECT SHELL

An isotropic circular cylindrical shell clamped at $x = 0$ and free at $x = L$ is considered. Calculations have been performed for a shell having the following dimensions and material properties: $L = 0.48$ m, $R = 0.24$ m, $h = 0.254$ mm, $E = 4.65 \times 10^9$ Pa, $r = 1400$ kg/m^3 and $n = 0.38$, which corresponds to the case of a polyester shell experimentally studied by Chiba (1993a,b).

Chebyshev polynomials of 15th power were used to obtain mode shapes of the problem (linear vibration study). The linear analysis shows that the fundamental mode has $n = 7$ circumferential waves and has natural frequency of 28.3 Hz according to the Sanders-Koiter shell theory. A nondimensional excitation in radial direction f_i is introduced, which is related to the dimensional force excitation by $f_i = \dfrac{\text{¥}}{m_i w_{1,n}^2 h}$, where $w_{1,n}$ is the fundamental natural frequency in rad/s and m_i is the modal mass of the shell, i.e. the *i*-th element of the mass matrix **M** in equation (6.9). The modal damping ratio $z = 0.0005$ is used for all modes.

The frequency-response curve of the fundamental mode (1,*n*) with *n*=7, without companion modes participation and without imperfections is shown in Figure 2 for different models. Each model has a different number of degrees of freedom (dofs). In particular, results for 18, 20, 22, 24, 26, 28, 30, 40, 43 and 47 dofs are presented. The response curves become less and less hardening increasing the number of degrees of freedom, reaching convergence for the model with 43 dofs, which shows a very mild softening behavior. In fact, the models with 43 and 47 dofs give almost coincident results as shown in Figure 3. The vibration amplitudes shown in the figures are the maximum amplitudes during an excitation period and they are shown at $x = L$, i.e. at the free edge of the shell where the largest vibration amplitudes is observed. In particular, the model with 43 dofs has the following generalized coordinates: for *w* and *u*, all the generalized coordinates with subscripts (1,*n*,*c*), (1,2*n*,*c*), (1,3*n*,*c*), (2,*n*,*c*), (2,2*n*,*c*), (3,*n*,*c*), (3,2*n*,*c*) plus the first 11 axisymmetric modes, i.e. (1,0), (2,0), (3,0), …, (11,0); for *v*, the same as *u* and *w* but

without axisymmetric modes since torsional axisymmetric modes are uncoupled from bending modes. The model with 47 dofs has the same generalized coordinates with the addition of two axisymmetric modes for both *w* and *u*: (12,0) and (13,0).

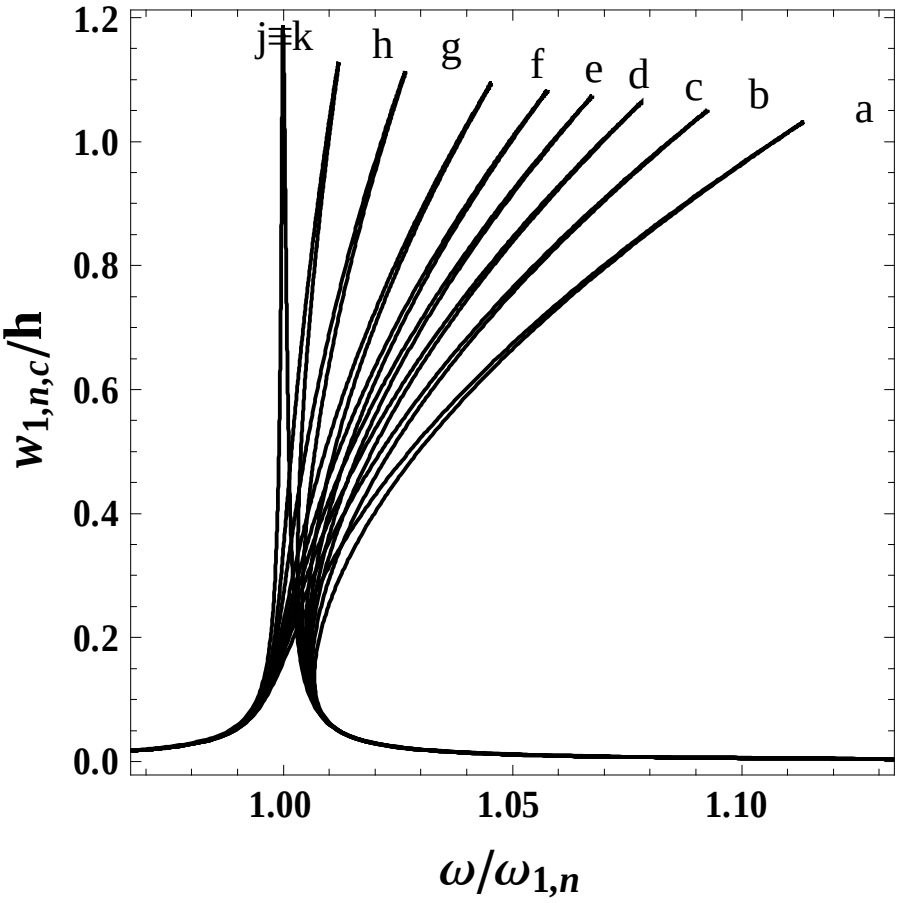

Figure 6.2. Frequency-response curve of the fundamental mode, without companion modes participation; no imperfections. Study of the convergence of the solution by comparison of models with different number of degrees of freedom (dofs): a, 18 dofs; b, 20 dofs; c, 22 dofs; d, 24 dofs; e, 26 dofs; f, 28 dofs; g, 30 dofs; h, 40 dofs; j, 43 dofs; k, 47 dofs. Nondimensional excitation f_1=0.0012.

The smallest model in Figure 6.2, i.e. the one with 18 dofs, uses the following generalized coordinates: for *w* and *u*, coordinates (1,n), (1,2n), (3,n), (3,2n) plus the first 3 axisymmetric modes; for *v*, the same as *u* and *w* but without axisymmetric modes. In the models with 20 to 30 degrees of freedom, an additional axisymmetric mode is progressively added for both *w* and *u*. The 40 dofs model has the same generalized coordinates of the previous models but the first 13

axisymmetric modes are included for both *w* and *u*. All these results have been obtained by using the base of natural modes; this applies also to axisymmetric modes.

6.3.1.1 "ARTIFICIAL" AXISYMMETRIC MODES VERSUS NATURAL AXISYMMETRIC MODES

The result of the convergence study shows that a large number of axisymmetric modes, at least 11 for each one of the displacements *w* and *u*, must be used in order to obtain accurate results. Therefore about half of the degrees of freedom are used by models in Figure 6.3 for axisymmetric generalized coordinates.

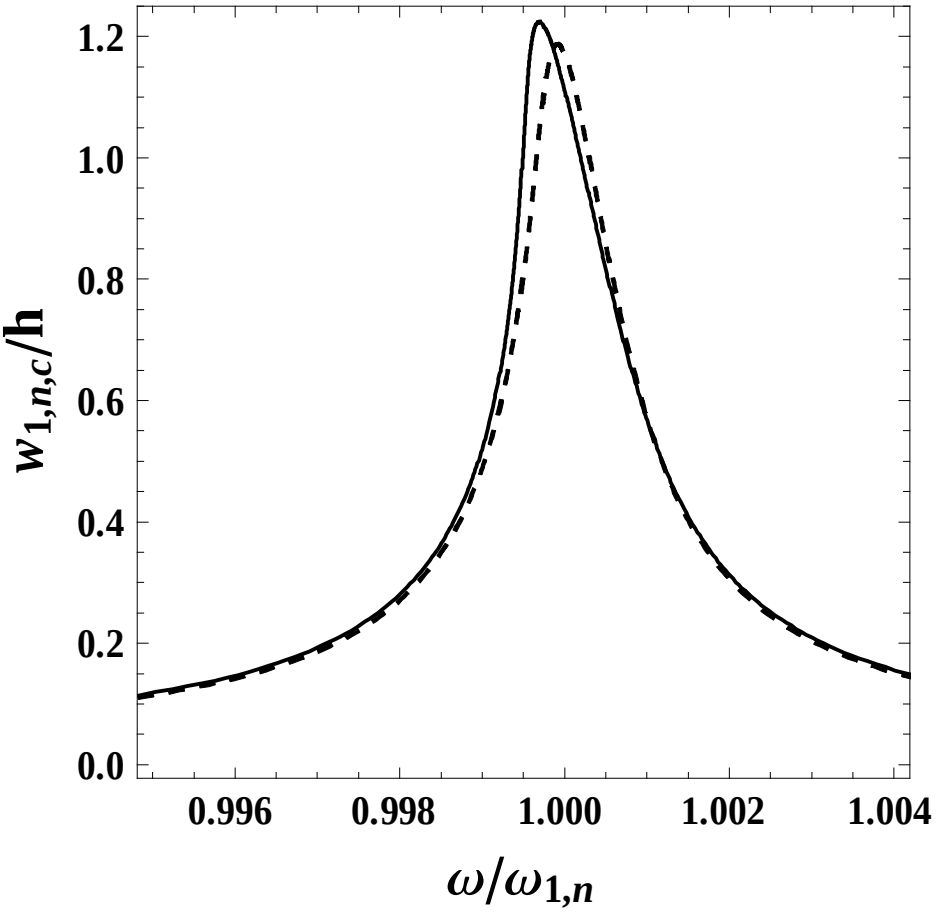

Figure 6.3. Frequency-response curve of the fundamental mode, without companion modes participation; no imperfections. Comparison of models with 43 dofs (dashed line) and 47 dofs (solid line). Nondimensional excitation f_1=0.0012.

It must be observed that, (i) axisymmetric modes have high natural frequency so they are evaluated with less accuracy in the linear eigenvalue analysis, (ii) the generalized coordinates corresponding to axisymmetric modes have much smaller amplitudes than the other coordinates during flexural vibrations. Therefore, it is convenient to reduce the number of axisymmetric modes in the model, but at the same time it is necessary to keep the accuracy of the solution. In order to do that, the natural axisymmetric modes are replaced by "artificial" axisymmetric modes. These "artificial" axisymmetric modes are build by taking the axial shape of the asymmetric modes with n circumferential waves (n = 7 in the present case) and making them artificially axisymmetric. The advantage of this technique is that asymmetric modes have much lower natural frequency and therefore the mode shapes can be evaluated with more accuracy.

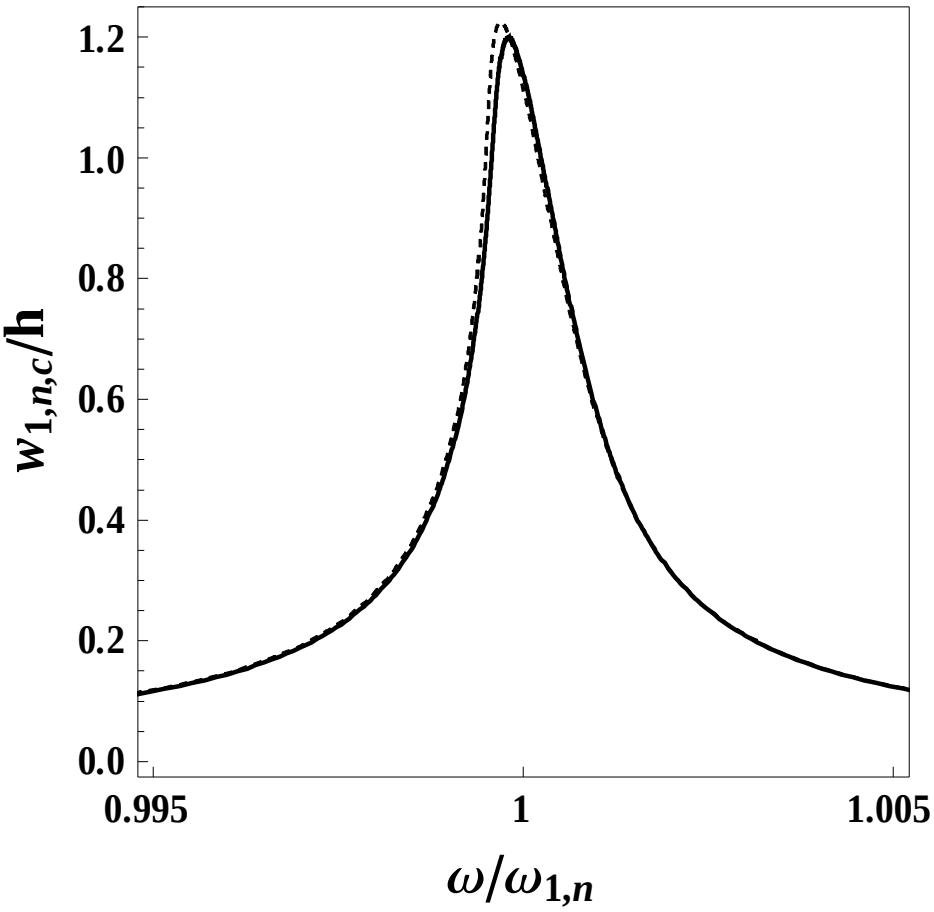

Figure 6.4. Frequency-response curve of the fundamental mode, without companion modes participation; no imperfections. Comparison of the model with "artificial" axisymmetric modes, 31 dofs (solid line), and the model with "natural" axisymmetric modes, 47 dofs (dashed line). Nondimensional excitation f_1=0.0012.

Figure 6.4 shows the frequency-response curve of the fundamental mode without companion modes participation and no imperfections obtained with the model with 31 dofs using "artificial" axisymmetric modes versus the 47 dofs model with natural modes. The 31 dofs model with "artificial" axisymmetric modes has the same generalized coordinates of the 47 dofs model but uses only the first 5 axisymmetric modes for bout *w* and *u* instead of 13, therefore reducing the model of 16 dofs. The two response curves are almost coincident, showing the efficiency of using "artificial" axisymmetric modes in reducing the order of the model.

A convergence study of the models with "artificial" axisymmetric modes is shown in Figure 6.5, where frequency-response curves obtained by using models with 22, 28, 31 and 37 degrees of freedom are compared. Excluding the model with 22 dofs, which is clearly inaccurate, the other three models present similar results.

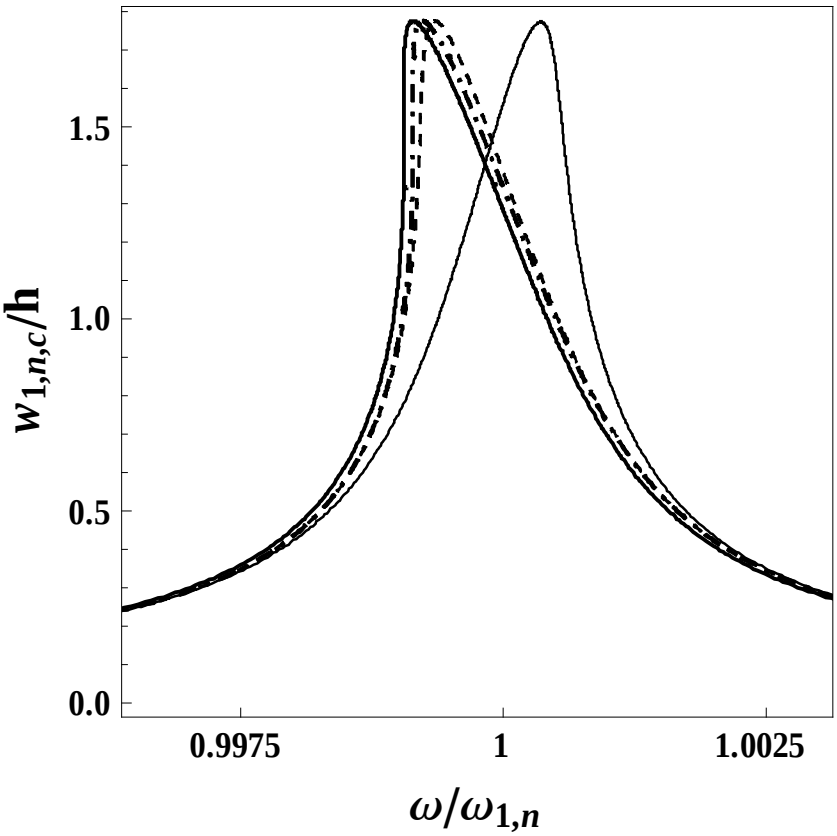

Figure 6.5. Frequency-response curve of the fundamental mode, without companion modes participation (using "artificial" axisymmetric modes); no imperfections. Study of the convergence of the solution by comparison of models with different degrees of freedom: —, 22 dofs; – –, 28 dofs; –·–, 31 dofs; ▬▬, 37dofs. Nondimensional excitation f_1=0.0018.

The 22 dofs model has the following generalized coordinates: for w and u the coordinates with subscript (1,n), (1,2n), (3,n), (3,2n) plus the first 5 "artificial" axisymmetric modes; for v, the same as u and w but without axisymmetric modes. The 28 dofs model has the same coordinates of the 22 dofs model with the addition of (2,n) and (2,2n) for all the three displacements. The 31 dofs model has the coordinates of the 28 dofs model with the addition of (1,3n) for all the three displacements. Finally, the 37 dofs model has the coordinates of the 31 dofs model with the addition of (2,3n) and (3,3n) for all the three displacements. Sample of equations for AUTO 97 should be found in Appendix B, namely for system with 37 dofs.

6.3.2 COMPANION MODE PARTICIPATION

In this section, a model with 52 dofs is used with the same generalized coordinates with "artificial" axisymmetric modes used in the 31 dofs model in Figure 6.5. It must be observed that now both driven (subscript c) and companion (subscript s) coordinates are used for all asymmetric modes; this doubles the degrees of freedom of modes that are not axisymmetric.

The frequency-response curve of the fundamental mode (1,n) with n=7, with companion modes participation and without imperfections, is shown in Figure 6.6 for nondimensional excitation f_1=0.0025.

This level of excitation is enough to obtain pitchfork bifurcation of the driven mode giving rise to a second branch of the solution with companion mode participation. The appearance of these pitchfork bifurcation and of the second branch is due to 1:1 internal resonance between driven and companion modes that, due to the axial symmetry of the perfect shell, have exactly the same natural frequency. The first pitchfork bifurcation of branch one is observed near the peak of the response on branch 1; the second bifurcation is near the exact linear resonance. Along the second branch, the response of the shell is a combination of cosine and sine modes in circumferential direction with some phase difference, giving nodes travelling around the shall (travelling wave) instead of fixed nodes as in linear vibrations. For the axial

symmetry of the shell, the travelling wave can be in clockwise or anti-clockwise direction around the shell according to initial conditions or transient history. On branch 1 there is no companion mode participation.

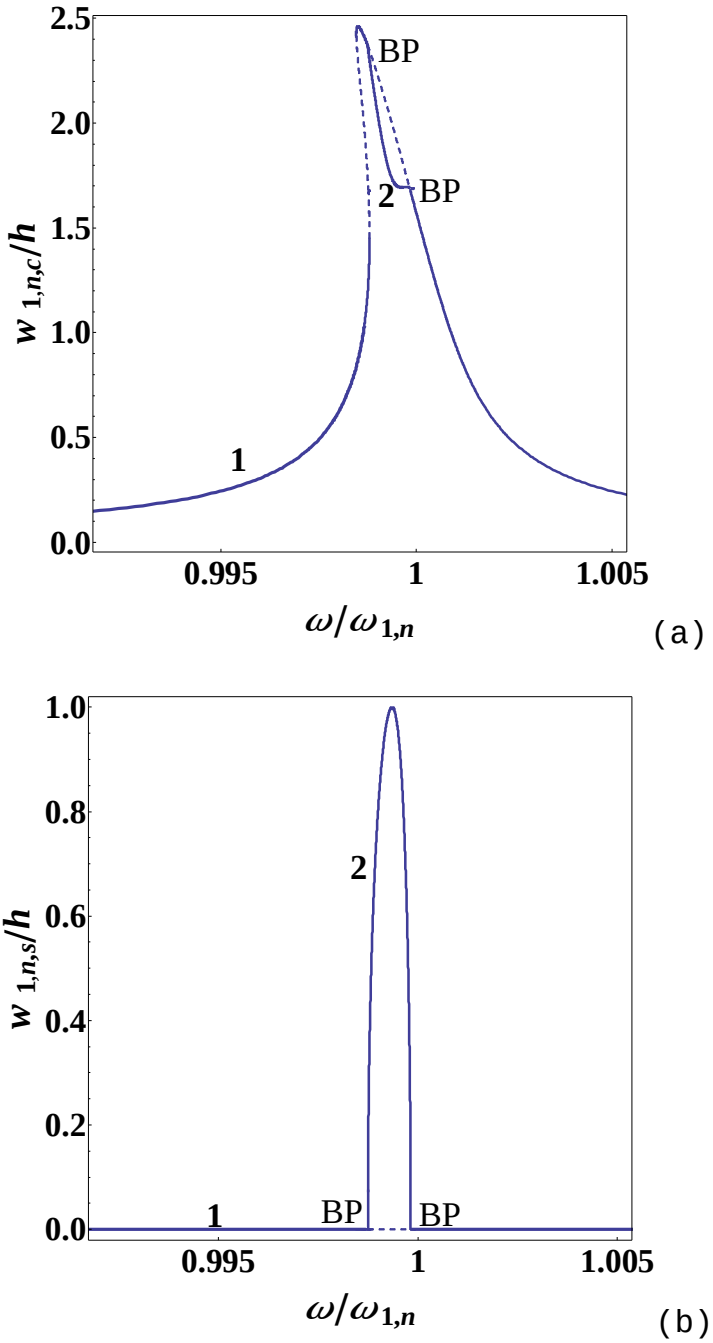

Figure 6.6. Frequency-response curve for the fundamental mode of the perfect shell with companion mode participation; 52 dofs model, nondimensional excitation f_1=0.0025. —, stable periodic solution; −·−, stable quasi-periodic solution; – –, unstable solutions; BP, pitchfork bifurcation; TR, Neimark-Sacker bifurcation; 1, branch 1; 2, branch 2. (a) Maximum of the generalized coordinate $w_{1,n,c}$; (b) maximum of the generalized coordinate $w_{1,n,s}$.

If a lower excitation level is used, e.g. f_1=0.0015, no pitchfork bifurcations are detected and the shell response is without companion mode participation. Increasing the excitation level to f_1=0.0033, the frequency-response curve shown in Figure 6 is modified into the one given in Figure 6.7.

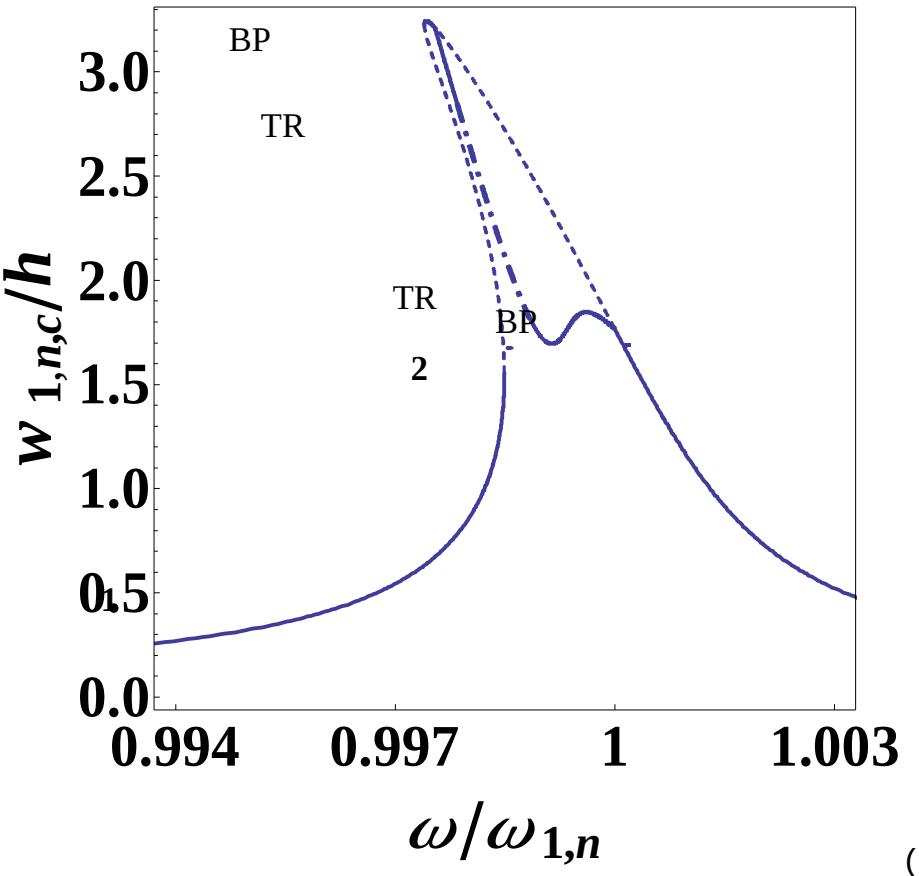

(a)

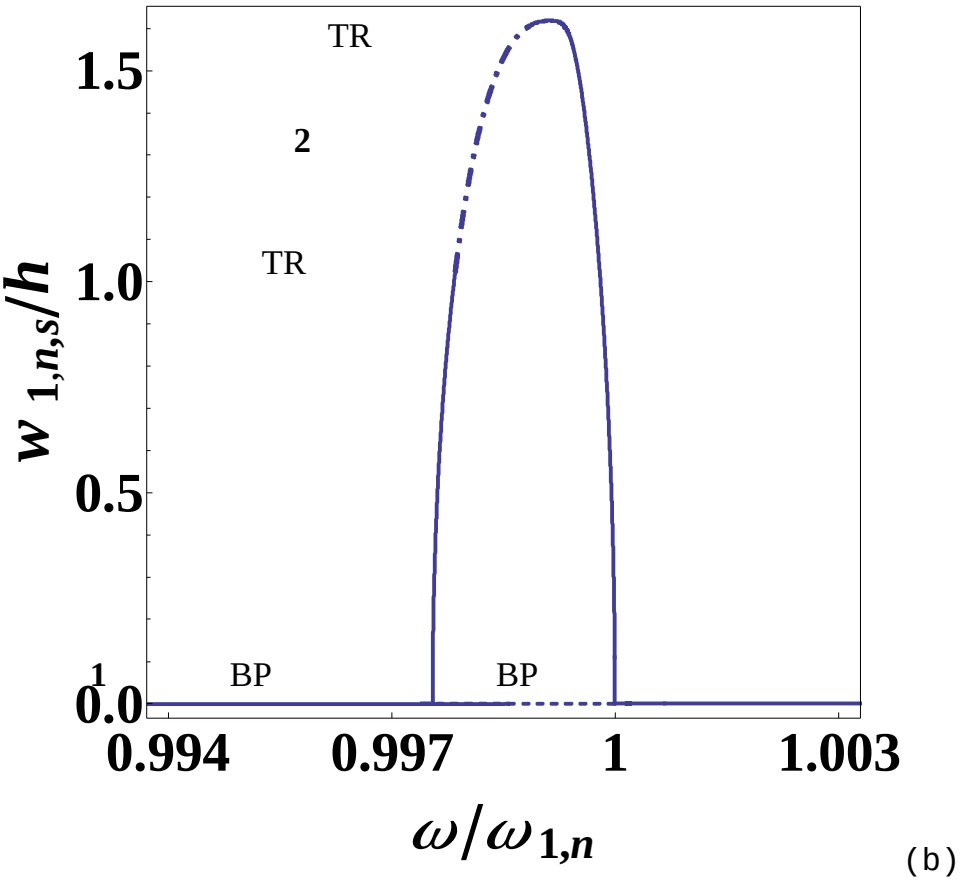

Figure 6.7. Frequency-response curve for the fundamental mode of the perfect shell with companion mode participation; 52 dofs model, nondimensional excitation f_1=0.0033. —, stable periodic solution; −·−, stable quasi-periodic solution; – –, unstable solutions; BP, pitchfork bifurcation; TR, Neimark-Sacker bifurcation; 1, branch 1; 2, branch 2. (a) Maximum of the generalized coordinate $w_{1,n,c}$; (b) maximum of the generalized coordinate $w_{1,n,s}$.

The main differences are that, (i) branch 2 extends over a larger frequency range around the linear resonance (i.e. $w/w_{1,n}=1$), (ii) the amplitude of the driven ($w_{1,n,c}$) and companion ($w_{1,n,s}$) coordinates is now almost equal on branch 2 near the linear resonance giving rise to a pure travelling wave response around the shell and, (iii) the response on branch 2 presents two Neimark-Sacker bifurcations. The shell response on branch 2 comprised between the two Neimark-Sacker bifurcations is quasi-periodic, i.e. it presents amplitude modulations. The response to harmonic excitation shown in Figure 6.7 is typical of circular cylindrical shells

without geometric imperfections and has been previously observed for simply supported and clamped shells, see e.g. Amabili (2008).

Increasing even more the excitation level to f_1=0.005, the frequency-response curve becomes the one given in Figure 6.8. Here a saturation phenomenon is observed on both branches. The shape of branch 1 is changed and the previous response peak is cut by an almost horizontal line appearing with a Neimark-Sacker bifurcation at vibration amplitude about 3.4*h*. After a second Neimark-Sacker bifurcation, the response on this horizontal line returns to be a stable periodic response without companion mode participation. Brach 2 appears with a single pitchfork bifurcation near the exact linear resonance. It presents almost the same amplitude of amplitude of the driven ($w_{1,n,c}$) and companion ($w_{1,n,s}$) coordinates, giving rise practically to a pure travelling wave. Two Neimark-Sacker bifurcations are detected on branch 2, giving rise to a quasi-periodic response as in Figure 6.7.

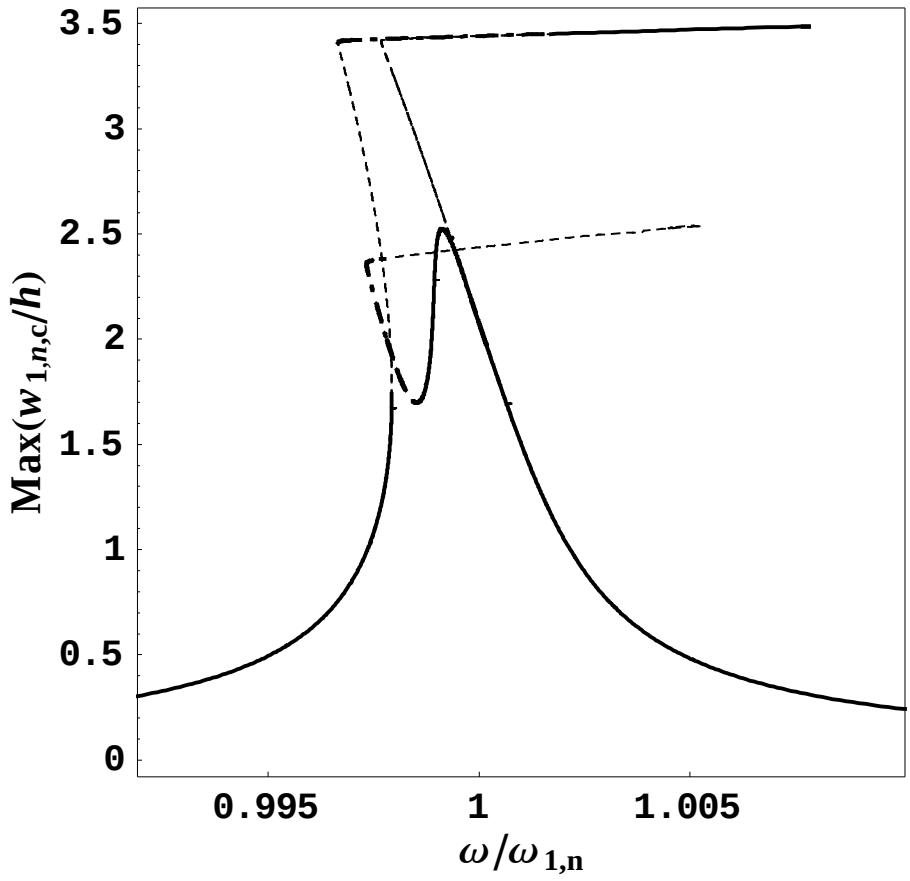

(a)

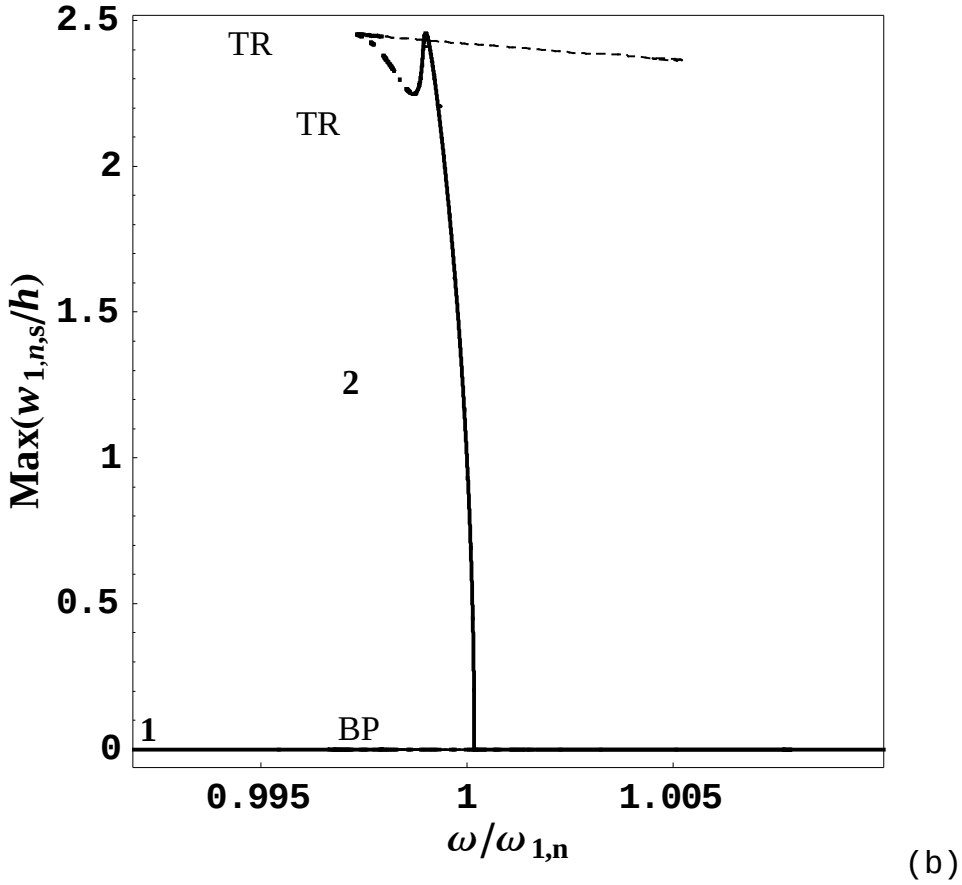

Figure 6.8. Frequency-response curve for the fundamental mode of the perfect shell with companion mode participation; 52 dofs model, nondimensional excitation f_1=0.005. —, stable periodic solution; −·−, stable quasi-periodic solution; – –, unstable solutions; BP, pitchfork bifurcation; TR, Neimark-Sacker bifurcation; 1, branch 1; 2, branch 2. (a) Maximum of the generalized coordinate $w_{1,n,c}$; (b) maximum of the generalized coordinate $w_{1,n,s}$.

Anyway, before the lowest frequency Neimark-Sacker bifurcation, the response loses stability on branch 2, differently from Figure 6.7, showing an unstable almost horizontal response that can be interpreted again as a kind of saturation. Being more precise, the saturation response is at vibration level 2.4h for both the driven and companion coordinates and, while for one coordinate it has a slight positive slope, for the other coordinate the slope is negative. But globally, it respects the condition $\sqrt{w_{1,n,c}^2 + w_{1,n,s}^2} \cong 3.4h$, indicating again a saturation phenomenon at vibration amplitude about 3.4h.

In order to better understand the shell response in Figure 8, additional generalized coordinates are shown in Figure 6.9. The in-plane coordinates associated to the main driven and companion coordinates are shown in Figures 6.9(a-c). They are slaves coordinates, reproducing the response of the main driven ($w_{1,n,c}$) and companion ($w_{1,n,s}$) coordinates. The coordinate $w_{1,3n,c}$ instead shows in Figure 6.9(d) that it is activated at the saturation, where some energy is transferred to this coordinate. The first axisymmetric coordinate is shown in Figure 6.9(e) showing generally a negative value, indicating that an axisymmetric contraction is necessary in order to keep the quasi-inextensibility of the shell during large-amplitude vibrations. This is the reason why, even if axisymmetric displacements are small, they must be retained in the expansion of w and u since in-plane stretching would erroneously introduce a strong hardening behavior of the shell.

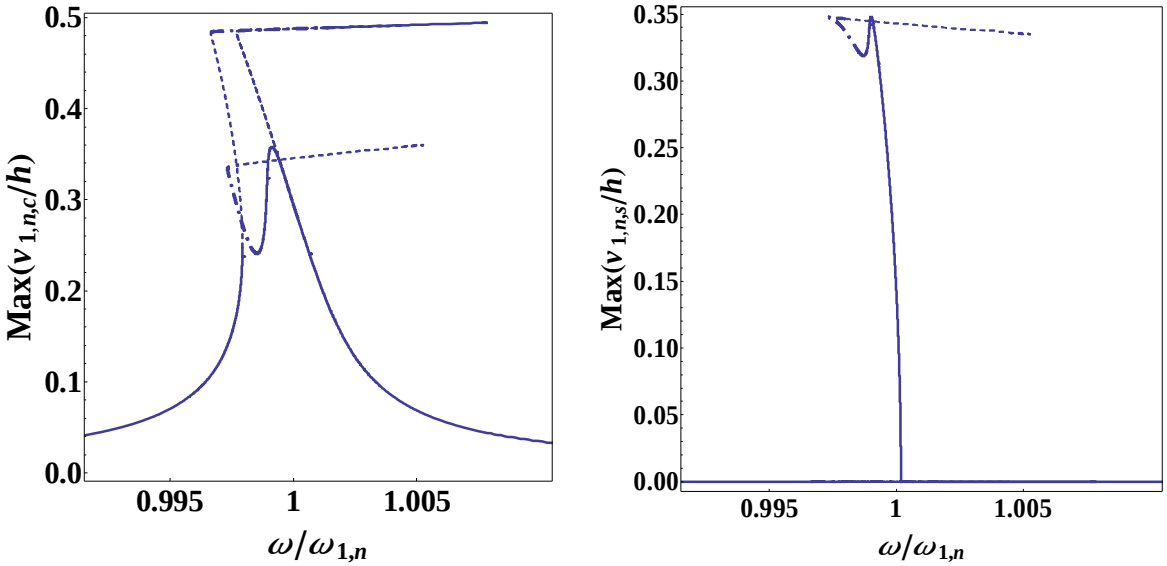

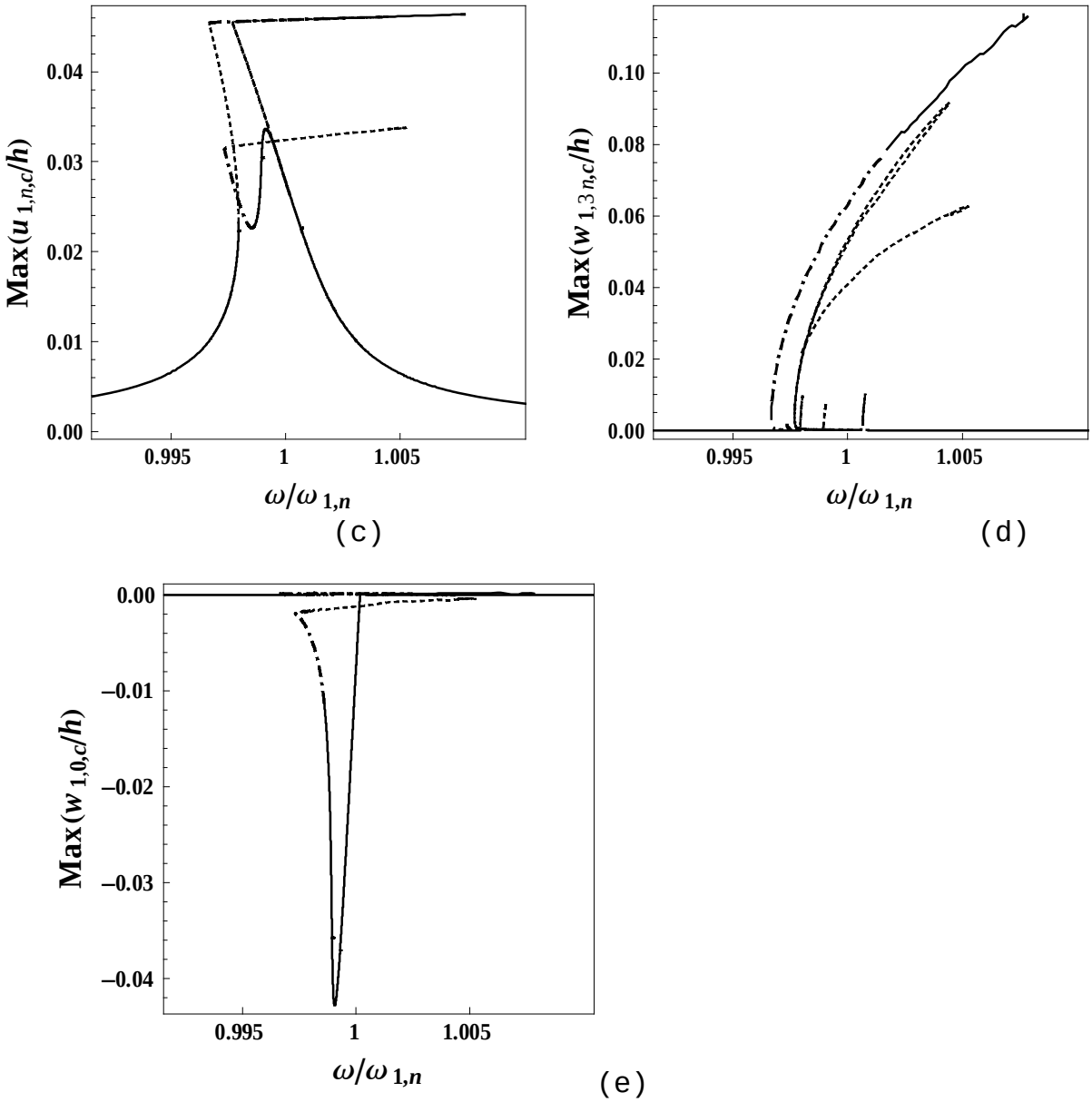

Figure 6.9. Frequency-response curve for perfect shell with companion mode participation; 52 dofs model, nondimensional excitation f_1=0.005. —, stable periodic solution; −·−, stable quasi-periodic solution; – –, unstable solutions; (a) Maximum of generalized coordinate $v_{1,n,c}$; (b) maximum of generalized coordinate $v_{1,n,s}$; (c) maximum of generalized coordinate $u_{1,n,c}$; (d) maximum of generalized coordinate $w_{1,3n,c}$; (e) maximum of generalized coordinate $w_{1,0,c}$.

Results in the time-domain, for the nonlinear response shown in Figure 8 and 9, are presented in Figure 6.10 for excitation frequency $w = 0.9986\,w_{1,n}$, i.e. at a specific point in the horizontal axes of Figures 6.8 and 6.9 corresponding to response on branch 2 of the solution with companion mode participation. Figure 6.10(a) shows the harmonic excitation. Comparing the

time responses of the generalized coordinates to the excitation, the relative phase angle can be obtained. Also, comparing Figure 6.10(b), driven mode, and Figure 6.10(c), companion mode, the relative phase angle can be observed, which leads to a travelling wave around the shell. At this specific excitation frequency, not a pure travelling wave is obtained because the phase angle is different from $p/2$ and the amplitudes of driven and companion modes is also different. The in-plane coordinates $v_{1,n,c}$ and $v_{1,n,s}$ are clearly slave of the corresponding $w_{1,n,c}$ and $w_{1,n,s}$, respectively, as shown in Figures 6.10(d,e). The generalized coordinate $w_{1,2n,c}$ presents two periods for an excitation period, showing its double frequency response in Figure 6.10(f). The same is observed for the first axisymmetric coordinate $w_{1,0,c}$ in Figure 6.10(g), which also shows always negative values representing axisymmetric double-frequency contraction.

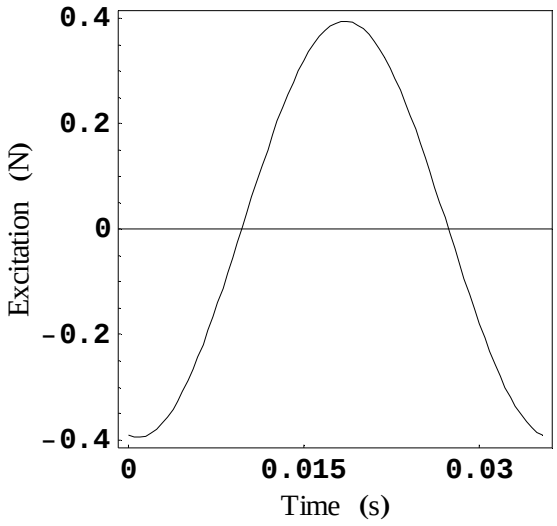

(a)

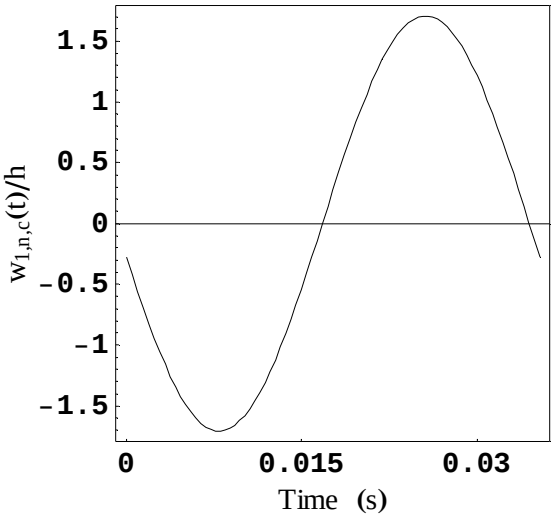

(b)

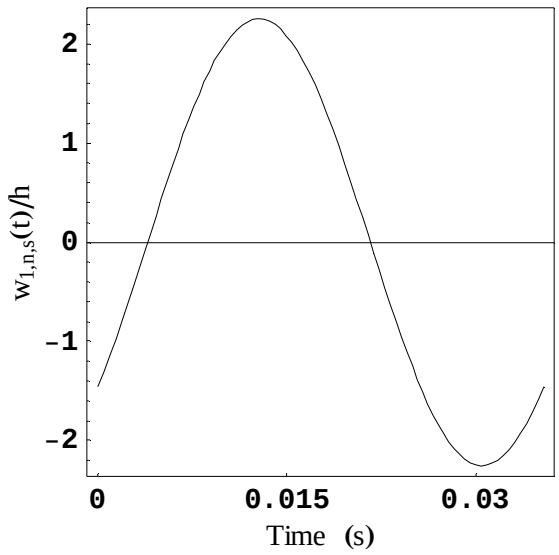

(c)

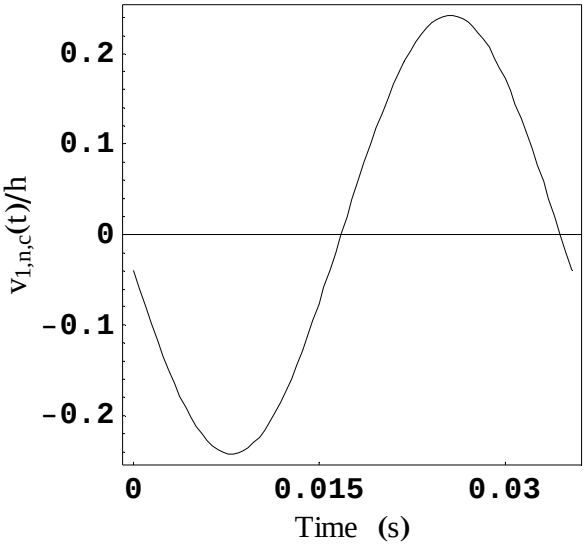

(d)

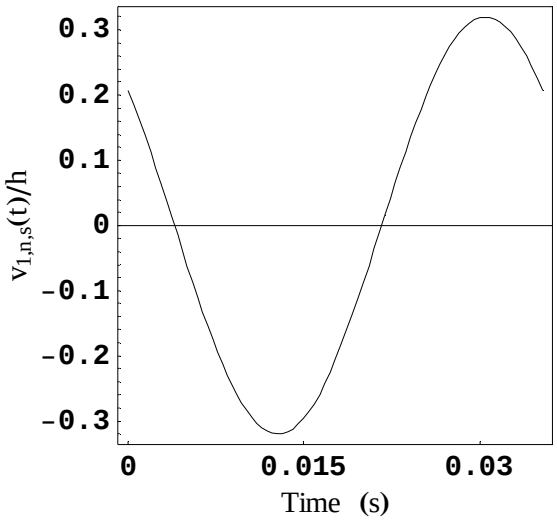

(e)

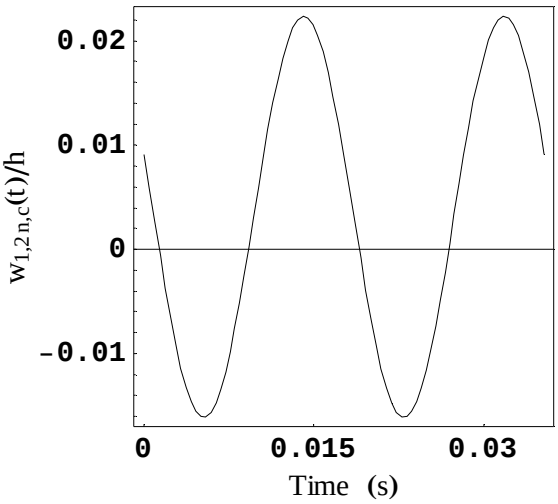

(f)

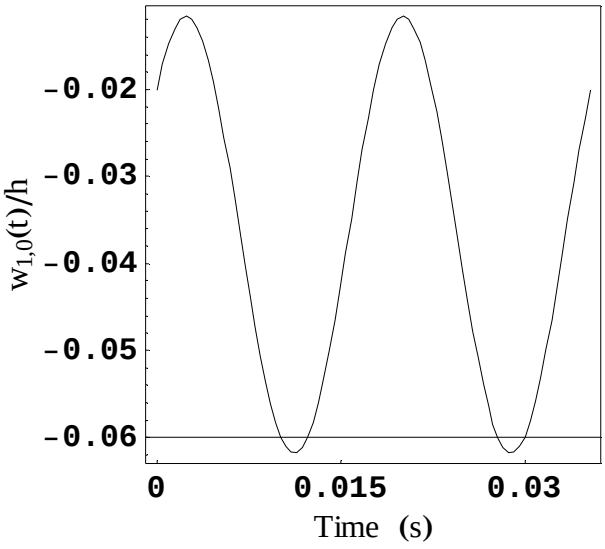

(g)

Figure 6.10. Time response of the shell with companion mode participation showing a travelling wave response; 52 dofs model, nondimensional excitation f_1=0.005, excitation frequency $w = 0.9986 w_{1,n}$. (a) Excitation; (b) generalized coordinate $w_{1,n,c}$; (c) generalized coordinate $w_{1,n,s}$; (d) generalized coordinate $v_{1,n,c}$; (e) generalized coordinate $v_{1,n,s}$; (f) generalized coordinate $w_{1,2n,c}$; (g) generalized coordinate $w_{1,0,c}$.

6.3.3 EFFECT OF GEOMETRIC IMPERFECTIONS AND COMPARISON TO EXPERIMENTS

Figure 6.11 shows the comparison of the frequency-response curve of the fundamental mode of the perfect shell without companion modes participation (model with 37 dofs previously used in Figure 6.5) with the experimental backbone curve from Chiba (1993a).

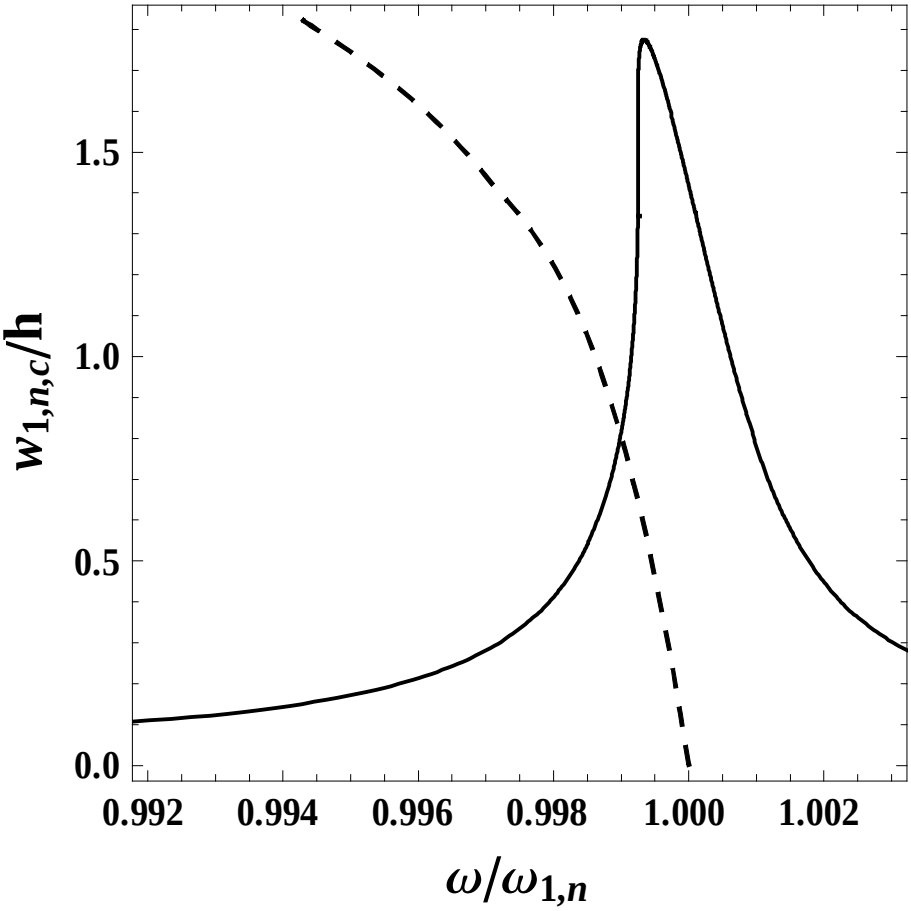

Figure 6.11. Comparison of the frequency-response curve of the fundamental mode of the perfect shell without companion modes participation (model with 37 dofs) with the experimental backbone curve from Chiba (1993a). Nondimensional excitation f_1=0.0018.

The backbone curve represents the nonlinear free vibration response, and should pass through the peak of the forced vibration response. A nondimensional excitation f_1=0.0018 has been used. Figure 6.11 clearly shows a significant difference between the computed and experimental results by Chiba. However, the calculation are for a perfect shell. For circular cylindrical shells with different boundary condition it has been shown that geometric imperfection can change the nonlinear response. For this reason, here the effect of geometric

imperfection is investigated in order to understand if the difference between numerical and experimental results can be attributed to geometric imperfections.

Initially the effect of geometric imperfection with shape corresponding to the first natural mode with circumferential shape cos(2$n\theta$), where n = 7 as in previous cases, is considered. This imperfection changes the natural frequencies of the shell introducing a frequency split between the fundamental driven and companion modes, that had before exactly the same natural frequency, as shown in Figure 6.12.

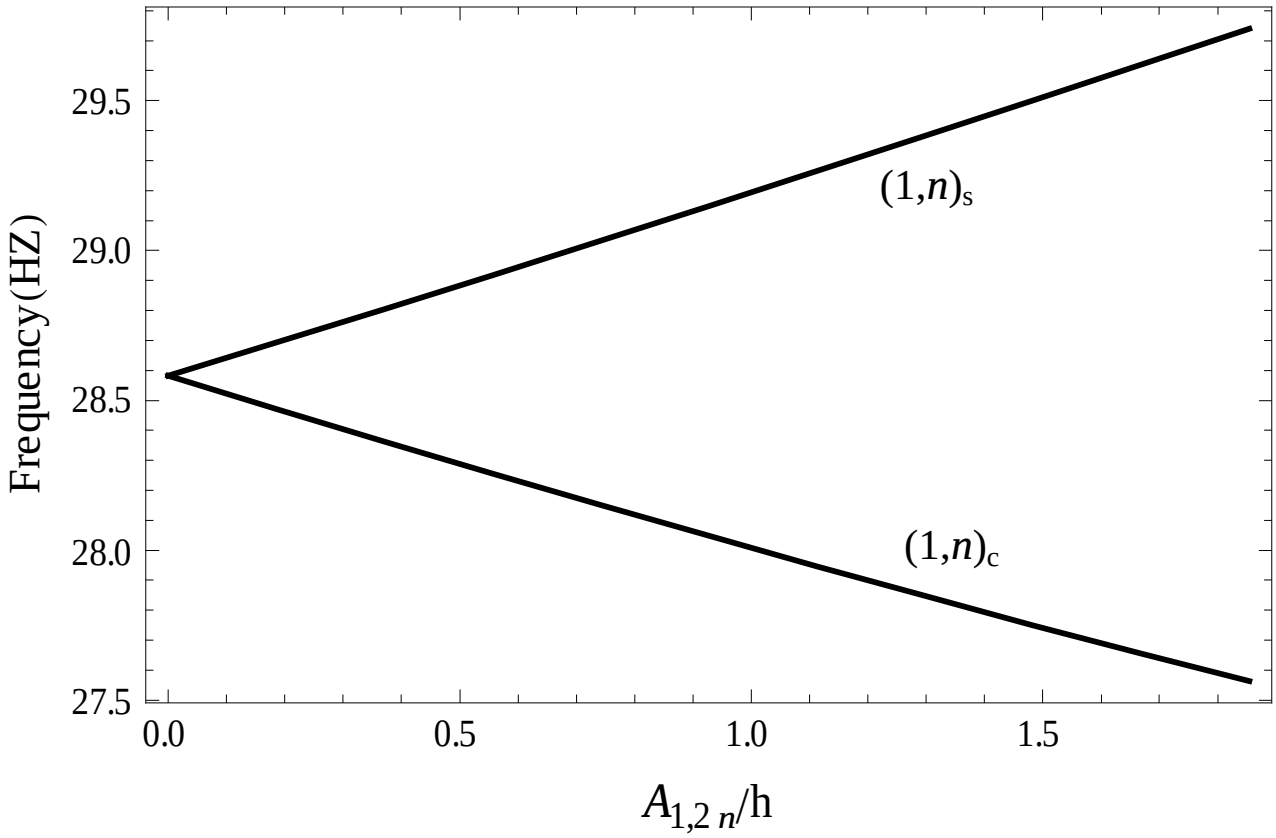

Figure 6.12. Fundamental natural frequencies of the shell versus imperfection with shape corresponding to the first natural mode with circumferential shape cos(2$n\theta$), where n = 7 as in previous cases. Natural frequency of driven mode, $\left(w_{1,n}\right)_c$, and of companion mode, $\left(w_{1,n}\right)_s$.

Results presented in Figure 6.12 have been obtained by using the simpler Donnell shell theory retaining in-plane inertia; this is the reason why the natural frequency of the perfect shell

(for zero imperfection) is slightly higher than the 28.3 Hz previously indicated. The effect of the geometric imperfection of amplitude 2h with circumferential shape cos(2$n\theta$) on the nonlinear response is shown in Figure 6.13 and is quite modest. Therefore, this geometric imperfection plays a small role. The same imperfection is increased to the amplitude 10h, which is a very large unrealistic value for this type of imperfection, in Figure 6.14, but still its effect is modest.

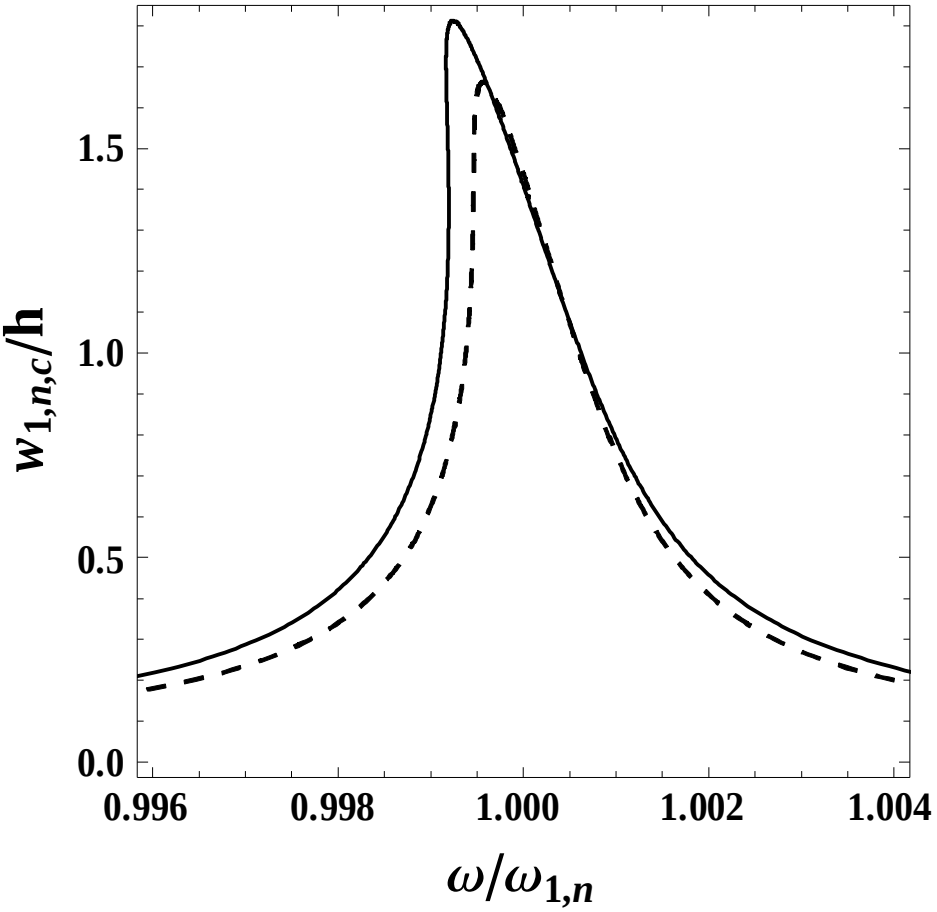

Figure 6.13. Frequency-response curve (dashed line) of the shell having imperfection with shape corresponding to the first natural mode with cos(2$n\theta$) and maximum amplitude of imperfection 2h (model with 37 dofs). Solid line, frequency-response curve of the perfect shell. Nondimensional excitation f_1=0.0018.

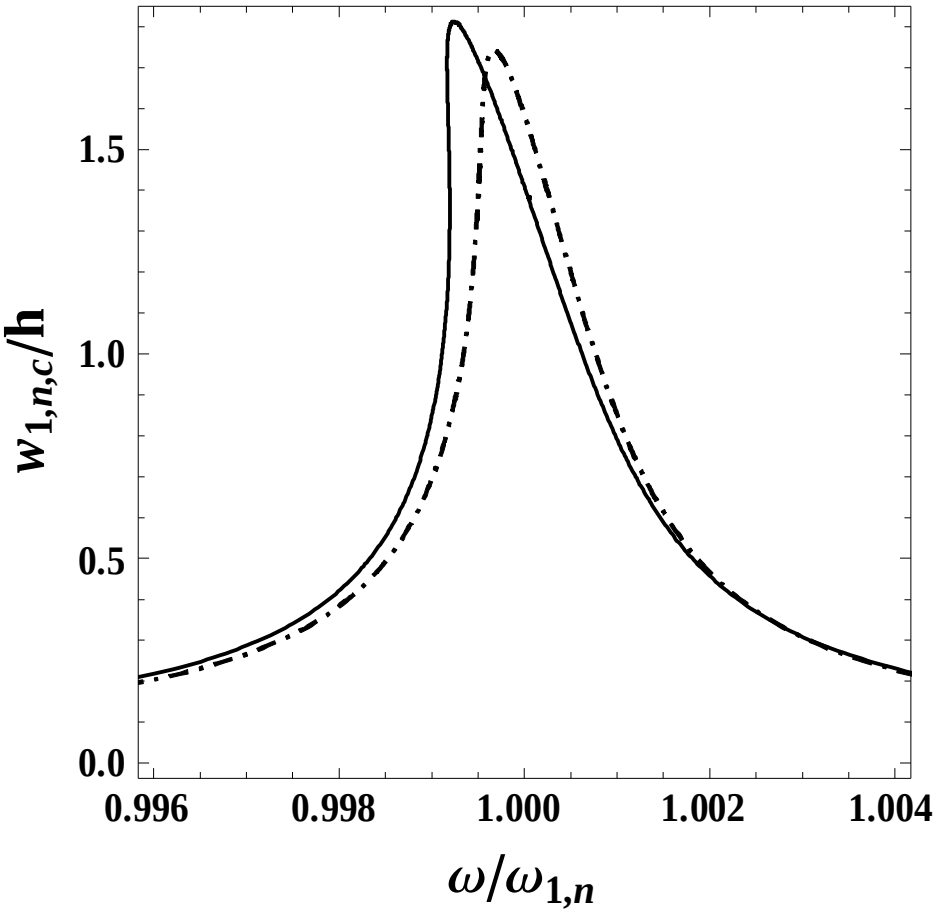

Figure 6.14. Frequency-response curve (dashed line) of the shell having imperfection with shape corresponding to the first natural mode with cos(2$n\theta$) and maximum amplitude of imperfection 10h, (model with 37 dofs). Solid line, frequency-response curve of the perfect shell. Nondimensional excitation f_1=0.0018.

The effect of imperfections of amplitude 2h with circumferential shape cos($n\theta$) and sin($n\theta$) is investigated in Figure 6.15. The effect of these imperfections on the nonlinear response is really very small.

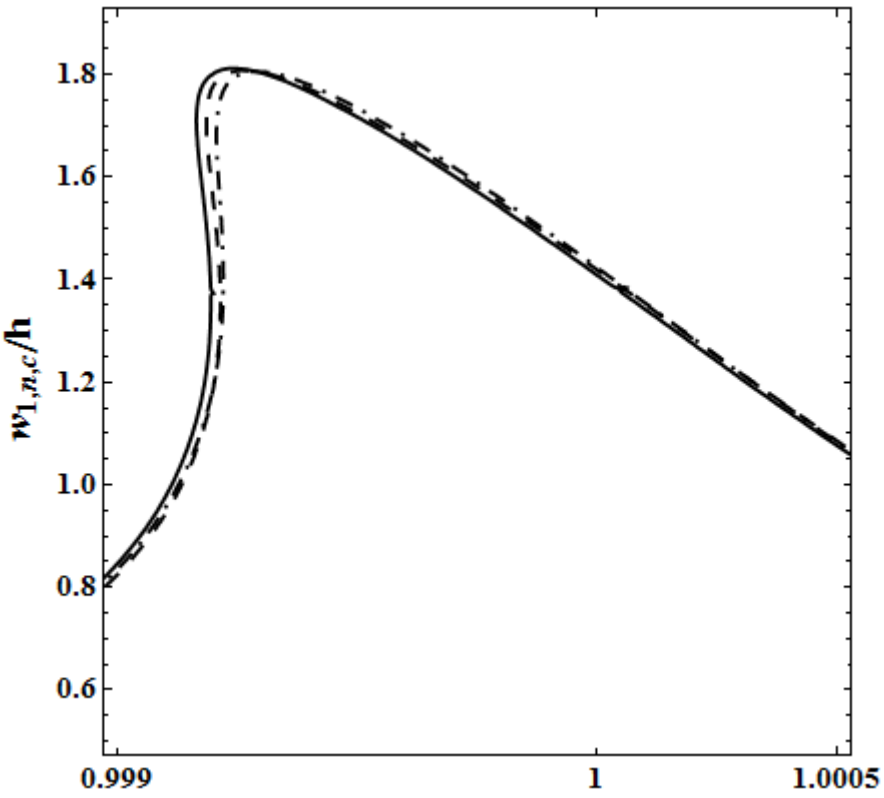

Figure 6.15. Frequency-response curve of the shell having imperfection of maximum amplitude 2*h* with shape corresponding to the fundamental mode. Solid line, perfect shell; dashed line, imperfection on mode sin($n\theta$); dashed-dotted line, imperfection on mode cos($n\theta$). Nondimensional excitation f_1=0.0018.

A shell with geometric axisymmetric imperfection of maximum amplitude 10*h* with the shape of the first axisymmetric mode is investigated in Figure 6.16. The effect of this type of imperfection is large, but it makes the shell response of hardening type. Therefore, this imperfection would increase the difference between the numerical and experimental results.

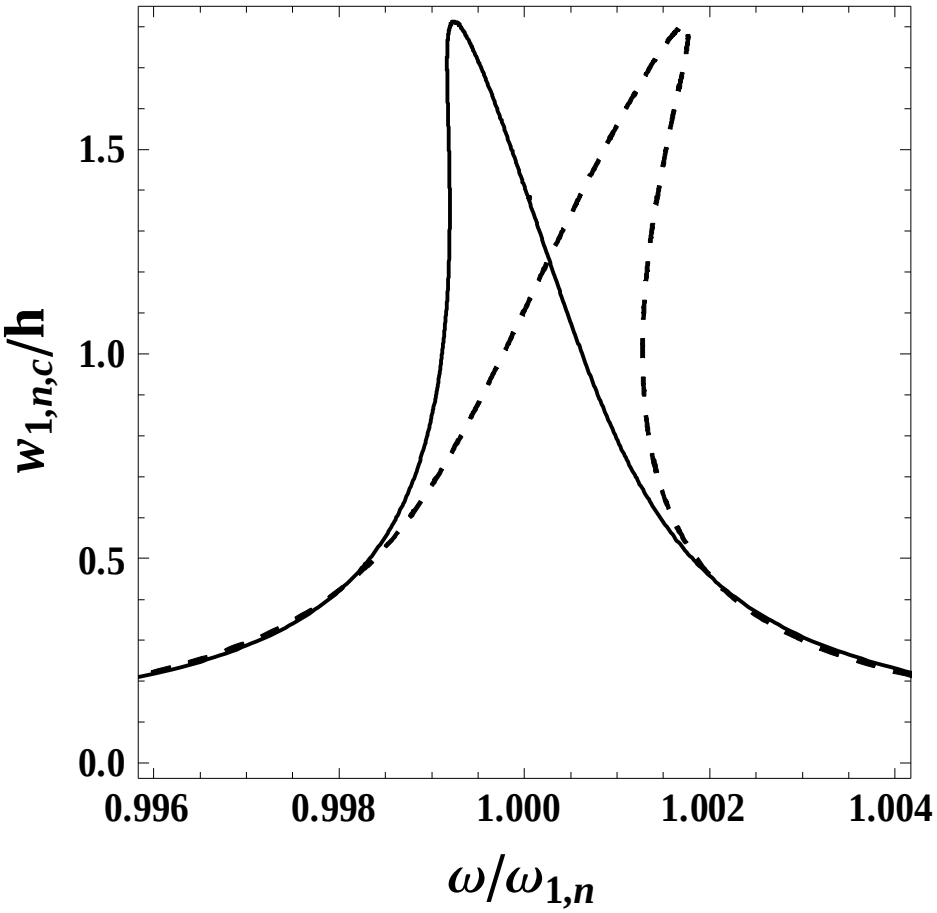

Figure 6.16. Frequency-response curve of the shell having axisymmetric imperfection of maximum amplitude 10*h* with the shape of the first axisymmetric mode (dashed line, 37 dofs). Solid line, frequency-response curve of the perfect shell. Nondimensional excitation f_1=0.0018.

The comparison of the frequency-response curves (without companion modes participation, 40 dofs model) of the fundamental mode of the shell having imperfections with the shape of the first mode cos(2θ) and different amplitudes is shown in Figure 6.17. The experimental backbone curve by Chiba (1993a) is also presented. The effect of maximum imperfection amplitude 3*h*, 4*h* and 5*h* at the tip is shown. Ovalization imperfections can be very large due to the manufacturing process of shells, so these values are all realistic. Figure 6.17 shows that these imperfections increase significantly the softening type behavior of the shell, reducing and eventually cancelling, in the case of imperfection amplitude 4*h*, the difference between the numerical and experimental results. Here it can be observed that the experimental shell tested by Chiba (1993a) was obtained by a polyester sheet with lap-joined seam, which can

easily lead to ovalization imperfection of the magnitude introduced. Unfortunately the actual geometry of the shell is not given, so it is impossible to know the actual value of the imperfections in Chiba's shell. The 40 dofs model used in the calculation has the same generalized coordinates of the 37 dofs model previously used, with the addition of coordinates (1,2,c) for *u*, *v* and *w*. The introduction of these additional coordinates is fundamental in order to obtain accurate results. The addition of additional coordinates, as (1,4,c), do not change the solution.

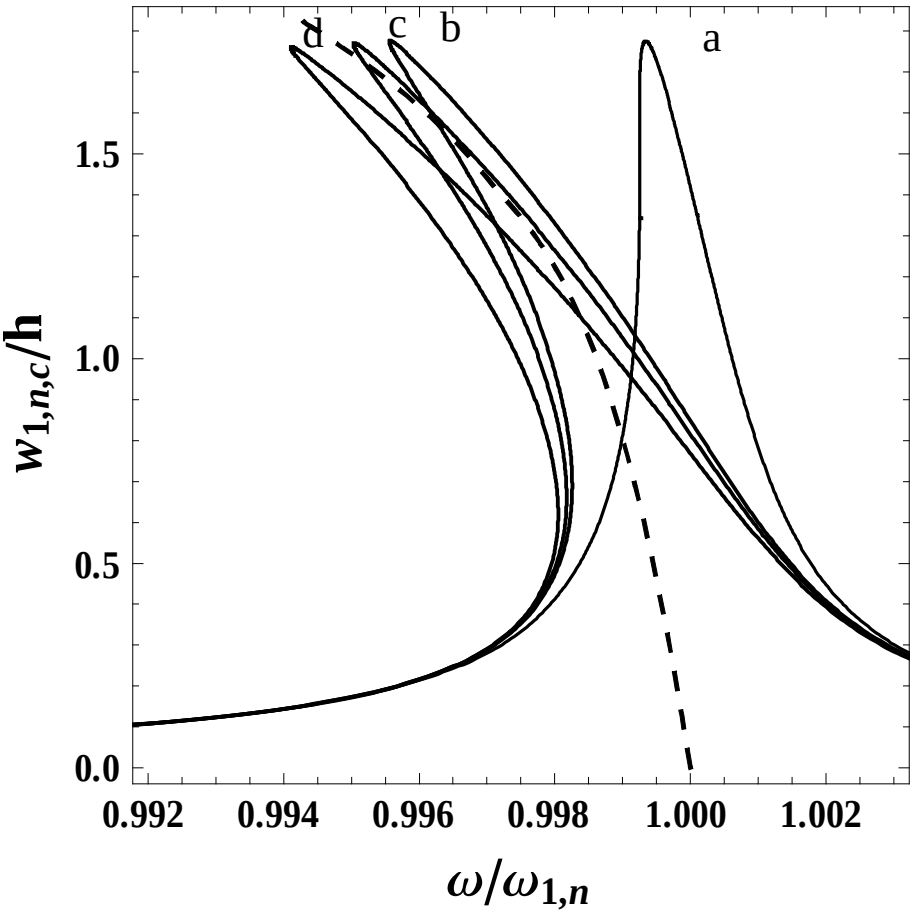

Figure 6.17. Comparison of the frequency-response curves (without companion modes participation, 40 dofs) of the fundamental mode of the shell having imperfections with the shape of the first mode cos(2θ) and different amplitudes. The experimental backbone curve by Chiba [30] is also shown as dashed line. a, perfect shell; b, imperfection with maximum amplitude 3*h*; c, imperfection with maximum amplitude 4*h*; d, imperfection with maximum amplitude 5*h*. Nondimensional excitation f_1=0.0018.

The fundamental natural frequency of the shell is changed significantly by the introduction of the ovalization imperfection, as shown in Figure 6.18. Anyway, this imperfection does not introduce any frequency split between the driven and companion modes.

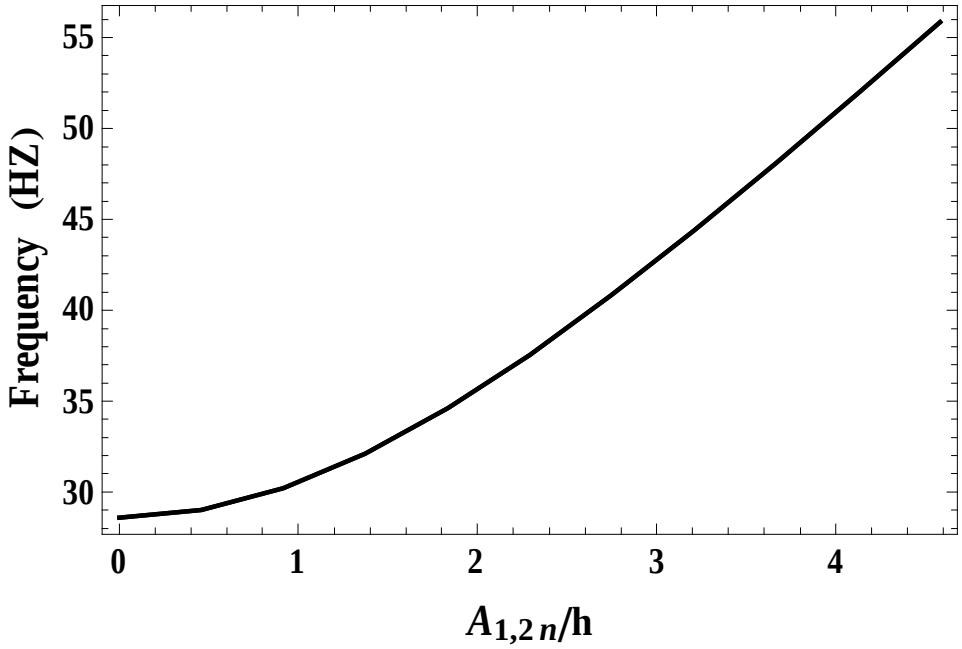

Figure 6.18. Natural frequency of the fundamental mode versus imperfection with shape corresponding to the first natural mode with circumferential shape cos(2θ).

CONCLUSIONS AND FUTURE WORK

The response of circular cylindrical shells with different boundary conditions has been studied by using Sanders-Koiter and Donnell theories. Displacements have been expanded by means of a double series: deformation in the circumferential direction is expanded by using trigonometric functions, while Chebyshev or ordinary power polynomials are applied to expand the displacements in the axial direction.

The approach used in the present study has the advantage of being suitable for different boundary conditions, and of being very flexible to structural modifications without complication of the solution procedure. Comparison of present results with results available in literature has been carried out, showing good agreement.

A minimum mode expansion necessary to capture the nonlinear response of the shell in the neighbourhood of a resonance has been determined and convergence of the solution has been numerically investigated for both simply supported and clamped shells. Models with about 20 degrees of freedom show very good convergence of results. They can be slightly reduced, but of a few units, and still presenting reasonably good results. In order to have a further reduction of the model, specific techniques can be used, as the nonlinear normal modes; otherwise the in-plane inertia has to be neglected. However, this further reduction can be paid with some loss of accuracy.

Nonlinear response of clamped-free circular cylindrical shells, available before only from experiment of Chiba (1993a), has been computed. Calculations has shown that for these boundary conditions mode expansion, necessary to capture the nonlinear response of the shell in the neighbourhood of a resonance, should have more modes than for cases of simply supported and clamped-clamped shells. Therefore approach allowing to reduce number of degrees of freedom is presented. Influence of imperfections on quality of system behaviour is also studied.

While simply supported shells and clamped-clamped shells are pretty well studied, clamped-free shells still represent a wide field for research. Future investigations should include study of complex nonlinear dynamics and chaos, fluid-structure interaction including clamped-free shell conveying flow. In the last case both the nonlinear vibrations under harmonic excitation and the shell stability under flow must be studied. The stability can be lost by pitchfork or Hopf bifurcations, the first one giving divergence (similar to buckling) and the second one giving flutter (dynamic oscillating instability). Also non-harmonic and impact (transient) excitations must be still studied and more experiments should be performed in order to measure the geometric imperfections on the shells tested.

Some experimental results on complex nonlinear dynamics of clamped-free shells are available but no theory is available yet to explain them. For example, Païdoussis and Denise (1972) during their experiments on clamped-free shell conveying fluid observed flutter phenomenon of the general character.

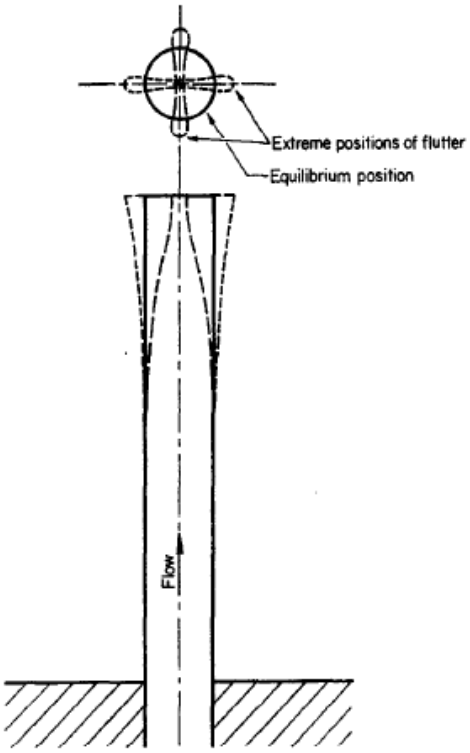

Observed flutter of a cantilever shell, Païdoussis and Denise (1972).

It was observed that, if the cantilever is sufficiently short (so that it remains stable with respect to the flexural instability to fairly high flows), another form of instability occurs spontaneously above a certain critical flow velocity: the cantilever vibrates in the second circumferential mode of a circular cylindrical shell, at fairly high frequency; the vibrations are mainly confined to the region of the free end and generate a shrill sound (see Figure). If the cantilever is not so short, this instability is then superposed on the flexural one. This and other phenomena of complex shell dynamics still need to be investigated theoretically.

Comparison of present thesis results with results available in literature showed good agreement, approving the efficiency of the proposed technique, which allow further studies of shells with different boundary conditions. Flexibility of the proposed technique should be used not only for studying of other poor investigated types of boundary conditions, but for studying of thin-walled structures with different geometries as well.

REFERENCES

A. ABE, Y. KOBAYASHI and G. YAMADA 2000 *Journal of Sound and Vibration* **234**, 405-426. Non-linear vibration characteristics of clamped laminated shallow shells.

V. L. AGAMIROV and A. S. VOL'MIR 1959 *Izvestiya Akademii Nauk SSSR, Ordelenie Tekhnicheskykh Nauk, Mekhanika i Mashinostroeni* **3**, 78-83. Behaviour of cylindrical shells under dynamic loading by hydrostatic pressure or by axial loading (in Russian). It was published in English in 1961 by *ARS Journal (Journal of the American Rocket Society)* **31**, 98-101.

M. AMABILI 2008 Nonlinear Vibrations and Stability of Shells and Plates. New York, USA: Cambridge University Press.

M. AMABILI 2003a *Journal of Sound and Vibration*, Vol. 264, No. 5, pp. 1091-1125. Comparison of shell theories for large-amplitude vibrations of circular cylindrical shells: Lagrangian approach.

M. AMABILI 2003b *AIAA Journal*, Vol. 41, No. 6, 1119-1130. Nonlinear vibrations of circular cylindrical shells with different boundary conditions.

M. AMABILI 2003c *Journal of Sound and Vibration* Vol. 262, No. 4, pp. 921-975. Theory and experiments for large-amplitude vibrations of empty and fluid-filled circular cylindrical shells with imperfections.

M. AMABILI, R. GARZIERA and A. NEGRI 2002 *Journal of Fluids and Structures* **16**, 213-227. Experimental study on large-amplitude vibrations of water-filled circular cylindrical shells.

M. AMABILI and M. P. PAÏDOUSSIS 2003 *Applied Mechanics Reviews*, Vol. 56, No. 4, 349-381. Review of studies on geometrically nonlinear vibrations and dynamics of circular cylindrical shells and panels, with and without fluid-structure interaction.

M. AMABILI, M. PELLEGRINI AND M. TOMMESANI 2003 *Journal of Sound and Vibration*, Vol. 260, No. 3, pp. 537-547. Experiments on large-amplitude vibrations of a circular cylindrical panel.

M. AMABILI, F. PELLICANO and M. P. PAÏDOUSSIS 1998 *Journal of Fluids and Structures* **12**, 883-918. Nonlinear vibrations of simply supported, circular cylindrical shells, coupled to quiescent fluid.

M. AMABILI, F. PELLICANO and M. P. PAÏDOUSSIS 1999a *Journal of Fluids and Structures* **13**, 785-788. Addendum to "Nonlinear vibrations of simply supported, circular cylindrical shells, coupled to quiescent fluid".

M. AMABILI, F. PELLICANO and M. P. PAÏDOUSSIS 1999b *Journal of Sound and Vibration* **225**, 655-699. Non-linear dynamics and stability of circular cylindrical shells containing flowing fluid. Part I: stability.

M. AMABILI, F. PELLICANO and M. P. PAÏDOUSSIS 1999c *Journal of Sound and Vibration* **228**, 1103-1124. Non-linear dynamics and stability of circular cylindrical shells containing flowing fluid, Part II: large-amplitude vibrations without flow.

M. AMABILI, F. PELLICANO and M. P. PAÏDOUSSIS 1999d *Journal of Fluids and Structures* **13**, 159-160. Further comments on the nonlinear vibrations of cylindrical shells.

M. AMABILI, F. PELLICANO and M. P. PAÏDOUSSIS 2000a *Journal of Sound and Vibration* **237**, 617-640. Non-linear dynamics and stability of circular cylindrical shells containing flowing fluid, Part III: truncation effect without flow and experiments.

M. AMABILI, F. PELLICANO and M. P. PAÏDOUSSIS 2000b *Journal of Sound and Vibration* **237**, 641-666. Non-linear dynamics and stability of circular cylindrical shells containing flowing fluid, Part IV: large-amplitude vibrations with flow.

M. AMABILI, F. PELLICANO and A. F. VAKAKIS 2000c *ASME Journal of Vibration and Acoustics* **122**, 346-354. Nonlinear vibrations and multiple resonances of fluid-filled, circular shells, Part 1: equations of motion and numerical results.

I. Y. AMIRO and N. Y. PROKOPENKO 1999 *International Applied Mechanics* **35**, 134-139. Study of nonlinear vibrations of cylindrical shells with allowance for energy dissipation.

I. V. ANDRIANOV and E. G. KHOLOD 1993 *Journal of Sound and Vibration* **165**, 9-17. Non-linear free vibration of shallow cylindrical shell by Bolotin's asymptotic method.

I. V. ANDRIANOV, E. G. KHOLOD and V. I. OLEVSKY 1996 *Journal of Sound and Vibration* **194**, 369-387. Approximate non-linear boundary value problems of reinforced shell dynamics.

A. ARGENTO and R. A. SCOTT 1993b *Journal of Sound and Vibration* **162**, 323-332. Dynamic instability of layered anisotropic circular cylindrical shells, Part II: numerical results.

S. Ashley 2001. *Scientific American.* Warp/drive Underwater.

S. ATLURI 1972 *International Journal of Solids and Structures* **8**, 549-569. A perturbation analysis of non-linear free flexural vibrations of a circular cylindrical shell.

V. BIRMAN and C. W. BERT 1987 *International Journal of Non-Linear Mechanics* **22**, 327-334. Non-linear beam-type vibrations of long cylindrical shells.

V. BIRMAN and P. TWINPRAWATE 1988 *Journal of Applied Mathematics and Physics (ZAMP)* **39**, 768-775. Free nonlinear vibrations of statically loaded long cylindrical shells.

M. N. BISMARCK-NASR 1992 *ASME Applied Mechanics Reviews* **45**, 461-482. Finite element analysis of aeroelasticity of plates and shells.

B. BUDIANSKY 1968 *ASME Journal of Applied Mechanics* **35**, 393-401. Notes on nonlinear shell theory.

L. CHEIKH, C. PAUCHON, C.-H. LAMARQUE, A. COMBESCURE and R. J. GIBERT 1996 *Mechanics Research Communications* **23**, 151-164. Nonlinear stability of a defective cylindrical shell.

J. C. CHEN and C. D. BABCOCK 1975 *AIAA Journal* **13**, 868-876. Nonlinear vibration of cylindrical shells.

C. Y. CHIA 1987a *International Journal of Solids and Structures* **23**, 1123-1132. Non-linear free vibration and postbuckling of symmetrically laminated orthotropic imperfect shallow cylindrical panels with two adjacent edges simply supported and the other edges clamped.

C. Y. CHIA 1987b *International Journal of Engineering Sciences* **25**, 427-441. Nonlinear vibration and postbuckling of unsymmetrically laminated imperfect shallow cylindrical panels with mixed boundary conditions resting on elastic foundation.

C. Y. CHIA 1988a *ASME Applied Mechanics Reviews* **41**, 439-451. Geometrically nonlinear behaviour of composite plates: a review.

C. Y. CHIA 1988b *Ingenieur Archiv* **58**, 252-264. Nonlinear analysis of doubly curved symmetrically laminated shallow shells with rectangular platform.

M. CHIBA 1993a *International Journal of Non-Linear Mechanics* **28**, 591-599. Non-linear hydroelastic vibration of a cantilever cylindrical tank. I Experiment (Empty case).

M. CHIBA 1993b *International Journal of Non-Linear Mechanics* **28**, 601-612. Non-linear hydroelastic vibration of a cantilever cylindrical tank. II Experiment (Liquid-filled case).

M. CHIBA 1993c *ASME Journal of Pressure Vessel Technology* **115**, 381-388. Experimental studies on a nonlinear hydroelastic vibration of a clamped cylindrical tank partially filled with liquid.

M. Chiba, N. Yamaki and J. Tani 1985 *Thin-walled structures* **3**, 1-14. Free vibration of a clamped-free circular cylindrical shell partially filled with liquid. Part III: Experimental results.

M. Chiba, N. Yamaki and J. Tani 1984 *Thin-walled structures* **2**, 265-284. Free vibration of a clamped-free circular cylindrical shell partially filled with liquid. Part I: Theoretical analysis.

H.-N. CHU 1961 *Journal of Aerospace Science* **28**, 602-609. Influence of large-amplitudes on flexural vibrations of a thin circular cylindrical shell.

B. E. CUMMINGS 1964 *AIAA Journal* **2**, 709-716. Large-amplitude vibration and response of curved panels.

E. J. DOEDEL, A. R. CHAMPNEYS, T. F. FAIRGRIEVE, Y. A. KUZNETSOV, B. SANDSTEDE and X. WANG 1998 *AUTO 97: Continuation and Bifurcation Software for Ordinary Differential Equations (with HomCont)*. Montreal, Canada: Concordia University.

L. H. DONNELL 1934 *Transactions of the ASME* **56**, 795-806. A new theory for the buckling of thin cylinders under axial compression and bending.

E. H. DOWELL 1967a *AIAA Journal* **5**, 1508-1509. On the nonlinear flexural vibrations of rings.

E. H. DOWELL 1970a *AIAA Journal* **8**, 385-399. Panel flutter: a review of the aeroelastic stability of plates and shells.

E. H. DOWELL 1978 *Journal of Sound and Vibration* **60**, 596-597. Comments on non-linear flexural vibrations of a cylindrical shell.

E. H. DOWELL 1998 *Journal of Fluids and Structures* **12**, 1087-1089. Comments on the nonlinear vibrations of cylindrical shells.

E. H. DOWELL and C. S. VENTRES 1968 *International Journal of Solids and Structures* **4**, 975-991. Modal equations for the nonlinear flexural vibrations of a cylindrical shell.

E. H. DOWELL, C. S. VENTRES and D. TANG 1998 *Duke University Research Report*, DT 98-1. Modal equations for the nonlinear flexural vibrations of a cylindrical shell.

I. ELISHAKOFF, V. BIRMAN and J. SINGER 1987 *Journal of Sound and Vibration* **114**, 57-63. Small vibrations of an imperfect panel in the vicinity of a non-linear static state.

B. R. EL-ZAOUK and C. L. DYM 1973 *Journal of Sound and Vibration* **31**, 89-103. Non-linear vibrations of orthotropic doubly-curved shallow shells.

D. A. EVENSEN 1963 *AIAA Journal* **1**, 2857-2858. Some observations on the nonlinear vibration of thin cylindrical shells.

D. A. EVENSEN 1964 *Non-Linear Flexural Vibrations of Thin Circular Rings*. Ph.D. thesis, California Institute of Technology, Pasadena, CA, USA.

D. A. EVENSEN 1965 *A Theoretical and Experimental Study of Nonlinear Flexural Vibrations of Thin Circular Rings*, NASA TR R-227. Washington, DC: Government Printing Office.

D. A. EVENSEN 1966 *ASME Journal of Applied Mechanics* **33**, 553-560. Nonlinear flexural vibrations of thin circular rings.

D. A. EVENSEN 1967 Nonlinear flexural vibrations of thin-walled circular cylinders. NASA TN D-4090.

D. A. EVENSEN 1968 *AIAA Journal* **6**, 1401-1403. Nonlinear vibrations of an infinitely long cylindrical shell.

D. A. EVENSEN 1974 Nonlinear vibrations of circular cylindrical shells. In *Thin-Shell Structures: Theory, Experiment and Design*, pp. 133-155 (eds Y. C. Fung & E. E. Sechler). Englewood Cliffs, NJ: Prentice-Hall.

D. A. EVENSEN 1977 *Journal of Sound and Vibration* **52**, 453-454. Comment on "Large-amplitude asymmetric vibrations of some thin shells of revolution".

D. A. EVENSEN 1978a *Journal of Sound and Vibration* **56**, 305-308. Author's reply.

D. A. EVENSEN 1978b *Journal of Sound and Vibration* **59**, 297-298. Author's reply.

D. A. EVENSEN 1978c *Journal of Sound and Vibration* **60**, 597-598. Author's reply.

D. A. EVENSEN 1999 *Journal of Fluids and Structures* **13**, 161-164. Non-linear vibrations of cylindrical shells – Logical rationale.

D. A. EVENSEN 2000 In *Nonlinear Dynamics of Shells and Plates* (eds. M. P. Païdoussis, M. Amabili and P. B. Gonçalves), *AMD Vol. 238*, pp. 47-59, ASME, New York. The influence of initial stress and boundary restraints on the nonlinear vibrations of cylindrical shells.

D. A. EVENSEN and R. E. FULTON 1967 *Proceedings of the International Conference on Dynamic Stability of Structures*, Evanston, IL, 18-20 October 1965, pp. 237-254, Pergamon Press. Some studies on the nonlinear dynamic response of shell-type structures.

S. FOALE, J. M. T. THOMPSON and F. A. MCROBIE 1998 *Journal of Sound and Vibration* **215**, 527-545. Numerical dimension-reduction methods for non-linear shell vibrations.

Y. M. FU and C. Y. CHIA 1989 *International Journal of Non-Linear Mechanics* **24**, 365-381. Multi-mode non-linear vibration and postbuckling of anti-symmetric imperfect angle-ply cylindrical thick panels.

Y. M. FU and C. Y. CHIA 1993 *International Journal of Non-Linear Mechanics* **28**, 313-327. Non-linear vibration and postbuckling of generally laminated circular cylindrical thick shells with non-uniform boundary conditions.

M. GANAPATHI and T. K. VARADAN 1995 *Composite Structures* **30**, 33-49. Nonlinear free flexural vibrations of laminated circular cylindrical shells.

M. GANAPATHI and T. K. VARADAN 1996 *Journal of Sound and Vibration* **192**, 1-14. Large-amplitude vibrations of circular cylindrical shells.

J. H. GINSBERG 1973 *ASME Journal of Applied Mechanics* **40**, 471-477. Large-amplitude forced vibrations of simply supported thin cylindrical shells.

J. H. GINSBERG 1974 *ASME Journal of Applied Mechanics* **41**, 310-311. Nonlinear axisymmetric free vibration in simply supported cylindrical shells.

P. B. GONÇALVES and R. C. BATISTA 1988 *Journal of Sound and Vibration* **127**, 133-143. Non-linear vibration analysis of fluid-filled cylindrical shells.

E. I. GRIGOLYUK 1955 *Prikladnaya Matematika i Mekhanika* **19**, 376-382. Vibrations of circular cylindrical panels subjected to finite deflections (in Russian).

L. GUNAWAN 1998 *Experimental study of nonlinear vibrations of thin-walled cylindrical shells.* Ph.D. Thesis, Technische Universiteit Delft, The Netherlands.

Q. HAN, H. HU and G. YANG 2000 *European Journal of Mechanics A: Solids* **18**, 351-360. A study of chaotic motion in elastic cylindrical shells.

T. HAUSE, L. LIBRESCU and T. F. JOHNSON 1998 *International Journal of Non-Linear Mechanics* **33**, 1039-1059. Non-linear response of geometrically imperfect sandwich curved panels under thermomechanical loading.

K. K. HU and P. G. KIRMSER 1971 *ASME Journal of Applied Mechanics* **38**, 461-466. Non-linear beam-type vibrations of long cylindrical shells.

D. HUI 1984 *ASME Journal of Applied Mechanics* **51**, 383-390. Influence of geometric imperfections and in-plane constraints on nonlinear vibrations of simply supported cylindrical panels.

J. HUTCHINSON 1965 *AIAA Journal* **3**, 1461-1466. Axial buckling of pressurized imperfect cylindrical shells.

E. L. JANSEN 1992 *Proceedings of the 17th International Seminar on Modal Analysis, Katholieke Universiteit Leuven, Leuven*, Vol. **3**, 1463-1479. Nonlinear vibrations of imperfect composite cylindrical shells.

E. L. JANSEN 2001 *Proceedings of the 42th AIAA/ASME/ASCE/AHS/ASC Structures, Structural Dynamics and Materials Conference*, Seattle, WA, pp. 1-10 (AIAA paper 2001-1314). Nonlinear vibration analysis of composite cylindrical shells using semi-analytical formulation.

E. L. JANSEN 2002 *International Journal of Non-Linear Mechanics* **37**, 937-949. Non-stationary flexural vibration behaviour of a cylindrical shell.

D. D. KAÑA 1966 in *The Dynamic Behaviour of Liquids in Moving Containers*, editor H. N. Abramson, NASA-SP-106, Washington, DC: Government Printing Office, pp. 303-352. Interaction between liquid propellants and the elastic structure.

D. D. KAÑA, U. S. LINDHOLM and H. N. ABRAMSON 1966 *Journal of Spacecraft and Rockets* **3**, 1183-1188. Experimental study of liquid instability in a vibrating elastic tank.

T. VON KÁRMÁN and H.-S. TSIEN 1941 *Journal of the Aeronautical Sciences* **8**, 303-312. The buckling of thin cylindrical shells under axial compression.

I. G. KIL'DIBEKOV 1977 *Prikladnaya Mekhanika* **13(11)**, 46-52. Investigation of the characteristic nonlinear oscillations of a cylindrical shell (in Russian). English version in *Soviet Applied Mechanics* **13**, 1109- 1114.

Y. KOBAYASHI and A. W. LEISSA 1995 *International Journal of Non-Linear Mechanics* **30**, 57-66. Large-amplitude free vibration of thick shallow shells supported by shear diaphragms.

W. T. KOITER 1963 *Proceedings Koninklijke Nederlandse Akademie van Wetenschappen* **B 66**, 265-279. The effect of axisymmetric imperfections on the buckling of cylindrical shells under axial compression.

W. T. KOITER 1966 *Proceedings Koninklijke Nederlandse Akademie van Wetenschappen* **B 69**, 1-54. On the nonlinear theory of thin elastic shells. I, II, III.

P. S. KOVAL'CHUK and T. S. KRASNOPOL'SKAYA 1980 *Soviet Applied Mechanics* **15**, 867-872. Resonance phenomena in nonlinear vibrations of cylindrical shells with initial imperfections.

P. S. KOVAL'CHUK and V. D. LAKIZA 1995 *International Applied Mechanics* **31**, 923-927. Experimental study of induced oscillations with large deflections of fiberglass shells of revolution.

P. S. KOVAL'CHUK and N. P. PODCHASOV 1988 *Soviet Applied Mechanics* **24**, 1086-1090. Nonlinear flexural waves in cylindrical shells with periodic excitation.

V. D. KUBENKO and P. S. KOVAL'CHUK 1998 *International Applied Mechanics* **34**, 703-728. Nonlinear problems of the vibration of thin shells (review).

V. D. KUBENKO and P. S. KOVAL'CHUK 2000a *Prikladnaya Mekhanika* **36**(4), 3-34. Nonlinear problems of the dynamics of elastic shells partially filled with a liquid (in Russian). English version in *International Applied Mechanics* **36**, 421-448.

V. D. KUBENKO and P. S. KOVAL'CHUK 2000b In *Nonlinear Dynamics of Shells and Plates* (eds. M. P. Païdoussis, M. Amabili and P. B. Gonçalves), *AMD Vol. 238*, pp. 147-153, ASME, New York. Problems of nonlinear multiple-mode vibrations of thin elastic shells of revolution.

V. D. KUBENKO, P. S. KOVAL'CHUK and T. S. KRASNOPOL'SKAYA 1982 *Soviet Applied Mechanics* **18**, 34-39. Effect of initial camber on natural nonlinear vibrations of cylindrical shells.

C. R. LAING, A. MCROBIE and J. M. T. THOMPSON 1999 *Dynamics and Stability of Systems* **14(**2), 163-181. The post-processed Galerkin method applied to non-linear shell vibrations.

Y-S. LEE and Y-W. KIM 1999 *Computers and Structures* **70**, 161-168. Nonlinear free vibration analysis of rotating hybrid cylindrical shells.

A. W. LEISSA 1973 *Vibration of Shells*, NASA SP-288. Washington, DC: Government Printing Office. Now available from The Acoustical Society of America (1993).

A. W. LEISSA and A. S. KADI 1971 *Journal of Sound and Vibration* **16**, 173-187. Curvature effects on shallow shell vibrations.

A. LIBAI and J. G. SIMMONDS 1988 *The Nonlinear Theory of Elastic Shells*. London, UK: Academic Press (2nd edition 1998).

L. LIBRESCU and M.-Y. CHANG 1993 *Acta Mechanica* **96**, 203-224. Effects of geometric imperfections on vibration of compressed shear deformable laminated composite curved panels.

L. LIBRESCU and W. LIN 1997a *International Journal of Solids and Structures* **34**, 2161-2181. Vibration of thermomechanically loaded flat and curved panels taking into account geometric imperfections and tangential edge restraints.

L. LIBRESCU and W. LIN 1997b *International Journal of Non-Linear Mechanics* **326**, 211-225. Postbuckling and vibration of shear deformable flat and curved panels on a non-linear elastic foundation.

L. LIBRESCU and W. LIN 1999 *International Journal of Solids and Structures* **36**, 4111-4147. Non-linear response of laminated plates and shells to thermomechanical loading: implications of violation of interlaminar shear traction continuity requirement.

L. LIBRESCU, W. LIN, M. P. NEMETH and J. H. STARNES JR. 1996 *Journal of Spacecraft and Rockets* **33**, 285-291. Vibration of geometrically imperfect panels subjected to thermal and mechanical loads.

A. I. LIKHODED 1976 *Mechanics of Solids* **11**, 127-132. Nonlinear vibrations of shells of revolution with concentrated masses.

G. Lin, B. Balachandran and E. Abed 2006 *Proceedings of the ASME International Mechanics Engineering Congress and Exposition, Chicago, IL*. Bifurcation behaviour of a supercavitating vehicle.

A. MAEWAL 1986a *International Journal of Non-Linear Mechanics* **21**, 433-438. Miles' evolution equations for axisymmetric shells: simple strange attractors in structural dynamics.

A. MAEWAL 1986b *Computer Methods in Applied Mechanics and Engineering* **58**, 37-50. Finite element analysis of steady nonlinear harmonic oscillations of axisymmetric shells.

R. MAO and F. W. WILLIAMS 1998a *Journal of Sound and Vibration* **210**, 307-327. Post-critical behaviour of orthotropic circular cylindrical shells under time dependent axial compression.

R. MAO and F. W. WILLIAMS 1998b *International Journal of Solids and Structures* **35**, 2151-2171. Nonlinear analysis of cross-ply thick cylindrical shells under axial compression.

Y. MATSUZAKI and S. KOBAYASHI 1969a *Journal of the Japan Society for Aeronautical and Space Sciences* **17**, 308-315. An analytical study of the nonlinear flexural vibration of thin circular cylindrical shells (in Japanese).

Y. MATSUZAKI and S. KOBAYASHI 1969b *Transactions of the Japan Society for Aeronautical and Space Sciences* **12**, 55-62. A theoretical and experimental study of the nonlinear flexural vibration of thin circular cylindrical shells with clamped ends.

J. MAYERS and B. G. WRENN 1967 On the nonlinear free vibrations of thin circular cylindrical shells. *Developments in Mechanics, Proceedings of the 10th Midwestern Mechanics Conference*, 819-846. New York: Johnson Publishing Co.

Y. V. MIKHLIN 2000 In *Nonlinear Dynamics of Shells and Plates* (eds. M. P. Païdoussis, M. Amabili and P. B. Gonçalves), *AMD Vol. 238*, pp. 95-103, ASME, New York. Stability of regular or chaotic post-buckling vibration of elastic shells.

F. MOUSSAOUI, R. BENAMAR and R. G. WHITE 2000 *Journal of Sound and Vibration* **232**, 917-943. The effects of large vibration amplitudes on the mode shapes and natural frequencies of thin elastic shells, Part I: coupled transverse-circumferential mode shapes of isotropic circular cylindrical shells of infinite length.

KH. M. MUSHTARI and K. Z. GALIMOV 1957 *Non-Linear Theory of Thin Elastic Shells*. Academy of Sciences (Nauka), Kazan'; English version, NASA-TT-F62 in 1961.

K. NAGAI and T. YAMAGUCHI 1995 ASME PVP Vol. 297, pp. 107-115. Chaotic oscillations of a shallow cylindrical shell with rectangular boundary under cyclic excitation.

K. NAGAI, T. YAMAGUCHI and T. MURATA 2001 *Proceedings of the 3rd International Symposium on Vibration of Continuous Systems*, 49-51, Grand Teton National Park, Wyoming, USA, July 23-27. Chaotic oscillations of a cylindrical shell-panel with concentrated mass under gravity and cyclic load.

P. M. NAGHDI and R. P. NORDGREN 1963 *Quarterly of Applied Mathematics* **21**, 49-59. On the nonlinear theory of elastic shells under the Kirchhoff hypothesis.

A. H. NAYFEH and R. A. RAOUF 1987a *International Journal of Solids and Structures* **23**, 1625-1638. Non-linear oscillation of circular cylindrical shells.

A. H. NAYFEH and R. A. RAOUF 1987b *ASME Journal of Applied Mechanics* **54**, 571-577. Nonlinear forced response of infinitely long circular cylindrical shells.

A. H. NAYFEH, R. A. RAOUF and J. F. NAYFEH 1991 *ASME Journal of Applied Mechanics* **58**, 1033-1041. Nonlinear response of infinitely long circular cylindrical shells to subharmonic radial loads.

J. F. NAYFEH and N. J. RIVIECCIO 2000 *Journal of Aerospace Engineering* **13**(2), 59-68. Nonlinear vibration of composite shell subjected to resonant excitations.

V. V. NOVOZHILOV 1953 *Foundations of the Nonlinear Theory of Elasticity*. Graylock Press, Rochester, USA (now available from Dover, N.Y., USA).

J. NOWINSKI 1963 *AIAA Journal* **1**, 617-620. Nonlinear transverse vibrations of orthotropic cylindrical shells.

M. D. OLSON 1965 *AIAA Journal* **3**, 1775-1777. Some experimental observations on the nonlinear vibration of cylindrical shells.

M. P. PAÏDOUSSIS 2002 *Fluid-Structure Interactions: Slender Structures and Axial Flow*. Vol. 2. London, UK: Academic Press.

M. P. PAÏDOUSSIS, M. AMABILI and P. B. GONÇALVES (editors) 2000 *Nonlinear Dynamics of Shells and Plates*, AMD-Vol. 238, Proceedings of the ASME International Mechanical Engineering Congress and Exposition, ASME, New York.

M. P. PAÏDOUSSIS and J.-P. DENISE 1972 *Journal of Sound and Vibration* **20**, 9-26. Flutter of thin cylindrical shells conveying fluid.

D. A. PALIWAL and V. BHALLA 1993 *International Journal of Pressure Vessels and Piping* **54**, 387-398. Large amplitude free vibrations of cylindrical shell on Pasternak foundations.

D. A. PALIWAL and V. BHALLA 1993 *Journal of Vibration and Acoustics* **115**, 70-74. Large amplitude free vibration of shallow spherical shell on a Pasternak foundation.

F. PELLICANO 2007 *Journal of Sound and Vibration* **303**, 154–170. Vibrations of circular cylindrical shells: Theory and experiments.

F. PELLICANO, M. AMABILI and M. P. PAÏDOUSSIS 2002 *International Journal of Non-Linear Mechanics* **37**, 1181-1198. Effect of the geometry on the non-linear vibration of circular cylindrical shells.

F. PELLICANO, M. AMABILI and A. F. VAKAKIS 2000 *ASME Journal of Vibration and Acoustics* **122**, 355-364. Nonlinear vibrations and multiple resonances of fluid-filled, circular shells, Part 2: perturbation analysis.

A. A. POPOV, J. M. T. THOMPSON and F. A. MCROBIE 1998a *Journal of Sound and Vibration* **209**, 163-186. Low dimensional models of shell vibrations. Parametrically excited vibrations of cylindrical shells.

A. A. POPOV, J. M. T. THOMPSON and F. A. MCROBIE 2001 *Journal of Sound and Vibration* **248**, 395-411. Chaotic energy exchange through auto-parametric resonance in cylindrical shells.

G. PRATHAP 1978a *Journal of Sound and Vibration* **56**, 303-305. Comments on the large-amplitude asymmetric vibrations of some thin shells of revolution.

G. PRATHAP 1978b *Journal of Sound and Vibration* **59**, 295-297. On the large amplitude vibration of circular cylindrical shells.

H. RADWAN and J. GENIN 1975 *International Journal of Non-Linear Mechanics* **10**, 15-29. Non-linear modal equations for thin elastic shells.

K. K. RAJU and G. V. RAO 1976 *Journal of Sound and Vibration* **44**, 327-333. Large-amplitude asymmetric vibrations of some thin shells of revolution.

R. A. RAOUF and A. H. NAYFEH 1990 *Computers and Structures* **35**, 163-173. One-to-one autoparametric resonances in infinitely long cylindrical shells.

E. REISSNER 1955 Nonlinear effects in vibrations of cylindrical shells. Ramo-Wooldridge Corporation Report AM5-6.

J. L. SANDERS JR. 1963 *Quarterly of Applied Mathematics* **21**, 21-36. Nonlinear theories for thin shells.

C. SANSOUR, W. WAGNER, P. WRIGGERS and J. SANSOUR 2002 *International Journal of Non-Linear Mechanics* **37**, 951-966. An energy-momentum integration scheme and enhanced strain finite elements for the non-linear dynamics of shells.

C. SANSOUR, P. WRIGGERS and J. SANSOUR 1997 *Nonlinear Dynamics* **13**, 279-305. Nonlinear dynamics of shells: theory, finite element formulation, and integration schemes.

A. SELMANE and A. A. LAKIS 1997a *International Journal for Numerical Methods in Engineering* **40**, 1115-1137. Influence of geometric non-linearities on free vibrations of orthotropic open cylindrical shells.

D. K. SHIN 1997 *Computers and Structures* **62**, 35-49. Large amplitude free vibration behaviour of doubly curved shallow open shells with simply-supported edges.

G. C. SINHARAY and B. BANERJEE 1985 *International Journal of Non-Linear Mechanics* **20**, 69-78. Large-amplitude free vibrations of shallow spherical shell and cylindrical shell – a new approach.

G. C. SINHARAY and B. BANERJEE 1986 *AIAA Journal* **24**, 998-1004. Large-amplitude free vibrations of shells of variable thickness – a new approach.

C. L. SUN and S. Y. LU 1968 *Nuclear Engineering Design* **7**, 113-122. Nonlinear dynamic behaviour of heated conical and cylindrical shells.

J. M. T. THOMPSON and J. R. DE SOUZA 1996 *Proceedings of the Royal Society of London Series A* **452**, 2527-2550. Suppression of escape be resonant modal interactions: in shell vibration and heave-roll capsize.

T. UEDA 1979 *Journal of Sound and Vibration* **64**, 85-95. Non-linear free vibrations of conical shells.

T. K. VARADAN, G. PRATHAP and H. V. RAMANI 1989 *AIAA Journal* **27**, 1303-1304. Nonlinear free flexural vibration of thin circular cylindrical shells.

A. S. VOL'MIR 1956 *Flexible Plates and Shells* (in Russian). Gittl, Moscow.

A. S. VOL'MIR 1972 *Nonlinear Dynamics of Plates and Shells* (in Russian). Academy of Sciences (Nauka), Moscow.

A. S. VOL'MIR, A. A. LOGVINSKAYA and V. V. ROGALEVICH 1973 *Soviet Physics – Doklady* **17**, 720-721. Nonlinear natural vibrations of rectangular plates and cylindrical panels.

I. I. VOROVICH 1999 *Nonlinear Theory of Shallow Shells*. Springer-Verlag, New York.

L. WATAWALA and W. A. NASH 1983 *Computers and Structures* **16**, 125-130. Influence of initial geometric imperfections on vibrations of thin circular cylindrical shells.

S. WOLFRAM 1999 *The Mathematica Book*, 4th edition. Cambridge, UK: Cambridge University Press.

T. YAMAGUCHI and K. NAGAI 1997 *Nonlinear Dynamics* **13**, 259-277. Chaotic vibration of a cylindrical shell-panel with an in-plane elastic-support at boundary.

T. YAMAGUCHI and K. NAGAI 2000 In *Nonlinear Dynamics of Shells and Plates* (eds. M. P. Païdoussis, M. Amabili and P. B. Gonçalves), *AMD Vol. 238*, pp. 85-94, ASME, New York. Chaotic oscillations of a shallow cylindrical shell-panel with a concentrated elastic-support.

N. YAMAKI 1982 In *Developments in Thin-Walled Structures* **1** (eds. J. Rhodes and A. C. Walker), pp. 81-118, Applied Science Publishers, London. Dynamic behaviour of a thin-walled circular cylindrical shell.

N. YAMAKI 1984 *Elastic Stability of Circular Cylindrical Shells.* Amsterdam: North-Holland.

J. C. YAO 1963 *AIAA Journal* **1**, 1391-1396. Dynamic stability of cylindrical shells under static and periodic axial and radial loads.

APPENDIX A: PROGRAM FOR SOLVING LINEAR PROBLEM

```
(*--------------------Chebyshev polynomials, Sanders-Koiter thery.
Eigenvectors and Eigenvalues of linear part for simply supported shell------------*)

SetDirectory["D:\\results\\simply supported\\eigenvector"];

M=15;
NN=6;Nmin=6;
L=SetPrecision[2/10,300];
R=SetPrecision[1/10,300]      ;
h=SetPrecision[247*10^-3/1000,300];
ρ=2796;
ν=SetPrecision[31/100,300];
EE=SetPrecision[7102/100*10^9,300];
num=3*M-5;

                (*-------------Boundary conditions simply support---------------*)


UU[eta_]=Sum[a1[i,n]ChebyshevT[i, 2*eta-1],{i,0,M}];
VV[eta_]=Sum[a2[i,n]ChebyshevT[i, 2*eta-1],{i,0,M}];
WW[eta_]=Sum[a3[i,n]ChebyshevT[i, 2*eta-1],{i,0,M}];

Do[

 W1=WW[0];
 W2=WW[1];
 W3=D[WW[eta],eta,eta] /.eta→0;
 W4= D[WW[eta],eta] /.eta→1;
 ww[n]=Chop[Solve[{W1==0,W2==0,W3==0,W4==0},{a3[0,n],a3[1,n],a3[2,n],a3[3,n]}]];
 a3[0,n]=a3[0,n]/.ww[n][[1]];
 a3[1,n]=a3[1,n]/.ww[n][[1]];
 a3[2,n]=a3[2,n]/.ww[n][[1]];
 a3[3,n]=a3[3,n]/.ww[n][[1]];

 V1=VV[0];
 V2=VV[1];
 vv[n]=Chop[Solve[{V1==0,V2==0},{a2[0,n],a2[1,n]}]];
 a2[0,n]=a2[0,n]/.vv[n][[1]];
 a2[1,n]=a2[1,n]/.vv[n][[1]];

 U1= D[UU [eta],eta] /.eta→0;
 U2= D[UU [eta],eta] /.eta→1;
 uu[n]=Chop[Solve[{U1==0,U2==0},{a1[1,n],a1[2,n]}]];
 a1[1,n]=a1[1,n]/.uu[n][[1]];
 a1[2,n]=a1[2,n]/.uu[n][[1]]

 ,{n,0,4*NN}]
```

```
(*---------- General expansion +rearranging variables  ----------*)

U[eta_, th_]=Sum[a1[i,n]ChebyshevT[i, 2*eta-1]*Cos[n*th],{i,0,M},{n,0,4*NN}];
V[eta_, th_]=Sum[a2[i,n]ChebyshevT[i, 2*eta-1]*Sin[n*th],{i,0,M},{n,1,4*NN}]
              + Sum[a2[i,0]ChebyshevT[i, 2*eta-1],{i,0,M}];
W[eta_, th_]=Sum[a3[i,n]ChebyshevT[i, 2*eta-1]*Cos[n*th],{i,0,M},{n,0,4*NN}];
U0[eta_, th_]=0;
V0[eta_, th_]=0;
W0[eta_, th_]=0;

Do[a1[m,n]=0;a2[m,n]=0;a3[m,n]=0,{m,0,M},{n,1,NN-1}];
Do[a1[m,n]=0;a2[m,n]=0;a3[m,n]=0,{m,0,M},{n,NN+1,2*NN-1}];
Do[a1[m,n]=0;a2[m,n]=0;a3[m,n]=0,{m,0,M},{n,2*NN+1,3*NN-1}];
Do[a1[m,n]=0;a2[m,n]=0;a3[m,n]=0,{m,0,M},{n,3*NN+1,4*NN-1}];

ii=1;
Do[a1[0,n]=qx[ii];ii=ii+1,{n,0,0}]
Do[a1[0,n]=qx[ii];ii=ii+1,{n,NN,NN}]
a1[0,2*NN]=qx[ii];ii=ii+1;
a1[0,3*NN]=qx[ii];ii=ii+1;
a1[0,4*NN]=qx[ii];ii=ii+1;

Do[Do[a1[m,n]=qx[ii];ii=ii+1,{m,3,M}],{n,0,0}]
Do[Do[a1[m,n]=qx[ii];ii=ii+1,{m,3,M}],{n,NN,NN}]
Do[Do[a1[m,2*NN]=qx[ii];ii=ii+1,{m,3,M}]]
Do[Do[a1[m,3*NN]=qx[ii];ii=ii+1,{m,3,M}]]
Do[Do[a1[m,4*NN]=qx[ii];ii=ii+1,{m,3,M}]]

Do[Do[a2[m,n]=qx[ii];ii=ii+1,{m,2,M}],{n,0,0}]
Do[Do[a2[m,n]=qx[ii];ii=ii+1,{m,2,M}],{n,NN,NN}]
Do[Do[a2[m,2*NN]=qx[ii];ii=ii+1,{m,2,M}]]
Do[Do[a2[m,3*NN]=qx[ii];ii=ii+1,{m,2,M}]]
Do[Do[a2[m,4*NN]=qx[ii];ii=ii+1,{m,2,M}]]

Do[Do[a3[m,n]=qx[ii];ii=ii+1,{m,4,M}],{n,0,0}]
Do[Do[a3[m,n]=qx[ii];ii=ii+1,{m,4,M}],{n,NN,NN}]
Do[Do[a3[m,2*NN]=qx[ii];ii=ii+1,{m,4,M}]]
Do[Do[a3[m,3*NN]=qx[ii];ii=ii+1,{m,4,M}]]
Do[Do[a3[m,4*NN]=qx[ii];ii=ii+1,{m,4,M}]]
Nmax=ii-1

                    (*-------normalization  with respect to h-------*)

Do[qx[ik]=h*q[ik],{ik,1,Nmax}]

U[eta_, th_]=Chop[Expand[U[eta, th]]];
V[eta_, th_]=Chop[Expand[V[eta, th]]];
W[eta_, th_]=Chop[Expand[W[eta, th]]];
U[eta_, th_]>>U.txt;
V[eta_, th_]>>V.txt;
W[eta_, th_]>>W.txt;
```

```
(*---------------------- Linear Sanders-Koiter theory ----------------------*)

∈x=Expand[D[U[eta,th],eta] /L]  ;
∈x>>epx.txt;

∈th=Expand[D[V[eta,th],th] /R+W[eta,th]/R]      ;
∈th>>epy.txt;

γxth=Expand[D[U[eta,th],th] /R+ D[V[eta,th],eta] /L] ;
γxth>>gxy.txt;

kx=Expand[-D[W[eta,th],eta,eta] /(L^2)];
kx>>kx.txt;

kth=Expand[D[V[eta,th],th] /(R^2)- D[W[eta,th],th,th]  /(R^2)];
kth>>ky.txt;

kxth=Expand[-(2/(R*L))*D[W[eta,th],eta,th]+(1/(2*R))*((3/L)*D[V[eta,th],eta]-
(1/R)*D[U[eta,th],th])];
kxth>>kxy.txt;

                (*-------------------------energy integrals-------------------------------*)

Ts=Expand[(1/2)*ρ*h*(U[eta,th]^2+V[eta,th]^2+W[eta,th]^2)];
Ts>>energia.txt;
en1=∈x^2;
en2=∈th^2;
en3=2 ν*∈x*∈th;
en4=(1-ν)/2*γxth^2;

aa1=en1+en2+en3+en4;

Us1=1/2 (EE*h)/(1-ν2)*aa1;
en5=kx^2;
en6=kth^2;
en7=2 ν*kx*kth;
en8=(1-ν)/2*kxth^2;
aa2=en5+en6+en7+en8;
Us2=1/2 (EE*h^3)/(12 (1-ν2))*aa2;
Us=Us1+Us2;
Us>>Us.txt;

                (*----------------------definitions of integrals-----------------*)

inthe[z_]:=Integrate[z,{th,0,2 Pi}];
intet[z_]:=Integrate[z,{eta,0,1}];
```

```
(*----------------------kinetic energy---------------------- *)

pp1=Map[inthe,Ts];
pp2=Map[intet,pp1];
TsI=L*R*pp2;
TsI>>TS.txt;

(*--------------------calculations  for  Lagrange equations ----------------------*)

F=Array[ff,Nmax];
F>>f.txt;
temp>>temp.txt;
Do[
    pp1=D[Us,q[ii]];
   {"derivative",ii}>>step.txt;
   Npol=4*M;
   pp2=0;
   Do[
 pp3=Coefficient[pp1,eta,kk];
 pp2=pp2+(1/(kk+1))*pp3,
 {kk,0,Npol}];
{"integral in eta",ii}>>>step.txt;
        pp2=Expand[pp2];
     pp2=Map[inthe,pp2];
    {"integral in theta",ii}>>>step.txt;
    {equation,ii}>>>temp.txt;
    ff[ii]=L*R*pp2;
    {storage,ii}>>>step.txt,
   {ii,1,Nmax}]

F>>f.txt;

Stiff=Array[KK,{Nmax,Nmax}];
Mass=Array[MM,{Nmax,Nmax}];

Do[MM[i,j]=D[TsI,q[i],q[j]],{i,1,Nmax}, {j,1,Nmax}];
Do[KKK[ii,jj]= D[ff,q[ii]],{ii,1,Nmax},{jj,1,Nmax}]
Do[KK[ii,jj]=KKK[ii,jj],{ii,1,Nmax},{jj,1,Nmax}]

Mass>>mass-matrix.txt;
MatrixForm[Mass]>>mass_m.txt;
Stiff>>stiff-matrix.txt;
MatrixForm[Stiff]>>stiff_m.txt;

Fnorm=Expand[Inverse[Mass] .F];
Fnorm>>Fnorm.txt;
Jacob=Table[D[Fnorm[[ii]],q[jj]],{ii,1,Nmax},{jj,1,Nmax}];
Do[q[jj]=0,{jj,1,Nmax}]
g=Eigenvalues[N[Jacob,300]]
uuuu=Table[Sqrt[g[[jj]]]/2/Pi,{jj,1,Nmax}]
vvv=Eigenvectors[Jacob];
vvv>>Eigenvect_up_3n4n.txt;
```

APPENDIX B:
SAMPLE OF EQUATIONS FOR AUTO 97, CASE OF CLAMPED-FREE SHELL, 37 DOF's, NO IMPERFECTIONS, DONNELL THEORY

```
function eq1p(q,gi1,gi2,gi3,crot)
IMPLICIT DOUBLE PRECISION (A-H,O-Z)
dimension q(37)

nxhat=0.d0

eq1p=       6.74e7*q(1) + 6.2e11*q(1)**3 + 1.48e10*q(1)*q(2) + 4.63e12*q(1)*q(2)**2 - 236.*q(3) +
-  3.72e11*q(1)**2*q(3) + 1.24e9*q(2)*q(3) + 9.85e11*q(2)**2*q(3) + 1.06e12*q(1)*q(3)**2 +
-  8.95e10*q(3)**3 + 8.45e8*q(1)*q(4) + 1.54e12*q(1)*q(2)*q(4) + 9.94e9*q(3)*q(4) +
-  4.9e12*q(2)*q(3)*q(4) + 2.53e12*q(1)*q(4)**2 + 5.49e11*q(3)*q(4)**2 + 1.55e12*q(1)**2*q(5) -
-  2.87e10*q(2)*q(5) - 5.88e12*q(2)**2*q(5) + 6.82e11*q(1)*q(3)*q(5) + 6.81e11*q(3)**2*q(5) -
-  3.22e9*q(4)*q(5) - 2.65e12*q(2)*q(4)*q(5) - 2.94e12*q(4)**2*q(5) + 8.03e12*q(1)*q(5)**2 +
-  2.48e12*q(3)*q(5)**2 - 270.*q(6) - 8.47e11*q(1)**2*q(6) - 4.4e9*q(2)*q(6) - 2.16e12*q(2)**2*q(6) -
-  1.68e12*q(1)*q(3)*q(6) - 2.e11*q(3)**2*q(6) - 5.e9*q(4)*q(6) - 3.69e12*q(2)*q(4)*q(6) -
-  4.29e11*q(4)**2*q(6) - 1.46e12*q(1)*q(5)*q(6) - 1.18e12*q(3)*q(5)*q(6) - 4.34e12*q(5)**2*q(6) +
-  1.1e12*q(1)*q(6)**2 + 5.61e11*q(3)*q(6)**2 + 8.36e11*q(5)*q(6)**2 - 7.33e10*q(6)**3 -
-  4.18e9*q(1)*q(7) - 4.1e12*q(1)*q(2)*q(7) - 5.94e9*q(3)*q(7) - 4.17e12*q(2)*q(3)*q(7) -
-  3.88e12*q(1)*q(4)*q(7) - 8.3e11*q(3)*q(4)*q(7) + 9.61e9*q(5)*q(7) + 5.77e12*q(2)*q(5)*q(7) +
-  4.89e12*q(4)*q(5)*q(7) + 1.05e10*q(6)*q(7) + 5.39e12*q(2)*q(6)*q(7) + 2.75e12*q(4)*q(6)*q(7) +
-  2.75e12*q(1)*q(7)**2 + 1.2e12*q(3)*q(7)**2 - 3.42e12*q(5)*q(7)**2 - 5.02e11*q(6)*q(7)**2 +
-  7.54e11*q(1)**2*q(8) - 8.17e9*q(2)*q(8) - 2.81e12*q(2)**2*q(8) + 1.5e12*q(1)*q(3)*q(8) +
-  1.16e10*q(3)**2*q(8) - 1.09e10*q(4)*q(8) - 5.57e12*q(2)*q(4)*q(8) - 2.97e11*q(4)**2*q(8) +
-  8.3e12*q(1)*q(5)*q(8) + 8.35e12*q(3)*q(5)*q(8) - 2.1e12*q(1)*q(6)*q(8) - 8.37e11*q(3)*q(6)*q(8) -
-  1.08e13*q(5)*q(6)*q(8) + 5.14e10*q(6)**2*q(8) + 2.45e10*q(7)*q(8) + 8.01e12*q(2)*q(7)*q(8) +
-  3.66e12*q(4)*q(7)*q(8) - 3.78e11*q(7)**2*q(8) + 6.29e12*q(1)*q(8)**2 + 2.57e12*q(3)*q(8)**2 -
-  1.21e10*q(6)*q(8)**2 - 2.71e11*q(1)**2*q(9) + 8.07e8*q(2)*q(9) + 9.86e11*q(2)**2*q(9) -
-  2.e12*q(1)*q(3)*q(9) - 1.15e11*q(3)**2*q(9) + 2.2e10*q(4)*q(9) + 7.37e12*q(2)*q(4)*q(9) +
-  5.58e11*q(4)**2*q(9) - 3.52e12*q(1)*q(5)*q(9) - 9.81e12*q(3)*q(5)*q(9) + 1.57e12*q(1)*q(6)*q(9) +
-  1.63e11*q(3)*q(6)*q(9) + 7.75e12*q(5)*q(6)*q(9) - 4.51e11*q(6)**2*q(9) - 1.27e10*q(7)*q(9) -
-  5.78e12*q(2)*q(7)*q(9) - 9.27e11*q(4)*q(7)*q(9) + 1.72e12*q(7)**2*q(9) - 8.87e12*q(1)*q(8)*q(9) -
-  6.28e11*q(3)*q(8)*q(9) + 5.22e12*q(6)*q(8)*q(9) + 5.81e12*q(1)*q(9)**2 + 5.65e11*q(3)*q(9)**2 -
-  5.6e11*q(6)*q(9)**2 + 1.03e10*q(1)*q(10) + 3.51e10*q(1)*q(2)*q(10) + 9.68e8*q(3)*q(10) +
-  7.59e10*q(2)*q(3)*q(10) - 3.89e10*q(1)*q(4)*q(10) + 3.26e10*q(3)*q(4)*q(10) -
-  6.01e10*q(2)*q(5)*q(10) - 1.01e11*q(4)*q(5)*q(10) - 3.19e9*q(6)*q(10) - 7.13e10*q(2)*q(6)*q(10) +
-  2.93e10*q(4)*q(6)*q(10) + 2.83e10*q(1)*q(7)*q(10) - 8.09e10*q(3)*q(7)*q(10) +
-  9.07e10*q(5)*q(7)*q(10) + 3.56e10*q(6)*q(7)*q(10) + 5.8e10*q(2)*q(8)*q(10) -
-  1.33e11*q(4)*q(8)*q(10) + 8.21e10*q(7)*q(8)*q(10) - 7.97e10*q(2)*q(9)*q(10) +
-  8.82e10*q(4)*q(9)*q(10) + 4.65e10*q(7)*q(9)*q(10) + 1.31e10*q(1)*q(10)**2 + 9.53e8*q(3)*q(10)**2 -
-  3.42e9*q(6)*q(10)**2 - 3.19e9*q(1)*q(11) - 1.01e11*q(1)*q(2)*q(11) - 4.41e9*q(3)*q(11) -
-  2.71e11*q(2)*q(3)*q(11) + 1.39e11*q(1)*q(4)*q(11) - 7.21e10*q(3)*q(4)*q(11) +
-  1.73e11*q(2)*q(5)*q(11) + 3.5e11*q(4)*q(5)*q(11) + 7.67e9*q(6)*q(11) + 2.3e11*q(2)*q(6)*q(11) -
-  3.2e10*q(4)*q(6)*q(11) - 5.9e10*q(1)*q(7)*q(11) + 2.11e11*q(3)*q(7)*q(11) -
-  3.07e11*q(5)*q(7)*q(11) - 7.96e10*q(6)*q(7)*q(11) - 1.07e11*q(2)*q(8)*q(11) +
-  3.84e11*q(4)*q(8)*q(11) - 1.36e11*q(7)*q(8)*q(11) + 2.78e11*q(2)*q(9)*q(11) -
-  1.66e11*q(4)*q(9)*q(11) - 3.42e10*q(7)*q(9)*q(11) - 7.48e10*q(1)*q(10)*q(11) -
-  1.01e10*q(3)*q(10)*q(11) + 3.68e10*q(6)*q(10)*q(11) + 1.17e11*q(1)*q(11)**2 + 2.8e10*q(3)*q(11)**2 -
-  5.8e10*q(6)*q(11)**2 + 9.68e8*q(1)*q(12) + 1.09e11*q(1)*q(2)*q(12) + 7.82e9*q(3)*q(12) +
-  4.63e11*q(2)*q(3)*q(12) - 1.81e11*q(1)*q(4)*q(12) + 8.93e10*q(3)*q(4)*q(12) -
-  1.89e11*q(2)*q(5)*q(12) - 6.15e11*q(4)*q(5)*q(12) - 4.41e9*q(6)*q(12) - 3.04e11*q(2)*q(6)*q(12) -
-  4.35e10*q(4)*q(6)*q(12) + 1.68e8*q(1)*q(7)*q(12) - 1.61e11*q(3)*q(7)*q(12) +
-  4.46e11*q(5)*q(7)*q(12) + 9.08e10*q(6)*q(7)*q(12) - 4.92e10*q(2)*q(8)*q(12) -
-  2.76e11*q(4)*q(8)*q(12) + 4.93e10*q(7)*q(8)*q(12) - 3.31e11*q(2)*q(9)*q(12) +
-  1.31e11*q(4)*q(9)*q(12) - 6.24e10*q(7)*q(9)*q(12) + 8.01e10*q(1)*q(10)*q(12) +
-  5.15e10*q(3)*q(10)*q(12) - 8.19e10*q(6)*q(10)*q(12) - 2.87e11*q(1)*q(11)*q(12) -
-  1.42e11*q(3)*q(11)*q(12) + 2.12e11*q(6)*q(11)*q(12) + 2.4e11*q(1)*q(12)**2 + 8.89e10*q(3)*q(12)**2 -
-  1.06e11*q(6)*q(12)**2 - 4.69e8*q(1)*q(13) - 1.05e11*q(1)*q(2)*q(13) - 5.13e9*q(3)*q(13) -
-  5.43e11*q(2)*q(3)*q(13) + 1.12e11*q(1)*q(4)*q(13) - 1.24e11*q(3)*q(4)*q(13) +
-  1.87e11*q(2)*q(5)*q(13) + 8.03e11*q(4)*q(5)*q(13) + 1.5e9*q(6)*q(13) + 2.98e11*q(2)*q(6)*q(13) +
-  2.45e10*q(4)*q(6)*q(13) + 3.03e10*q(1)*q(7)*q(13) + 2.16e11*q(3)*q(7)*q(13) -
```

```
-  4.62e11*q(5)*q(7)*q(13) - 1.95e11*q(6)*q(7)*q(13) + 1.15e11*q(2)*q(8)*q(13) +
-  1.97e11*q(4)*q(8)*q(13) - 2.92e11*q(7)*q(8)*q(13) + 1.5e11*q(2)*q(9)*q(13) -
-  1.96e11*q(4)*q(9)*q(13) - 7.81e10*q(7)*q(9)*q(13) - 7.85e10*q(1)*q(10)*q(13) -
-  1.03e11*q(3)*q(10)*q(13) + 9.11e10*q(6)*q(10)*q(13) + 2.73e11*q(1)*q(11)*q(13) +
-  2.67e11*q(3)*q(11)*q(13) - 3.14e11*q(6)*q(11)*q(13) - 5.32e11*q(1)*q(12)*q(13) -
-  2.37e11*q(3)*q(12)*q(13) + 3.88e11*q(6)*q(12)*q(13) + 4.22e11*q(1)*q(13)**2 + 1.37e11*q(3)*q(13)**2 -
-  1.55e11*q(6)*q(13)**2 + 4.21e8*q(1)*q(14) + 1.04e11*q(1)*q(2)*q(14) + 1.59e9*q(3)*q(14) +
-  4.66e11*q(2)*q(3)*q(14) - 4.98e10*q(1)*q(4)*q(14) + 1.56e11*q(3)*q(4)*q(14) -
-  1.87e11*q(2)*q(5)*q(14) - 7.62e11*q(4)*q(5)*q(14) - 9.46e8*q(6)*q(14) - 2.74e11*q(2)*q(6)*q(14) -
-  9.96e10*q(4)*q(6)*q(14) - 2.78e10*q(1)*q(7)*q(14) - 4.11e11*q(3)*q(7)*q(14) +
-  4.34e11*q(5)*q(7)*q(14) + 2.28e11*q(6)*q(7)*q(14) - 9.87e10*q(2)*q(8)*q(14) -
-  6.08e11*q(4)*q(8)*q(14) + 4.07e11*q(7)*q(8)*q(14) - 1.65e10*q(2)*q(9)*q(14) +
-  1.03e11*q(4)*q(9)*q(14) - 9.17e10*q(7)*q(9)*q(14) + 7.83e10*q(1)*q(10)*q(14) +
-  1.05e11*q(3)*q(10)*q(14) - 8.54e10*q(6)*q(10)*q(14) - 2.52e11*q(1)*q(11)*q(14) -
-  3.68e11*q(3)*q(11)*q(14) + 3.03e11*q(6)*q(11)*q(14) + 4.39e11*q(1)*q(12)*q(14) +
-  4.73e11*q(3)*q(12)*q(14) - 5.64e11*q(6)*q(12)*q(14) - 8.55e11*q(1)*q(13)*q(14) -
-  3.34e11*q(3)*q(13)*q(14) + 6.12e11*q(6)*q(13)*q(14) + 6.66e11*q(1)*q(14)**2 + 1.73e11*q(3)*q(14)**2 -
-  1.99e11*q(6)*q(14)**2 + 8.62e6*q(15) + 2.4e9*q(2)*q(15) - 4.16e9*q(4)*q(15) + 6.77e9*q(7)*q(15) +
-  4.e9*q(10)*q(15) - 1.e10*q(11)*q(15) + 8.31e9*q(12)*q(15) - 8.33e9*q(13)*q(15) + 8.29e9*q(14)*q(15) +
-  6.58e9*q(1)*q(16) + 8.07e9*q(3)*q(16) - 6.e9*q(5)*q(16) - 8.68e9*q(6)*q(16) + 1.35e10*q(8)*q(16) -
-  8.74e9*q(9)*q(16) + 4.27e7*q(17) + 6.72e9*q(2)*q(17) - 9.49e9*q(4)*q(17) + 1.29e9*q(7)*q(17) +
-  1.96e9*q(10)*q(17) - 7.54e9*q(11)*q(17) + 1.2e10*q(12)*q(17) - 1.02e10*q(13)*q(17) +
-  8.27e9*q(14)*q(17) - 8.87e7*q(1)*q(18) + 1.57e10*q(3)*q(18) - 8.96e9*q(5)*q(18) - 8.93e9*q(6)*q(18) -
-  7.14e8*q(8)*q(18) - 1.81e10*q(9)*q(18) + 6.68e9*q(2)*q(19) + 1.14e10*q(4)*q(19) - 9.07e9*q(7)*q(19) -
-  2.81e7*q(20) - 4.25e9*q(2)*q(20) + 7.26e9*q(4)*q(20) - 5.78e9*q(7)*q(20) - 3.21e9*q(10)*q(20) +
-  9.6e9*q(11)*q(20) - 9.85e9*q(12)*q(20) + 8.36e9*q(13)*q(20) - 8.23e9*q(14)*q(20) -
-  4.37e9*q(1)*q(21) - 1.03e10*q(3)*q(21) + 6.81e9*q(5)*q(21) + 1.17e10*q(6)*q(21) -
-  1.07e10*q(8)*q(21) + 1.65e10*q(9)*q(21) - 1.03e10*q(2)*q(22) - 1.18e10*q(4)*q(22) +
-  1.87e10*q(7)*q(22) + 1.34e9*q(2)*q(23) + 2.6e10*q(4)*q(23) - 1.82e10*q(7)*q(23) + 7.45e8*q(1)*q(24) -
-  4.e7*q(3)*q(24) + 8.68e8*q(6)*q(24) - 3.21e9*q(1)*q(25) + 1.96e9*q(3)*q(25) - 1.7e9*q(6)*q(25) +
-  6.44e9*q(1)*q(26) - 3.65e9*q(3)*q(26) - 7.81e8*q(6)*q(26) - 7.02e9*q(1)*q(27) - 4.54e8*q(3)*q(27) +
-  4.53e9*q(6)*q(27) + 7.51e9*q(1)*q(28) + 3.84e9*q(3)*q(28) - 5.07e9*q(6)*q(28) - 4.74e8*q(29) -
-  6.89e10*q(2)*q(29) - 4.18e9*q(4)*q(29) + 2.01e10*q(7)*q(29) - 9.06e7*q(10)*q(29) +
-  2.34e8*q(11)*q(29) - 2.06e8*q(12)*q(29) + 2.06e8*q(13)*q(29) - 2.18e8*q(14)*q(29) +
-  6.99e10*q(1)*q(30) + 4.6e9*q(3)*q(30) + 1.75e11*q(5)*q(30) - 1.95e10*q(6)*q(30) +
-  5.09e10*q(8)*q(30) - 5.44e9*q(9)*q(30) - 1.83e7*q(31) + 2.28e9*q(2)*q(31) + 4.94e10*q(4)*q(31) -
-  2.68e10*q(7)*q(31) - 8.41e8*q(10)*q(31) + 3.96e9*q(11)*q(31) - 6.52e9*q(12)*q(31) +
-  4.35e9*q(13)*q(31) - 2.72e9*q(14)*q(31) - 3.3e9*q(1)*q(32) - 4.83e10*q(3)*q(32) -
-  1.62e10*q(5)*q(32) + 2.47e10*q(6)*q(32) - 6.37e10*q(8)*q(32) + 1.35e11*q(9)*q(32) +
-  1.78e11*q(2)*q(33) + 1.81e10*q(4)*q(33) - 5.77e10*q(7)*q(33) + 8.53e6*q(34) - 1.85e10*q(2)*q(34) -
-  2.49e10*q(4)*q(34) + 4.99e10*q(7)*q(34) + 1.11e9*q(10)*q(34) - 2.74e9*q(11)*q(34) +
-  1.88e9*q(12)*q(34) - 1.55e9*q(13)*q(34) + 1.51e9*q(14)*q(34) + 1.99e10*q(1)*q(35) +
-  2.66e10*q(3)*q(35) + 5.64e10*q(5)*q(35) - 4.99e10*q(6)*q(35) + 1.5e11*q(8)*q(35) -
-  7.94e10*q(9)*q(35) - 5.1e10*q(2)*q(36) - 6.43e10*q(4)*q(36) + 1.52e11*q(7)*q(36) + 4.2e9*q(2)*q(37) +
-  1.36e11*q(4)*q(37) - 7.98e10*q(7)*q(37)


return
end

function eq2p(q,gi1,gi2,gi3,crot)
IMPLICIT DOUBLE PRECISION (A-H,O-Z)
dimension q(37)

nxhat=0.d0

eq2p=       7.95e9*q(1)**2 + 6.76e7*q(2) + 4.98e12*q(1)**2*q(2) + 9.31e12*q(2)**3 + 1.33e9*q(1)*q(3) +
-  2.12e12*q(1)*q(2)*q(3) + 5.43e9*q(3)**2 + 3.11e12*q(2)*q(3)**2 - 3.01e3*q(4) + 8.3e11*q(1)**2*q(4) +
-  5.02e12*q(2)**2*q(4) + 5.27e12*q(1)*q(3)*q(4) + 6.86e11*q(3)**2*q(4) + 1.48e13*q(2)*q(4)**2 +
-  1.1e12*q(4)**3 - 3.08e10*q(1)*q(5) - 1.26e13*q(1)*q(2)*q(5) - 4.32e9*q(3)*q(5) -
-  3.29e12*q(2)*q(3)*q(5) - 2.85e12*q(1)*q(4)*q(5) - 7.22e12*q(3)*q(4)*q(5) + 3.24e13*q(2)*q(5)**2 +
-  8.88e12*q(4)*q(5)**2 - 4.73e9*q(1)*q(6) - 4.64e12*q(1)*q(2)*q(6) - 6.14e9*q(3)*q(6) -
-  4.82e12*q(2)*q(3)*q(6) - 3.96e12*q(1)*q(4)*q(6) - 9.79e11*q(3)*q(4)*q(6) + 1.07e10*q(5)*q(6) +
-  6.36e12*q(2)*q(5)*q(6) + 5.57e12*q(4)*q(5)*q(6) + 5.64e9*q(6)**2 + 3.09e12*q(2)*q(6)**2 +
-  1.45e12*q(4)*q(6)**2 + 22.5*q(7) - 2.21e12*q(1)**2*q(7) - 1.27e13*q(2)**2*q(7) -
-  4.48e12*q(1)*q(3)*q(7) - 5.6e11*q(3)**2*q(7) - 2.32e13*q(2)*q(4)*q(7) - 2.51e12*q(4)**2*q(7) +
```

- 6.2e12*q(1)*q(5)*q(7) + 6.09e12*q(3)*q(5)*q(7) - 1.71e13*q(5)**2*q(7) + 5.8e12*q(1)*q(6)*q(7) +
- 3.03e12*q(3)*q(6)*q(7) - 7.69e12*q(5)*q(6)*q(7) - 5.93e11*q(6)**2*q(7) + 1.64e13*q(2)*q(7)**2 +
- 8.01e12*q(4)*q(7)**2 - 1.04e12*q(7)**3 - 8.78e9*q(1)*q(8) - 6.03e12*q(1)*q(2)*q(8) -
- 1.36e10*q(3)*q(8) - 6.22e12*q(2)*q(3)*q(8) - 5.99e12*q(1)*q(4)*q(8) - 9.38e11*q(3)*q(4)*q(8) +
- 3.41e13*q(2)*q(5)*q(8) + 3.09e13*q(4)*q(5)*q(8) + 2.64e10*q(6)*q(8) + 8.3e12*q(2)*q(6)*q(8) +
- 4.54e12*q(4)*q(6)*q(8) + 8.61e12*q(1)*q(7)*q(8) + 3.78e12*q(3)*q(7)*q(8) - 4.36e13*q(5)*q(7)*q(8) -
- 9.13e11*q(6)*q(7)*q(8) + 2.53e13*q(2)*q(8)**2 + 1.17e13*q(4)*q(8)**2 - 2.95e11*q(7)*q(8)**2 +
- 8.71e8*q(1)*q(9) + 2.12e12*q(1)*q(2)*q(9) + 2.39e10*q(3)*q(9) + 7.38e12*q(2)*q(3)*q(9) +
- 7.92e12*q(1)*q(4)*q(9) + 1.34e12*q(3)*q(4)*q(9) - 1.51e13*q(2)*q(5)*q(9) - 3.88e13*q(4)*q(5)*q(9) -
- 1.31e10*q(6)*q(9) - 5.75e12*q(2)*q(6)*q(9) - 1.16e12*q(4)*q(6)*q(9) - 6.21e12*q(1)*q(7)*q(9) -
- 9.51e11*q(3)*q(7)*q(9) + 3.22e13*q(5)*q(7)*q(9) + 3.5e12*q(6)*q(7)*q(9) - 3.59e13*q(2)*q(8)*q(9) -
- 3.04e12*q(4)*q(8)*q(9) + 2.03e13*q(7)*q(8)*q(9) + 2.33e13*q(2)*q(9)**2 + 2.39e12*q(4)*q(9)**2 -
- 2.23e12*q(7)*q(9)**2 + 1.89e10*q(1)**2*q(10) + 4.09e10*q(2)*q(10) + 8.16e10*q(1)*q(3)*q(10) +
- 3.01e10*q(3)**2*q(10) + 2.53e9*q(4)*q(10) - 6.46e10*q(1)*q(5)*q(10) - 2.12e11*q(3)*q(5)*q(10) -
- 7.67e10*q(1)*q(6)*q(10) - 7.59e10*q(3)*q(6)*q(10) + 1.84e11*q(5)*q(6)*q(10) +
- 2.44e10*q(6)**2*q(10) - 1.17e10*q(7)*q(10) + 6.23e10*q(1)*q(8)*q(10) - 2.38e11*q(3)*q(8)*q(10) +
- 8.72e10*q(6)*q(8)*q(10) - 8.57e10*q(1)*q(9)*q(10) + 8.34e10*q(3)*q(9)*q(10) +
- 6.89e10*q(6)*q(9)*q(10) + 5.07e10*q(2)*q(10)**2 + 1.42e9*q(4)*q(10)**2 - 9.e9*q(7)*q(10)**2 -
- 5.43e10*q(1)**2*q(11) - 1.23e10*q(2)*q(11) - 2.91e11*q(1)*q(3)*q(11) - 1.02e11*q(3)**2*q(11) -
- 1.37e10*q(4)*q(11) + 1.86e11*q(1)*q(5)*q(11) + 7.39e11*q(3)*q(5)*q(11) + 2.47e11*q(1)*q(6)*q(11) +
- 2.03e11*q(3)*q(6)*q(11) - 5.8e11*q(5)*q(6)*q(11) - 9.03e10*q(6)**2*q(11) + 2.89e10*q(7)*q(11) -
- 1.15e11*q(1)*q(8)*q(11) + 5.82e11*q(3)*q(8)*q(11) - 2.16e11*q(6)*q(8)*q(11) +
- 2.99e11*q(1)*q(9)*q(11) - 2.1e11*q(3)*q(9)*q(11) - 8.35e10*q(6)*q(9)*q(11) -
- 2.92e11*q(2)*q(10)*q(11) - 5.58e9*q(4)*q(10)*q(11) + 1.16e11*q(7)*q(10)*q(11) +
- 4.55e11*q(2)*q(11)**2 + 4.82e10*q(4)*q(11)**2 - 1.9e11*q(7)*q(11)**2 + 5.83e10*q(1)**2*q(12) +
- 3.61e9*q(2)*q(12) + 4.97e11*q(1)*q(3)*q(12) + 1.45e11*q(3)**2*q(12) + 2.71e10*q(4)*q(12) -
- 2.03e11*q(1)*q(5)*q(12) - 1.21e12*q(3)*q(5)*q(12) - 3.26e11*q(1)*q(6)*q(12) -
- 2.73e11*q(3)*q(6)*q(12) + 7.5e11*q(5)*q(6)*q(12) + 1.93e11*q(6)**2*q(12) - 1.63e10*q(7)*q(12) -
- 5.29e10*q(1)*q(8)*q(12) - 4.06e11*q(3)*q(8)*q(12) + 3.35e11*q(6)*q(8)*q(12) -
- 3.55e11*q(1)*q(9)*q(12) + 2.55e11*q(3)*q(9)*q(12) - 1.36e11*q(6)*q(9)*q(12) +
- 3.2e11*q(2)*q(10)*q(12) + 1.14e11*q(4)*q(10)*q(12) - 3.e11*q(7)*q(10)*q(12) -
- 1.13e12*q(2)*q(11)*q(12) - 3.75e11*q(4)*q(11)*q(12) + 7.5e11*q(7)*q(11)*q(12) +
- 9.33e11*q(2)*q(12)**2 + 2.83e11*q(4)*q(12)**2 - 3.55e11*q(7)*q(12)**2 - 5.65e10*q(1)**2*q(13) -
- 1.56e9*q(2)*q(13) - 5.84e11*q(1)*q(3)*q(13) - 1.77e11*q(3)**2*q(13) - 1.87e10*q(4)*q(13) +
- 2.01e11*q(1)*q(5)*q(13) + 1.4e12*q(3)*q(5)*q(13) + 3.2e11*q(1)*q(6)*q(13) +
- 5.83e11*q(3)*q(6)*q(13) - 7.51e11*q(5)*q(6)*q(13) - 2.87e11*q(6)**2*q(13) + 4.76e9*q(7)*q(13) +
- 1.23e11*q(1)*q(8)*q(13) + 7.11e11*q(3)*q(8)*q(13) - 6.67e11*q(6)*q(8)*q(13) +
- 1.62e11*q(1)*q(9)*q(13) - 3.3e11*q(3)*q(9)*q(13) + 2.34e11*q(6)*q(9)*q(13) -
- 3.17e11*q(2)*q(10)*q(13) - 3.42e11*q(4)*q(10)*q(13) + 3.58e11*q(7)*q(10)*q(13) +
- 1.1e12*q(2)*q(11)*q(13) + 8.04e11*q(4)*q(11)*q(13) - 1.18e12*q(7)*q(11)*q(13) -
- 2.1e12*q(2)*q(12)*q(13) - 6.72e11*q(4)*q(12)*q(13) + 1.35e12*q(7)*q(12)*q(13) +
- 1.64e12*q(2)*q(13)**2 + 4.39e11*q(4)*q(13)**2 - 5.08e11*q(7)*q(13)**2 + 5.59e10*q(1)**2*q(14) +
- 1.19e9*q(2)*q(14) + 5.01e11*q(1)*q(3)*q(14) + 3.99e11*q(3)**2*q(14) + 5.45e9*q(4)*q(14) -
- 2.01e11*q(1)*q(5)*q(14) - 1.24e12*q(3)*q(5)*q(14) - 2.95e11*q(1)*q(6)*q(14) -
- 8.67e11*q(3)*q(6)*q(14) + 7.13e11*q(5)*q(6)*q(14) + 2.78e11*q(6)**2*q(14) - 2.45e9*q(7)*q(14) -
- 1.06e11*q(1)*q(8)*q(14) - 1.36e12*q(3)*q(8)*q(14) + 7.18e11*q(6)*q(8)*q(14) -
- 1.77e10*q(1)*q(9)*q(14) + 6.29e11*q(3)*q(9)*q(14) - 5.07e11*q(6)*q(9)*q(14) +
- 3.18e11*q(2)*q(10)*q(14) + 4.07e11*q(4)*q(10)*q(14) - 3.34e11*q(7)*q(10)*q(14) -
- 1.02e12*q(2)*q(11)*q(14) - 1.31e12*q(4)*q(11)*q(14) + 1.2e12*q(7)*q(11)*q(14) +
- 1.78e12*q(2)*q(12)*q(14) + 1.39e12*q(4)*q(12)*q(14) - 2.16e12*q(7)*q(12)*q(14) -
- 3.38e12*q(2)*q(13)*q(14) - 9.35e11*q(4)*q(13)*q(14) + 2.11e12*q(7)*q(13)*q(14) +
- 2.57e12*q(2)*q(14)**2 + 5.52e11*q(4)*q(14)**2 - 6.16e11*q(7)*q(14)**2 + 2.58e9*q(1)*q(15) +
- 8.67e9*q(3)*q(15) - 1.92e9*q(5)*q(15) - 9.89e9*q(6)*q(15) + 1.54e10*q(8)*q(15) - 9.26e9*q(9)*q(15) +
- 1.25e7*q(16) + 1.51e10*q(10)*q(16) - 3.88e10*q(11)*q(16) + 3.4e10*q(12)*q(16) - 3.49e10*q(13)*q(16) +
- 3.52e10*q(14)*q(16) + 7.22e9*q(1)*q(17) + 7.45e9*q(3)*q(17) - 1.47e10*q(5)*q(17) -
- 5.87e9*q(6)*q(17) + 4.38e9*q(8)*q(17) - 2.49e10*q(9)*q(17) + 4.49e7*q(18) + 6.64e9*q(10)*q(18) -
- 2.68e10*q(11)*q(18) + 5.e10*q(12)*q(18) - 5.05e10*q(13)*q(18) + 3.61e10*q(14)*q(18) +
- 7.18e9*q(1)*q(19) + 2.29e10*q(3)*q(19) - 1.99e10*q(6)*q(19) - 4.57e9*q(1)*q(20) - 9.19e9*q(3)*q(20) +
- 7.11e9*q(5)*q(20) + 7.03e9*q(6)*q(20) - 1.56e10*q(8)*q(20) + 1.71e10*q(9)*q(20) - 3.11e7*q(21) -
- 1.23e10*q(10)*q(21) + 3.89e10*q(11)*q(21) - 4.36e10*q(12)*q(21) + 3.5e10*q(13)*q(21) -
- 3.43e10*q(14)*q(21) - 1.11e10*q(1)*q(22) - 3.04e10*q(3)*q(22) + 3.3e10*q(6)*q(22) +
- 1.45e9*q(1)*q(23) + 4.64e10*q(3)*q(23) - 2.54e10*q(6)*q(23) + 2.68e9*q(2)*q(24) + 2.88e8*q(4)*q(24) +
- 3.3e9*q(7)*q(24) - 1.2e10*q(2)*q(25) + 5.71e9*q(4)*q(25) - 8.11e9*q(7)*q(25) + 2.47e10*q(2)*q(26) -
- 1.66e10*q(4)*q(26) + 6.07e8*q(7)*q(26) - 2.74e10*q(2)*q(27) + 6.31e9*q(4)*q(27) +
- 1.52e10*q(7)*q(27) + 2.95e10*q(2)*q(28) + 9.92e9*q(4)*q(28) - 1.82e10*q(7)*q(28) -
- 7.41e10*q(1)*q(29) - 5.26e9*q(3)*q(29) + 1.85e11*q(5)*q(29) + 2.11e10*q(6)*q(29) +

```
-  5.4e10*q(8)*q(29) - 5.74e9*q(9)*q(29) - 9.63e8*q(30) - 2.42e8*q(10)*q(30) + 6.22e8*q(11)*q(30) -
-  6.23e8*q(12)*q(30) + 6.84e8*q(13)*q(30) - 7.4e8*q(14)*q(30) + 2.45e9*q(1)*q(31) +
-  4.35e10*q(3)*q(31) - 1.88e10*q(5)*q(31) - 2.41e10*q(6)*q(31) - 8.18e10*q(8)*q(31) +
-  1.54e11*q(9)*q(31) - 1.15e7*q(32) - 1.61e9*q(10)*q(32) + 7.65e9*q(11)*q(32) - 1.34e10*q(12)*q(32) +
-  1.02e10*q(13)*q(32) - 6.57e9*q(14)*q(32) + 1.91e11*q(1)*q(33) + 2.52e10*q(3)*q(33) -
-  6.51e10*q(6)*q(33) - 1.99e10*q(1)*q(34) - 2.45e10*q(3)*q(34) + 6.15e10*q(5)*q(34) +
-  4.92e10*q(6)*q(34) + 1.62e11*q(8)*q(34) - 8.29e10*q(9)*q(34) + 5.08e6*q(35) + 2.17e9*q(10)*q(35) -
-  5.49e9*q(11)*q(35) + 3.92e9*q(12)*q(35) - 3.07e9*q(13)*q(35) + 2.96e9*q(14)*q(35) -
-  5.48e10*q(1)*q(36) - 8.23e10*q(3)*q(36) + 1.64e11*q(6)*q(36) + 4.54e9*q(1)*q(37) +
-  1.51e11*q(3)*q(37) - 8.32e10*q(6)*q(37)


 return
 end

 function eq3p(q,gi1,gi2,gi3,crot)
 IMPLICIT DOUBLE PRECISION (A-H,O-Z)
 dimension q(37)

 nxhat=0.d0

 eq3p=       -185.*q(1) + 1.e11*q(1)**3 + 9.97e8*q(1)*q(2) + 7.95e11*q(1)*q(2)**2 + 6.74e7*q(3) +
-  8.59e11*q(1)**2*q(3) + 8.16e9*q(2)*q(3) + 2.34e12*q(2)**2*q(3) + 2.17e11*q(1)*q(3)**2 +
-  6.39e11*q(3)**3 + 8.02e9*q(1)*q(4) + 3.96e12*q(1)*q(2)*q(4) + 6.07e9*q(3)*q(4) +
-  1.03e12*q(2)*q(3)*q(4) + 4.44e11*q(1)*q(4)**2 + 3.91e12*q(3)*q(4)**2 + 2.75e11*q(1)**2*q(5) -
-  3.24e9*q(2)*q(5) - 1.24e12*q(2)**2*q(5) + 1.1e12*q(1)*q(3)*q(5) + 8.47e10*q(3)**2*q(5) -
-  1.48e10*q(4)*q(5) - 5.42e12*q(2)*q(4)*q(5) - 8.18e11*q(4)**2*q(5) + 2.e12*q(1)*q(5)**2 +
-  4.04e12*q(3)*q(5)**2 - 122.*q(6) - 6.78e11*q(1)**2*q(6) - 4.62e9*q(2)*q(6) - 1.81e12*q(2)**2*q(6) -
-  3.23e11*q(1)*q(3)*q(6) - 7.21e10*q(3)**2*q(6) + 4.45e9*q(4)*q(6) - 7.36e11*q(2)*q(4)*q(6) -
-  6.23e10*q(4)**2*q(6) - 9.53e11*q(1)*q(5)*q(6) - 1.16e11*q(3)*q(5)*q(6) - 3.32e12*q(5)**2*q(6) +
-  4.52e11*q(1)*q(6)**2 + 1.15e12*q(3)*q(6)**2 + 2.88e11*q(5)*q(6)**2 - 8.41e10*q(6)**3 -
-  4.8e9*q(1)*q(7) - 3.37e12*q(1)*q(2)*q(7) + 4.39e9*q(3)*q(7) - 8.43e11*q(2)*q(3)*q(7) -
-  6.69e11*q(1)*q(4)*q(7) - 4.01e11*q(3)*q(4)*q(7) + 9.32e9*q(5)*q(7) + 4.57e12*q(2)*q(5)*q(7) +
-  1.38e12*q(4)*q(5)*q(7) + 5.13e9*q(6)*q(7) + 2.27e12*q(2)*q(6)*q(7) + 4.94e12*q(4)*q(6)*q(7) +
-  9.64e11*q(1)*q(7)**2 + 2.74e12*q(3)*q(7)**2 - 1.57e12*q(5)*q(7)**2 - 7.08e11*q(6)*q(7)**2 +
-  6.06e11*q(1)**2*q(8) - 1.02e10*q(2)*q(8) - 2.34e12*q(2)**2*q(8) + 1.84e10*q(1)*q(3)*q(8) -
-  1.83e11*q(3)**2*q(8) + 1.26e10*q(4)*q(8) - 7.07e11*q(2)*q(4)*q(8) + 2.59e11*q(4)**2*q(8) +
-  6.74e12*q(1)*q(5)*q(8) + 1.77e12*q(3)*q(5)*q(8) - 6.75e11*q(1)*q(6)*q(8) - 1.79e12*q(3)*q(6)*q(8) -
-  4.86e12*q(5)*q(6)*q(8) + 4.87e10*q(6)**2*q(8) + 1.18e10*q(7)*q(8) + 2.83e12*q(2)*q(7)*q(8) +
-  8.03e12*q(4)*q(7)*q(8) - 8.33e11*q(7)**2*q(8) + 2.08e12*q(1)*q(8)**2 + 7.56e12*q(3)*q(8)**2 -
-  5.88e11*q(6)*q(8)**2 - 8.06e11*q(1)**2*q(9) + 1.8e10*q(2)*q(9) + 2.77e12*q(2)**2*q(9) -
-  1.85e11*q(1)*q(3)*q(9) - 1.29e12*q(3)**2*q(9) + 1.1e10*q(4)*q(9) + 1.e12*q(2)*q(4)*q(9) +
-  5.28e12*q(4)**2*q(9) - 7.92e12*q(1)*q(5)*q(9) - 2.25e12*q(3)*q(5)*q(9) + 1.31e11*q(1)*q(6)*q(9) -
-  1.39e11*q(3)*q(6)*q(9) + 1.81e12*q(5)*q(6)*q(9) - 9.04e11*q(6)**2*q(9) + 9.87e9*q(7)*q(9) -
-  7.15e11*q(2)*q(7)*q(9) - 7.72e11*q(4)*q(7)*q(9) + 3.32e12*q(7)**2*q(9) - 5.05e11*q(1)*q(8)*q(9) +
-  1.38e11*q(3)*q(8)*q(9) + 1.23e13*q(6)*q(8)*q(9) + 4.57e11*q(1)*q(9)**2 + 8.87e12*q(3)*q(9)**2 -
-  4.67e11*q(6)*q(9)**2 + 7.81e8*q(1)*q(10) + 6.13e10*q(1)*q(2)*q(10) + 6.31e9*q(3)*q(10) +
-  4.51e10*q(2)*q(3)*q(10) + 2.63e10*q(1)*q(4)*q(10) + 4.2e10*q(3)*q(4)*q(10) -
-  1.59e11*q(2)*q(5)*q(10) - 8.34e10*q(4)*q(5)*q(10) - 3.56e9*q(6)*q(10) - 5.69e10*q(2)*q(6)*q(10) -
-  6.e10*q(4)*q(6)*q(10) - 6.52e10*q(1)*q(7)*q(10) - 5.95e10*q(3)*q(7)*q(10) +
-  1.42e11*q(5)*q(7)*q(10) + 2.42e10*q(6)*q(7)*q(10) - 1.78e11*q(2)*q(8)*q(10) -
-  1.16e11*q(4)*q(8)*q(10) + 6.17e8*q(7)*q(8)*q(10) + 6.25e10*q(2)*q(9)*q(10) +
-  7.52e10*q(4)*q(9)*q(10) - 9.95e10*q(7)*q(9)*q(10) + 7.71e8*q(1)*q(10)**2 + 1.77e10*q(3)*q(10)**2 -
-  7.25e9*q(6)*q(10)**2 - 3.56e9*q(1)*q(11) - 2.19e11*q(1)*q(2)*q(11) + 3.24e9*q(3)*q(11) -
-  1.53e11*q(2)*q(3)*q(11) - 5.81e10*q(1)*q(4)*q(11) - 2.02e11*q(3)*q(4)*q(11) +
-  5.55e11*q(2)*q(5)*q(11) + 2.88e11*q(4)*q(5)*q(11) + 4.26e9*q(6)*q(11) + 1.53e11*q(2)*q(6)*q(11) +
-  2.07e11*q(4)*q(6)*q(11) + 1.7e11*q(1)*q(7)*q(11) + 1.37e11*q(3)*q(7)*q(11) -
-  3.76e11*q(5)*q(7)*q(11) - 1.6e11*q(6)*q(7)*q(11) + 4.37e11*q(2)*q(8)*q(11) +
-  2.16e11*q(4)*q(8)*q(11) - 3.1e11*q(7)*q(8)*q(11) - 1.58e11*q(2)*q(9)*q(11) -
-  3.24e11*q(4)*q(9)*q(11) + 3.37e11*q(7)*q(9)*q(11) - 8.12e9*q(1)*q(10)*q(11) -
-  6.45e10*q(3)*q(10)*q(11) + 6.08e10*q(6)*q(10)*q(11) + 2.26e10*q(1)*q(11)**2 + 1.37e11*q(3)*q(11)**2 -
-  7.03e10*q(6)*q(11)**2 + 6.31e9*q(1)*q(12) + 3.73e11*q(1)*q(2)*q(12) + 5.23e9*q(3)*q(12) +
-  2.17e11*q(2)*q(3)*q(12) + 7.22e10*q(1)*q(4)*q(12) + 5.e11*q(3)*q(4)*q(12) -
-  9.08e11*q(2)*q(5)*q(12) - 4.43e11*q(4)*q(5)*q(12) + 3.24e9*q(6)*q(12) - 2.05e11*q(2)*q(6)*q(12) -
-  1.63e11*q(4)*q(6)*q(12) - 1.3e11*q(1)*q(7)*q(12) - 2.31e11*q(3)*q(7)*q(12) +
-  4.54e11*q(5)*q(7)*q(12) + 4.21e11*q(6)*q(7)*q(12) - 3.05e11*q(2)*q(8)*q(12) -
```

```
-  3.13e11*q(4)*q(8)*q(12) + 1.08e12*q(7)*q(8)*q(12) + 1.91e11*q(2)*q(9)*q(12) +
-  8.42e11*q(4)*q(9)*q(12) - 3.48e11*q(7)*q(9)*q(12) + 4.16e10*q(1)*q(10)*q(12) +
-  5.54e10*q(3)*q(10)*q(12) - 6.74e10*q(6)*q(10)*q(12) - 1.15e11*q(1)*q(11)*q(12) -
-  2.33e11*q(3)*q(11)*q(12) + 2.18e11*q(6)*q(11)*q(12) + 7.18e10*q(1)*q(12)**2 + 3.42e11*q(3)*q(12)**2 -
-  1.25e11*q(6)*q(12)**2 - 4.13e9*q(1)*q(13) - 4.38e11*q(1)*q(2)*q(13) + 2.73e9*q(3)*q(13) -
-  2.66e11*q(2)*q(3)*q(13) - 9.98e10*q(1)*q(4)*q(13) - 2.41e11*q(3)*q(4)*q(13) +
-  1.05e12*q(2)*q(5)*q(13) + 5.3e11*q(4)*q(5)*q(13) + 3.7e9*q(6)*q(13) + 4.38e11*q(2)*q(6)*q(13) +
-  2.07e11*q(4)*q(6)*q(13) + 1.75e11*q(1)*q(7)*q(13) + 6.67e11*q(3)*q(7)*q(13) -
-  8.82e11*q(5)*q(7)*q(13) - 2.87e11*q(6)*q(7)*q(13) + 5.34e11*q(2)*q(8)*q(13) +
-  1.36e12*q(4)*q(8)*q(13) - 6.21e11*q(7)*q(8)*q(13) - 2.48e11*q(2)*q(9)*q(13) -
-  5.28e11*q(4)*q(9)*q(13) + 5.41e11*q(7)*q(9)*q(13) - 8.34e10*q(1)*q(10)*q(13) -
-  9.44e10*q(3)*q(10)*q(13) + 3.82e10*q(6)*q(10)*q(13) + 2.15e11*q(1)*q(11)*q(13) +
-  2.04e11*q(3)*q(11)*q(13) - 2.47e11*q(6)*q(11)*q(13) - 1.92e11*q(1)*q(12)*q(13) -
-  3.58e11*q(3)*q(12)*q(13) + 5.19e11*q(6)*q(12)*q(13) + 1.1e11*q(1)*q(13)**2 + 6.97e11*q(3)*q(13)**2 -
-  1.79e11*q(6)*q(13)**2 + 1.28e9*q(1)*q(14) + 3.76e11*q(1)*q(2)*q(14) + 3.32e9*q(3)*q(14) +
-  5.99e11*q(2)*q(3)*q(14) + 1.26e11*q(1)*q(4)*q(14) + 2.7e11*q(3)*q(4)*q(14) -
-  9.33e11*q(2)*q(5)*q(14) - 1.06e12*q(4)*q(5)*q(14) - 5.92e9*q(6)*q(14) - 6.51e11*q(2)*q(6)*q(14) -
-  2.98e11*q(4)*q(6)*q(14) - 3.31e11*q(1)*q(7)*q(14) - 4.4e11*q(3)*q(7)*q(14) +
-  1.33e12*q(5)*q(7)*q(14) + 1.19e11*q(6)*q(7)*q(14) - 1.02e12*q(2)*q(8)*q(14) -
-  1.e12*q(4)*q(8)*q(14) + 5.34e10*q(7)*q(8)*q(14) + 4.73e11*q(2)*q(9)*q(14) +
-  4.24e11*q(4)*q(9)*q(14) - 5.69e11*q(7)*q(9)*q(14) + 8.45e10*q(1)*q(10)*q(14) +
-  7.58e10*q(3)*q(10)*q(14) - 8.18e10*q(6)*q(10)*q(14) - 2.97e11*q(1)*q(11)*q(14) -
-  3.19e11*q(3)*q(11)*q(14) + 1.78e11*q(6)*q(11)*q(14) + 3.82e11*q(1)*q(12)*q(14) +
-  3.68e11*q(3)*q(12)*q(14) - 4.13e11*q(6)*q(12)*q(14) - 2.7e11*q(1)*q(13)*q(14) -
-  4.67e11*q(3)*q(13)*q(14) + 8.93e11*q(6)*q(13)*q(14) + 1.4e11*q(1)*q(14)**2 + 1.18e12*q(3)*q(14)**2 -
-  2.48e11*q(6)*q(14)**2 + 1.43e7*q(15) + 6.52e9*q(2)*q(15) + 2.16e9*q(4)*q(15) - 1.e10*q(7)*q(15) -
-  1.48e8*q(10)*q(15) + 2.92e9*q(11)*q(15) + 4.08e9*q(12)*q(15) - 1.25e10*q(13)*q(15) +
-  8.1e9*q(14)*q(15) + 6.51e9*q(1)*q(16) + 4.31e9*q(3)*q(16) - 1.71e10*q(5)*q(16) - 7.77e9*q(6)*q(16) -
-  3.03e10*q(8)*q(16) + 6.23e9*q(9)*q(16) - 4.75e7*q(17) + 5.59e9*q(2)*q(17) + 3.22e9*q(4)*q(17) -
-  5.5e9*q(7)*q(17) + 8.39e8*q(10)*q(17) - 2.83e9*q(11)*q(17) + 6.21e9*q(12)*q(17) -
-  4.43e9*q(13)*q(17) + 8.81e9*q(14)*q(17) + 1.27e10*q(1)*q(18) + 8.38e9*q(3)*q(18) -
-  1.82e10*q(5)*q(18) + 4.52e8*q(6)*q(18) - 7.73e9*q(8)*q(18) + 6.18e9*q(9)*q(18) + 1.72e10*q(2)*q(19) +
-  9.21e9*q(4)*q(19) - 1.71e10*q(7)*q(19) + 9.99e6*q(20) - 6.9e9*q(2)*q(20) - 4.16e9*q(4)*q(20) +
-  5.93e9*q(7)*q(20) + 9.05e8*q(10)*q(20) + 1.34e9*q(11)*q(20) - 4.24e9*q(12)*q(20) +
-  7.72e9*q(13)*q(20) - 9.09e9*q(14)*q(20) - 8.34e9*q(1)*q(21) - 4.03e9*q(3)*q(21) + 2.e10*q(5)*q(21) +
-  6.55e9*q(6)*q(21) + 1.47e10*q(8)*q(21) - 8.86e9*q(9)*q(21) - 2.28e10*q(2)*q(22) - 5.72e9*q(4)*q(22) +
-  1.85e10*q(7)*q(22) + 3.49e10*q(2)*q(23) + 1.79e10*q(4)*q(23) + 3.83e9*q(7)*q(23) -
-  3.13e7*q(1)*q(24) + 4.55e9*q(3)*q(24) + 1.61e9*q(6)*q(24) + 1.58e9*q(1)*q(25) - 4.7e9*q(3)*q(25) +
-  1.12e9*q(6)*q(25) - 2.95e9*q(1)*q(26) + 3.47e9*q(3)*q(26) - 6.18e9*q(6)*q(26) - 3.7e8*q(1)*q(27) -
-  6.19e9*q(3)*q(27) + 3.42e9*q(6)*q(27) + 3.1e9*q(1)*q(28) + 6.57e9*q(3)*q(28) - 2.84e9*q(6)*q(28) +
-  1.35e6*q(29) - 3.95e9*q(2)*q(29) - 3.84e10*q(4)*q(29) + 2.18e10*q(7)*q(29) - 8.12e8*q(10)*q(29) +
-  3.66e9*q(11)*q(29) - 6.28e9*q(12)*q(29) + 4.89e9*q(13)*q(29) - 3.13e9*q(14)*q(29) +
-  3.72e9*q(1)*q(30) + 3.03e10*q(3)*q(30) + 1.93e10*q(5)*q(30) - 1.76e10*q(6)*q(30) +
-  6.22e10*q(8)*q(30) - 1.13e11*q(9)*q(30) + 4.99e8*q(31) + 3.26e10*q(2)*q(31) + 2.64e10*q(4)*q(31) +
-  2.2e10*q(7)*q(31) + 1.98e7*q(10)*q(31) - 8.17e7*q(11)*q(31) + 2.51e8*q(12)*q(31) +
-  1.99e8*q(13)*q(31) + 7.41e8*q(14)*q(31) - 3.9e10*q(1)*q(32) - 2.62e10*q(3)*q(32) -
-  8.27e10*q(5)*q(32) - 2.27e10*q(6)*q(32) + 7.81e10*q(8)*q(32) + 6.49e10*q(9)*q(32) +
-  1.89e10*q(2)*q(33) + 8.14e10*q(4)*q(33) - 5.25e10*q(7)*q(33) - 3.04e6*q(34) - 1.84e10*q(2)*q(34) +
-  2.24e10*q(4)*q(34) + 2.19e10*q(7)*q(34) - 1.53e9*q(10)*q(34) + 1.95e9*q(11)*q(34) +
-  1.16e9*q(12)*q(34) + 2.82e9*q(13)*q(34) - 3.94e9*q(14)*q(34) + 2.15e10*q(1)*q(35) -
-  2.05e10*q(3)*q(35) + 5.3e10*q(5)*q(35) - 2.16e10*q(6)*q(35) + 6.96e10*q(8)*q(35) +
-  6.24e10*q(9)*q(35) - 6.19e10*q(2)*q(36) + 7.77e10*q(4)*q(36) + 6.97e10*q(7)*q(36) +
-  1.14e11*q(2)*q(37) + 6.49e10*q(4)*q(37) + 6.39e10*q(7)*q(37)


 return
 end

 function eq4p(q,gi1,gi2,gi3,crot)
 IMPLICIT DOUBLE PRECISION (A-H,O-Z)
 dimension q(37)

 nxhat=0.d0

 eq4p=       4.05e8*q(1)**2 - 2.68e3*q(2) + 7.39e11*q(1)**2*q(2) + 1.49e12*q(2)**3 + 9.52e9*q(1)*q(3) +
-  4.69e12*q(1)*q(2)*q(3) + 3.61e9*q(3)**2 + 6.11e11*q(2)*q(3)**2 + 6.77e7*q(4) + 2.42e12*q(1)**2*q(4) +
```

- 1.32e13*q(2)**2*q(4) + 1.05e12*q(1)*q(3)*q(4) + 4.64e12*q(3)**2*q(4) + 2.93e12*q(2)*q(4)**2 +
- 7.65e12*q(4)**3 - 3.09e9*q(1)*q(5) - 2.54e12*q(1)*q(2)*q(5) - 1.76e10*q(3)*q(5) -
- 6.43e12*q(2)*q(3)*q(5) - 5.63e12*q(1)*q(4)*q(5) - 1.94e12*q(3)*q(4)*q(5) + 7.91e12*q(2)*q(5)**2 +
- 1.57e13*q(4)*q(5)**2 - 4.78e9*q(1)*q(6) - 3.53e12*q(1)*q(2)*q(6) + 5.3e9*q(3)*q(6) -
- 8.72e11*q(2)*q(3)*q(6) - 8.19e11*q(1)*q(4)*q(6) - 1.39e11*q(3)*q(4)*q(6) + 9.45e9*q(5)*q(6) +
- 4.96e12*q(2)*q(5)*q(6) + 1.47e12*q(4)*q(5)*q(6) + 3.6e9*q(6)**2 + 1.29e12*q(2)*q(6)**2 +
- 3.1e12*q(4)*q(6)**2 - 5.38e3*q(7) - 1.86e12*q(1)**2*q(7) - 1.03e13*q(2)**2*q(7) -
- 7.92e11*q(1)*q(3)*q(7) - 2.34e11*q(3)**2*q(7) - 4.47e12*q(2)*q(4)*q(7) - 7.47e11*q(4)**2*q(7) +
- 4.68e12*q(1)*q(5)*q(7) + 1.63e12*q(3)*q(5)*q(7) - 1.31e13*q(5)**2*q(7) + 2.64e12*q(1)*q(6)*q(7) +
- 5.87e12*q(3)*q(6)*q(7) - 3.63e12*q(5)*q(6)*q(7) - 4.4e11*q(6)**2*q(7) + 7.13e12*q(2)*q(7)**2 +
- 1.57e13*q(4)*q(7)**2 - 1.06e12*q(7)**3 - 1.04e10*q(1)*q(8) - 5.33e12*q(1)*q(2)*q(8) +
- 1.5e10*q(3)*q(8) - 8.36e11*q(2)*q(3)*q(8) - 5.65e11*q(1)*q(4)*q(8) + 6.27e11*q(3)*q(4)*q(8) +
- 2.75e13*q(2)*q(5)*q(8) + 6.61e12*q(4)*q(5)*q(8) + 1.68e10*q(6)*q(8) + 4.04e12*q(2)*q(6)*q(8) +
- 8.88e12*q(4)*q(6)*q(8) + 3.5e12*q(1)*q(7)*q(8) + 9.54e12*q(3)*q(7)*q(8) - 2.07e13*q(5)*q(7)*q(8) -
- 6.71e11*q(6)*q(7)*q(8) + 1.05e13*q(2)*q(8)**2 + 2.96e13*q(4)*q(8)**2 - 1.87e11*q(7)*q(8)**2 +
- 2.1e10*q(1)*q(9) + 7.05e12*q(1)*q(2)*q(9) + 1.31e10*q(3)*q(9) + 1.19e12*q(2)*q(3)*q(9) +
- 1.07e12*q(1)*q(4)*q(9) + 1.25e13*q(3)*q(4)*q(9) - 3.46e13*q(2)*q(5)*q(9) - 8.66e12*q(4)*q(5)*q(9) +
- 1.18e10*q(6)*q(9) - 1.04e12*q(2)*q(6)*q(9) - 1.8e11*q(4)*q(6)*q(9) - 8.84e11*q(1)*q(7)*q(9) -
- 9.04e11*q(3)*q(7)*q(9) + 7.51e12*q(5)*q(7)*q(9) + 8.42e12*q(6)*q(7)*q(9) - 2.71e12*q(2)*q(8)*q(9) +
- 1.77e12*q(4)*q(8)*q(9) + 5.09e13*q(7)*q(8)*q(9) + 2.13e12*q(2)*q(9)**2 + 3.48e13*q(4)*q(9)**2 -
- 2.79e12*q(7)*q(9)**2 - 1.86e10*q(1)**2*q(10) + 2.26e9*q(2)*q(10) + 3.12e10*q(1)*q(3)*q(10) +
- 2.49e10*q(3)**2*q(10) + 2.39e10*q(4)*q(10) - 9.66e10*q(1)*q(5)*q(10) - 9.89e10*q(3)*q(5)*q(10) +
- 2.81e10*q(1)*q(6)*q(10) - 7.12e10*q(3)*q(6)*q(10) + 9.25e10*q(5)*q(6)*q(10) +
- 4.24e10*q(6)**2*q(10) - 1.28e10*q(7)*q(10) - 1.27e11*q(1)*q(8)*q(10) - 1.37e11*q(3)*q(8)*q(10) +
- 7.64e10*q(6)*q(8)*q(10) + 8.44e10*q(1)*q(9)*q(10) + 8.92e10*q(3)*q(9)*q(10) -
- 1.11e11*q(6)*q(9)*q(10) + 1.26e9*q(2)*q(10)**2 + 4.6e10*q(4)*q(10)**2 - 1.73e10*q(7)*q(10)**2 +
- 6.64e10*q(1)**2*q(11) - 1.22e10*q(2)*q(11) - 6.9e10*q(1)*q(3)*q(11) - 1.2e11*q(3)**2*q(11) +
- 1.3e10*q(4)*q(11) + 3.35e11*q(1)*q(5)*q(11) + 3.41e11*q(3)*q(5)*q(11) - 3.06e10*q(1)*q(6)*q(11) +
- 2.45e11*q(3)*q(6)*q(11) - 2.75e11*q(5)*q(6)*q(11) - 5.55e10*q(6)**2*q(11) + 1.73e10*q(7)*q(11) +
- 3.67e11*q(1)*q(8)*q(11) + 2.56e11*q(3)*q(8)*q(11) - 3.04e11*q(6)*q(8)*q(11) -
- 1.59e11*q(1)*q(9)*q(11) - 3.84e11*q(3)*q(9)*q(11) + 5.09e11*q(6)*q(9)*q(11) -
- 4.97e9*q(2)*q(10)*q(11) - 1.56e11*q(4)*q(10)*q(11) + 1.69e11*q(7)*q(10)*q(11) +
- 4.29e10*q(2)*q(11)**2 + 3.41e11*q(4)*q(11)**2 - 1.72e11*q(7)*q(11)**2 - 8.64e10*q(1)**2*q(12) +
- 2.41e10*q(2)*q(12) + 8.56e10*q(1)*q(3)*q(12) + 2.97e11*q(3)**2*q(12) + 1.71e10*q(4)*q(12) -
- 5.89e11*q(1)*q(5)*q(12) - 5.25e11*q(3)*q(5)*q(12) - 4.17e10*q(1)*q(6)*q(12) -
- 1.93e11*q(3)*q(6)*q(12) + 4.31e11*q(5)*q(6)*q(12) + 1.43e10*q(6)**2*q(12) + 1.25e10*q(7)*q(12) -
- 2.64e11*q(1)*q(8)*q(12) - 3.7e11*q(3)*q(8)*q(12) + 8.05e11*q(6)*q(8)*q(12) +
- 1.25e11*q(1)*q(9)*q(12) + 9.99e11*q(3)*q(9)*q(12) - 4.54e11*q(6)*q(9)*q(12) +
- 1.02e11*q(2)*q(10)*q(12) + 1.24e11*q(4)*q(10)*q(12) - 1.81e11*q(7)*q(10)*q(12) -
- 3.34e11*q(2)*q(11)*q(12) - 5.7e11*q(4)*q(11)*q(12) + 4.46e11*q(7)*q(11)*q(12) +
- 2.52e11*q(2)*q(12)**2 + 6.89e11*q(4)*q(12)**2 - 2.61e11*q(7)*q(12)**2 + 5.38e10*q(1)**2*q(13) -
- 1.67e10*q(2)*q(13) - 1.18e11*q(1)*q(3)*q(13) - 1.43e11*q(3)**2*q(13) + 8.03e9*q(4)*q(13) +
- 7.69e11*q(1)*q(5)*q(13) + 6.29e11*q(3)*q(5)*q(13) + 2.35e10*q(1)*q(6)*q(13) +
- 2.45e11*q(3)*q(6)*q(13) - 8.64e11*q(5)*q(6)*q(13) - 9.39e10*q(6)**2*q(13) + 8.88e9*q(7)*q(13) +
- 1.89e11*q(1)*q(8)*q(13) + 1.61e12*q(3)*q(8)*q(13) - 6.89e11*q(6)*q(8)*q(13) -
- 1.87e11*q(1)*q(9)*q(13) - 6.27e11*q(3)*q(9)*q(13) + 1.61e11*q(6)*q(9)*q(13) -
- 3.05e11*q(2)*q(10)*q(13) - 2.26e11*q(4)*q(10)*q(13) - 7.27e9*q(7)*q(10)*q(13) +
- 7.16e11*q(2)*q(11)*q(13) + 1.47e11*q(4)*q(11)*q(13) - 6.26e11*q(7)*q(11)*q(13) -
- 5.98e11*q(2)*q(12)*q(13) - 7.66e11*q(4)*q(12)*q(13) + 1.46e12*q(7)*q(12)*q(13) +
- 3.91e11*q(2)*q(13)**2 + 1.75e12*q(4)*q(13)**2 - 3.98e11*q(7)*q(13)**2 - 2.38e10*q(1)**2*q(14) +
- 4.86e9*q(2)*q(14) + 1.49e11*q(1)*q(3)*q(14) + 1.6e11*q(3)**2*q(14) + 4.37e9*q(4)*q(14) -
- 7.29e11*q(1)*q(5)*q(14) - 1.26e12*q(3)*q(5)*q(14) - 9.55e10*q(1)*q(6)*q(14) -
- 3.53e11*q(3)*q(6)*q(14) + 1.34e12*q(5)*q(6)*q(14) + 6.22e10*q(6)**2*q(14) - 2.16e10*q(7)*q(14) -
- 5.82e11*q(1)*q(8)*q(14) - 1.19e12*q(3)*q(8)*q(14) + 1.16e11*q(6)*q(8)*q(14) +
- 9.87e10*q(1)*q(9)*q(14) + 5.03e11*q(3)*q(9)*q(14) - 5.29e11*q(6)*q(9)*q(14) +
- 3.62e11*q(2)*q(10)*q(14) + 6.15e9*q(4)*q(10)*q(14) - 2.03e11*q(7)*q(10)*q(14) -
- 1.17e12*q(2)*q(11)*q(14) - 6.97e11*q(4)*q(11)*q(14) + 3.28e11*q(7)*q(11)*q(14) +
- 1.24e12*q(2)*q(12)*q(14) + 7.2e11*q(4)*q(12)*q(14) - 1.27e12*q(7)*q(12)*q(14) -
- 8.33e11*q(2)*q(13)*q(14) - 1.19e12*q(4)*q(13)*q(14) + 2.47e12*q(7)*q(13)*q(14) +
- 4.91e11*q(2)*q(14)**2 + 2.93e12*q(4)*q(14)**2 - 5.63e11*q(7)*q(14)**2 - 3.97e9*q(1)*q(15) +
- 2.59e9*q(3)*q(15) - 1.02e10*q(5)*q(15) + 1.08e10*q(6)*q(15) - 1.68e10*q(8)*q(15) +
- 1.18e10*q(9)*q(15) + 1.3e7*q(16) + 3.02e8*q(10)*q(16) + 1.03e10*q(11)*q(16) + 7.38e9*q(12)*q(16) -
- 5.54e10*q(13)*q(16) + 3.73e10*q(14)*q(16) - 9.08e9*q(1)*q(17) + 3.81e9*q(3)*q(17) -
- 4.42e9*q(5)*q(17) - 6.68e9*q(6)*q(17) - 1.84e10*q(8)*q(17) + 5.65e9*q(9)*q(17) - 6.6e7*q(18) +
- 2.68e9*q(10)*q(18) - 7.46e9*q(11)*q(18) + 1.84e10*q(12)*q(18) - 8.06e9*q(13)*q(18) +
- 2.3e10*q(14)*q(18) + 1.09e10*q(1)*q(19) + 1.09e10*q(3)*q(19) - 9.64e9*q(6)*q(19) +

```
-  6.94e9*q(1)*q(20) - 4.94e9*q(3)*q(20) + 9.47e9*q(5)*q(20) - 3.44e9*q(6)*q(20) + 1.03e10*q(8)*q(20) -
-  1.29e10*q(9)*q(20) + 8.98e6*q(21) + 3.67e9*q(10)*q(21) + 3.23e9*q(11)*q(21) - 1.15e10*q(12)*q(21) +
-  2.15e10*q(13)*q(21) - 5.64e10*q(14)*q(21) - 1.13e10*q(1)*q(22) - 6.78e9*q(3)*q(22) +
-  1.48e10*q(6)*q(22) + 2.49e10*q(1)*q(23) + 2.13e10*q(3)*q(23) + 2.28e9*q(6)*q(23) +
-  2.57e8*q(2)*q(24) + 1.17e10*q(4)*q(24) + 5.26e9*q(7)*q(24) + 5.09e9*q(2)*q(25) - 1.52e10*q(4)*q(25) +
-  5.85e8*q(7)*q(25) - 1.47e10*q(2)*q(26) + 5.54e9*q(4)*q(26) - 2.19e10*q(7)*q(26) + 5.61e9*q(2)*q(27) -
-  2.01e10*q(4)*q(27) + 8.83e9*q(7)*q(27) + 8.83e9*q(2)*q(28) + 1.75e10*q(4)*q(28) + 2.71e9*q(7)*q(28) -
-  4.01e9*q(1)*q(29) - 4.56e10*q(3)*q(29) + 1.74e10*q(5)*q(29) + 2.38e10*q(6)*q(29) +
-  6.11e10*q(8)*q(29) - 1.26e11*q(9)*q(29) + 7.29e5*q(30) - 1.87e9*q(10)*q(30) + 8.28e9*q(11)*q(30) -
-  1.49e10*q(12)*q(30) + 1.3e10*q(13)*q(30) - 8.74e9*q(14)*q(30) + 4.73e10*q(1)*q(31) +
-  3.15e10*q(3)*q(31) - 1.e11*q(5)*q(31) + 2.82e10*q(6)*q(31) + 9.73e10*q(8)*q(31) +
-  7.56e10*q(9)*q(31) + 9.76e8*q(32) + 1.47e8*q(10)*q(32) - 3.95e8*q(11)*q(32) + 9.49e8*q(12)*q(32) -
-  1.92e8*q(13)*q(32) + 1.16e9*q(14)*q(32) + 1.73e10*q(1)*q(33) + 9.66e10*q(3)*q(33) -
-  5.19e10*q(6)*q(33) - 2.38e10*q(1)*q(34) + 2.67e10*q(3)*q(34) + 5.24e10*q(5)*q(34) +
-  3.43e10*q(6)*q(34) + 9.73e10*q(8)*q(34) + 7.58e10*q(9)*q(34) - 1.54e6*q(35) - 3.5e9*q(10)*q(35) +
-  5.41e9*q(11)*q(35) + 1.39e9*q(12)*q(35) + 5.85e9*q(13)*q(35) - 1.04e10*q(14)*q(35) -
-  6.15e10*q(1)*q(36) + 9.24e10*q(3)*q(36) + 9.86e10*q(6)*q(36) + 1.3e11*q(1)*q(37) +
-  7.72e10*q(3)*q(37) + 7.62e10*q(6)*q(37)


 return
 end

 function eq5p(q,gi1,gi2,gi3,crot)
 IMPLICIT DOUBLE PRECISION (A-H,O-Z)
 dimension q(37)

 nxhat=0.d0

 eq5p=  7.69e11*q(1)**3 - 4.28e10*q(1)*q(2) - 8.77e12*q(1)*q(2)**2 + 5.08e11*q(1)**2*q(3) - 5.99e9*q(2)*q(3) -
-  2.28e12*q(2)**2*q(3) + 1.01e12*q(1)*q(3)**2 + 5.23e10*q(3)**3 - 4.81e9*q(1)*q(4) -
-  3.95e12*q(1)*q(2)*q(4) - 2.74e10*q(3)*q(4) - 1.e13*q(2)*q(3)*q(4) - 4.38e12*q(1)*q(4)**2 -
-  1.51e12*q(3)*q(4)**2 + 6.86e7*q(5) + 1.2e13*q(1)**2*q(5) + 4.49e13*q(2)**2*q(5) +
-  7.38e12*q(1)*q(3)*q(5) + 7.46e12*q(3)**2*q(5) + 2.46e13*q(2)*q(4)*q(5) + 2.44e13*q(4)**2*q(5) +
-  3.99e13*q(5)**3 - 1.09e12*q(1)**2*q(6) + 1.49e10*q(2)*q(6) + 4.41e12*q(2)**2*q(6) -
-  1.76e12*q(1)*q(3)*q(6) - 1.06e11*q(3)**2*q(6) + 1.47e10*q(4)*q(6) + 7.73e12*q(2)*q(4)*q(6) +
-  1.15e12*q(4)**2*q(6) - 1.29e13*q(1)*q(5)*q(6) - 1.23e13*q(3)*q(5)*q(6) + 1.25e12*q(1)*q(6)**2 +
-  5.33e11*q(3)*q(6)**2 + 7.6e12*q(5)*q(6)**2 - 7.9e10*q(6)**3 + 1.43e10*q(1)*q(7) +
-  8.6e12*q(1)*q(2)*q(7) + 1.72e10*q(3)*q(7) + 8.44e12*q(2)*q(3)*q(7) + 7.29e12*q(1)*q(4)*q(7) +
-  2.54e12*q(3)*q(4)*q(7) - 4.75e13*q(2)*q(5)*q(7) - 4.07e13*q(4)*q(5)*q(7) - 2.97e10*q(6)*q(7) -
-  1.07e13*q(2)*q(6)*q(7) - 5.65e12*q(4)*q(6)*q(7) - 5.1e12*q(1)*q(7)**2 - 2.9e12*q(3)*q(7)**2 +
-  2.73e13*q(5)*q(7)**2 + 1.51e12*q(6)*q(7)**2 - 2.6e3*q(8) + 6.18e12*q(1)**2*q(8) +
-  2.37e13*q(2)**2*q(8) + 1.24e13*q(1)*q(3)*q(8) + 1.63e12*q(3)**2*q(8) + 4.28e13*q(2)*q(4)*q(8) +
-  5.15e12*q(4)**2*q(8) + 7.23e13*q(5)**2*q(8) - 1.61e13*q(1)*q(6)*q(8) - 9.e12*q(3)*q(6)*q(8) +
-  1.74e12*q(6)**2*q(8) - 6.05e13*q(2)*q(7)*q(8) - 3.23e13*q(4)*q(7)*q(8) + 6.24e12*q(7)**2*q(8) +
-  9.15e13*q(5)*q(8)**2 + 8.47e11*q(8)**3 + 6.28e3*q(9) - 2.62e12*q(1)**2*q(9) - 1.05e13*q(2)**2*q(9) -
-  1.46e13*q(1)*q(3)*q(9) - 2.08e12*q(3)**2*q(9) - 5.38e13*q(2)*q(4)*q(9) - 6.74e12*q(4)**2*q(9) -
-  4.03e13*q(5)**2*q(9) + 1.15e13*q(1)*q(6)*q(9) + 3.34e12*q(3)*q(6)*q(9) - 3.88e12*q(6)**2*q(9) +
-  4.46e13*q(2)*q(7)*q(9) + 1.17e13*q(4)*q(7)*q(9) - 1.4e13*q(7)**2*q(9) - 1.35e14*q(5)*q(8)*q(9) -
-  4.63e13*q(8)**2*q(9) + 8.15e13*q(5)*q(9)**2 + 1.07e13*q(8)*q(9)**2 - 4.18e12*q(9)**3 -
-  8.97e10*q(1)*q(2)*q(10) - 2.94e11*q(2)*q(3)*q(10) - 1.5e11*q(1)*q(4)*q(10) -
-  1.54e11*q(3)*q(4)*q(10) + 9.54e10*q(5)*q(10) + 2.55e11*q(2)*q(6)*q(10) + 1.44e11*q(4)*q(6)*q(10) +
-  1.35e11*q(1)*q(7)*q(10) + 2.63e11*q(3)*q(7)*q(10) - 1.37e11*q(6)*q(7)*q(10) + 3.28e10*q(8)*q(10) -
-  8.77e9*q(9)*q(10) + 1.17e11*q(5)*q(10)**2 + 2.49e10*q(8)*q(10)**2 - 5.94e9*q(9)*q(10)**2 +
-  2.58e11*q(1)*q(2)*q(11) + 1.03e12*q(2)*q(3)*q(11) + 5.22e11*q(1)*q(4)*q(11) +
-  5.31e11*q(3)*q(4)*q(11) - 3.78e10*q(5)*q(11) - 8.05e11*q(2)*q(6)*q(11) - 4.28e11*q(4)*q(6)*q(11) -
-  4.58e11*q(1)*q(7)*q(11) - 6.95e11*q(3)*q(7)*q(11) + 4.84e11*q(6)*q(7)*q(11) - 7.96e10*q(8)*q(11) +
-  4.11e10*q(9)*q(11) - 6.85e11*q(5)*q(10)*q(11) - 3.2e11*q(8)*q(10)*q(11) + 3.46e10*q(9)*q(10)*q(11) +
-  1.07e12*q(5)*q(11)**2 + 5.16e11*q(8)*q(11)**2 - 1.54e11*q(9)*q(11)**2 - 2.82e11*q(1)*q(2)*q(12) -
-  1.68e12*q(2)*q(3)*q(12) - 9.17e11*q(1)*q(4)*q(12) - 8.18e11*q(3)*q(4)*q(12) + 1.84e10*q(5)*q(12) +
-  1.04e12*q(2)*q(6)*q(12) + 6.72e11*q(4)*q(6)*q(12) + 6.65e11*q(1)*q(7)*q(12) +
-  8.39e11*q(3)*q(7)*q(12) - 9.92e11*q(6)*q(7)*q(12) + 4.25e10*q(8)*q(12) - 7.19e10*q(9)*q(12) +
-  8.13e11*q(5)*q(10)*q(12) + 8.19e11*q(8)*q(10)*q(12) - 3.41e11*q(9)*q(10)*q(12) -
-  2.79e12*q(5)*q(11)*q(12) - 2.03e12*q(8)*q(11)*q(12) + 1.07e12*q(9)*q(11)*q(12) +
-  2.24e12*q(5)*q(12)**2 + 9.57e11*q(8)*q(12)**2 - 7.73e11*q(9)*q(12)**2 + 2.79e11*q(1)*q(2)*q(13) +
-  1.94e12*q(2)*q(3)*q(13) + 1.2e12*q(1)*q(4)*q(13) + 9.79e11*q(3)*q(4)*q(13) - 1.07e10*q(5)*q(13) -
```

```
-  1.04e12*q(2)*q(6)*q(13) - 1.35e12*q(4)*q(6)*q(13) - 6.89e11*q(1)*q(7)*q(13) -
-  1.63e12*q(3)*q(7)*q(13) + 1.5e12*q(6)*q(7)*q(13) - 1.4e10*q(8)*q(13) + 4.67e10*q(9)*q(13) -
-  8.7e11*q(5)*q(10)*q(13) - 9.65e11*q(8)*q(10)*q(13) + 9.35e11*q(9)*q(10)*q(13) +
-  2.93e12*q(5)*q(11)*q(13) + 3.24e12*q(8)*q(11)*q(13) - 2.23e12*q(9)*q(11)*q(13) -
-  5.22e12*q(5)*q(12)*q(13) - 3.73e12*q(8)*q(12)*q(13) + 1.93e12*q(9)*q(12)*q(13) +
-  3.9e12*q(5)*q(13)**2 + 1.37e12*q(8)*q(13)**2 - 1.22e12*q(9)*q(13)**2 - 2.79e11*q(1)*q(2)*q(14) -
-  1.72e12*q(2)*q(3)*q(14) - 1.14e12*q(1)*q(4)*q(14) - 1.95e12*q(3)*q(4)*q(14) + 7.26e9*q(5)*q(14) +
-  9.89e11*q(2)*q(6)*q(14) + 2.09e12*q(4)*q(6)*q(14) + 6.47e11*q(1)*q(7)*q(14) +
-  2.46e12*q(3)*q(7)*q(14) - 1.52e12*q(6)*q(7)*q(14) + 9.24e9*q(8)*q(14) - 1.48e10*q(9)*q(14) +
-  9.06e11*q(5)*q(10)*q(14) + 9.27e11*q(8)*q(10)*q(14) - 1.1e12*q(9)*q(10)*q(14) -
-  2.91e12*q(5)*q(11)*q(14) - 3.29e12*q(8)*q(11)*q(14) + 3.58e12*q(9)*q(11)*q(14) +
-  4.87e12*q(5)*q(12)*q(14) + 5.93e12*q(8)*q(12)*q(14) - 3.94e12*q(9)*q(12)*q(14) -
-  8.36e12*q(5)*q(13)*q(14) - 5.84e12*q(8)*q(13)*q(14) + 2.76e12*q(9)*q(13)*q(14) +
-  6.06e12*q(5)*q(14)**2 + 1.66e12*q(8)*q(14)**2 - 1.55e12*q(9)*q(14)**2 - 2.66e9*q(2)*q(15) -
-  1.6e10*q(4)*q(15) + 1.48e10*q(7)*q(15) - 8.95e9*q(1)*q(16) - 3.16e10*q(3)*q(16) +
-  3.31e10*q(6)*q(16) - 2.04e10*q(2)*q(17) - 6.88e9*q(4)*q(17) + 9.05e9*q(7)*q(17) -
-  1.34e10*q(1)*q(18) - 3.36e10*q(3)*q(18) + 2.06e10*q(6)*q(18) - 3.45e7*q(19) - 2.7e10*q(10)*q(19) +
-  7.64e10*q(11)*q(19) - 8.73e10*q(12)*q(19) + 9.82e10*q(13)*q(19) - 1.02e11*q(14)*q(19) +
-  9.87e9*q(2)*q(20) + 1.48e10*q(4)*q(20) - 8.15e9*q(7)*q(20) + 1.02e10*q(1)*q(21) +
-  3.69e10*q(3)*q(21) - 2.75e10*q(6)*q(21) + 3.43e7*q(22) + 3.25e10*q(10)*q(22) - 1.03e11*q(11)*q(22) +
-  1.14e11*q(12)*q(22) - 9.44e10*q(13)*q(22) + 9.98e10*q(14)*q(22) - 4.91e7*q(23) - 1.93e10*q(10)*q(23) +
-  7.61e10*q(11)*q(23) - 1.39e11*q(12)*q(23) + 1.4e11*q(13)*q(23) - 1.02e11*q(14)*q(23) +
-  5.19e9*q(5)*q(24) - 9.38e9*q(8)*q(24) - 2.77e8*q(9)*q(24) - 2.35e10*q(5)*q(25) + 2.24e10*q(8)*q(25) -
-  1.61e10*q(9)*q(25) + 5.11e10*q(5)*q(26) - 1.14e9*q(8)*q(26) + 4.31e10*q(9)*q(26) -
-  6.19e10*q(5)*q(27) - 4.03e10*q(8)*q(27) - 1.41e10*q(9)*q(27) + 7.07e10*q(5)*q(28) +
-  4.73e10*q(8)*q(28) - 2.73e10*q(9)*q(28) + 2.57e11*q(2)*q(29) + 2.71e10*q(4)*q(29) -
-  8.44e10*q(7)*q(29) + 2.61e11*q(1)*q(30) + 3.57e10*q(3)*q(30) - 9.01e10*q(6)*q(30) -
-  2.61e10*q(2)*q(31) - 1.56e11*q(4)*q(31) + 9.66e10*q(7)*q(31) - 2.42e10*q(1)*q(32) -
-  1.53e11*q(3)*q(32) + 8.08e10*q(6)*q(32) + 1.47e9*q(33) + 6.15e8*q(10)*q(33) - 1.67e9*q(11)*q(33) +
-  2.04e9*q(12)*q(33) - 2.4e9*q(13)*q(33) + 2.64e9*q(14)*q(33) + 8.53e10*q(2)*q(34) +
-  8.16e10*q(4)*q(34) - 1.74e11*q(7)*q(34) + 8.41e10*q(1)*q(35) + 9.78e10*q(3)*q(35) -
-  1.75e11*q(6)*q(35) + 3.99e6*q(36) + 3.47e9*q(10)*q(36) - 8.37e9*q(11)*q(36) + 4.58e9*q(12)*q(36) -
-  2.53e9*q(13)*q(36) + 2.1e9*q(14)*q(36) - 8.74e6*q(37) - 2.95e9*q(10)*q(37) + 1.33e10*q(11)*q(37) -
-  2.19e10*q(12)*q(37) + 1.54e10*q(13)*q(37) - 8.77e9*q(14)*q(37)


return
end

function eq6p(q,gi1,gi2,gi3,crot)
IMPLICIT DOUBLE PRECISION (A-H,O-Z)
dimension q(37)

nxhat=0.d0

eq6p=       -237.*q(1) - 2.5e11*q(1)**3 - 3.9e9*q(1)*q(2) - 1.91e12*q(1)*q(2)**2 - 149.*q(3) -
-  7.44e11*q(1)**2*q(3) - 5.06e9*q(2)*q(3) - 1.99e12*q(2)**2*q(3) - 1.77e11*q(1)*q(3)**2 -
-  2.68e10*q(3)**3 - 4.43e9*q(1)*q(4) - 3.27e12*q(1)*q(2)*q(4) + 4.88e9*q(3)*q(4) -
-  8.09e11*q(2)*q(3)*q(4) - 3.8e11*q(1)*q(4)**2 - 7.05e10*q(3)*q(4)**2 - 6.46e11*q(1)**2*q(5) +
-  8.85e9*q(2)*q(5) + 2.62e12*q(2)**2*q(5) - 1.05e12*q(1)*q(3)*q(5) - 6.35e10*q(3)**2*q(5) +
-  8.75e9*q(4)*q(5) + 4.6e12*q(2)*q(4)*q(5) + 6.82e11*q(4)**2*q(5) - 3.84e12*q(1)*q(5)**2 -
-  3.65e12*q(3)*q(5)**2 + 6.74e7*q(6) + 9.78e11*q(1)**2*q(6) + 9.3e9*q(2)*q(6) + 2.55e12*q(2)**2*q(6) +
-  9.94e11*q(1)*q(3)*q(6) + 1.26e12*q(3)**2*q(6) + 6.65e9*q(4)*q(6) + 2.38e12*q(2)*q(4)*q(6) +
-  2.87e12*q(4)**2*q(6) + 1.48e12*q(1)*q(5)*q(6) + 6.32e11*q(3)*q(5)*q(6) + 4.52e12*q(5)**2*q(6) -
-  1.95e11*q(1)*q(6)**2 - 2.76e11*q(3)*q(6)**2 - 1.41e11*q(5)*q(6)**2 + 5.4e11*q(6)**3 +
-  9.3e9*q(1)*q(7) + 4.78e12*q(1)*q(2)*q(7) + 5.64e9*q(3)*q(7) + 2.49e12*q(2)*q(3)*q(7) +
-  2.44e12*q(1)*q(4)*q(7) + 5.42e12*q(3)*q(4)*q(7) - 1.76e10*q(5)*q(7) - 6.34e12*q(2)*q(5)*q(7) -
-  3.36e12*q(4)*q(5)*q(7) + 5.23e9*q(6)*q(7) - 9.81e11*q(2)*q(6)*q(7) - 8.21e11*q(4)*q(6)*q(7) -
-  4.45e11*q(1)*q(7)**2 - 7.75e11*q(3)*q(7)**2 + 8.98e11*q(5)*q(7)**2 + 3.84e12*q(6)*q(7)**2 -
-  9.29e11*q(1)**2*q(8) + 2.17e10*q(2)*q(8) + 3.42e12*q(2)**2*q(8) - 7.42e11*q(1)*q(3)*q(8) -
-  9.84e11*q(3)**2*q(8) + 1.55e10*q(4)*q(8) + 3.74e12*q(2)*q(4)*q(8) + 4.1e12*q(4)**2*q(8) -
-  9.57e12*q(1)*q(5)*q(8) - 5.34e12*q(3)*q(5)*q(8) + 9.16e10*q(1)*q(6)*q(8) + 1.05e11*q(3)*q(6)*q(8) +
-  2.08e12*q(5)*q(6)*q(8) - 1.52e12*q(6)**2*q(8) + 1.53e10*q(7)*q(8) - 7.59e11*q(2)*q(7)*q(8) -
-  6.33e11*q(4)*q(7)*q(8) + 5.98e12*q(7)**2*q(8) - 1.27e10*q(1)*q(8)**2 - 6.41e11*q(3)*q(8)**2 +
-  1.05e13*q(6)*q(8)**2 + 6.95e11*q(1)**2*q(9) - 1.08e10*q(2)*q(9) - 2.37e12*q(2)**2*q(9) +
-  1.45e11*q(1)*q(3)*q(9) - 7.55e10*q(3)**2*q(9) + 1.09e10*q(4)*q(9) - 9.62e11*q(2)*q(4)*q(9) -
```

- 9.14e10*q(4)**2*q(9) + 6.86e12*q(1)*q(5)*q(9) + 1.99e12*q(3)*q(5)*q(9) - 7.99e11*q(1)*q(6)*q(9) -
- 1.98e12*q(3)*q(6)*q(9) - 4.61e12*q(5)*q(6)*q(9) + 1.45e11*q(6)**2*q(9) + 1.13e10*q(7)*q(9) +
- 2.88e12*q(2)*q(7)*q(9) + 7.78e12*q(4)*q(7)*q(9) - 1.03e12*q(7)**2*q(9) + 4.62e12*q(1)*q(8)*q(9) +
- 1.35e13*q(3)*q(8)*q(9) - 1.9e12*q(6)*q(8)*q(9) - 4.96e11*q(1)*q(9)**2 - 5.16e11*q(3)*q(9)**2 +
- 6.3e12*q(6)*q(9)**2 - 2.82e9*q(1)*q(10) - 6.32e10*q(1)*q(2)*q(10) - 3.91e9*q(3)*q(10) -
- 6.25e10*q(2)*q(3)*q(10) + 2.59e10*q(1)*q(4)*q(10) - 6.58e10*q(3)*q(4)*q(10) +
- 1.51e11*q(2)*q(5)*q(10) + 8.56e10*q(4)*q(5)*q(10) + 6.79e9*q(6)*q(10) + 4.03e10*q(2)*q(6)*q(10) +
- 7.85e10*q(4)*q(6)*q(10) + 3.16e10*q(1)*q(7)*q(10) + 2.66e10*q(3)*q(7)*q(10) -
- 8.18e10*q(5)*q(7)*q(10) - 5.23e10*q(6)*q(7)*q(10) + 7.2e10*q(2)*q(8)*q(10) +
- 7.08e10*q(4)*q(8)*q(10) - 9.65e10*q(7)*q(8)*q(10) + 5.66e10*q(2)*q(9)*q(10) -
- 1.03e11*q(4)*q(9)*q(10) + 1.64e11*q(7)*q(9)*q(10) - 3.03e9*q(1)*q(10)**2 - 7.96e9*q(3)*q(10)**2 +
- 1.41e10*q(6)*q(10)**2 + 6.79e9*q(1)*q(11) + 2.04e11*q(1)*q(2)*q(11) + 4.67e9*q(3)*q(11) +
- 1.68e11*q(2)*q(3)*q(11) - 2.82e10*q(1)*q(4)*q(11) + 2.27e11*q(3)*q(4)*q(11) -
- 4.78e11*q(2)*q(5)*q(11) - 2.55e11*q(4)*q(5)*q(11) + 3.6e9*q(6)*q(11) - 1.49e11*q(2)*q(6)*q(11) -
- 1.03e11*q(4)*q(6)*q(11) - 7.06e10*q(1)*q(7)*q(11) - 1.76e11*q(3)*q(7)*q(11) +
- 2.88e11*q(5)*q(7)*q(11) + 1.88e11*q(6)*q(7)*q(11) - 1.78e11*q(2)*q(8)*q(11) -
- 2.81e11*q(4)*q(8)*q(11) + 3.84e11*q(7)*q(8)*q(11) - 6.85e10*q(2)*q(9)*q(11) +
- 4.71e11*q(4)*q(9)*q(11) - 2.06e11*q(7)*q(9)*q(11) + 3.26e10*q(1)*q(10)*q(11) +
- 6.67e10*q(3)*q(10)*q(11) - 5.22e10*q(6)*q(10)*q(11) - 5.14e10*q(1)*q(11)**2 - 7.72e10*q(3)*q(11)**2 +
- 9.57e10*q(6)*q(11)**2 - 3.91e9*q(1)*q(12) - 2.69e11*q(1)*q(2)*q(12) + 3.55e9*q(3)*q(12) -
- 2.26e11*q(2)*q(3)*q(12) - 3.85e10*q(1)*q(4)*q(12) - 1.79e11*q(3)*q(4)*q(12) +
- 6.19e11*q(2)*q(5)*q(12) + 3.99e11*q(4)*q(5)*q(12) + 4.67e9*q(6)*q(12) + 3.19e11*q(2)*q(6)*q(12) +
- 2.66e10*q(4)*q(6)*q(12) + 8.06e10*q(1)*q(7)*q(12) + 4.62e11*q(3)*q(7)*q(12) -
- 5.89e11*q(5)*q(7)*q(12) - 1.86e11*q(6)*q(7)*q(12) + 2.76e11*q(2)*q(8)*q(12) +
- 7.45e11*q(4)*q(8)*q(12) - 3.8e11*q(7)*q(8)*q(12) - 1.12e11*q(2)*q(9)*q(12) -
- 4.21e11*q(4)*q(9)*q(12) - 4.4e9*q(7)*q(9)*q(12) - 7.25e10*q(1)*q(10)*q(12) -
- 7.4e10*q(3)*q(10)*q(12) + 2.63e10*q(6)*q(10)*q(12) + 1.88e11*q(1)*q(11)*q(12) +
- 2.39e11*q(3)*q(11)*q(12) - 1.96e11*q(6)*q(11)*q(12) - 9.41e10*q(1)*q(12)**2 - 1.38e11*q(3)*q(12)**2 +
- 2.66e11*q(6)*q(12)**2 + 1.33e9*q(1)*q(13) + 2.64e11*q(1)*q(2)*q(13) + 4.05e9*q(3)*q(13) +
- 4.8e11*q(2)*q(3)*q(13) + 2.18e10*q(1)*q(4)*q(13) + 2.27e11*q(3)*q(4)*q(13) -
- 6.2e11*q(2)*q(5)*q(13) - 7.99e11*q(4)*q(5)*q(13) - 5.61e9*q(6)*q(13) - 4.73e11*q(2)*q(6)*q(13) -
- 1.74e11*q(4)*q(6)*q(13) - 1.73e11*q(1)*q(7)*q(13) - 3.16e11*q(3)*q(7)*q(13) +
- 8.94e11*q(5)*q(7)*q(13) + 1.26e11*q(6)*q(7)*q(13) - 5.49e11*q(2)*q(8)*q(13) -
- 6.39e11*q(4)*q(8)*q(13) + 1.66e11*q(7)*q(8)*q(13) + 1.93e11*q(2)*q(9)*q(13) +
- 1.49e11*q(4)*q(9)*q(13) - 2.93e11*q(7)*q(9)*q(13) + 8.07e10*q(1)*q(10)*q(13) +
- 4.2e10*q(3)*q(10)*q(13) - 7.54e10*q(6)*q(10)*q(13) - 2.78e11*q(1)*q(11)*q(13) -
- 2.71e11*q(3)*q(11)*q(13) + 1.48e11*q(6)*q(11)*q(13) + 3.43e11*q(1)*q(12)*q(13) +
- 5.7e11*q(3)*q(12)*q(13) - 3.53e11*q(6)*q(12)*q(13) - 1.37e11*q(1)*q(13)**2 - 1.97e11*q(3)*q(13)**2 +
- 5.11e11*q(6)*q(13)**2 - 8.4e8*q(1)*q(14) - 2.43e11*q(1)*q(2)*q(14) - 6.5e9*q(3)*q(14) -
- 7.14e11*q(2)*q(3)*q(14) - 8.84e10*q(1)*q(4)*q(14) - 3.27e11*q(3)*q(4)*q(14) +
- 5.88e11*q(2)*q(5)*q(14) + 1.24e12*q(4)*q(5)*q(14) + 2.04e9*q(6)*q(14) + 4.58e11*q(2)*q(6)*q(14) +
- 1.15e11*q(4)*q(6)*q(14) + 2.02e11*q(1)*q(7)*q(14) + 1.31e11*q(3)*q(7)*q(14) -
- 9.04e11*q(5)*q(7)*q(14) - 3.32e11*q(6)*q(7)*q(14) + 5.93e11*q(2)*q(8)*q(14) +
- 1.09e11*q(4)*q(8)*q(14) - 7.09e11*q(7)*q(8)*q(14) - 4.18e11*q(2)*q(9)*q(14) -
- 4.89e11*q(4)*q(9)*q(14) + 1.74e11*q(7)*q(9)*q(14) - 7.57e10*q(1)*q(10)*q(14) -
- 8.97e10*q(3)*q(10)*q(14) + 9.42e10*q(6)*q(10)*q(14) + 2.68e11*q(1)*q(11)*q(14) +
- 1.95e11*q(3)*q(11)*q(14) - 2.84e11*q(6)*q(11)*q(14) - 5.e11*q(1)*q(12)*q(14) -
- 4.54e11*q(3)*q(12)*q(14) + 1.95e11*q(6)*q(12)*q(14) + 5.42e11*q(1)*q(13)*q(14) +
- 9.8e11*q(3)*q(13)*q(14) - 5.31e11*q(6)*q(13)*q(14) - 1.76e11*q(1)*q(14)**2 - 2.72e11*q(3)*q(14)**2 +
- 8.4e11*q(6)*q(14)**2 + 1.81e7*q(15) - 8.15e9*q(2)*q(15) + 1.e10*q(4)*q(15) + 3.1e9*q(7)*q(15) +
- 8.95e8*q(10)*q(15) + 3.33e9*q(11)*q(15) - 1.1e10*q(12)*q(15) + 7.83e9*q(13)*q(15) -
- 7.64e9*q(14)*q(15) - 7.69e9*q(1)*q(16) - 8.53e9*q(3)*q(16) + 1.96e10*q(5)*q(16) + 4.97e9*q(6)*q(16) +
- 8.35e9*q(8)*q(16) + 1.96e10*q(9)*q(16) - 5.25e6*q(17) - 4.84e9*q(2)*q(17) - 6.17e9*q(4)*q(17) +
- 3.28e9*q(7)*q(17) - 2.76e9*q(10)*q(17) + 5.52e9*q(11)*q(17) - 2.49e9*q(12)*q(17) +
- 8.94e9*q(13)*q(17) - 9.08e9*q(14)*q(17) - 7.91e9*q(1)*q(18) + 4.88e8*q(3)*q(18) +
- 1.23e10*q(5)*q(18) + 9.84e9*q(6)*q(18) + 6.34e9*q(8)*q(18) - 1.35e10*q(9)*q(18) -
- 1.64e10*q(2)*q(19) - 8.93e9*q(4)*q(19) + 9.98e9*q(7)*q(19) - 2.77e7*q(20) + 5.8e9*q(2)*q(20) -
- 3.18e9*q(4)*q(20) - 5.37e9*q(7)*q(20) + 1.09e9*q(10)*q(20) - 2.74e9*q(11)*q(20) +
- 7.27e9*q(12)*q(20) - 9.87e9*q(13)*q(20) + 7.81e9*q(14)*q(20) + 1.04e10*q(1)*q(21) +
- 7.2e9*q(3)*q(21) - 1.64e10*q(5)*q(21) - 1.51e9*q(6)*q(21) - 1.05e10*q(8)*q(21) - 4.31e9*q(9)*q(21) +
- 2.72e10*q(2)*q(22) + 1.37e10*q(4)*q(22) - 1.06e9*q(7)*q(22) - 2.09e10*q(2)*q(23) +
- 2.06e9*q(4)*q(23) + 1.92e10*q(7)*q(23) + 7.69e8*q(1)*q(24) + 1.76e9*q(3)*q(24) + 2.7e9*q(6)*q(24) -
- 1.5e9*q(1)*q(25) + 1.23e9*q(3)*q(25) - 5.15e9*q(6)*q(25) - 6.9e8*q(1)*q(26) - 6.78e9*q(3)*q(26) +
- 2.6e9*q(6)*q(26) + 4.01e9*q(1)*q(27) + 3.76e9*q(3)*q(27) - 1.42e9*q(6)*q(27) - 4.49e9*q(1)*q(28) -
- 3.12e9*q(3)*q(28) + 5.54e9*q(6)*q(28) + 1.71e6*q(29) + 1.74e10*q(2)*q(29) + 2.2e10*q(4)*q(29) -
- 4.37e10*q(7)*q(29) + 1.15e9*q(10)*q(29) - 3.07e9*q(11)*q(29) + 2.62e9*q(12)*q(29) -

```
-  2.13e9*q(13)*q(29) + 2.05e9*q(14)*q(29) - 1.72e10*q(1)*q(30) - 1.93e10*q(3)*q(30) -
-  5.35e10*q(5)*q(30) + 3.99e10*q(6)*q(30) - 1.34e11*q(8)*q(30) + 6.87e10*q(9)*q(30) + 2.24e6*q(31) -
-  1.99e10*q(2)*q(31) + 2.6e10*q(4)*q(31) + 2.38e10*q(7)*q(31) + 1.56e9*q(10)*q(31) -
-  1.82e9*q(11)*q(31) - 1.32e9*q(12)*q(31) - 1.87e9*q(13)*q(31) + 1.53e9*q(14)*q(31) +
-  2.19e10*q(1)*q(32) - 2.49e10*q(3)*q(32) + 4.81e10*q(5)*q(32) - 3.18e10*q(6)*q(32) +
-  9.07e10*q(8)*q(32) + 7.e10*q(9)*q(32) - 5.37e10*q(2)*q(33) - 4.81e10*q(4)*q(33) +
-  1.04e11*q(7)*q(33) + 4.83e8*q(34) + 4.05e10*q(2)*q(34) + 3.17e10*q(4)*q(34) + 2.63e10*q(7)*q(34) +
-  4.9e7*q(10)*q(34) - 1.05e8*q(11)*q(34) + 4.39e8*q(12)*q(34) - 9.1e8*q(13)*q(34) +
-  5.87e8*q(14)*q(34) - 4.42e10*q(1)*q(35) - 2.38e10*q(3)*q(35) - 1.04e11*q(5)*q(35) -
-  2.6e10*q(6)*q(35) + 9.52e10*q(8)*q(35) + 6.97e10*q(9)*q(35) + 1.35e11*q(2)*q(36) +
-  9.1e10*q(4)*q(36) + 9.66e10*q(7)*q(36) - 6.86e10*q(2)*q(37) + 7.02e10*q(4)*q(37) + 7.01e10*q(7)*q(37)


 return
 end

 function eq7p(q,gi1,gi2,gi3,crot)
 IMPLICIT DOUBLE PRECISION (A-H,O-Z)
 dimension q(37)

 nxhat=0.d0

 eq7p=       -2.05e9*q(1)**2 + 21.*q(2) - 2.02e12*q(1)**2*q(2) - 3.86e12*q(2)**3 - 5.83e9*q(1)*q(3) -
-  4.1e12*q(1)*q(2)*q(3) + 2.68e9*q(3)**2 - 5.12e11*q(2)*q(3)**2 - 5.52e3*q(4) - 1.9e12*q(1)**2*q(4) -
-  1.06e13*q(2)**2*q(4) - 8.13e11*q(1)*q(3)*q(4) - 2.4e11*q(3)**2*q(4) - 2.29e12*q(2)*q(4)**2 -
-  2.56e11*q(4)**3 + 9.43e9*q(1)*q(5) + 5.67e12*q(1)*q(2)*q(5) + 1.13e10*q(3)*q(5) +
-  5.56e12*q(2)*q(3)*q(5) + 4.8e12*q(1)*q(4)*q(5) + 1.67e12*q(3)*q(4)*q(5) - 1.57e13*q(2)*q(5)**2 -
-  1.34e13*q(4)*q(5)**2 + 1.03e10*q(1)*q(6) + 5.3e12*q(1)*q(2)*q(6) + 6.27e9*q(3)*q(6) +
-  2.77e12*q(2)*q(3)*q(6) + 2.7e12*q(1)*q(4)*q(6) + 6.03e12*q(3)*q(4)*q(6) - 1.96e10*q(5)*q(6) -
-  7.03e12*q(2)*q(5)*q(6) - 3.73e12*q(4)*q(5)*q(6) + 2.91e9*q(6)**2 - 5.42e11*q(2)*q(6)**2 -
-  4.52e11*q(4)*q(6)**2 + 6.77e7*q(7) + 2.7e12*q(1)**2*q(7) + 1.5e13*q(2)**2*q(7) +
-  2.35e12*q(1)*q(3)*q(7) + 3.34e12*q(3)**2*q(7) + 1.46e13*q(2)*q(4)*q(7) + 1.61e13*q(4)**2*q(7) -
-  6.73e12*q(1)*q(5)*q(7) - 3.82e12*q(3)*q(5)*q(7) + 1.8e13*q(5)**2*q(7) - 9.84e11*q(1)*q(6)*q(7) -
-  1.71e12*q(3)*q(6)*q(7) + 1.99e12*q(5)*q(6)*q(7) + 4.26e12*q(6)**2*q(7) - 2.85e12*q(2)*q(7)**2 -
-  3.26e12*q(4)*q(7)**2 + 7.68e12*q(7)**3 + 2.41e10*q(1)*q(8) + 7.87e12*q(1)*q(2)*q(8) +
-  1.44e10*q(3)*q(8) + 3.45e12*q(2)*q(3)*q(8) + 3.6e12*q(1)*q(4)*q(8) + 9.79e12*q(3)*q(4)*q(8) -
-  3.99e13*q(2)*q(5)*q(8) - 2.13e13*q(4)*q(5)*q(8) + 1.7e10*q(6)*q(8) - 8.35e11*q(2)*q(6)*q(8) -
-  6.89e11*q(4)*q(6)*q(8) - 7.39e11*q(1)*q(7)*q(8) - 2.01e12*q(3)*q(7)*q(8) + 8.23e12*q(5)*q(7)*q(8) +
-  1.33e13*q(6)*q(7)*q(8) - 2.7e11*q(2)*q(8)**2 - 1.91e11*q(4)*q(8)**2 + 4.19e13*q(7)*q(8)**2 -
-  1.25e10*q(1)*q(9) - 5.67e12*q(1)*q(2)*q(9) + 1.2e10*q(3)*q(9) - 8.69e11*q(2)*q(3)*q(9) -
-  9.07e11*q(1)*q(4)*q(9) - 9.29e11*q(3)*q(4)*q(9) + 2.94e13*q(2)*q(5)*q(9) + 7.71e12*q(4)*q(5)*q(9) +
-  1.25e10*q(6)*q(9) + 3.2e12*q(2)*q(6)*q(9) + 8.64e12*q(4)*q(6)*q(9) + 3.39e12*q(1)*q(7)*q(9) +
-  8.08e12*q(3)*q(7)*q(9) - 1.84e13*q(5)*q(7)*q(9) - 2.27e12*q(6)*q(7)*q(9) + 1.86e13*q(2)*q(8)*q(9) +
-  5.23e13*q(4)*q(8)*q(9) - 1.08e13*q(7)*q(8)*q(9) - 2.04e12*q(2)*q(9)**2 - 2.87e12*q(4)*q(9)**2 +
-  2.43e13*q(7)*q(9)**2 + 1.39e10*q(1)**2*q(10) - 1.07e10*q(2)*q(10) - 7.94e10*q(1)*q(3)*q(10) -
-  3.62e10*q(3)**2*q(10) - 1.31e10*q(4)*q(10) + 8.92e10*q(1)*q(5)*q(10) + 1.73e11*q(3)*q(5)*q(10) +
-  3.5e10*q(1)*q(6)*q(10) + 2.95e10*q(3)*q(6)*q(10) - 9.06e10*q(5)*q(6)*q(10) - 2.91e10*q(6)**2*q(10) +
-  2.65e10*q(7)*q(10) + 8.06e10*q(1)*q(8)*q(10) + 6.35e8*q(3)*q(8)*q(10) - 1.07e11*q(6)*q(8)*q(10) +
-  4.57e10*q(1)*q(9)*q(10) - 1.21e11*q(3)*q(9)*q(10) + 1.82e11*q(6)*q(9)*q(10) - 8.22e9*q(2)*q(10)**2 -
-  1.78e10*q(4)*q(10)**2 + 4.43e10*q(7)*q(10)**2 - 2.9e10*q(1)**2*q(11) + 2.64e10*q(2)*q(11) +
-  2.07e11*q(1)*q(3)*q(11) + 8.35e10*q(3)**2*q(11) + 1.77e10*q(4)*q(11) - 3.02e11*q(1)*q(5)*q(11) -
-  4.58e11*q(3)*q(5)*q(11) - 7.82e10*q(1)*q(6)*q(11) - 1.95e11*q(3)*q(6)*q(11) +
-  3.19e11*q(5)*q(6)*q(11) + 1.04e11*q(6)**2*q(11) + 1.45e10*q(7)*q(11) - 1.34e11*q(1)*q(8)*q(11) -
-  3.77e11*q(3)*q(8)*q(11) + 4.26e11*q(6)*q(8)*q(11) - 3.35e10*q(1)*q(9)*q(11) +
-  4.11e11*q(3)*q(9)*q(11) - 2.28e11*q(6)*q(9)*q(11) + 1.06e11*q(2)*q(10)*q(11) +
-  1.73e11*q(4)*q(10)*q(11) - 1.45e11*q(7)*q(10)*q(11) - 1.74e11*q(2)*q(11)**2 - 1.77e11*q(4)*q(11)**2 +
-  2.6e11*q(7)*q(11)**2 + 7.95e7*q(1)**2*q(12) - 1.49e10*q(2)*q(12) - 1.58e11*q(1)*q(3)*q(12) -
-  1.41e11*q(3)**2*q(12) + 1.29e10*q(4)*q(12) + 4.38e11*q(1)*q(5)*q(12) + 5.53e11*q(3)*q(5)*q(12) +
-  8.93e10*q(1)*q(6)*q(12) + 5.13e11*q(3)*q(6)*q(12) - 6.54e11*q(5)*q(6)*q(12) -
-  1.03e11*q(6)**2*q(12) + 1.49e10*q(7)*q(12) + 4.88e10*q(1)*q(8)*q(12) + 1.32e12*q(3)*q(8)*q(12) -
-  4.2e11*q(6)*q(8)*q(12) - 6.15e10*q(1)*q(9)*q(12) - 4.24e11*q(3)*q(9)*q(12) -
-  5.49e9*q(6)*q(9)*q(12) - 2.74e11*q(2)*q(10)*q(12) - 1.86e11*q(4)*q(10)*q(12) +
-  1.64e10*q(7)*q(10)*q(12) + 6.85e11*q(2)*q(11)*q(12) + 4.58e11*q(4)*q(11)*q(12) -
-  5.28e11*q(7)*q(11)*q(12) - 3.24e11*q(2)*q(12)**2 - 2.68e11*q(4)*q(12)**2 + 8.37e11*q(7)*q(12)**2 +
-  1.49e10*q(1)**2*q(13) + 4.36e9*q(2)*q(13) + 2.13e11*q(1)*q(3)*q(13) + 4.06e11*q(3)**2*q(13) +
-  9.11e9*q(4)*q(13) - 4.54e11*q(1)*q(5)*q(13) - 1.07e12*q(3)*q(5)*q(13) - 1.92e11*q(1)*q(6)*q(13) -
```

```
-  3.49e11*q(3)*q(6)*q(13) + 9.91e11*q(5)*q(6)*q(13) + 6.99e10*q(6)**2*q(13) - 2.06e10*q(7)*q(13) -
-  2.87e11*q(1)*q(8)*q(13) - 7.56e11*q(3)*q(8)*q(13) + 1.84e11*q(6)*q(8)*q(13) -
-  7.65e10*q(1)*q(9)*q(13) + 6.58e11*q(3)*q(9)*q(13) - 3.25e11*q(6)*q(9)*q(13) +
-  3.27e11*q(2)*q(10)*q(13) - 7.44e9*q(4)*q(10)*q(13) - 2.19e11*q(7)*q(10)*q(13) -
-  1.08e12*q(2)*q(11)*q(13) - 6.43e11*q(4)*q(11)*q(13) + 3.5e11*q(7)*q(11)*q(13) +
-  1.24e12*q(2)*q(12)*q(13) + 1.49e12*q(4)*q(12)*q(13) - 1.04e12*q(7)*q(12)*q(13) -
-  4.64e11*q(2)*q(13)**2 - 4.09e11*q(4)*q(13)**2 + 1.6e12*q(7)*q(13)**2 - 1.37e10*q(1)**2*q(14) -
-  2.24e9*q(2)*q(14) - 4.04e11*q(1)*q(3)*q(14) - 2.68e11*q(3)**2*q(14) - 2.22e10*q(4)*q(14) +
-  4.26e11*q(1)*q(5)*q(14) + 1.62e12*q(3)*q(5)*q(14) + 2.24e11*q(1)*q(6)*q(14) +
-  1.45e11*q(3)*q(6)*q(14) - 1.e12*q(5)*q(6)*q(14) - 1.84e11*q(6)**2*q(14) + 6.88e9*q(7)*q(14) +
-  4.e11*q(1)*q(8)*q(14) + 6.42e10*q(3)*q(8)*q(14) - 7.87e11*q(6)*q(8)*q(14) -
-  9.02e10*q(1)*q(9)*q(14) - 6.94e11*q(3)*q(9)*q(14) + 1.93e11*q(6)*q(9)*q(14) -
-  3.05e11*q(2)*q(10)*q(14) - 2.08e11*q(4)*q(10)*q(14) + 3.57e11*q(7)*q(10)*q(14) +
-  1.1e12*q(2)*q(11)*q(14) + 3.36e11*q(4)*q(11)*q(14) - 9.4e11*q(7)*q(11)*q(14) -
-  1.97e12*q(2)*q(12)*q(14) - 1.31e12*q(4)*q(12)*q(14) + 3.41e11*q(7)*q(12)*q(14) +
-  1.93e12*q(2)*q(13)*q(14) + 2.54e12*q(4)*q(13)*q(14) - 1.61e12*q(7)*q(13)*q(14) -
-  5.63e11*q(2)*q(14)**2 - 5.78e11*q(4)*q(14)**2 + 2.64e12*q(7)*q(14)**2 + 6.64e9*q(1)*q(15) -
-  1.22e10*q(3)*q(15) + 9.73e9*q(5)*q(15) + 3.43e9*q(6)*q(15) + 9.65e9*q(8)*q(15) + 2.06e10*q(9)*q(15) +
-  1.25e7*q(16) + 2.95e9*q(10)*q(16) + 1.2e10*q(11)*q(16) - 4.5e10*q(12)*q(16) + 3.37e10*q(13)*q(16) -
-  3.26e10*q(14)*q(16) + 1.27e9*q(1)*q(17) - 6.7e9*q(3)*q(17) + 5.96e9*q(5)*q(17) + 3.64e9*q(6)*q(17) +
-  4.5e9*q(8)*q(17) - 1.84e10*q(9)*q(17) - 1.17e7*q(18) - 9.55e9*q(10)*q(18) + 1.96e10*q(11)*q(18) -
-  3.88e9*q(12)*q(18) + 2.93e10*q(13)*q(18) - 5.54e10*q(14)*q(18) - 8.91e9*q(1)*q(19) -
-  2.09e10*q(3)*q(19) + 1.11e10*q(6)*q(19) - 5.68e9*q(1)*q(20) + 7.21e9*q(3)*q(20) - 5.37e9*q(5)*q(20) -
-  5.96e9*q(6)*q(20) - 1.66e10*q(8)*q(20) - 4.92e9*q(9)*q(20) - 3.39e7*q(21) + 4.09e9*q(10)*q(21) -
-  8.42e9*q(11)*q(21) + 2.59e10*q(12)*q(21) - 5.e10*q(13)*q(21) + 3.43e10*q(14)*q(21) +
-  1.84e10*q(1)*q(22) + 2.26e10*q(3)*q(22) - 1.14e9*q(6)*q(22) - 1.78e10*q(1)*q(23) +
-  4.69e9*q(3)*q(23) + 2.13e10*q(6)*q(23) + 3.01e9*q(2)*q(24) + 5.4e9*q(4)*q(24) + 8.74e9*q(7)*q(24) -
-  7.41e9*q(2)*q(25) + 5.99e8*q(4)*q(25) - 1.89e10*q(7)*q(25) + 5.55e8*q(2)*q(26) - 2.25e10*q(4)*q(26) +
-  6.09e9*q(7)*q(26) + 1.39e10*q(2)*q(27) + 9.06e9*q(4)*q(27) + 3.81e9*q(7)*q(27) - 1.66e10*q(2)*q(28) +
-  2.78e9*q(4)*q(28) + 1.48e10*q(7)*q(28) + 1.97e10*q(1)*q(29) + 2.65e10*q(3)*q(29) -
-  5.56e10*q(5)*q(29) - 4.85e10*q(6)*q(29) - 1.45e11*q(8)*q(29) + 7.7e10*q(9)*q(29) + 6.66e5*q(30) +
-  2.46e9*q(10)*q(30) - 6.73e9*q(11)*q(30) + 6.e9*q(12)*q(30) - 4.86e9*q(13)*q(30) +
-  4.78e9*q(14)*q(30) - 2.63e10*q(1)*q(31) + 2.69e10*q(3)*q(31) + 6.37e10*q(5)*q(31) +
-  2.65e10*q(6)*q(31) + 8.34e10*q(8)*q(31) + 8.21e10*q(9)*q(31) + 2.93e6*q(32) + 3.15e9*q(10)*q(32) -
-  4.29e9*q(11)*q(32) - 2.04e9*q(12)*q(32) - 3.39e9*q(13)*q(32) + 4.04e9*q(14)*q(32) -
-  5.67e10*q(1)*q(33) - 6.38e10*q(3)*q(33) + 1.16e11*q(6)*q(33) + 4.91e10*q(1)*q(34) +
-  2.68e10*q(3)*q(34) - 1.15e11*q(5)*q(34) + 2.93e10*q(6)*q(34) + 1.08e11*q(8)*q(34) +
-  7.6e10*q(9)*q(34) + 9.66e8*q(35) + 1.79e8*q(10)*q(35) - 3.71e8*q(11)*q(35) + 1.06e9*q(12)*q(35) -
-  2.18e9*q(13)*q(35) + 1.53e9*q(14)*q(35) + 1.49e11*q(1)*q(36) + 8.52e10*q(3)*q(36) +
-  1.07e11*q(6)*q(36) - 7.83e10*q(1)*q(37) + 7.79e10*q(3)*q(37) + 7.8e10*q(6)*q(37)


 return
 end

 function eq8p(q,gi1,gi2,gi3,crot)
 IMPLICIT DOUBLE PRECISION (A-H,O-Z)
 dimension q(37)

 nxhat=0.d0

 eq8p=   1.95e11*q(1)**3 - 6.35e9*q(1)*q(2) - 2.18e12*q(1)*q(2)**2 + 5.83e11*q(1)**2*q(3) - 9.81e9*q(2)*q(3) -
-  2.25e12*q(2)**2*q(3) + 8.62e9*q(1)*q(3)**2 - 5.92e10*q(3)**3 - 8.48e9*q(1)*q(4) -
-  4.33e12*q(1)*q(2)*q(4) + 1.22e10*q(3)*q(4) - 6.79e11*q(2)*q(3)*q(4) - 2.29e11*q(1)*q(4)**2 +
-  2.55e11*q(3)*q(4)**2 - 1.35e3*q(5) + 3.23e12*q(1)**2*q(5) + 1.24e13*q(2)**2*q(5) +
-  6.49e12*q(1)*q(3)*q(5) + 8.52e11*q(3)**2*q(5) + 2.23e13*q(2)*q(4)*q(5) + 2.69e12*q(4)**2*q(5) +
-  1.26e13*q(5)**3 - 8.16e11*q(1)**2*q(6) + 1.91e10*q(2)*q(6) + 3.e12*q(2)**2*q(6) -
-  6.52e11*q(1)*q(3)*q(6) - 8.66e11*q(3)**2*q(6) + 1.37e10*q(4)*q(6) + 3.29e12*q(2)*q(4)*q(6) +
-  3.61e12*q(4)**2*q(6) - 8.4e12*q(1)*q(5)*q(6) - 4.69e12*q(3)*q(5)*q(6) + 3.94e10*q(1)*q(6)**2 +
-  4.48e10*q(3)*q(6)**2 + 9.09e11*q(5)*q(6)**2 - 4.44e11*q(6)**3 + 1.91e10*q(1)*q(7) +
-  6.23e12*q(1)*q(2)*q(7) + 1.14e10*q(3)*q(7) + 2.73e12*q(2)*q(3)*q(7) + 2.85e12*q(1)*q(4)*q(7) +
-  7.75e12*q(3)*q(4)*q(7) - 3.16e13*q(2)*q(5)*q(7) - 1.68e13*q(4)*q(5)*q(7) + 1.35e10*q(6)*q(7) -
-  6.6e11*q(2)*q(6)*q(7) - 5.44e11*q(4)*q(6)*q(7) - 2.92e11*q(1)*q(7)**2 - 7.95e11*q(3)*q(7)**2 +
-  3.25e12*q(5)*q(7)**2 + 5.25e12*q(6)*q(7)**2 + 6.86e7*q(8) + 4.89e12*q(1)**2*q(8) +
-  1.83e13*q(2)**2*q(8) + 4.01e12*q(1)*q(3)*q(8) + 7.29e12*q(3)**2*q(8) + 1.7e13*q(2)*q(4)*q(8) +
-  2.41e13*q(4)**2*q(8) + 4.77e13*q(5)**2*q(8) - 1.21e10*q(1)*q(6)*q(8) - 1.1e12*q(3)*q(6)*q(8) +
```

```
-  9.22e12*q(6)**2*q(8) - 4.26e11*q(2)*q(7)*q(8) - 2.97e11*q(4)*q(7)*q(8) + 3.31e13*q(7)**2*q(8) +
-  1.33e12*q(5)*q(8)**2 + 4.67e13*q(8)**3 - 5.17e3*q(9) - 3.45e12*q(1)**2*q(9) - 1.3e13*q(2)**2*q(9) -
-  4.84e11*q(1)*q(3)*q(9) + 7.59e10*q(3)**2*q(9) - 2.2e12*q(2)*q(4)*q(9) + 7.22e11*q(4)**2*q(9) -
-  3.53e13*q(5)**2*q(9) + 4.06e12*q(1)*q(6)*q(9) + 1.18e13*q(3)*q(6)*q(9) - 8.27e11*q(6)**2*q(9) +
-  1.47e13*q(2)*q(7)*q(9) + 4.14e13*q(4)*q(7)*q(9) - 4.27e12*q(7)**2*q(9) - 4.83e13*q(5)*q(8)*q(9) -
-  1.67e12*q(8)**2*q(9) + 5.56e12*q(5)*q(9)**2 + 7.9e13*q(8)*q(9)**2 - 1.16e12*q(9)**3 +
-  4.5e10*q(1)*q(2)*q(10) - 1.72e11*q(2)*q(3)*q(10) - 1.03e11*q(1)*q(4)*q(10) -
-  1.12e11*q(3)*q(4)*q(10) + 1.71e10*q(5)*q(10) + 6.31e10*q(2)*q(6)*q(10) + 6.21e10*q(4)*q(6)*q(10) +
-  6.38e10*q(1)*q(7)*q(10) + 4.88e8*q(3)*q(7)*q(10) - 8.49e10*q(6)*q(7)*q(10) + 5.19e10*q(8)*q(10) -
-  2.46e10*q(9)*q(10) + 1.3e10*q(5)*q(10)**2 + 8.67e10*q(8)*q(10)**2 - 3.e10*q(9)*q(10)**2 -
-  8.31e10*q(1)*q(2)*q(11) + 4.21e11*q(2)*q(3)*q(11) + 2.98e11*q(1)*q(4)*q(11) +
-  2.08e11*q(3)*q(4)*q(11) - 4.15e10*q(5)*q(11) - 1.56e11*q(2)*q(6)*q(11) - 2.47e11*q(4)*q(6)*q(11) -
-  1.06e11*q(1)*q(7)*q(11) - 2.98e11*q(3)*q(7)*q(11) + 3.38e11*q(6)*q(7)*q(11) + 4.48e10*q(8)*q(11) +
-  2.89e10*q(9)*q(11) - 1.67e11*q(5)*q(10)*q(11) - 2.18e11*q(8)*q(10)*q(11) + 3.e11*q(9)*q(10)*q(11) +
-  2.69e11*q(5)*q(11)**2 + 4.39e11*q(8)*q(11)**2 - 2.58e11*q(9)*q(11)**2 - 3.83e10*q(1)*q(2)*q(12) -
-  2.94e11*q(2)*q(3)*q(12) - 2.15e11*q(1)*q(4)*q(12) - 3.01e11*q(3)*q(4)*q(12) + 2.22e10*q(5)*q(12) +
-  2.42e11*q(2)*q(6)*q(12) + 6.54e11*q(4)*q(6)*q(12) + 3.86e10*q(1)*q(7)*q(12) +
-  1.04e12*q(3)*q(7)*q(12) - 3.32e11*q(6)*q(7)*q(12) + 3.36e10*q(8)*q(12) + 3.28e10*q(9)*q(12) +
-  4.27e11*q(5)*q(10)*q(12) - 1.18e11*q(8)*q(10)*q(12) - 2.44e11*q(9)*q(10)*q(12) -
-  1.06e12*q(5)*q(11)*q(12) - 7.72e11*q(8)*q(11)*q(12) + 5.86e11*q(9)*q(11)*q(12) +
-  4.99e11*q(5)*q(12)**2 + 1.62e12*q(8)*q(12)**2 - 3.98e11*q(9)*q(12)**2 + 8.92e10*q(1)*q(2)*q(13) +
-  5.15e11*q(2)*q(3)*q(13) + 1.53e11*q(1)*q(4)*q(13) + 1.31e12*q(3)*q(4)*q(13) - 7.32e9*q(5)*q(13) -
-  4.82e11*q(2)*q(6)*q(13) - 5.6e11*q(4)*q(6)*q(13) - 2.27e11*q(1)*q(7)*q(13) -
-  5.99e11*q(3)*q(7)*q(13) + 1.45e11*q(6)*q(7)*q(13) - 4.01e10*q(8)*q(13) + 2.04e10*q(9)*q(13) -
-  5.03e11*q(5)*q(10)*q(13) - 3.9e11*q(8)*q(10)*q(13) - 1.81e11*q(9)*q(10)*q(13) +
-  1.69e12*q(5)*q(11)*q(13) + 2.27e11*q(8)*q(11)*q(13) - 8.9e11*q(9)*q(11)*q(13) -
-  1.95e12*q(5)*q(12)*q(13) - 1.39e12*q(8)*q(12)*q(13) + 2.54e12*q(9)*q(12)*q(13) +
-  7.16e11*q(5)*q(13)**2 + 3.18e12*q(8)*q(13)**2 - 5.19e11*q(9)*q(13)**2 - 7.69e10*q(1)*q(2)*q(14) -
-  9.85e11*q(2)*q(3)*q(14) - 4.73e11*q(1)*q(4)*q(14) - 9.67e11*q(3)*q(4)*q(14) + 4.82e9*q(5)*q(14) +
-  5.2e11*q(2)*q(6)*q(14) + 9.42e10*q(4)*q(6)*q(14) + 3.16e11*q(1)*q(7)*q(14) +
-  5.07e10*q(3)*q(7)*q(14) - 6.23e11*q(6)*q(7)*q(14) + 7.33e9*q(8)*q(14) - 4.16e10*q(9)*q(14) +
-  4.84e11*q(5)*q(10)*q(14) + 6.42e11*q(8)*q(10)*q(14) - 3.51e11*q(9)*q(10)*q(14) -
-  1.72e12*q(5)*q(11)*q(14) - 1.67e12*q(8)*q(11)*q(14) + 2.13e11*q(9)*q(11)*q(14) +
-  3.09e12*q(5)*q(12)*q(14) - 2.7e11*q(8)*q(12)*q(14) - 1.77e12*q(9)*q(12)*q(14) -
-  3.05e12*q(5)*q(13)*q(14) - 2.05e12*q(8)*q(13)*q(14) + 4.36e12*q(9)*q(13)*q(14) +
-  8.67e11*q(5)*q(14)**2 + 5.32e12*q(8)*q(14)**2 - 7.45e11*q(9)*q(14)**2 + 1.11e10*q(2)*q(15) -
-  1.36e10*q(4)*q(15) + 7.64e9*q(7)*q(15) + 1.05e10*q(1)*q(16) - 2.92e10*q(3)*q(16) + 7.3e9*q(6)*q(16) +
-  3.17e9*q(2)*q(17) - 1.49e10*q(4)*q(17) + 3.56e9*q(7)*q(17) - 5.56e8*q(1)*q(18) - 7.44e9*q(3)*q(18) +
-  5.56e9*q(6)*q(18) - 1.57e6*q(19) - 3.32e8*q(10)*q(19) + 2.03e10*q(11)*q(19) - 5.4e10*q(12)*q(19) +
-  4.93e10*q(13)*q(19) - 5.48e10*q(14)*q(19) - 1.13e10*q(2)*q(20) + 8.35e9*q(4)*q(20) -
-  1.32e10*q(7)*q(20) - 8.31e9*q(1)*q(21) + 1.42e10*q(3)*q(21) - 9.25e9*q(6)*q(21) - 3.45e7*q(22) +
-  5.93e9*q(10)*q(22) - 7.63e9*q(11)*q(22) + 4.78e10*q(12)*q(22) - 9.76e10*q(13)*q(22) +
-  4.75e10*q(14)*q(22) - 1.15e7*q(23) - 1.77e10*q(10)*q(23) + 3.23e10*q(11)*q(23) + 7.54e9*q(12)*q(23) +
-  5.5e10*q(13)*q(23) - 1.15e11*q(14)*q(23) - 4.89e9*q(5)*q(24) + 2.16e10*q(8)*q(24) +
-  1.07e10*q(9)*q(24) + 1.17e10*q(5)*q(25) - 4.28e10*q(8)*q(25) + 3.57e9*q(9)*q(25) -
-  5.93e8*q(5)*q(26) + 4.16e9*q(8)*q(26) - 4.68e10*q(9)*q(26) - 2.1e10*q(5)*q(27) + 1.76e10*q(8)*q(27) +
-  8.57e9*q(9)*q(27) + 2.47e10*q(5)*q(28) + 2.76e10*q(8)*q(28) + 1.51e10*q(9)*q(28) +
-  3.91e10*q(2)*q(29) + 4.96e10*q(4)*q(29) - 1.14e11*q(7)*q(29) + 3.96e10*q(1)*q(30) +
-  5.99e10*q(3)*q(30) - 1.18e11*q(6)*q(30) - 5.92e10*q(2)*q(31) + 7.91e10*q(4)*q(31) +
-  6.6e10*q(7)*q(31) - 4.95e10*q(1)*q(32) + 7.55e10*q(3)*q(32) + 7.99e10*q(6)*q(32) - 1.28e5*q(33) +
-  2.49e9*q(10)*q(33) - 6.63e9*q(11)*q(33) + 5.51e9*q(12)*q(33) - 4.28e9*q(13)*q(33) +
-  4.38e9*q(14)*q(33) + 1.17e11*q(2)*q(34) + 7.9e10*q(4)*q(34) + 8.56e10*q(7)*q(34) +
-  1.17e11*q(1)*q(35) + 6.74e10*q(3)*q(35) + 8.39e10*q(6)*q(35) - 1.47e9*q(36) - 2.53e8*q(10)*q(36) +
-  4.41e8*q(11)*q(36) - 1.59e9*q(12)*q(36) + 3.1e9*q(13)*q(36) - 1.74e9*q(14)*q(36) - 1.91e6*q(37) -
-  4.12e9*q(10)*q(37) + 4.87e9*q(11)*q(37) + 4.5e9*q(12)*q(37) + 3.58e9*q(13)*q(37) - 4.51e9*q(14)*q(37)


return
end

function eq9p(q,gi1,gi2,gi3,crot)
IMPLICIT DOUBLE PRECISION (A-H,O-Z)
dimension q(37)

nxhat=0.d0
```

```
 eq9p=       -8.28e10*q(1)**3 + 7.44e8*q(1)*q(2) + 9.06e11*q(1)*q(2)**2 - 9.17e11*q(1)**2*q(3) +
-  2.04e10*q(2)*q(3) + 3.15e12*q(2)**2*q(3) - 1.06e11*q(1)*q(3)**2 - 4.89e11*q(3)**3 +
-  2.02e10*q(1)*q(4) + 6.76e12*q(1)*q(2)*q(4) + 1.25e10*q(3)*q(4) + 1.14e12*q(2)*q(3)*q(4) +
-  5.15e11*q(1)*q(4)**2 + 6.02e12*q(3)*q(4)**2 + 3.87e3*q(5) - 1.62e12*q(1)**2*q(5) -
-  6.46e12*q(2)**2*q(5) - 9.01e12*q(1)*q(3)*q(5) - 1.28e12*q(3)**2*q(5) - 3.31e13*q(2)*q(4)*q(5) -
-  4.15e12*q(4)**2*q(5) - 8.27e12*q(5)**3 + 7.2e11*q(1)**2*q(6) - 1.12e10*q(2)*q(6) -
-  2.46e12*q(2)**2*q(6) + 1.49e11*q(1)*q(3)*q(6) - 8.06e10*q(3)**2*q(6) + 1.14e10*q(4)*q(6) -
-  9.94e11*q(2)*q(4)*q(6) - 8.57e10*q(4)**2*q(6) + 7.11e12*q(1)*q(5)*q(6) + 2.06e12*q(3)*q(5)*q(6) -
-  4.14e11*q(1)*q(6)**2 - 1.03e12*q(3)*q(6)**2 - 2.39e12*q(5)*q(6)**2 + 4.98e10*q(6)**3 -
-  1.16e10*q(1)*q(7) - 5.3e12*q(1)*q(2)*q(7) + 1.13e10*q(3)*q(7) - 8.12e11*q(2)*q(3)*q(7) -
-  8.48e11*q(1)*q(4)*q(7) - 8.67e11*q(3)*q(4)*q(7) + 2.75e13*q(2)*q(5)*q(7) + 7.2e12*q(4)*q(5)*q(7) +
-  1.17e10*q(6)*q(7) + 2.99e12*q(2)*q(6)*q(7) + 8.08e12*q(4)*q(6)*q(7) + 1.58e12*q(1)*q(7)**2 +
-  3.78e12*q(3)*q(7)**2 - 8.62e12*q(5)*q(7)**2 - 1.06e12*q(6)*q(7)**2 - 6.1e3*q(8) -
-  4.07e12*q(1)**2*q(8) - 1.53e13*q(2)**2*q(8) - 5.71e11*q(1)*q(3)*q(8) + 8.97e10*q(3)**2*q(8) -
-  2.6e12*q(2)*q(4)*q(8) + 8.52e11*q(4)**2*q(8) - 4.17e13*q(5)**2*q(8) + 4.79e12*q(1)*q(6)*q(8) +
-  1.4e13*q(3)*q(6)*q(8) - 9.76e11*q(6)**2*q(8) + 1.73e13*q(2)*q(7)*q(8) + 4.89e13*q(4)*q(7)*q(8) -
-  5.04e12*q(7)**2*q(8) - 2.85e13*q(5)*q(8)**2 - 6.59e11*q(8)**3 + 6.87e7*q(9) + 5.34e12*q(1)**2*q(9) +
-  1.99e13*q(2)**2*q(9) + 1.04e12*q(1)*q(3)*q(9) + 1.01e13*q(3)**2*q(9) + 4.09e12*q(2)*q(4)*q(9) +
-  3.34e13*q(4)**2*q(9) + 5.02e13*q(5)**2*q(9) - 1.02e12*q(1)*q(6)*q(9) - 1.04e12*q(3)*q(6)*q(9) +
-  6.54e12*q(6)**2*q(9) - 3.82e12*q(2)*q(7)*q(9) - 5.35e12*q(4)*q(7)*q(9) + 2.27e13*q(7)**2*q(9) +
-  1.31e13*q(5)*q(8)*q(9) + 9.33e13*q(8)**2*q(9) - 7.72e12*q(5)*q(9)**2 - 4.11e12*q(8)*q(9)**2 +
-  3.88e13*q(9)**3 - 7.32e10*q(1)*q(2)*q(10) + 7.12e10*q(2)*q(3)*q(10) + 8.09e10*q(1)*q(4)*q(10) +
-  8.55e10*q(3)*q(4)*q(10) - 5.4e9*q(5)*q(10) + 5.88e10*q(2)*q(6)*q(10) - 1.06e11*q(4)*q(6)*q(10) +
-  4.27e10*q(1)*q(7)*q(10) - 1.13e11*q(3)*q(7)*q(10) + 1.7e11*q(6)*q(7)*q(10) - 2.9e10*q(8)*q(10) +
-  5.34e10*q(9)*q(10) - 3.66e9*q(5)*q(10)**2 - 3.54e10*q(8)*q(10)**2 + 9.09e10*q(9)*q(10)**2 +
-  2.55e11*q(1)*q(2)*q(11) - 1.79e11*q(2)*q(3)*q(11) - 1.52e11*q(1)*q(4)*q(11) -
-  3.69e11*q(3)*q(4)*q(11) + 2.53e10*q(5)*q(11) - 7.13e10*q(2)*q(6)*q(11) + 4.88e11*q(4)*q(6)*q(11) -
-  3.14e10*q(1)*q(7)*q(11) + 3.84e11*q(3)*q(7)*q(11) - 2.13e11*q(6)*q(7)*q(11) + 3.41e10*q(8)*q(11) +
-  3.09e10*q(9)*q(11) + 2.13e10*q(5)*q(10)*q(11) + 3.54e11*q(8)*q(10)*q(11) -
-  3.03e11*q(9)*q(10)*q(11) - 9.51e10*q(5)*q(11)**2 - 3.05e11*q(8)*q(11)**2 + 6.57e11*q(9)*q(11)**2 -
-  3.03e11*q(1)*q(2)*q(12) + 2.18e11*q(2)*q(3)*q(12) + 1.2e11*q(1)*q(4)*q(12) +
-  9.58e11*q(3)*q(4)*q(12) - 4.43e10*q(5)*q(12) - 1.17e11*q(2)*q(6)*q(12) - 4.35e11*q(4)*q(6)*q(12) -
-  5.75e10*q(1)*q(7)*q(12) - 3.96e11*q(3)*q(7)*q(12) - 5.18e9*q(6)*q(7)*q(12) + 3.88e10*q(8)*q(12) +
-  2.8e10*q(9)*q(12) - 2.1e11*q(5)*q(10)*q(12) - 2.88e11*q(8)*q(10)*q(12) + 2.02e11*q(9)*q(10)*q(12) +
-  6.61e11*q(5)*q(11)*q(12) + 6.91e11*q(8)*q(11)*q(12) - 9.25e11*q(9)*q(11)*q(12) -
-  4.76e11*q(5)*q(12)**2 - 4.7e11*q(8)*q(12)**2 + 1.16e12*q(9)*q(12)**2 + 1.38e11*q(1)*q(2)*q(13) -
-  2.82e11*q(2)*q(3)*q(13) - 1.8e11*q(1)*q(4)*q(13) - 6.02e11*q(3)*q(4)*q(13) + 2.87e10*q(5)*q(13) +
-  2.e11*q(2)*q(6)*q(13) + 1.54e11*q(4)*q(6)*q(13) - 7.15e10*q(1)*q(7)*q(13) +
-  6.15e11*q(3)*q(7)*q(13) - 3.04e11*q(6)*q(7)*q(13) + 2.41e10*q(8)*q(13) + 2.11e10*q(9)*q(13) +
-  5.76e11*q(5)*q(10)*q(13) - 2.14e11*q(8)*q(10)*q(13) - 2.87e11*q(9)*q(10)*q(13) -
-  1.38e12*q(5)*q(11)*q(13) - 1.05e12*q(8)*q(11)*q(13) - 1.71e11*q(9)*q(11)*q(13) +
-  1.19e12*q(5)*q(12)*q(13) + 3.e12*q(8)*q(12)*q(13) - 1.32e12*q(9)*q(12)*q(13) -
-  7.52e11*q(5)*q(13)**2 - 6.13e11*q(8)*q(13)**2 + 3.41e12*q(9)*q(13)**2 - 1.51e10*q(1)*q(2)*q(14) +
-  5.37e11*q(2)*q(3)*q(14) + 9.46e10*q(1)*q(4)*q(14) + 4.82e11*q(3)*q(4)*q(14) - 9.12e9*q(5)*q(14) -
-  4.33e11*q(2)*q(6)*q(14) - 5.07e11*q(4)*q(6)*q(14) - 8.43e10*q(1)*q(7)*q(14) -
-  6.48e11*q(3)*q(7)*q(14) + 1.8e11*q(6)*q(7)*q(14) - 4.92e10*q(8)*q(14) + 1.54e10*q(9)*q(14) -
-  6.76e11*q(5)*q(10)*q(14) - 4.15e11*q(8)*q(10)*q(14) - 2.21e11*q(9)*q(10)*q(14) +
-  2.2e12*q(5)*q(11)*q(14) + 2.51e11*q(8)*q(11)*q(14) - 9.46e11*q(9)*q(11)*q(14) -
-  2.43e12*q(5)*q(12)*q(14) - 2.09e12*q(8)*q(12)*q(14) + 1.1e12*q(9)*q(12)*q(14) +
-  1.7e12*q(5)*q(13)*q(14) + 5.15e12*q(8)*q(13)*q(14) - 2.e12*q(9)*q(13)*q(14) -
-  9.55e11*q(5)*q(14)**2 - 8.8e11*q(8)*q(14)**2 + 5.7e12*q(9)*q(14)**2 - 7.91e9*q(2)*q(15) +
-  1.13e10*q(4)*q(15) + 1.92e10*q(7)*q(15) - 8.01e9*q(1)*q(16) + 7.13e9*q(3)*q(16) +
-  2.04e10*q(6)*q(16) - 2.13e10*q(2)*q(17) + 5.42e9*q(4)*q(17) - 1.72e10*q(7)*q(17) -
-  1.66e10*q(1)*q(18) + 7.e9*q(3)*q(18) - 1.4e10*q(6)*q(18) + 5.12e6*q(19) + 1.69e9*q(10)*q(19) +
-  3.23e9*q(11)*q(19) + 2.32e10*q(12)*q(19) - 7.66e10*q(13)*q(19) + 6.52e10*q(14)*q(19) +
-  1.46e10*q(2)*q(20) - 1.24e10*q(4)*q(20) - 4.6e9*q(7)*q(20) + 1.52e10*q(1)*q(21) -
-  1.01e10*q(3)*q(21) - 4.48e9*q(6)*q(21) + 2.63e6*q(22) + 9.62e9*q(10)*q(22) + 4.61e9*q(11)*q(22) -
-  2.e10*q(12)*q(22) + 4.96e10*q(13)*q(22) - 1.37e11*q(14)*q(22) - 7.53e7*q(23) + 5.17e9*q(10)*q(23) -
-  1.28e10*q(11)*q(23) + 3.21e10*q(12)*q(23) - 6.06e9*q(13)*q(23) + 5.36e10*q(14)*q(23) -
-  1.7e8*q(5)*q(24) + 1.26e10*q(8)*q(24) + 2.36e10*q(9)*q(24) - 9.9e9*q(5)*q(25) + 4.21e9*q(8)*q(25) -
-  3.24e10*q(9)*q(25) + 2.66e10*q(5)*q(26) - 5.53e10*q(8)*q(26) + 1.61e10*q(9)*q(26) -
-  8.7e9*q(5)*q(27) + 1.01e10*q(8)*q(27) - 4.45e10*q(9)*q(27) - 1.68e10*q(5)*q(28) +
-  1.79e10*q(8)*q(28) + 2.57e10*q(9)*q(28) - 4.91e9*q(2)*q(29) - 1.21e11*q(4)*q(29) +
-  7.2e10*q(7)*q(29) - 5.01e9*q(1)*q(30) - 1.29e11*q(3)*q(30) + 7.11e10*q(6)*q(30) +
-  1.32e11*q(2)*q(31) + 7.25e10*q(4)*q(31) + 7.68e10*q(7)*q(31) + 1.24e11*q(1)*q(32) +
-  7.4e10*q(3)*q(32) + 7.28e10*q(6)*q(32) + 4.06e5*q(33) - 2.57e9*q(10)*q(33) + 1.07e10*q(11)*q(33) -
```

```
-  1.82e10*q(12)*q(33) + 1.53e10*q(13)*q(33) - 1.01e10*q(14)*q(33) - 7.08e10*q(2)*q(34) +
-  7.27e10*q(4)*q(34) + 7.1e10*q(7)*q(34) - 7.28e10*q(1)*q(35) + 7.12e10*q(3)*q(35) +
-  7.25e10*q(6)*q(35) + 4.34e5*q(36) + 5.67e9*q(10)*q(36) - 7.86e9*q(11)*q(36) - 4.57e9*q(12)*q(36) -
-  9.e9*q(13)*q(36) + 1.62e10*q(14)*q(36) - 1.47e9*q(37) - 2.84e8*q(10)*q(37) + 7.01e8*q(11)*q(37) -
-  1.48e9*q(12)*q(37) + 4.21e8*q(13)*q(37) - 2.5e9*q(14)*q(37)


 return
 end

 function eq10p(q,gi1,gi2,gi3,crot)
 IMPLICIT DOUBLE PRECISION (A-H,O-Z)
 dimension q(37)

 nxhat=0.d0

 eq10p=  2.58e9*q(1)**2 + 8.76e9*q(1)**2*q(2) + 9.52e9*q(2)**2 + 4.83e8*q(1)*q(3) + 3.78e10*q(1)*q(2)*q(3) +
-  1.95e9*q(3)**2 + 1.39e10*q(2)*q(3)**2 - 9.71e9*q(1)**2*q(4) + 1.18e9*q(2)*q(4) +
-  1.63e10*q(1)*q(3)*q(4) + 1.29e10*q(3)**2*q(4) + 6.25e9*q(4)**2 - 3.e10*q(1)*q(2)*q(5) -
-  9.81e10*q(2)*q(3)*q(5) - 5.02e10*q(1)*q(4)*q(5) - 5.14e10*q(3)*q(4)*q(5) + 1.6e10*q(5)**2 -
-  1.59e9*q(1)*q(6) - 3.56e10*q(1)*q(2)*q(6) - 2.2e9*q(3)*q(6) - 3.51e10*q(2)*q(3)*q(6) +
-  1.47e10*q(1)*q(4)*q(6) - 3.71e10*q(3)*q(4)*q(6) + 8.52e10*q(2)*q(5)*q(6) + 4.8e10*q(4)*q(5)*q(6) +
-  1.92e9*q(6)**2 + 1.13e10*q(2)*q(6)**2 + 2.22e10*q(4)*q(6)**2 + 7.08e9*q(1)**2*q(7) -
-  5.45e9*q(2)*q(7) - 4.04e10*q(1)*q(3)*q(7) - 1.84e10*q(3)**2*q(7) - 6.68e9*q(4)*q(7) +
-  4.52e10*q(1)*q(5)*q(7) + 8.77e10*q(3)*q(5)*q(7) + 1.78e10*q(1)*q(6)*q(7) + 1.49e10*q(3)*q(6)*q(7) -
-  4.58e10*q(5)*q(6)*q(7) - 1.48e10*q(6)**2*q(7) + 6.74e9*q(7)**2 + 2.9e10*q(1)*q(2)*q(8) -
-  1.1e11*q(2)*q(3)*q(8) - 6.65e10*q(1)*q(4)*q(8) - 7.14e10*q(3)*q(4)*q(8) + 1.1e10*q(5)*q(8) +
-  4.04e10*q(2)*q(6)*q(8) + 3.98e10*q(4)*q(6)*q(8) + 4.09e10*q(1)*q(7)*q(8) + 7.76e7*q(3)*q(7)*q(8) -
-  5.44e10*q(6)*q(7)*q(8) + 1.67e10*q(8)**2 - 3.98e10*q(1)*q(2)*q(9) + 3.87e10*q(2)*q(3)*q(9) +
-  4.41e10*q(1)*q(4)*q(9) + 4.63e10*q(3)*q(4)*q(9) - 2.94e9*q(5)*q(9) + 3.22e10*q(2)*q(6)*q(9) -
-  5.78e10*q(4)*q(6)*q(9) + 2.33e10*q(1)*q(7)*q(9) - 6.14e10*q(3)*q(7)*q(9) + 9.26e10*q(6)*q(7)*q(9) -
-  1.58e10*q(8)*q(9) + 1.45e10*q(9)**2 + 6.74e7*q(10) + 6.55e9*q(1)**2*q(10) + 2.35e10*q(2)**2*q(10) +
-  9.26e8*q(1)*q(3)*q(10) + 1.1e10*q(3)**2*q(10) + 1.22e9*q(2)*q(4)*q(10) + 2.4e10*q(4)**2*q(10) +
-  3.91e10*q(5)**2*q(10) - 3.39e9*q(1)*q(6)*q(10) - 8.95e9*q(3)*q(6)*q(10) + 7.96e9*q(6)**2*q(10) -
-  8.27e9*q(2)*q(7)*q(10) - 1.81e10*q(4)*q(7)*q(10) + 2.25e10*q(7)**2*q(10) + 1.65e10*q(5)*q(8)*q(10) +
-  5.57e10*q(8)**2*q(10) - 3.78e9*q(5)*q(9)*q(10) - 3.86e10*q(8)*q(9)*q(10) + 4.95e10*q(9)**2*q(10) +
-  1.e8*q(10)**2 + 2.46e8*q(10)**3 + 12.5*q(11) - 1.87e10*q(1)**2*q(11) - 6.78e10*q(2)**2*q(11) -
-  4.93e9*q(1)*q(3)*q(11) - 1.99e10*q(3)**2*q(11) - 2.3e9*q(2)*q(4)*q(11) - 4.06e10*q(4)**2*q(11) -
-  1.15e11*q(5)**2*q(11) + 1.83e10*q(1)*q(6)*q(11) + 3.76e10*q(3)*q(6)*q(11) - 1.47e10*q(6)**2*q(11) +
-  5.35e10*q(2)*q(7)*q(11) + 8.8e10*q(4)*q(7)*q(11) - 3.69e10*q(7)**2*q(11) - 1.07e11*q(5)*q(8)*q(11) -
-  6.98e10*q(8)**2*q(11) + 1.1e10*q(5)*q(9)*q(11) + 1.93e11*q(8)*q(9)*q(11) - 8.25e10*q(9)**2*q(11) -
-  3.23e8*q(10)*q(11) - 1.64e9*q(10)**2*q(11) + 3.24e8*q(11)**2 + 5.28e9*q(10)*q(11)**2 -
-  4.84e9*q(11)**3 + 192.*q(12) + 1.99e10*q(1)**2*q(12) + 7.42e10*q(2)**2*q(12) +
-  2.57e10*q(1)*q(3)*q(12) + 1.7e10*q(3)**2*q(12) + 5.28e10*q(2)*q(4)*q(12) + 3.21e10*q(4)**2*q(12) +
-  1.36e11*q(5)**2*q(12) - 4.08e10*q(1)*q(6)*q(12) - 4.17e10*q(3)*q(6)*q(12) + 7.33e9*q(6)**2*q(12) -
-  1.39e11*q(2)*q(7)*q(12) - 9.45e10*q(4)*q(7)*q(12) + 4.01e9*q(7)**2*q(12) + 2.74e11*q(5)*q(8)*q(12) -
-  3.83e10*q(8)**2*q(12) - 1.14e11*q(5)*q(9)*q(12) - 1.56e11*q(8)*q(9)*q(12) + 5.49e10*q(9)**2*q(12) +
-  2.83e8*q(10)*q(12) + 9.47e8*q(10)**2*q(12) - 7.61e8*q(11)*q(12) - 1.03e10*q(10)*q(11)*q(12) +
-  1.78e10*q(11)**2*q(12) + 6.25e8*q(12)**2 + 1.19e10*q(10)*q(12)**2 - 2.6e10*q(11)*q(12)**2 +
-  7.65e9*q(12)**3 + 250.*q(13) - 1.95e10*q(1)**2*q(13) - 7.33e10*q(2)**2*q(13) -
-  5.16e10*q(1)*q(3)*q(13) - 2.92e10*q(3)**2*q(13) - 1.59e11*q(2)*q(4)*q(13) - 5.88e10*q(4)**2*q(13) -
-  1.45e11*q(5)**2*q(13) + 4.54e10*q(1)*q(6)*q(13) + 2.34e10*q(3)*q(6)*q(13) - 2.12e10*q(6)**2*q(13) +
-  1.66e11*q(2)*q(7)*q(13) - 4.45e9*q(4)*q(7)*q(13) - 5.54e10*q(7)**2*q(13) - 3.23e11*q(5)*q(8)*q(13) -
-  1.25e11*q(8)**2*q(13) + 3.13e11*q(5)*q(9)*q(13) - 1.18e11*q(8)*q(9)*q(13) - 7.75e10*q(9)**2*q(13) -
-  2.82e8*q(10)*q(13) - 1.07e9*q(10)**2*q(13) + 6.04e8*q(11)*q(13) + 5.65e9*q(10)*q(11)*q(13) -
-  1.51e10*q(11)**2*q(13) - 1.27e9*q(12)*q(13) - 1.86e10*q(10)*q(12)*q(13) + 7.03e10*q(11)*q(12)*q(13) -
-  4.08e10*q(12)**2*q(13) + 1.1e9*q(13)**2 + 2.26e10*q(10)*q(13)**2 - 4.32e10*q(11)*q(13)**2 +
-  3.64e10*q(12)*q(13)**2 - 1.99e10*q(13)**3 + 369.*q(14) + 1.94e10*q(1)**2*q(14) +
-  7.35e10*q(2)**2*q(14) + 5.23e10*q(1)*q(3)*q(14) + 2.32e10*q(3)**2*q(14) + 1.89e11*q(2)*q(4)*q(14) +
-  1.05e9*q(4)**2*q(14) + 1.51e11*q(5)**2*q(14) - 4.26e10*q(1)*q(6)*q(14) - 5.04e10*q(3)*q(6)*q(14) +
-  2.64e10*q(6)**2*q(14) - 1.55e11*q(2)*q(7)*q(14) - 1.05e11*q(4)*q(7)*q(14) + 9.05e10*q(7)**2*q(14) +
-  3.1e11*q(5)*q(8)*q(14) + 2.06e11*q(8)**2*q(14) - 3.68e11*q(5)*q(9)*q(14) - 2.25e11*q(8)*q(9)*q(14) -
-  6.12e10*q(9)**2*q(14) + 2.85e8*q(10)*q(14) + 1.15e9*q(10)**2*q(14) - 5.9e8*q(11)*q(14) -
-  6.65e9*q(10)*q(11)*q(14) + 8.04e9*q(11)**2*q(14) + 8.28e8*q(12)*q(14) + 6.79e9*q(10)*q(12)*q(14) -
-  4.69e10*q(11)*q(12)*q(14) + 6.71e10*q(12)**2*q(14) - 1.93e9*q(13)*q(14) - 2.95e10*q(10)*q(13)*q(14) +
-  1.19e11*q(11)*q(13)*q(14) - 1.22e11*q(12)*q(13)*q(14) + 5.53e10*q(13)**2*q(14) + 1.75e9*q(14)**2 +
```

```
-  3.75e10*q(10)*q(14)**2 - 6.76e10*q(11)*q(14)**2 + 5.12e10*q(12)*q(14)**2 - 7.78e10*q(13)*q(14)**2 +
-  2.6e10*q(14)**3 + 2.e9*q(1)*q(15) - 9.44e7*q(3)*q(15) + 5.1e8*q(6)*q(15) + 7.01e9*q(2)*q(16) +
-  1.45e8*q(4)*q(16) + 1.52e9*q(7)*q(16) + 9.75e8*q(1)*q(17) + 5.15e8*q(3)*q(17) - 1.56e9*q(6)*q(17) +
-  3.08e9*q(2)*q(18) + 1.39e9*q(4)*q(18) - 4.85e9*q(7)*q(18) - 9.03e9*q(5)*q(19) - 1.9e8*q(8)*q(19) +
-  8.99e8*q(9)*q(19) - 1.6e9*q(1)*q(20) + 5.65e8*q(3)*q(20) + 6.12e8*q(6)*q(20) - 5.73e9*q(2)*q(21) +
-  1.93e9*q(4)*q(21) + 2.07e9*q(7)*q(21) + 1.09e10*q(5)*q(22) + 3.79e9*q(8)*q(22) + 5.27e9*q(9)*q(22) -
-  6.46e9*q(5)*q(23) - 1.13e10*q(8)*q(23) + 2.8e9*q(9)*q(23) + 8.61e6*q(24) + 8.95e7*q(10)*q(24) +
-  3.e7*q(11)*q(24) - 9.56e7*q(12)*q(24) - 7.79e7*q(13)*q(24) - 4.71e7*q(14)*q(24) - 2.81e7*q(25) -
-  2.43e8*q(10)*q(25) + 3.84e8*q(11)*q(25) + 4.35e8*q(12)*q(25) - 9.38e7*q(13)*q(25) -
-  2.71e7*q(14)*q(25) + 4.27e7*q(26) + 2.86e8*q(10)*q(26) - 1.04e9*q(11)*q(26) + 5.89e8*q(12)*q(26) +
-  1.08e9*q(13)*q(26) - 1.56e8*q(14)*q(26) - 3.89e7*q(27) - 2.13e8*q(10)*q(27) + 8.74e8*q(11)*q(27) -
-  1.89e9*q(12)*q(27) + 7.79e8*q(13)*q(27) + 1.66e9*q(14)*q(27) + 4.29e7*q(28) + 2.59e8*q(10)*q(28) -
-  7.37e8*q(11)*q(28) + 1.24e9*q(12)*q(28) - 2.66e9*q(13)*q(28) + 9.64e8*q(14)*q(28) -
-  4.52e7*q(1)*q(29) - 5.01e8*q(3)*q(29) + 6.49e8*q(6)*q(29) - 1.12e8*q(2)*q(30) - 9.72e8*q(4)*q(30) +
-  1.25e9*q(7)*q(30) - 4.19e8*q(1)*q(31) + 1.34e7*q(3)*q(31) + 8.84e8*q(6)*q(31) - 7.48e8*q(2)*q(32) +
-  7.64e7*q(4)*q(32) + 1.6e9*q(7)*q(32) + 2.06e8*q(5)*q(33) + 1.6e9*q(8)*q(33) - 1.4e9*q(9)*q(33) +
-  5.53e8*q(1)*q(34) - 9.5e8*q(3)*q(34) + 2.63e7*q(6)*q(34) + 1.01e9*q(2)*q(35) - 1.83e9*q(4)*q(35) +
-  9.06e7*q(7)*q(35) + 1.16e9*q(5)*q(36) - 1.62e8*q(8)*q(36) + 3.09e9*q(9)*q(36) - 9.88e8*q(5)*q(37) -
-  2.65e9*q(8)*q(37) - 1.54e8*q(9)*q(37)


 return
 end

 function eq11p(q,gi1,gi2,gi3,crot)
 IMPLICIT DOUBLE PRECISION (A-H,O-Z)
 dimension q(37)

 nxhat=0.d0

 eq11p= -7.06e8*q(1)**2 - 2.24e10*q(1)**2*q(2) - 2.54e9*q(2)**2 - 1.96e9*q(1)*q(3) - 1.2e11*q(1)*q(2)*q(3) +
-  8.87e8*q(3)**2 - 4.21e10*q(2)*q(3)**2 + 3.07e10*q(1)**2*q(4) - 5.67e9*q(2)*q(4) -
-  3.2e10*q(1)*q(3)*q(4) - 5.55e10*q(3)**2*q(4) + 3.e9*q(4)**2 + 7.68e10*q(1)*q(2)*q(5) +
-  3.05e11*q(2)*q(3)*q(5) + 1.56e11*q(1)*q(4)*q(5) + 1.59e11*q(3)*q(4)*q(5) - 5.61e9*q(5)**2 +
-  3.39e9*q(1)*q(6) + 1.02e11*q(1)*q(2)*q(6) + 2.34e9*q(3)*q(6) + 8.41e10*q(2)*q(3)*q(6) -
-  1.41e10*q(1)*q(4)*q(6) + 1.14e11*q(3)*q(4)*q(6) - 2.39e11*q(2)*q(5)*q(6) - 1.28e11*q(4)*q(5)*q(6) +
-  8.99e8*q(6)**2 - 3.74e10*q(2)*q(6)**2 - 2.57e10*q(4)*q(6)**2 - 1.3e10*q(1)**2*q(7) +
-  1.19e10*q(2)*q(7) + 9.36e10*q(1)*q(3)*q(7) + 3.78e10*q(3)**2*q(7) + 7.98e9*q(4)*q(7) -
-  1.36e11*q(1)*q(5)*q(7) - 2.07e11*q(3)*q(5)*q(7) - 3.54e10*q(1)*q(6)*q(7) - 8.83e10*q(3)*q(6)*q(7) +
-  1.45e11*q(5)*q(6)*q(7) + 4.7e10*q(6)**2*q(7) + 3.25e9*q(7)**2 - 4.72e10*q(1)*q(2)*q(8) +
-  2.4e11*q(2)*q(3)*q(8) + 1.7e11*q(1)*q(4)*q(8) + 1.19e11*q(3)*q(4)*q(8) - 2.36e10*q(5)*q(8) -
-  8.94e10*q(2)*q(6)*q(8) - 1.41e11*q(4)*q(6)*q(8) - 6.05e10*q(1)*q(7)*q(8) - 1.71e11*q(3)*q(7)*q(8) +
-  1.92e11*q(6)*q(7)*q(8) + 1.27e10*q(8)**2 + 1.23e11*q(1)*q(2)*q(9) - 8.68e10*q(2)*q(3)*q(9) -
-  7.34e10*q(1)*q(4)*q(9) - 1.78e11*q(3)*q(4)*q(9) + 1.22e10*q(5)*q(9) - 3.41e10*q(2)*q(6)*q(9) +
-  2.36e11*q(4)*q(6)*q(9) - 1.5e10*q(1)*q(7)*q(9) + 1.85e11*q(3)*q(7)*q(9) - 1.03e11*q(6)*q(7)*q(9) +
-  1.64e10*q(8)*q(9) + 7.42e9*q(9)**2 + 12.2*q(10) - 1.66e10*q(1)**2*q(10) - 6.02e10*q(2)**2*q(10) -
-  4.53e9*q(1)*q(3)*q(10) - 1.77e10*q(3)**2*q(10) - 2.53e9*q(2)*q(4)*q(10) - 3.6e10*q(4)**2*q(10) -
-  1.02e11*q(5)**2*q(10) + 1.64e10*q(1)*q(6)*q(10) + 3.34e10*q(3)*q(6)*q(10) - 1.3e10*q(6)**2*q(10) +
-  4.79e10*q(2)*q(7)*q(10) + 7.81e10*q(4)*q(7)*q(10) - 3.28e10*q(7)**2*q(10) -
-  9.55e10*q(5)*q(8)*q(10) - 6.2e10*q(8)**2*q(10) + 1.07e10*q(5)*q(9)*q(10) + 1.71e11*q(8)*q(9)*q(10) -
-  7.3e10*q(9)**2*q(10) - 1.43e8*q(10)**2 - 4.84e8*q(10)**3 + 6.74e7*q(11) + 5.17e10*q(1)**2*q(11) +
-  1.88e11*q(2)**2*q(11) + 2.5e10*q(1)*q(3)*q(11) + 7.54e10*q(3)**2*q(11) + 4.04e10*q(2)*q(4)*q(11) +
-  1.58e11*q(4)**2*q(11) + 3.19e11*q(5)**2*q(11) - 5.16e10*q(1)*q(6)*q(11) - 7.72e10*q(3)*q(6)*q(11) +
-  4.79e10*q(6)**2*q(11) - 1.57e11*q(2)*q(7)*q(11) - 1.6e11*q(4)*q(7)*q(11) + 1.17e11*q(7)**2*q(11) +
-  3.08e11*q(5)*q(8)*q(11) + 2.5e11*q(8)**2*q(11) - 9.31e10*q(5)*q(9)*q(11) - 2.94e11*q(8)*q(9)*q(11) +
-  3.17e11*q(9)**2*q(11) + 5.76e8*q(10)*q(11) + 4.69e9*q(10)**2*q(11) - 1.33e8*q(11)**2 -
-  1.29e10*q(10)*q(11)**2 + 1.49e10*q(11)**3 + 1.4e3*q(12) - 6.38e10*q(1)**2*q(12) -
-  2.34e11*q(2)**2*q(12) - 6.32e10*q(1)*q(3)*q(12) - 6.43e10*q(3)**2*q(12) - 1.55e11*q(2)*q(4)*q(12) -
-  1.32e11*q(4)**2*q(12) - 4.16e11*q(5)**2*q(12) + 9.41e10*q(1)*q(6)*q(12) + 1.2e11*q(3)*q(6)*q(12) -
-  4.92e10*q(6)**2*q(12) + 3.1e11*q(2)*q(7)*q(12) + 2.07e11*q(4)*q(7)*q(12) - 1.2e11*q(7)**2*q(12) -
-  6.05e11*q(5)*q(8)*q(12) - 2.21e11*q(8)**2*q(12) + 3.2e11*q(5)*q(9)*q(12) + 3.35e11*q(8)*q(9)*q(12) -
-  2.24e11*q(9)**2*q(12) - 6.76e8*q(10)*q(12) - 4.59e9*q(10)**2*q(12) + 7.7e8*q(11)*q(12) +
-  3.17e10*q(10)*q(11)*q(12) - 4.86e10*q(11)**2*q(12) - 8.17e7*q(12)**2 - 2.31e10*q(10)*q(12)**2 +
-  8.48e10*q(11)*q(12)**2 - 3.03e10*q(12)**3 + 2.35e3*q(13) + 6.06e10*q(1)**2*q(13) +
-  2.28e11*q(2)**2*q(13) + 1.18e11*q(1)*q(3)*q(13) + 5.62e10*q(3)**2*q(13) + 3.31e11*q(2)*q(4)*q(13) +
-  3.47e10*q(4)**2*q(13) + 4.37e11*q(5)**2*q(13) - 1.39e11*q(1)*q(6)*q(13) - 1.36e11*q(3)*q(6)*q(13) +
```

```
-  3.71e10*q(6)**2*q(13) - 4.89e11*q(2)*q(7)*q(13) - 2.91e11*q(4)*q(7)*q(13) + 7.96e10*q(7)**2*q(13) +
-  9.63e11*q(5)*q(8)*q(13) + 6.59e10*q(8)**2*q(13) - 6.64e11*q(5)*q(9)*q(13) - 5.1e11*q(8)*q(9)*q(13) -
-  4.e10*q(9)**2*q(13) + 5.38e8*q(10)*q(13) + 2.56e9*q(10)**2*q(13) - 1.23e9*q(11)*q(13) -
-  2.71e10*q(10)*q(11)*q(13) + 4.59e10*q(11)**2*q(13) + 1.08e9*q(12)*q(13) + 6.26e10*q(10)*q(12)*q(13) -
-  1.6e11*q(11)*q(12)*q(13) + 1.31e11*q(12)**2*q(13) + 1.11e8*q(13)**2 - 3.84e10*q(10)*q(13)**2 +
-  1.59e11*q(11)*q(13)**2 - 1.36e11*q(12)*q(13)**2 + 4.46e10*q(13)**3 + 3.07e3*q(14) -
-  5.61e10*q(1)**2*q(14) - 2.12e11*q(2)**2*q(14) - 1.63e11*q(1)*q(3)*q(14) - 8.81e10*q(3)**2*q(14) -
-  5.42e11*q(2)*q(4)*q(14) - 1.62e11*q(4)**2*q(14) - 4.35e11*q(5)**2*q(14) + 1.34e11*q(1)*q(6)*q(14) +
-  9.8e10*q(3)*q(6)*q(14) - 7.14e10*q(6)**2*q(14) + 4.96e11*q(2)*q(7)*q(14) + 1.53e11*q(4)*q(7)*q(14) -
-  2.13e11*q(7)**2*q(14) - 9.8e11*q(5)*q(8)*q(14) - 4.76e11*q(8)**2*q(14) + 1.06e12*q(5)*q(9)*q(14) +
-  1.24e11*q(8)*q(9)*q(14) - 2.3e11*q(9)**2*q(14) - 5.26e8*q(10)*q(14) - 3.01e9*q(10)**2*q(14) +
-  8.34e8*q(11)*q(14) + 1.46e10*q(10)*q(11)*q(14) - 3.63e10*q(11)**2*q(14) - 1.88e9*q(12)*q(14) -
-  4.19e10*q(10)*q(12)*q(14) + 1.61e11*q(11)*q(12)*q(14) - 1.16e11*q(12)**2*q(14) + 1.57e9*q(13)*q(14) +
-  1.06e11*q(10)*q(13)*q(14) - 2.41e11*q(11)*q(13)*q(14) + 4.42e11*q(12)*q(13)*q(14) -
-  1.9e11*q(13)**2*q(14) + 4.34e8*q(14)**2 - 6.e10*q(10)*q(14)**2 + 2.56e11*q(11)*q(14)**2 -
-  1.89e11*q(12)*q(14)**2 + 1.89e11*q(13)*q(14)**2 - 8.11e10*q(14)**3 - 4.43e9*q(1)*q(15) +
-  1.6e9*q(3)*q(15) + 1.68e9*q(6)*q(15) - 1.6e10*q(2)*q(16) + 4.73e9*q(4)*q(16) + 5.44e9*q(7)*q(16) -
-  3.35e9*q(1)*q(17) - 1.56e9*q(3)*q(17) + 2.76e9*q(6)*q(17) - 1.11e10*q(2)*q(18) - 3.47e9*q(4)*q(18) +
-  8.86e9*q(7)*q(18) + 2.27e10*q(5)*q(19) + 1.16e10*q(8)*q(19) + 1.51e9*q(9)*q(19) + 4.25e9*q(1)*q(20) +
-  7.4e8*q(3)*q(20) - 1.38e9*q(6)*q(20) + 1.6e10*q(2)*q(21) + 1.52e9*q(4)*q(21) - 3.82e9*q(7)*q(21) -
-  3.05e10*q(5)*q(22) - 4.41e9*q(8)*q(22) + 2.29e9*q(9)*q(22) + 2.27e10*q(5)*q(23) +
-  1.84e10*q(8)*q(23) - 6.21e9*q(9)*q(23) + 1.81e7*q(24) + 2.7e7*q(10)*q(24) + 5.2e8*q(11)*q(24) +
-  3.72e8*q(12)*q(24) - 1.51e8*q(13)*q(24) - 1.29e8*q(14)*q(24) - 2.77e7*q(25) + 3.39e8*q(10)*q(25) -
-  8.08e8*q(11)*q(25) + 8.27e8*q(12)*q(25) + 1.59e9*q(13)*q(25) + 6.23e7*q(14)*q(25) - 5.26e6*q(26) -
-  9.21e8*q(10)*q(26) + 2.04e9*q(11)*q(26) - 1.33e9*q(12)*q(26) + 1.05e9*q(13)*q(26) +
-  3.39e9*q(14)*q(26) + 2.61e7*q(27) + 7.75e8*q(10)*q(27) - 3.02e9*q(11)*q(27) + 3.16e9*q(12)*q(27) -
-  2.13e9*q(13)*q(27) + 9.23e8*q(14)*q(27) - 1.7e7*q(28) - 6.57e8*q(10)*q(28) + 2.43e9*q(11)*q(28) -
-  4.93e9*q(12)*q(28) + 4.02e9*q(13)*q(28) - 2.94e9*q(14)*q(28) + 1.04e8*q(1)*q(29) +
-  2.01e9*q(3)*q(29) - 1.54e9*q(6)*q(29) + 2.57e8*q(2)*q(30) + 3.84e9*q(4)*q(30) - 3.03e9*q(7)*q(30) +
-  1.76e9*q(1)*q(31) - 4.6e7*q(3)*q(31) - 9.11e8*q(6)*q(31) + 3.16e9*q(2)*q(32) - 1.83e8*q(4)*q(32) -
-  1.93e9*q(7)*q(32) - 4.96e8*q(5)*q(33) - 3.77e9*q(8)*q(33) + 5.17e9*q(9)*q(33) - 1.21e9*q(1)*q(34) +
-  1.07e9*q(3)*q(34) - 5.23e7*q(6)*q(34) - 2.26e9*q(2)*q(35) + 2.5e9*q(4)*q(35) - 1.68e8*q(7)*q(35) -
-  2.49e9*q(5)*q(36) + 2.53e8*q(8)*q(36) - 3.79e9*q(9)*q(36) + 3.97e9*q(5)*q(37) + 2.77e9*q(8)*q(37) +
-  3.4e8*q(9)*q(37)


return
end

function eq12p(q,gi1,gi2,gi3,crot)
IMPLICIT DOUBLE PRECISION (A-H,O-Z)
dimension q(37)

nxhat=0.d0

eq12p= 1.95e8*q(1)**2 + 2.19e10*q(1)**2*q(2) + 6.78e8*q(2)**2 + 3.16e9*q(1)*q(3) + 1.87e11*q(1)*q(2)*q(3) +
-  1.31e9*q(3)**2 + 5.45e10*q(2)*q(3)**2 - 3.65e10*q(1)**2*q(4) + 1.02e10*q(2)*q(4) +
-  3.62e10*q(1)*q(3)*q(4) + 1.25e11*q(3)**2*q(4) + 3.59e9*q(4)**2 - 7.64e10*q(1)*q(2)*q(5) -
-  4.55e11*q(2)*q(3)*q(5) - 2.49e11*q(1)*q(4)*q(5) - 2.22e11*q(3)*q(4)*q(5) + 2.49e9*q(5)**2 -
-  1.78e9*q(1)*q(6) - 1.23e11*q(1)*q(2)*q(6) + 1.62e9*q(3)*q(6) - 1.03e11*q(2)*q(3)*q(6) -
-  1.76e10*q(1)*q(4)*q(6) - 8.18e10*q(3)*q(4)*q(6) + 2.82e11*q(2)*q(5)*q(6) + 1.83e11*q(4)*q(5)*q(6) +
-  1.07e9*q(6)**2 + 7.27e10*q(2)*q(6)**2 + 6.1e9*q(4)*q(6)**2 + 3.42e7*q(1)**2*q(7) - 6.14e9*q(2)*q(7) -
-  6.5e10*q(1)*q(3)*q(7) - 5.8e10*q(3)**2*q(7) + 5.26e9*q(4)*q(7) + 1.8e11*q(1)*q(5)*q(7) +
-  2.28e11*q(3)*q(5)*q(7) + 3.68e10*q(1)*q(6)*q(7) + 2.11e11*q(3)*q(6)*q(7) - 2.69e11*q(5)*q(6)*q(7) -
-  4.23e10*q(6)**2*q(7) + 3.05e9*q(7)**2 - 1.99e10*q(1)*q(2)*q(8) - 1.53e11*q(2)*q(3)*q(8) -
-  1.12e11*q(1)*q(4)*q(8) - 1.57e11*q(3)*q(4)*q(8) + 1.15e10*q(5)*q(8) + 1.26e11*q(2)*q(6)*q(8) +
-  3.4e11*q(4)*q(6)*q(8) + 2.03e10*q(1)*q(7)*q(8) + 5.42e11*q(3)*q(7)*q(8) - 1.73e11*q(6)*q(7)*q(8) +
-  8.69e9*q(8)**2 - 1.33e11*q(1)*q(2)*q(9) + 9.59e10*q(2)*q(3)*q(9) + 5.29e10*q(1)*q(4)*q(9) +
-  4.21e11*q(3)*q(4)*q(9) - 1.95e10*q(5)*q(9) - 5.13e10*q(2)*q(6)*q(9) - 1.92e11*q(4)*q(6)*q(9) -
-  2.52e10*q(1)*q(7)*q(9) - 1.75e11*q(3)*q(7)*q(9) - 1.92e9*q(6)*q(7)*q(9) + 1.7e10*q(8)*q(9) +
-  6.13e9*q(9)**2 + 159.*q(10) + 1.62e10*q(1)**2*q(10) + 6.02e10*q(2)**2*q(10) +
-  2.08e10*q(1)*q(3)*q(10) + 1.39e10*q(3)**2*q(10) + 4.31e10*q(2)*q(4)*q(10) + 2.61e10*q(4)**2*q(10) +
-  1.1e11*q(5)**2*q(10) - 3.31e10*q(1)*q(6)*q(10) - 3.38e10*q(3)*q(6)*q(10) + 6.01e9*q(6)**2*q(10) -
-  1.13e11*q(2)*q(7)*q(10) - 7.66e10*q(4)*q(7)*q(10) + 3.51e9*q(7)**2*q(10) + 2.22e11*q(5)*q(8)*q(10) -
-  3.03e10*q(8)**2*q(10) - 9.28e10*q(5)*q(9)*q(10) - 1.27e11*q(8)*q(9)*q(10) + 4.46e10*q(9)**2*q(10) +
-  1.15e8*q(10)**2 + 2.57e8*q(10)**3 + 1.29e3*q(11) - 5.81e10*q(1)**2*q(11) - 2.13e11*q(2)**2*q(11) -
```

```
-  5.76e10*q(1)*q(3)*q(11) - 5.85e10*q(3)**2*q(11) - 1.41e11*q(2)*q(4)*q(11) - 1.2e11*q(4)**2*q(11) -
-  3.79e11*q(5)**2*q(11) + 8.58e10*q(1)*q(6)*q(11) + 1.09e11*q(3)*q(6)*q(11) - 4.48e10*q(6)**2*q(11) +
-  2.82e11*q(2)*q(7)*q(11) + 1.88e11*q(4)*q(7)*q(11) - 1.09e11*q(7)**2*q(11) -
-  5.51e11*q(5)*q(8)*q(11) - 2.01e11*q(8)**2*q(11) + 2.92e11*q(5)*q(9)*q(11) +
-  3.05e11*q(8)*q(9)*q(11) - 2.03e11*q(9)**2*q(11) - 6.16e8*q(10)*q(11) - 4.18e9*q(10)**2*q(11) +
-  3.51e8*q(11)**2 + 1.44e10*q(10)*q(11)**2 - 1.47e10*q(11)**3 + 6.74e7*q(12) + 9.69e10*q(1)**2*q(12) +
-  3.51e11*q(2)**2*q(12) + 7.2e10*q(1)*q(3)*q(12) + 1.71e11*q(3)**2*q(12) + 2.13e11*q(2)*q(4)*q(12) +
-  2.91e11*q(4)**2*q(12) + 6.06e11*q(5)**2*q(12) - 8.6e10*q(1)*q(6)*q(12) - 1.26e11*q(3)*q(6)*q(12) +
-  1.21e11*q(6)**2*q(12) - 2.68e11*q(2)*q(7)*q(12) - 2.21e11*q(4)*q(7)*q(12) + 3.44e11*q(7)**2*q(12) +
-  5.2e11*q(5)*q(8)*q(12) + 8.4e11*q(8)**2*q(12) - 4.2e11*q(5)*q(9)*q(12) - 4.15e11*q(8)*q(9)*q(12) +
-  5.12e11*q(9)**2*q(12) + 1.01e9*q(10)*q(12) + 9.66e9*q(10)**2*q(12) - 1.49e8*q(11)*q(12) -
-  4.22e10*q(10)*q(11)*q(12) + 7.73e10*q(11)**2*q(12) + 5.18e8*q(12)**2 + 1.87e10*q(10)*q(12)**2 -
-  8.27e10*q(11)*q(12)**2 + 8.03e10*q(12)**3 + 5.43e3*q(13) - 1.08e11*q(1)**2*q(13) -
-  3.96e11*q(2)**2*q(13) - 9.6e10*q(1)*q(3)*q(13) - 9.e10*q(3)**2*q(13) - 2.53e11*q(2)*q(4)*q(13) -
-  1.62e11*q(4)**2*q(13) - 7.08e11*q(5)**2*q(13) + 1.57e11*q(1)*q(6)*q(13) + 2.6e11*q(3)*q(6)*q(13) -
-  8.07e10*q(6)**2*q(13) + 5.09e11*q(2)*q(7)*q(13) + 6.14e11*q(4)*q(7)*q(13) - 2.15e11*q(7)**2*q(13) -
-  1.01e12*q(5)*q(8)*q(13) - 3.63e11*q(8)**2*q(13) + 5.25e11*q(5)*q(9)*q(13) +
-  1.32e12*q(8)*q(9)*q(13) - 2.93e11*q(9)**2*q(13) - 1.03e9*q(10)*q(13) - 7.56e9*q(10)**2*q(13) +
-  9.82e8*q(11)*q(13) + 5.71e10*q(10)*q(11)*q(13) - 7.31e10*q(11)**2*q(13) - 7.97e7*q(12)*q(13) -
-  6.63e10*q(10)*q(12)*q(13) + 2.38e11*q(11)*q(12)*q(13) - 1.33e11*q(12)**2*q(13) + 6.76e8*q(13)**2 +
-  2.98e10*q(10)*q(13)**2 - 1.24e11*q(11)*q(13)**2 + 3.68e11*q(12)*q(13)**2 - 6.4e10*q(13)**3 +
-  6.97e3*q(14) + 8.89e10*q(1)**2*q(14) + 3.36e11*q(2)**2*q(14) + 1.91e11*q(1)*q(3)*q(14) +
-  9.24e10*q(3)**2*q(14) + 5.24e11*q(2)*q(4)*q(14) + 1.53e11*q(4)**2*q(14) + 6.62e11*q(5)**2*q(14) -
-  2.28e11*q(1)*q(6)*q(14) - 2.08e11*q(3)*q(6)*q(14) + 4.48e10*q(6)**2*q(14) -
-  8.11e11*q(2)*q(7)*q(14) - 5.38e11*q(4)*q(7)*q(14) + 7.11e10*q(7)**2*q(14) +
-  1.61e12*q(5)*q(8)*q(14) - 6.73e10*q(8)**2*q(14) - 1.07e12*q(5)*q(9)*q(14) -
-  9.19e11*q(8)*q(9)*q(14) + 2.44e11*q(9)**2*q(14) + 6.72e8*q(10)*q(14) + 2.8e9*q(10)**2*q(14) -
-  1.72e9*q(11)*q(14) - 3.82e10*q(10)*q(11)*q(14) + 7.32e10*q(11)**2*q(14) + 1.19e9*q(12)*q(14) +
-  1.09e11*q(10)*q(12)*q(14) - 2.12e11*q(11)*q(12)*q(14) + 1.3e11*q(12)**2*q(14) + 2.58e8*q(13)*q(14) -
-  9.89e10*q(10)*q(13)*q(14) + 4.03e11*q(11)*q(13)*q(14) - 3.66e11*q(12)*q(13)*q(14) +
-  4.44e11*q(13)**2*q(14) + 8.81e8*q(14)**2 + 4.18e10*q(10)*q(14)**2 - 1.72e11*q(11)*q(14)**2 +
-  6.14e11*q(12)*q(14)**2 - 2.48e11*q(13)*q(14)**2 + 1.1e11*q(14)**3 + 3.36e9*q(1)*q(15) +
-  2.04e9*q(3)*q(15) - 5.02e9*q(6)*q(15) + 1.28e10*q(2)*q(16) + 3.14e9*q(4)*q(16) - 1.85e10*q(7)*q(16) +
-  4.84e9*q(1)*q(17) + 3.11e9*q(3)*q(17) - 1.14e9*q(6)*q(17) + 1.88e10*q(2)*q(18) + 7.76e9*q(4)*q(18) -
-  1.63e9*q(7)*q(18) - 2.37e10*q(5)*q(19) - 2.81e10*q(8)*q(19) + 1.02e10*q(9)*q(19) -
-  3.98e9*q(1)*q(20) - 2.13e9*q(3)*q(20) + 3.32e9*q(6)*q(20) - 1.64e10*q(2)*q(21) - 4.85e9*q(4)*q(21) +
-  1.07e10*q(7)*q(21) + 3.1e10*q(5)*q(22) + 2.49e10*q(8)*q(22) - 8.83e9*q(9)*q(22) -
-  3.78e10*q(5)*q(23) + 3.82e9*q(8)*q(23) + 1.41e10*q(9)*q(23) + 1.43e7*q(24) - 7.64e7*q(10)*q(24) +
-  3.4e8*q(11)*q(24) + 1.81e9*q(12)*q(24) + 1.31e9*q(13)*q(24) + 4.4e7*q(14)*q(24) + 9.98e6*q(25) +
-  3.51e8*q(10)*q(25) + 7.53e8*q(11)*q(25) - 1.98e9*q(12)*q(25) + 1.92e9*q(13)*q(25) +
-  3.77e9*q(14)*q(25) - 4.75e7*q(26) + 4.76e8*q(10)*q(26) - 1.21e9*q(11)*q(26) + 3.03e9*q(12)*q(26) -
-  3.33e9*q(13)*q(26) + 1.79e9*q(14)*q(26) - 7.42e5*q(27) - 1.52e9*q(10)*q(27) + 2.88e9*q(11)*q(27) -
-  1.47e9*q(12)*q(27) + 4.31e9*q(13)*q(27) - 5.2e9*q(14)*q(27) + 1.89e7*q(28) + 1.e9*q(10)*q(28) -
-  4.49e9*q(11)*q(28) + 4.76e9*q(12)*q(28) - 2.43e9*q(13)*q(28) + 4.62e9*q(14)*q(28) -
-  8.39e7*q(1)*q(29) - 3.15e9*q(3)*q(29) + 1.19e9*q(6)*q(29) - 2.34e8*q(2)*q(30) - 6.31e9*q(4)*q(30) +
-  2.47e9*q(7)*q(30) - 2.64e9*q(1)*q(31) + 1.24e8*q(3)*q(31) - 6.01e8*q(6)*q(31) - 5.03e9*q(2)*q(32) +
-  4.e8*q(4)*q(32) - 8.3e8*q(7)*q(32) + 5.53e8*q(5)*q(33) + 2.86e9*q(8)*q(33) - 8.e9*q(9)*q(33) +
-  7.6e8*q(1)*q(34) + 5.75e8*q(3)*q(34) + 2.02e8*q(6)*q(34) + 1.47e9*q(2)*q(35) + 5.76e8*q(4)*q(35) +
-  4.38e8*q(7)*q(35) + 1.24e9*q(5)*q(36) - 8.25e8*q(8)*q(36) - 1.99e9*q(9)*q(36) - 5.93e9*q(5)*q(37) +
-  2.32e9*q(8)*q(37) - 6.49e8*q(9)*q(37)


 return
 end

 function eq13p(q,gi1,gi2,gi3,crot)
 IMPLICIT DOUBLE PRECISION (A-H,O-Z)
 dimension q(37)

 nxhat=0.d0

 eq13p= -8.8e7*q(1)**2 - 1.97e10*q(1)**2*q(2) - 2.71e8*q(2)**2 - 1.92e9*q(1)*q(3) - 2.03e11*q(1)*q(2)*q(3) +
-  6.3e8*q(3)**2 - 6.17e10*q(2)*q(3)**2 + 2.1e10*q(1)**2*q(4) - 6.52e9*q(2)*q(4) -
-  4.62e10*q(1)*q(3)*q(4) - 5.6e10*q(3)**2*q(4) + 1.56e9*q(4)**2 + 7.e10*q(1)*q(2)*q(5) +
-  4.87e11*q(2)*q(3)*q(5) + 3.e11*q(1)*q(4)*q(5) + 2.46e11*q(3)*q(4)*q(5) - 1.34e9*q(5)**2 +
-  5.61e8*q(1)*q(6) + 1.11e11*q(1)*q(2)*q(6) + 1.71e9*q(3)*q(6) + 2.03e11*q(2)*q(3)*q(6) +
```

- 9.22e9*q(1)*q(4)*q(6) + 9.58e10*q(3)*q(4)*q(6) - 2.61e11*q(2)*q(5)*q(6) - 3.37e11*q(4)*q(5)*q(6) -
- 1.18e9*q(6)**2 - 9.97e10*q(2)*q(6)**2 - 3.66e10*q(4)*q(6)**2 + 5.65e9*q(1)**2*q(7) +
- 1.67e9*q(2)*q(7) + 8.1e10*q(1)*q(3)*q(7) + 1.54e11*q(3)**2*q(7) + 3.46e9*q(4)*q(7) -
- 1.73e11*q(1)*q(5)*q(7) - 4.09e11*q(3)*q(5)*q(7) - 7.29e10*q(1)*q(6)*q(7) - 1.33e11*q(3)*q(6)*q(7) +
- 3.77e11*q(5)*q(6)*q(7) + 2.67e10*q(6)**2*q(7) - 3.91e9*q(7)**2 + 4.28e10*q(1)*q(2)*q(8) +
- 2.48e11*q(2)*q(3)*q(8) + 7.39e10*q(1)*q(4)*q(8) + 6.29e11*q(3)*q(4)*q(8) - 3.53e9*q(5)*q(8) -
- 2.32e11*q(2)*q(6)*q(8) - 2.69e11*q(4)*q(6)*q(8) - 1.09e11*q(1)*q(7)*q(8) - 2.88e11*q(3)*q(7)*q(8) +
- 7.03e10*q(6)*q(7)*q(8) - 9.62e9*q(8)**2 + 5.63e10*q(1)*q(2)*q(9) - 1.15e11*q(2)*q(3)*q(9) -
- 7.31e10*q(1)*q(4)*q(9) - 2.45e11*q(3)*q(4)*q(9) + 1.17e10*q(5)*q(9) + 8.16e10*q(2)*q(6)*q(9) +
- 6.31e10*q(4)*q(6)*q(9) - 2.9e10*q(1)*q(7)*q(9) + 2.51e11*q(3)*q(7)*q(9) - 1.23e11*q(6)*q(7)*q(9) +
- 9.8e9*q(8)*q(9) + 4.28e9*q(9)**2 + 191.*q(10) - 1.47e10*q(1)**2*q(10) - 5.52e10*q(2)**2*q(10) -
- 3.86e10*q(1)*q(3)*q(10) - 2.19e10*q(3)**2*q(10) - 1.19e11*q(2)*q(4)*q(10) - 4.41e10*q(4)**2*q(10) -
- 1.09e11*q(5)**2*q(10) + 3.4e10*q(1)*q(6)*q(10) + 1.77e10*q(3)*q(6)*q(10) - 1.59e10*q(6)**2*q(10) +
- 1.24e11*q(2)*q(7)*q(10) - 2.62e9*q(4)*q(7)*q(10) - 4.16e10*q(7)**2*q(10) - 2.42e11*q(5)*q(8)*q(10) -
- 9.36e10*q(8)**2*q(10) + 2.34e11*q(5)*q(9)*q(10) - 8.64e10*q(8)*q(9)*q(10) - 5.83e10*q(9)**2*q(10) -
- 1.06e8*q(10)**2 - 2.7e8*q(10)**3 + 1.99e3*q(11) + 5.1e10*q(1)**2*q(11) + 1.91e11*q(2)**2*q(11) +
- 9.97e10*q(1)*q(3)*q(11) + 4.73e10*q(3)**2*q(11) + 2.8e11*q(2)*q(4)*q(11) + 2.9e10*q(4)**2*q(11) +
- 3.67e11*q(5)**2*q(11) - 1.17e11*q(1)*q(6)*q(11) - 1.14e11*q(3)*q(6)*q(11) + 3.12e10*q(6)**2*q(11) -
- 4.12e11*q(2)*q(7)*q(11) - 2.45e11*q(4)*q(7)*q(11) + 6.68e10*q(7)**2*q(11) +
- 8.11e11*q(5)*q(8)*q(11) + 5.51e10*q(8)**2*q(11) - 5.6e11*q(5)*q(9)*q(11) - 4.27e11*q(8)*q(9)*q(11) -
- 3.42e10*q(9)**2*q(11) + 4.53e8*q(10)*q(11) + 2.14e9*q(10)**2*q(11) - 5.2e8*q(11)**2 -
- 1.14e10*q(10)*q(11)**2 + 1.29e10*q(11)**3 + 5.03e3*q(12) - 9.95e10*q(1)**2*q(12) -
- 3.66e11*q(2)**2*q(12) - 8.88e10*q(1)*q(3)*q(12) - 8.31e10*q(3)**2*q(12) - 2.34e11*q(2)*q(4)*q(12) -
- 1.5e11*q(4)**2*q(12) - 6.54e11*q(5)**2*q(12) + 1.45e11*q(1)*q(6)*q(12) + 2.4e11*q(3)*q(6)*q(12) -
- 7.45e10*q(6)**2*q(12) + 4.71e11*q(2)*q(7)*q(12) + 5.68e11*q(4)*q(7)*q(12) - 1.99e11*q(7)**2*q(12) -
- 9.36e11*q(5)*q(8)*q(12) - 3.35e11*q(8)**2*q(12) + 4.86e11*q(5)*q(9)*q(12) +
- 1.22e12*q(8)*q(9)*q(12) - 2.7e11*q(9)**2*q(12) - 9.48e8*q(10)*q(12) - 6.98e9*q(10)**2*q(12) +
- 9.09e8*q(11)*q(12) + 5.27e10*q(10)*q(11)*q(12) - 6.75e10*q(11)**2*q(12) - 3.68e7*q(12)**2 -
- 3.06e10*q(10)*q(12)**2 + 1.1e11*q(11)*q(12)**2 - 4.11e10*q(12)**3 + 6.74e7*q(13) +
- 1.58e11*q(1)**2*q(13) + 5.7e11*q(2)**2*q(13) + 1.02e11*q(1)*q(3)*q(13) + 3.22e11*q(3)**2*q(13) +
- 3.05e11*q(2)*q(4)*q(13) + 6.84e11*q(4)**2*q(13) + 9.78e11*q(5)**2*q(13) - 1.16e11*q(1)*q(6)*q(13) -
- 1.66e11*q(3)*q(6)*q(13) + 2.16e11*q(6)**2*q(13) - 3.54e11*q(2)*q(7)*q(13) -
- 3.12e11*q(4)*q(7)*q(13) + 6.08e11*q(7)**2*q(13) + 6.9e11*q(5)*q(8)*q(13) + 1.53e12*q(8)**2*q(13) -
- 6.13e11*q(5)*q(9)*q(13) - 5.02e11*q(8)*q(9)*q(13) + 1.39e12*q(9)**2*q(13) + 1.64e9*q(10)*q(13) +
- 1.69e10*q(10)**2*q(13) + 1.87e8*q(11)*q(13) - 6.48e10*q(10)*q(11)*q(13) + 1.34e11*q(11)**2*q(13) +
- 1.25e9*q(12)*q(13) + 5.51e10*q(10)*q(12)*q(13) - 2.29e11*q(11)*q(12)*q(13) + 3.4e11*q(12)**2*q(13) -
- 4.94e7*q(13)**2 - 4.47e10*q(10)*q(13)**2 + 1.13e11*q(11)*q(13)**2 - 1.77e11*q(12)*q(13)**2 +
- 3.03e11*q(13)**3 + 1.11e4*q(14) - 1.6e11*q(1)**2*q(14) - 5.88e11*q(2)**2*q(14) -
- 1.25e11*q(1)*q(3)*q(14) - 1.08e11*q(3)**2*q(14) - 3.26e11*q(2)*q(4)*q(14) - 2.33e11*q(4)**2*q(14) -
- 1.05e12*q(5)**2*q(14) + 2.29e11*q(1)*q(6)*q(14) + 4.14e11*q(3)*q(6)*q(14) - 1.12e11*q(6)**2*q(14) +
- 7.33e11*q(2)*q(7)*q(14) + 9.65e11*q(4)*q(7)*q(14) - 3.07e11*q(7)**2*q(14) -
- 1.46e12*q(5)*q(8)*q(14) - 4.95e11*q(8)**2*q(14) + 6.92e11*q(5)*q(9)*q(14) +
- 2.09e12*q(8)*q(9)*q(14) - 4.08e11*q(9)**2*q(14) - 1.45e9*q(10)*q(14) - 1.11e10*q(10)**2*q(14) +
- 1.32e9*q(11)*q(14) + 8.9e10*q(10)*q(11)*q(14) - 1.02e11*q(11)**2*q(14) + 2.39e8*q(12)*q(14) -
- 9.15e10*q(10)*q(12)*q(14) + 3.73e11*q(11)*q(12)*q(14) - 1.69e11*q(12)**2*q(14) + 1.47e9*q(13)*q(14) +
- 8.39e10*q(10)*q(13)*q(14) - 3.18e11*q(11)*q(13)*q(14) + 8.21e11*q(12)*q(13)*q(14) -
- 2.09e11*q(13)**2*q(14) + 3.92e7*q(14)**2 - 5.84e10*q(10)*q(14)**2 + 1.59e11*q(11)*q(14)**2 -
- 2.29e11*q(12)*q(14)**2 + 1.17e12*q(13)*q(14)**2 - 8.41e10*q(14)**3 - 3.12e9*q(1)*q(15) -
- 5.81e9*q(3)*q(15) + 3.3e9*q(6)*q(15) - 1.21e10*q(2)*q(16) - 2.16e10*q(4)*q(16) + 1.28e10*q(7)*q(16) -
- 3.82e9*q(1)*q(17) - 2.06e9*q(3)*q(17) + 3.77e9*q(6)*q(17) - 1.75e10*q(2)*q(18) - 3.16e9*q(4)*q(18) +
- 1.11e10*q(7)*q(18) + 2.46e10*q(5)*q(19) + 2.37e10*q(8)*q(19) - 3.12e10*q(9)*q(19) +
- 3.13e9*q(1)*q(20) + 3.58e9*q(3)*q(20) - 4.17e9*q(6)*q(20) + 1.22e10*q(2)*q(21) + 8.41e9*q(4)*q(21) -
- 1.9e10*q(7)*q(21) - 2.37e10*q(5)*q(22) - 4.69e10*q(8)*q(22) + 2.02e10*q(9)*q(22) +
- 3.52e10*q(5)*q(23) + 2.64e10*q(8)*q(23) - 2.51e9*q(9)*q(23) + 8.75e6*q(24) - 5.71e7*q(10)*q(24) -
- 1.25e8*q(11)*q(24) + 1.21e9*q(12)*q(24) + 3.99e9*q(13)*q(24) + 2.74e9*q(14)*q(24) + 1.26e7*q(25) -
- 6.76e7*q(10)*q(25) + 1.35e9*q(11)*q(25) + 1.77e9*q(12)*q(25) - 3.69e9*q(13)*q(25) +
- 3.38e9*q(14)*q(25) + 7.92e6*q(26) + 8.02e8*q(10)*q(26) + 8.75e8*q(11)*q(26) - 3.08e9*q(12)*q(26) +
- 4.63e9*q(13)*q(26) - 5.99e9*q(14)*q(26) - 5.79e7*q(27) + 5.85e8*q(10)*q(27) - 1.79e9*q(11)*q(27) +
- 3.99e9*q(12)*q(27) - 3.9e9*q(13)*q(27) + 5.6e9*q(14)*q(27) - 5.01e5*q(28) - 1.99e9*q(10)*q(28) +
- 3.39e9*q(11)*q(28) - 2.24e9*q(12)*q(28) + 6.79e9*q(13)*q(28) - 5.73e9*q(14)*q(28) +
- 7.77e7*q(1)*q(29) + 2.27e9*q(3)*q(29) - 8.97e8*q(6)*q(29) + 2.38e8*q(2)*q(30) + 5.08e9*q(4)*q(30) -
- 1.85e9*q(7)*q(30) + 1.63e9*q(1)*q(31) + 9.08e7*q(3)*q(31) - 7.88e8*q(6)*q(31) + 3.55e9*q(2)*q(32) -
- 7.61e7*q(4)*q(32) - 1.29e9*q(7)*q(32) - 6.01e8*q(5)*q(33) - 2.06e9*q(8)*q(33) + 6.21e9*q(9)*q(33) -
- 5.78e8*q(1)*q(34) + 1.31e9*q(3)*q(34) - 3.82e8*q(6)*q(34) - 1.07e9*q(2)*q(35) + 2.28e9*q(4)*q(35) -
- 8.28e8*q(7)*q(35) - 6.35e8*q(5)*q(36) + 1.49e9*q(8)*q(36) - 3.66e9*q(9)*q(36) + 3.86e9*q(5)*q(37) +
- 1.72e9*q(8)*q(37) + 1.73e8*q(9)*q(37)

```
return
end

function eq14p(q,gi1,gi2,gi3,crot)
IMPLICIT DOUBLE PRECISION (A-H,O-Z)
dimension q(37)

nxhat=0.d0

eq14p= 7.45e7*q(1)**2 + 1.85e10*q(1)**2*q(2) + 1.96e8*q(2)**2 + 5.69e8*q(1)*q(3) + 1.66e11*q(1)*q(2)*q(3) +
-  7.27e8*q(3)**2 + 1.32e11*q(2)*q(3)**2 - 8.89e9*q(1)**2*q(4) + 1.81e9*q(2)*q(4) +
-  5.53e10*q(1)*q(3)*q(4) + 5.95e10*q(3)**2*q(4) + 8.04e8*q(4)**2 - 6.66e10*q(1)*q(2)*q(5) -
-  4.11e11*q(2)*q(3)*q(5) - 2.71e11*q(1)*q(4)*q(5) - 4.65e11*q(3)*q(4)*q(5) + 8.65e8*q(5)**2 -
-  3.39e8*q(1)*q(6) - 9.74e10*q(1)*q(2)*q(6) - 2.61e9*q(3)*q(6) - 2.86e11*q(2)*q(3)*q(6) -
-  3.54e10*q(1)*q(4)*q(6) - 1.31e11*q(3)*q(4)*q(6) + 2.36e11*q(2)*q(5)*q(6) + 4.98e11*q(4)*q(5)*q(6) +
-  4.08e8*q(6)**2 + 9.17e10*q(2)*q(6)**2 + 2.31e10*q(4)*q(6)**2 - 4.94e9*q(1)**2*q(7) -
-  8.21e8*q(2)*q(7) - 1.46e11*q(1)*q(3)*q(7) - 9.7e10*q(3)**2*q(7) - 8.02e9*q(4)*q(7) +
-  1.54e11*q(1)*q(5)*q(7) + 5.85e11*q(3)*q(5)*q(7) + 8.08e10*q(1)*q(6)*q(7) + 5.26e10*q(3)*q(6)*q(7) -
-  3.62e11*q(5)*q(6)*q(7) - 6.66e10*q(6)**2*q(7) + 1.24e9*q(7)**2 - 3.51e10*q(1)*q(2)*q(8) -
-  4.49e11*q(2)*q(3)*q(8) - 2.16e11*q(1)*q(4)*q(8) - 4.42e11*q(3)*q(4)*q(8) + 2.22e9*q(5)*q(8) +
-  2.37e11*q(2)*q(6)*q(8) + 4.34e10*q(4)*q(6)*q(8) + 1.44e11*q(1)*q(7)*q(8) + 2.38e10*q(3)*q(7)*q(8) -
-  2.84e11*q(6)*q(7)*q(8) + 1.67e9*q(8)**2 - 6.04e9*q(1)*q(2)*q(9) + 2.08e11*q(2)*q(3)*q(9) +
-  3.67e10*q(1)*q(4)*q(9) + 1.87e11*q(3)*q(4)*q(9) - 3.55e9*q(5)*q(9) - 1.67e11*q(2)*q(6)*q(9) -
-  1.96e11*q(4)*q(6)*q(9) - 3.25e10*q(1)*q(7)*q(9) - 2.51e11*q(3)*q(7)*q(9) + 6.97e10*q(6)*q(7)*q(9) -
-  1.9e10*q(8)*q(9) + 2.95e9*q(9)**2 + 273.*q(10) + 1.39e10*q(1)**2*q(10) + 5.26e10*q(2)**2*q(10) +
-  3.72e10*q(1)*q(3)*q(10) + 1.67e10*q(3)**2*q(10) + 1.34e11*q(2)*q(4)*q(10) + 1.22e9*q(4)**2*q(10) +
-  1.08e11*q(5)**2*q(10) - 3.03e10*q(1)*q(6)*q(10) - 3.6e10*q(3)*q(6)*q(10) + 1.89e10*q(6)**2*q(10) -
-  1.1e11*q(2)*q(7)*q(10) - 7.51e10*q(4)*q(7)*q(10) + 6.45e10*q(7)**2*q(10) + 2.21e11*q(5)*q(8)*q(10) +
-  1.47e11*q(8)**2*q(10) - 2.61e11*q(5)*q(9)*q(10) - 1.6e11*q(8)*q(9)*q(10) - 4.25e10*q(9)**2*q(10) +
-  1.02e8*q(10)**2 + 2.77e8*q(10)**3 + 2.49e3*q(11) - 4.47e10*q(1)**2*q(11) - 1.69e11*q(2)**2*q(11) -
-  1.31e11*q(1)*q(3)*q(11) - 7.02e10*q(3)**2*q(11) - 4.34e11*q(2)*q(4)*q(11) - 1.29e11*q(4)**2*q(11) -
-  3.47e11*q(5)**2*q(11) + 1.07e11*q(1)*q(6)*q(11) + 7.82e10*q(3)*q(6)*q(11) - 5.7e10*q(6)**2*q(11) +
-  3.97e11*q(2)*q(7)*q(11) + 1.22e11*q(4)*q(7)*q(11) - 1.7e11*q(7)**2*q(11) - 7.84e11*q(5)*q(8)*q(11) -
-  3.8e11*q(8)**2*q(11) + 8.52e11*q(5)*q(9)*q(11) + 9.78e10*q(8)*q(9)*q(11) - 1.83e11*q(9)**2*q(11) -
-  4.19e8*q(10)*q(11) - 2.39e9*q(10)**2*q(11) + 3.34e8*q(11)**2 + 5.82e9*q(10)*q(11)**2 -
-  9.64e9*q(11)**3 + 6.13e3*q(12) + 7.8e10*q(1)**2*q(12) + 2.95e11*q(2)**2*q(12) +
-  1.68e11*q(1)*q(3)*q(12) + 8.1e10*q(3)**2*q(12) + 4.6e11*q(2)*q(4)*q(12) + 1.34e11*q(4)**2*q(12) +
-  5.81e11*q(5)**2*q(12) - 2.e11*q(1)*q(6)*q(12) - 1.82e11*q(3)*q(6)*q(12) + 3.91e10*q(6)**2*q(12) -
-  7.12e11*q(2)*q(7)*q(12) - 4.72e11*q(4)*q(7)*q(12) + 6.19e10*q(7)**2*q(12) +
-  1.41e12*q(5)*q(8)*q(12) - 6.06e10*q(8)**2*q(12) - 9.38e11*q(5)*q(9)*q(12) -
-  8.07e11*q(8)*q(9)*q(12) + 2.13e11*q(9)**2*q(12) + 5.89e8*q(10)*q(12) + 2.45e9*q(10)**2*q(12) -
-  1.51e9*q(11)*q(12) - 3.35e10*q(10)*q(11)*q(12) + 6.42e10*q(11)**2*q(12) + 5.23e8*q(12)**2 +
-  4.78e10*q(10)*q(12)**2 - 9.28e10*q(11)*q(12)**2 + 3.81e10*q(12)**3 + 1.06e4*q(13) -
-  1.52e11*q(1)**2*q(13) - 5.58e11*q(2)**2*q(13) - 1.19e11*q(1)*q(3)*q(13) - 1.03e11*q(3)**2*q(13) -
-  3.09e11*q(2)*q(4)*q(13) - 2.21e11*q(4)**2*q(13) - 9.96e11*q(5)**2*q(13) + 2.17e11*q(1)*q(6)*q(13) +
-  3.93e11*q(3)*q(6)*q(13) - 1.06e11*q(6)**2*q(13) + 6.96e11*q(2)*q(7)*q(13) +
-  9.17e11*q(4)*q(7)*q(13) - 2.92e11*q(7)**2*q(13) - 1.39e12*q(5)*q(8)*q(13) - 4.69e11*q(8)**2*q(13) +
-  6.57e11*q(5)*q(9)*q(13) + 1.99e12*q(8)*q(9)*q(13) - 3.87e11*q(9)**2*q(13) - 1.37e9*q(10)*q(13) -
-  1.05e10*q(10)**2*q(13) + 1.26e9*q(11)*q(13) + 8.46e10*q(10)*q(11)*q(13) - 9.64e10*q(11)**2*q(13) +
-  2.29e8*q(12)*q(13) - 8.68e10*q(10)*q(12)*q(13) + 3.54e11*q(11)*q(12)*q(13) - 1.61e11*q(12)**2*q(13) +
-  6.98e8*q(13)**2 + 3.98e10*q(10)*q(13)**2 - 1.51e11*q(11)*q(13)**2 + 3.9e11*q(12)*q(13)**2 -
-  6.61e10*q(13)**3 + 6.74e7*q(14) + 2.36e11*q(1)**2*q(14) + 8.5e11*q(2)**2*q(14) +
-  1.23e11*q(1)*q(3)*q(14) + 5.17e11*q(3)**2*q(14) + 3.65e11*q(2)*q(4)*q(14) + 1.08e12*q(4)**2*q(14) +
-  1.44e12*q(5)**2*q(14) - 1.41e11*q(1)*q(6)*q(14) - 2.17e11*q(3)*q(6)*q(14) + 3.37e11*q(6)**2*q(14) -
-  4.07e11*q(2)*q(7)*q(14) - 4.18e11*q(4)*q(7)*q(14) + 9.52e11*q(7)**2*q(14) +
-  7.93e11*q(5)*q(8)*q(14) + 2.43e12*q(8)**2*q(14) - 7.39e11*q(5)*q(9)*q(14) -
-  6.82e11*q(8)*q(9)*q(14) + 2.2e12*q(9)**2*q(14) + 2.49e9*q(10)*q(14) + 2.66e10*q(10)**2*q(14) +
-  6.98e8*q(11)*q(14) - 9.61e10*q(10)*q(11)*q(14) + 2.05e11*q(11)**2*q(14) + 1.55e9*q(12)*q(14) +
-  7.33e10*q(10)*q(12)*q(14) - 3.01e11*q(11)*q(12)*q(14) + 5.4e11*q(12)**2*q(14) + 7.63e7*q(13)*q(14) -
-  1.11e11*q(10)*q(13)*q(14) + 3.02e11*q(11)*q(13)*q(14) - 4.33e11*q(12)*q(13)*q(14) +
-  1.11e12*q(13)**2*q(14) + 8.35e8*q(14)**2 + 5.64e10*q(10)*q(14)**2 - 1.93e11*q(11)*q(14)**2 +
-  2.88e11*q(12)*q(14)**2 - 2.38e11*q(13)*q(14)**2 + 8.49e11*q(14)**3 + 2.95e9*q(1)*q(15) +
-  3.56e9*q(3)*q(15) - 3.06e9*q(6)*q(15) + 1.16e10*q(2)*q(16) + 1.38e10*q(4)*q(16) -
-  1.18e10*q(7)*q(16) + 2.94e9*q(1)*q(17) + 3.87e9*q(3)*q(17) - 3.64e9*q(6)*q(17) + 1.19e10*q(2)*q(18) +
```

```
-  8.52e9*q(4)*q(18) - 2.e10*q(7)*q(18) - 2.44e10*q(5)*q(19) - 2.5e10*q(8)*q(19) + 2.52e10*q(9)*q(19) -
-  2.93e9*q(1)*q(20) - 4.e9*q(3)*q(20) + 3.13e9*q(6)*q(20) - 1.13e10*q(2)*q(21) - 2.09e10*q(4)*q(21) +
-  1.24e10*q(7)*q(21) + 2.38e10*q(5)*q(22) + 2.17e10*q(8)*q(22) - 5.28e10*q(9)*q(22) -
-  2.43e10*q(5)*q(23) - 5.25e10*q(8)*q(23) + 2.07e10*q(9)*q(23) + 6.59e6*q(24) - 3.14e7*q(10)*q(24) -
-  9.91e7*q(11)*q(24) + 3.87e7*q(12)*q(24) + 2.61e9*q(13)*q(24) + 6.84e9*q(14)*q(24) + 7.48e6*q(25) -
-  2.04e7*q(10)*q(25) + 4.86e7*q(11)*q(25) + 3.32e9*q(12)*q(25) + 3.21e9*q(13)*q(25) -
-  6.25e9*q(14)*q(25) + 1.22e7*q(26) - 1.06e8*q(10)*q(26) + 2.72e9*q(11)*q(26) + 1.58e9*q(12)*q(26) -
-  5.69e9*q(13)*q(26) + 7.31e9*q(14)*q(26) + 4.37e6*q(27) + 1.17e9*q(10)*q(27) + 7.32e8*q(11)*q(27) -
-  4.57e9*q(12)*q(27) + 5.31e9*q(13)*q(27) - 6.68e9*q(14)*q(27) - 5.67e7*q(28) + 6.91e8*q(10)*q(28) -
-  2.35e9*q(11)*q(28) + 4.05e9*q(12)*q(28) - 5.44e9*q(13)*q(28) + 8.78e9*q(14)*q(28) -
-  7.76e7*q(1)*q(29) - 1.38e9*q(3)*q(29) + 8.24e8*q(6)*q(29) - 2.45e8*q(2)*q(30) - 3.25e9*q(4)*q(30) +
-  1.73e9*q(7)*q(30) - 9.66e8*q(1)*q(31) + 3.26e8*q(3)*q(31) + 6.16e8*q(6)*q(31) - 2.18e9*q(2)*q(32) +
-  4.29e8*q(4)*q(32) + 1.46e9*q(7)*q(32) + 6.28e8*q(5)*q(33) + 2.e9*q(8)*q(33) - 3.93e9*q(9)*q(33) +
-  5.35e8*q(1)*q(34) - 1.74e9*q(3)*q(34) + 2.34e8*q(6)*q(34) + 9.8e8*q(2)*q(35) - 3.85e9*q(4)*q(35) +
-  5.53e8*q(7)*q(35) + 5.02e8*q(5)*q(36) - 7.94e8*q(8)*q(36) + 6.26e9*q(9)*q(36) - 2.1e9*q(5)*q(37) -
-  2.06e9*q(8)*q(37) - 9.66e8*q(9)*q(37)


 return
 end

 function eq15p(q,gi1,gi2,gi3,crot)
 IMPLICIT DOUBLE PRECISION (A-H,O-Z)
 dimension q(37)

 nxhat=0.d0

 eq15p=      -5.2e6*q(1) + 4.97e8*q(1)*q(2) + 2.89e6*q(3) + 7.97e8*q(2)*q(3) + 1.67e8*q(1)*q(4) -
-  1.89e9*q(3)*q(4) - 4.75e8*q(2)*q(5) - 4.92e8*q(4)*q(5) - 2.34e7*q(6) - 3.84e9*q(2)*q(6) +
-  3.19e9*q(4)*q(6) + 5.66e7*q(1)*q(7) - 6.83e9*q(3)*q(7) + 6.32e9*q(5)*q(7) - 2.41e9*q(6)*q(7) -
-  2.15e9*q(2)*q(8) - 1.43e10*q(4)*q(8) - 9.76e9*q(7)*q(8) - 4.11e8*q(2)*q(9) - 1.84e9*q(4)*q(9) +
-  4.96e9*q(7)*q(9) + 9.57e8*q(1)*q(10) + 1.86e9*q(3)*q(10) + 9.94e8*q(6)*q(10) - 1.74e9*q(1)*q(11) +
-  4.06e9*q(3)*q(11) + 3.18e9*q(6)*q(11) + 2.04e9*q(1)*q(12) + 2.45e9*q(3)*q(12) - 3.53e9*q(6)*q(12) -
-  3.11e9*q(1)*q(13) - 6.43e9*q(3)*q(13) - 1.45e8*q(6)*q(13) + 2.16e9*q(1)*q(14) + 1.39e9*q(3)*q(14) -
-  2.81e9*q(6)*q(14) + 1.11e9*q(15) + 1.63e8*q(17) + 2.58e8*q(20) + 1.41e8*q(29) - 4.81e7*q(31) -
-  2.44e8*q(34)


 return
 end

 function eq16p(q,gi1,gi2,gi3,crot)
 IMPLICIT DOUBLE PRECISION (A-H,O-Z)
 dimension q(37)

 nxhat=0.d0

 eq16p=       1.28e9*q(1)**2 - 6.23e6*q(2) + 1.31e9*q(1)*q(3) + 1.1e9*q(3)**2 + 1.09e7*q(4) - 1.3e9*q(1)*q(5) -
-  3.03e9*q(3)*q(5) - 5.84e7*q(1)*q(6) - 2.44e9*q(3)*q(6) + 7.51e9*q(5)*q(6) + 2.47e9*q(6)**2 -
-  1.54e7*q(7) + 3.92e9*q(1)*q(8) - 2.07e10*q(3)*q(8) + 3.5e8*q(6)*q(8) + 2.36e9*q(1)*q(9) -
-  3.64e8*q(3)*q(9) + 1.42e10*q(6)*q(9) + 4.61e9*q(2)*q(10) + 3.39e9*q(4)*q(10) + 4.56e9*q(7)*q(10) -
-  8.09e9*q(2)*q(11) + 1.1e10*q(4)*q(11) + 6.7e9*q(7)*q(11) + 3.43e9*q(2)*q(12) + 1.95e8*q(4)*q(12) -
-  2.14e10*q(7)*q(12) - 9.97e9*q(2)*q(13) - 3.52e10*q(4)*q(13) - 3.81e9*q(7)*q(13) + 9.2e9*q(2)*q(14) -
-  6.14e9*q(4)*q(14) - 9.93e9*q(7)*q(14) + 4.18e9*q(16) + 1.09e8*q(18) + 2.42e8*q(21) + 3.11e8*q(30) +
-  1.28e8*q(32) - 2.59e8*q(35)


 return
 end

 function eq17p(q,gi1,gi2,gi3,crot)
 IMPLICIT DOUBLE PRECISION (A-H,O-Z)
 dimension q(37)

 nxhat=0.d0
```

```
 eq17p=       4.46e7*q(1) + 7.89e9*q(1)*q(2) - 9.06e7*q(3) + 4.1e9*q(2)*q(3) - 9.44e9*q(1)*q(4) +
-  8.79e8*q(3)*q(4) - 1.78e10*q(2)*q(5) + 1.53e9*q(4)*q(5) - 5.43e7*q(6) - 5.09e9*q(2)*q(6) -
-  1.43e10*q(4)*q(6) - 3.5e9*q(1)*q(7) - 8.26e9*q(3)*q(7) + 8.55e9*q(5)*q(7) - 7.99e8*q(6)*q(7) -
-  8.48e9*q(2)*q(8) - 3.07e10*q(4)*q(8) - 1.4e10*q(7)*q(8) - 2.53e10*q(2)*q(9) - 4.05e9*q(4)*q(9) -
-  3.57e10*q(7)*q(9) + 7.34e8*q(1)*q(10) + 3.94e9*q(3)*q(10) - 3.77e9*q(6)*q(10) - 4.61e9*q(1)*q(11) -
-  2.44e9*q(3)*q(11) + 9.59e9*q(6)*q(11) + 1.24e10*q(1)*q(12) + 9.65e9*q(3)*q(12) + 1.45e9*q(6)*q(12) -
-  1.13e10*q(1)*q(13) - 3.45e9*q(3)*q(13) + 6.6e9*q(6)*q(13) + 7.49e9*q(1)*q(14) + 8.74e9*q(3)*q(14) -
-  1.08e10*q(6)*q(14) + 7.99e6*q(15) + 2.e9*q(17) + 2.11e8*q(20) - 3.13e8*q(29) - 1.53e9*q(31) -
-  4.5e8*q(34)


 return
 end

 function eq18p(q,gi1,gi2,gi3,crot)
 IMPLICIT DOUBLE PRECISION (A-H,O-Z)
 dimension q(37)

 nxhat=0.d0

 eq18p=       -1.08e9*q(1)**2 + 3.25e7*q(2) + 1.3e10*q(1)*q(3) + 4.9e9*q(3)**2 - 7.46e7*q(4) - 7.e9*q(1)*q(5) -
-  1.34e10*q(3)*q(5) - 4.11e9*q(1)*q(6) + 4.8e9*q(3)*q(6) + 7.17e9*q(5)*q(6) + 6.41e9*q(6)**2 -
-  3.5e7*q(7) - 6.17e9*q(1)*q(8) - 3.99e9*q(3)*q(8) + 1.97e9*q(6)*q(8) - 1.2e10*q(1)*q(9) +
-  2.93e9*q(3)*q(9) - 1.88e10*q(6)*q(9) + 1.61e9*q(2)*q(10) + 5.83e9*q(4)*q(10) - 8.58e9*q(7)*q(10) -
-  1.07e10*q(2)*q(11) - 5.91e9*q(4)*q(11) + 1.97e10*q(7)*q(11) + 3.31e10*q(2)*q(12) +
-  1.61e10*q(4)*q(12) + 6.96e9*q(7)*q(12) - 3.88e10*q(2)*q(13) - 2.22e9*q(4)*q(13) + 6.76e9*q(7)*q(13) +
-  2.33e10*q(2)*q(14) - 4.72e9*q(4)*q(14) - 4.86e10*q(7)*q(14) + 4.63e7*q(16) + 5.11e9*q(18) +
-  1.9e8*q(21) - 4.62e8*q(30) - 2.37e9*q(32) - 5.29e8*q(35)


 return
 end

 function eq19p(q,gi1,gi2,gi3,crot)
 IMPLICIT DOUBLE PRECISION (A-H,O-Z)
 dimension q(37)

 nxhat=0.d0

 eq19p=       5.14e9*q(1)*q(2) + 5.84e9*q(2)*q(3) + 6.23e9*q(1)*q(4) + 1.42e10*q(3)*q(4) - 2.26e7*q(5) -
-  2.82e9*q(2)*q(6) - 9.75e9*q(4)*q(6) + 6.24e9*q(1)*q(7) - 3.33e10*q(3)*q(7) + 2.18e10*q(6)*q(7) -
-  5.83e7*q(8) + 5.54e7*q(9) - 1.81e10*q(5)*q(10) + 1.87e10*q(8)*q(10) + 1.68e10*q(9)*q(10) +
-  3.56e10*q(5)*q(11) + 4.49e10*q(8)*q(11) + 2.29e10*q(9)*q(11) - 2.82e10*q(5)*q(12) -
-  1.24e11*q(8)*q(12) + 2.94e10*q(9)*q(12) + 6.68e10*q(5)*q(13) - 1.27e10*q(8)*q(13) -
-  1.68e11*q(9)*q(13) - 8.1e10*q(5)*q(14) - 6.01e10*q(8)*q(14) - 1.59e10*q(9)*q(14) + 9.44e9*q(19) +
-  4.74e8*q(22) + 1.02e8*q(23) + 9.88e7*q(33) + 1.32e9*q(36) - 1.18e9*q(37)


 return
 end

 function eq20p(q,gi1,gi2,gi3,crot)
 IMPLICIT DOUBLE PRECISION (A-H,O-Z)
 dimension q(37)

 nxhat=0.d0

 eq20p=       -1.17e6*q(1) + 1.73e9*q(1)*q(2) - 3.92e7*q(3) - 3.4e9*q(2)*q(3) + 3.28e8*q(1)*q(4) -
-  5.28e9*q(3)*q(4) - 5.54e9*q(2)*q(5) + 7.92e9*q(4)*q(5) - 7.76e7*q(6) - 1.67e9*q(2)*q(6) -
-  7.74e9*q(4)*q(6) - 6.33e9*q(1)*q(7) - 5.8e9*q(3)*q(7) + 6.89e9*q(5)*q(7) - 7.44e9*q(6)*q(7) -
-  1.8e10*q(2)*q(8) - 2.33e10*q(4)*q(8) - 3.04e10*q(7)*q(8) - 2.65e9*q(2)*q(9) - 1.43e10*q(4)*q(9) -
-  1.92e10*q(7)*q(9) - 1.09e9*q(1)*q(10) + 4.91e9*q(3)*q(10) - 2.3e8*q(6)*q(10) + 2.99e9*q(1)*q(11) +
-  3.86e9*q(3)*q(11) + 6.21e9*q(6)*q(11) + 1.52e9*q(1)*q(12) + 3.88e9*q(3)*q(12) + 3.61e9*q(6)*q(12) -
-  3.12e9*q(1)*q(13) - 9.81e8*q(3)*q(13) - 4.88e9*q(6)*q(13) + 1.09e8*q(1)*q(14) - 2.25e9*q(3)*q(14) -
-  2.16e9*q(6)*q(14) + 7.11e7*q(15) + 6.39e8*q(17) + 1.59e9*q(20) + 1.49e7*q(29) - 5.64e8*q(31) -
-  1.03e9*q(34)
```

```
return
end

function eq21p(q,gi1,gi2,gi3,crot)
IMPLICIT DOUBLE PRECISION (A-H,O-Z)
dimension q(37)

nxhat=0.d0

eq21p= -1.07e9*q(1)**2 - 1.05e7*q(2) - 3.31e8*q(1)*q(3) + 1.35e9*q(3)**2 - 1.95e7*q(4) + 6.18e8*q(1)*q(5) +
-  9.16e9*q(3)*q(5) + 6.43e9*q(1)*q(6) + 6.16e9*q(3)*q(6) - 4.06e9*q(5)*q(6) + 4.28e9*q(6)**2 -
-  5.28e7*q(7) - 7.47e9*q(1)*q(8) - 4.8e9*q(3)*q(8) - 7.32e9*q(6)*q(8) + 8.09e9*q(1)*q(9) -
-  6.78e9*q(3)*q(9) - 1.24e9*q(6)*q(9) - 3.89e9*q(2)*q(10) + 8.07e9*q(4)*q(10) + 2.53e9*q(7)*q(10) +
-  1.46e10*q(2)*q(11) + 8.17e9*q(4)*q(11) + 8.21e9*q(7)*q(11) - 1.09e10*q(2)*q(12) - 9.35e8*q(4)*q(12) +
-  5.52e9*q(7)*q(12) - 2.42e9*q(2)*q(13) - 1.22e10*q(4)*q(13) - 3.62e10*q(7)*q(13) - 4.92e9*q(2)*q(14) -
-  4.91e10*q(4)*q(14) - 5.27e9*q(7)*q(14) + 8.76e7*q(16) + 5.38e8*q(18) + 4.61e9*q(21) + 1.54e8*q(30) -
-  4.17e8*q(32) - 1.5e9*q(35)


return
end

function eq22p(q,gi1,gi2,gi3,crot)
IMPLICIT DOUBLE PRECISION (A-H,O-Z)
dimension q(37)

nxhat=0.d0

eq22p=       -5.33e9*q(1)*q(2) - 4.93e9*q(2)*q(3) + 2.36e9*q(1)*q(4) + 8.46e9*q(3)*q(4) - 3.41e6*q(5) +
-  1.49e10*q(2)*q(6) + 8.56e9*q(4)*q(6) + 1.14e10*q(1)*q(7) + 4.52e9*q(3)*q(7) + 1.64e10*q(6)*q(7) -
-  6.65e7*q(8) - 3.03e5*q(9) + 4.53e9*q(5)*q(10) + 6.81e9*q(8)*q(10) + 1.78e10*q(9)*q(10) -
-  2.06e10*q(5)*q(11) + 2.69e10*q(8)*q(11) + 9.67e9*q(9)*q(11) + 1.58e10*q(5)*q(12) -
-  5.09e9*q(8)*q(12) + 8.16e9*q(9)*q(12) + 1.26e10*q(5)*q(13) - 8.06e10*q(8)*q(13) -
-  3.65e10*q(9)*q(13) - 7.47e9*q(5)*q(14) - 2.96e10*q(8)*q(14) - 1.04e11*q(9)*q(14) + 1.27e8*q(19) +
-  9.85e9*q(22) + 5.29e8*q(23) - 6.65e7*q(33) + 2.58e9*q(36) + 9.91e7*q(37)


return
end

function eq23p(q,gi1,gi2,gi3,crot)
IMPLICIT DOUBLE PRECISION (A-H,O-Z)
dimension q(37)

nxhat=0.d0

eq23p=       -3.07e9*q(1)*q(2) + 2.81e10*q(2)*q(3) + 1.83e10*q(1)*q(4) + 1.54e10*q(3)*q(4) - 1.83e7*q(5) -
-  1.02e10*q(2)*q(6) + 8.83e9*q(4)*q(6) - 1.08e10*q(1)*q(7) + 1.7e10*q(3)*q(7) + 1.58e10*q(6)*q(7) -
-  1.97e7*q(8) - 8.05e7*q(9) - 1.5e9*q(5)*q(10) - 2.05e10*q(8)*q(10) + 6.09e9*q(9)*q(10) +
-  1.69e10*q(5)*q(11) + 2.71e10*q(8)*q(11) - 1.42e10*q(9)*q(11) - 5.32e10*q(5)*q(12) +
-  4.8e10*q(8)*q(12) + 1.95e10*q(9)*q(12) + 5.27e10*q(5)*q(13) + 2.24e10*q(8)*q(13) +
-  3.74e10*q(9)*q(13) - 2.64e10*q(5)*q(14) - 1.02e11*q(8)*q(14) + 4.04e9*q(9)*q(14) + 7.51e7*q(19) +
-  2.14e8*q(22) + 1.02e10*q(23) - 3.94e8*q(33) + 4.52e8*q(36) + 3.53e9*q(37)


return
end

function eq24p(q,gi1,gi2,gi3,crot)
IMPLICIT DOUBLE PRECISION (A-H,O-Z)
dimension q(37)

nxhat=0.d0
```

```
 eq24p=       1.83e8*q(1)**2 + 8.13e8*q(2)**2 + 1.94e9*q(1)*q(3) - 5.48e8*q(3)**2 + 7.41e9*q(2)*q(4) -
-  7.9e9*q(4)**2 + 2.42e9*q(5)**2 - 1.45e9*q(1)*q(6) - 1.61e9*q(3)*q(6) + 2.11e8*q(6)**2 -
-  5.48e9*q(2)*q(7) - 3.69e9*q(4)*q(7) + 1.37e9*q(7)**2 + 1.09e10*q(5)*q(8) + 2.26e9*q(8)**2 -
-  1.39e10*q(5)*q(9) - 1.14e10*q(8)*q(9) - 2.23e10*q(9)**2 - 2.5e6*q(10) - 2.64e7*q(10)**2 -
-  3.04e7*q(11) - 5.33e7*q(10)*q(11) - 1.9e8*q(11)**2 - 9.43e6*q(12) - 3.46e6*q(10)*q(12) -
-  1.3e8*q(11)*q(12) + 5.19e9*q(12)**2 - 8.64e7*q(13) - 8.26e8*q(10)*q(13) + 9.74e9*q(11)*q(13) +
-  9.99e9*q(12)*q(13) + 5.67e9*q(13)**2 - 3.14e7*q(14) + 5.08e9*q(10)*q(14) + 4.8e9*q(11)*q(14) +
-  1.38e10*q(12)*q(14) + 1.03e10*q(13)*q(14) + 6.1e9*q(14)**2 + 9.14e7*q(24) + 3.25e8*q(25) +
-  3.85e8*q(26) + 8.16e8*q(27) + 4.46e8*q(28)


 return
 end

 function eq25p(q,gi1,gi2,gi3,crot)
 IMPLICIT DOUBLE PRECISION (A-H,O-Z)
 dimension q(37)

 nxhat=0.d0

 eq25p=       2.28e9*q(1)**2 + 8.68e9*q(2)**2 + 5.07e9*q(1)*q(3) - 4.05e8*q(3)**2 + 1.48e10*q(2)*q(4) -
-  1.36e10*q(4)**2 + 1.69e10*q(5)**2 - 6.39e9*q(1)*q(6) - 6.71e9*q(3)*q(6) + 4.33e8*q(6)**2 -
-  2.24e10*q(2)*q(7) - 1.35e10*q(4)*q(7) + 7.12e8*q(7)**2 + 4.39e10*q(5)*q(8) - 5.06e9*q(8)**2 -
-  2.88e10*q(5)*q(9) - 3.06e10*q(8)*q(9) - 4.06e10*q(9)**2 + 3.18e7*q(10) + 2.5e7*q(10)**2 -
-  1.19e8*q(11) - 1.11e9*q(10)*q(11) + 1.18e9*q(11)**2 - 2.63e7*q(12) + 2.17e9*q(10)*q(12) -
-  5.83e9*q(11)*q(12) + 1.12e10*q(12)**2 - 1.25e8*q(13) - 3.37e9*q(10)*q(13) + 2.4e10*q(11)*q(13) +
-  1.32e10*q(12)*q(13) + 1.24e10*q(13)**2 - 1.12e8*q(14) + 9.45e9*q(10)*q(14) + 7.68e9*q(11)*q(14) +
-  3.6e10*q(12)*q(14) + 8.09e9*q(13)*q(14) + 1.31e10*q(14)**2 + 8.36e7*q(24) + 6.92e8*q(25) +
-  9.4e8*q(26) + 9.88e8*q(27) + 1.41e9*q(28)


 return
 end

 function eq26p(q,gi1,gi2,gi3,crot)
 IMPLICIT DOUBLE PRECISION (A-H,O-Z)
 dimension q(37)

 nxhat=0.d0

 eq26p=       1.58e9*q(1)**2 + 5.82e9*q(2)**2 - 9.06e8*q(1)*q(3) - 1.23e9*q(3)**2 - 2.74e9*q(2)*q(4) -
-  1.35e10*q(4)**2 + 9.6e9*q(5)**2 - 1.42e9*q(1)*q(6) - 7.8e9*q(3)*q(6) + 3.57e8*q(6)**2 -
-  3.27e9*q(2)*q(7) - 2.4e10*q(4)*q(7) + 2.07e9*q(7)**2 + 7.35e9*q(5)*q(8) - 1.72e8*q(8)**2 +
-  5.5e9*q(5)*q(9) - 6.91e10*q(8)*q(9) - 3.35e10*q(9)**2 + 3.4e7*q(10) + 9.01e7*q(10)**2 - 4.95e7*q(11) -
-  1.26e9*q(10)*q(11) + 4.28e8*q(11)**2 - 1.26e8*q(12) + 2.47e7*q(10)*q(12) - 1.58e8*q(11)*q(12) +
-  8.04e9*q(12)**2 - 1.34e8*q(13) + 1.65e9*q(10)*q(13) + 1.3e10*q(11)*q(13) + 8.23e9*q(12)*q(13) +
-  8.51e9*q(13)**2 + 2.32e6*q(14) + 6.89e9*q(10)*q(14) + 1.39e10*q(11)*q(14) + 1.82e10*q(12)*q(14) +
-  2.87e9*q(13)*q(14) + 9.69e9*q(14)**2 + 2.44e7*q(24) + 3.01e8*q(25) + 1.35e9*q(26) + 1.11e9*q(27) +
-  3.35e8*q(28)


 return
 end

 function eq27p(q,gi1,gi2,gi3,crot)
 IMPLICIT DOUBLE PRECISION (A-H,O-Z)
 dimension q(37)

 nxhat=0.d0

 eq27p=       -7.13e7*q(1)**2 - 9.49e7*q(2)**2 + 2.93e9*q(1)*q(3) - 2.e9*q(3)**2 + 1.59e10*q(2)*q(4) -
-  1.61e10*q(4)**2 + 1.53e9*q(5)**2 - 3.4e8*q(1)*q(6) - 3.01e9*q(3)*q(6) + 1.83e9*q(6)**2 -
-  1.73e9*q(2)*q(7) - 2.64e9*q(4)*q(7) + 9.79e9*q(7)**2 + 3.77e9*q(5)*q(8) + 2.73e10*q(8)**2 -
-  2.86e10*q(5)*q(9) - 1.68e10*q(8)*q(9) - 4.6e10*q(9)**2 - 3.6e6*q(10) - 9.95e5*q(10)**2 - 5.76e6*q(11) +
-  1.01e8*q(10)*q(11) - 1.54e9*q(11)**2 - 3.96e7*q(12) - 2.28e9*q(10)*q(12) - 5.64e8*q(11)*q(12) +
-  9.73e9*q(12)**2 - 2.9e8*q(13) - 1.8e9*q(10)*q(13) + 1.39e10*q(11)*q(13) + 1.74e10*q(12)*q(13) +
```

```
-  9.06e9*q(13)**2 - 1.2e8*q(14) + 1.16e10*q(10)*q(14) + 7.55e9*q(11)*q(14) + 1.2e10*q(12)*q(14) +
-  1.26e10*q(13)*q(14) + 7.98e9*q(14)**2 + 2.34e7*q(24) + 1.46e8*q(25) + 5.32e8*q(26) + 2.32e9*q(27) +
-  1.03e9*q(28)


 return
 end

 function eq28p(q,gi1,gi2,gi3,crot)
 IMPLICIT DOUBLE PRECISION (A-H,O-Z)
 dimension q(37)

 nxhat=0.d0

 eq28p=       4.61e9*q(1)**2 + 1.72e10*q(2)**2 + 9.85e9*q(1)*q(3) + 3.41e9*q(3)**2 + 3.07e10*q(2)*q(4) -
-  3.75e8*q(4)**2 + 3.22e10*q(5)**2 - 9.32e9*q(1)*q(6) - 5.53e9*q(3)*q(6) + 4.35e9*q(6)**2 -
-  3.31e10*q(2)*q(7) + 6.98e9*q(4)*q(7) + 1.25e10*q(7)**2 + 6.29e10*q(5)*q(8) + 3.e10*q(8)**2 -
-  5.91e10*q(5)*q(9) + 3.34e10*q(8)*q(9) - 1.82e10*q(9)**2 + 9.08e7*q(10) + 2.36e8*q(10)**2 - 1.e8*q(11) -
-  1.55e9*q(10)*q(11) + 2.58e9*q(11)**2 + 8.54e7*q(12) + 2.91e9*q(10)*q(12) - 1.67e10*q(11)*q(12) +
-  1.39e10*q(12)**2 - 1.69e8*q(13) - 1.02e10*q(10)*q(13) + 2.56e10*q(11)*q(13) + 5.85e9*q(12)*q(13) +
-  1.7e10*q(13)**2 - 3.27e8*q(14) + 1.06e10*q(10)*q(14) - 6.89e9*q(11)*q(14) + 3.14e10*q(12)*q(14) -
-  8.27e9*q(13)*q(14) + 1.9e10*q(14)**2 + 2.23e6*q(24) + 1.5e8*q(25) + 9.24e7*q(26) + 7.44e8*q(27) +
-  2.99e9*q(28)


 return
 end

 function eq29p(q,gi1,gi2,gi3,crot)
 IMPLICIT DOUBLE PRECISION (A-H,O-Z)
 dimension q(37)

 nxhat=0.d0

 eq29p=       -4.7e8*q(1) - 6.88e10*q(1)*q(2) - 1.72e7*q(3) - 6.36e9*q(2)*q(3) - 5.95e9*q(1)*q(4) -
-  4.79e10*q(3)*q(4) + 1.73e11*q(2)*q(5) + 2.18e10*q(4)*q(5) + 8.22e6*q(6) + 2.07e10*q(2)*q(6) +
-  2.42e10*q(4)*q(6) + 2.14e10*q(1)*q(7) + 2.63e10*q(3)*q(7) - 5.96e10*q(5)*q(7) - 4.95e10*q(6)*q(7) +
-  5.41e10*q(2)*q(8) + 6.16e10*q(4)*q(8) - 1.48e11*q(7)*q(8) - 1.06e10*q(2)*q(9) - 1.32e11*q(4)*q(9) +
-  7.63e10*q(7)*q(9) - 5.12e7*q(1)*q(10) - 1.02e9*q(3)*q(10) + 1.24e9*q(6)*q(10) + 8.06e7*q(1)*q(11) +
-  4.53e9*q(3)*q(11) - 3.39e9*q(6)*q(11) + 1.28e7*q(1)*q(12) - 7.73e9*q(3)*q(12) + 2.99e9*q(6)*q(12) +
-  5.69e7*q(1)*q(13) + 6.06e9*q(3)*q(13) - 2.33e9*q(6)*q(13) - 1.17e8*q(1)*q(14) - 3.94e9*q(3)*q(14) +
-  2.26e9*q(6)*q(14) + 1.86e8*q(15) - 2.22e8*q(17) + 4.92e7*q(20) + 3.33e9*q(29) - 3.27e7*q(31) +
-  4.34e7*q(34)


 return
 end

 function eq30p(q,gi1,gi2,gi3,crot)
 IMPLICIT DOUBLE PRECISION (A-H,O-Z)
 dimension q(37)

 nxhat=0.d0

 eq30p=3.61e10*q(1)**2 - 9.25e8*q(2) + 5.43e9*q(1)*q(3) + 1.95e10*q(3)**2 - 1.09e7*q(4) + 1.81e11*q(1)*q(5) +
-  2.62e10*q(3)*q(5) - 2.06e10*q(1)*q(6) - 2.23e10*q(3)*q(6) - 6.35e10*q(5)*q(6) + 2.34e10*q(6)**2 +
-  4.84e6*q(7) + 5.39e10*q(1)*q(8) + 7.88e10*q(3)*q(8) - 1.57e11*q(6)*q(8) - 7.52e9*q(1)*q(9) -
-  1.45e11*q(3)*q(9) + 7.94e10*q(6)*q(9) - 2.07e8*q(2)*q(10) - 2.03e9*q(4)*q(10) + 2.55e9*q(7)*q(10) +
-  4.95e8*q(2)*q(11) + 8.96e9*q(4)*q(11) - 7.02e9*q(7)*q(11) - 4.41e8*q(2)*q(12) - 1.61e10*q(4)*q(12) +
-  6.34e9*q(7)*q(12) + 5.37e8*q(2)*q(13) + 1.41e10*q(4)*q(13) - 5.08e9*q(7)*q(13) - 6.29e8*q(2)*q(14) -
-  9.49e9*q(4)*q(14) + 4.98e9*q(7)*q(14) + 2.89e8*q(16) - 4.98e8*q(18) + 1.69e8*q(21) + 1.32e10*q(30) -
-  2.87e7*q(32) + 4.16e7*q(35)


 return
 end
```

```
function eq31p(q,gi1,gi2,gi3,crot)
IMPLICIT DOUBLE PRECISION (A-H,O-Z)
dimension q(37)

nxhat=0.d0

eq31p=       1.25e6*q(1) + 3.71e9*q(1)*q(2) + 4.46e8*q(3) + 2.93e10*q(2)*q(3) + 3.58e10*q(1)*q(4) +
-  2.51e10*q(3)*q(4) - 1.78e10*q(2)*q(5) - 7.59e10*q(4)*q(5) + 2.68e6*q(6) - 1.67e10*q(2)*q(6) +
-  2.05e10*q(4)*q(6) - 1.99e10*q(1)*q(7) + 1.89e10*q(3)*q(7) + 4.84e10*q(5)*q(7) + 2.1e10*q(6)*q(7) -
-  5.63e10*q(2)*q(8) + 7.14e10*q(4)*q(8) + 6.57e10*q(7)*q(8) + 1.04e11*q(2)*q(9) + 6.1e10*q(4)*q(9) +
-  5.8e10*q(7)*q(9) - 6.02e8*q(1)*q(10) + 4.9e7*q(3)*q(10) + 1.23e9*q(6)*q(10) + 2.85e9*q(1)*q(11) -
-  2.09e8*q(3)*q(11) - 1.38e9*q(6)*q(11) - 4.7e9*q(1)*q(12) + 4.56e8*q(3)*q(12) - 1.17e9*q(6)*q(12) +
-  3.13e9*q(1)*q(13) - 4.11e6*q(3)*q(13) - 1.45e9*q(6)*q(13) - 1.95e9*q(1)*q(14) + 7.78e8*q(3)*q(14) +
-  1.18e9*q(6)*q(14) - 4.48e7*q(15) - 7.9e8*q(17) + 3.28e8*q(20) - 1.31e7*q(29) + 3.65e9*q(31) -
-  8.07e7*q(34)


return
end

function eq32p(q,gi1,gi2,gi3,crot)
IMPLICIT DOUBLE PRECISION (A-H,O-Z)
dimension q(37)

nxhat=0.d0

eq32p= -1.9e9*q(1)**2 + 6.78e5*q(2) - 4.33e10*q(1)*q(3) - 1.48e10*q(3)**2 + 9.12e8*q(4) - 1.66e10*q(1)*q(5) -
-  9.21e10*q(3)*q(5) + 2.23e10*q(1)*q(6) - 2.5e10*q(3)*q(6) + 4.94e10*q(5)*q(6) - 1.64e10*q(6)**2 +
-  1.42e6*q(7) - 5.77e10*q(1)*q(8) + 8.59e10*q(3)*q(8) + 9.35e10*q(6)*q(8) + 1.21e11*q(1)*q(9) +
-  7.37e10*q(3)*q(9) + 7.e10*q(6)*q(9) - 1.34e9*q(2)*q(10) + 1.65e8*q(4)*q(10) + 2.84e9*q(7)*q(10) +
-  6.37e9*q(2)*q(11) - 4.76e8*q(4)*q(11) - 3.83e9*q(7)*q(11) - 1.11e10*q(2)*q(12) + 1.06e9*q(4)*q(12) -
-  1.93e9*q(7)*q(12) + 8.49e9*q(2)*q(13) - 3.44e8*q(4)*q(13) - 3.03e9*q(7)*q(13) - 5.47e9*q(2)*q(14) +
-  1.2e9*q(4)*q(14) + 3.62e9*q(7)*q(14) - 2.05e8*q(16) - 2.15e9*q(18) + 7.33e8*q(21) - 2.06e7*q(30) +
-  1.36e10*q(32) - 9.93e7*q(35)


return
end

function eq33p(q,gi1,gi2,gi3,crot)
IMPLICIT DOUBLE PRECISION (A-H,O-Z)
dimension q(37)

nxhat=0.d0

eq33p=       2.46e11*q(1)*q(2) + 3.33e10*q(2)*q(3) + 2.59e10*q(1)*q(4) + 1.4e11*q(3)*q(4) + 1.36e9*q(5) -
-  8.46e10*q(2)*q(6) - 7.47e10*q(4)*q(6) - 8.05e10*q(1)*q(7) - 8.96e10*q(3)*q(7) + 1.63e11*q(6)*q(7) +
-  3.66e6*q(8) - 8.06e6*q(9) + 5.55e8*q(5)*q(10) + 4.4e9*q(8)*q(10) - 3.89e9*q(9)*q(10) -
-  1.48e9*q(5)*q(11) - 1.18e10*q(8)*q(11) + 1.61e10*q(9)*q(11) + 1.8e9*q(5)*q(12) + 9.83e9*q(8)*q(12) -
-  2.74e10*q(9)*q(12) - 2.16e9*q(5)*q(13) - 7.59e9*q(8)*q(13) + 2.3e10*q(9)*q(13) + 2.41e9*q(5)*q(14) +
-  7.77e9*q(8)*q(14) - 1.53e10*q(9)*q(14) - 7.01e7*q(19) + 5.77e7*q(22) - 5.9e8*q(23) + 2.98e10*q(33) -
-  7.29e7*q(36) + 7.1e7*q(37)


return
end

function eq34p(q,gi1,gi2,gi3,crot)
IMPLICIT DOUBLE PRECISION (A-H,O-Z)
dimension q(37)

nxhat=0.d0

eq34p=       1.64e6*q(1) - 1.65e10*q(1)*q(2) - 2.13e6*q(3) - 1.93e10*q(2)*q(3) - 2.1e10*q(1)*q(4) +
-  2.3e10*q(3)*q(4) + 5.03e10*q(2)*q(5) + 4.63e10*q(4)*q(5) + 4.61e8*q(6) + 3.88e10*q(2)*q(6) +
```

```
-  3.05e10*q(4)*q(6) + 4.23e10*q(1)*q(7) + 2.33e10*q(3)*q(7) - 9.91e10*q(5)*q(7) + 2.46e10*q(6)*q(7) +
-  1.28e11*q(2)*q(8) + 8.65e10*q(4)*q(8) + 9.1e10*q(7)*q(8) - 6.51e10*q(2)*q(9) + 6.52e10*q(4)*q(9) +
-  6.62e10*q(7)*q(9) + 9.32e8*q(1)*q(10) - 1.61e9*q(3)*q(10) + 6.12e7*q(6)*q(10) - 2.3e9*q(1)*q(11) +
-  2.09e9*q(3)*q(11) - 1.41e8*q(6)*q(11) + 1.58e9*q(1)*q(12) + 1.12e9*q(3)*q(12) + 4.56e8*q(6)*q(12) -
-  1.3e9*q(1)*q(13) + 3.03e9*q(3)*q(13) - 8.93e8*q(6)*q(13) + 1.27e9*q(1)*q(14) - 4.17e9*q(3)*q(14) +
-  5.83e8*q(6)*q(14) + 4.67e8*q(15) + 1.81e8*q(17) - 5.94e8*q(20) + 3.25e7*q(29) - 9.31e7*q(31) +
-  3.45e9*q(34)


 return
 end

 function eq35p(q,gi1,gi2,gi3,crot)
 IMPLICIT DOUBLE PRECISION (A-H,O-Z)
 dimension q(37)

 nxhat=0.d0

 eq35p= 9.48e9*q(1)**2 + 6.37e5*q(2) + 2.5e10*q(1)*q(3) - 1.18e10*q(3)**2 - 2.79e6*q(4) + 5.37e10*q(1)*q(5) +
-  6.18e10*q(3)*q(5) - 4.69e10*q(1)*q(6) - 2.53e10*q(3)*q(6) - 1.1e11*q(5)*q(6) - 1.37e10*q(6)**2 +
-  9.22e8*q(7) + 1.41e11*q(1)*q(8) + 8.14e10*q(3)*q(8) + 1.e11*q(6)*q(8) - 7.46e10*q(1)*q(9) +
-  7.2e10*q(3)*q(9) + 7.42e10*q(6)*q(9) + 1.89e9*q(2)*q(10) - 3.44e9*q(4)*q(10) + 1.77e8*q(7)*q(10) -
-  4.79e9*q(2)*q(11) + 5.34e9*q(4)*q(11) - 3.77e8*q(7)*q(11) + 3.43e9*q(2)*q(12) + 1.29e9*q(4)*q(12) +
-  1.04e9*q(7)*q(12) - 2.69e9*q(2)*q(13) + 5.79e9*q(4)*q(13) - 2.1e9*q(7)*q(13) + 2.59e9*q(2)*q(14) -
-  1.02e10*q(4)*q(14) + 1.48e9*q(7)*q(14) + 8.49e8*q(16) + 2.51e8*q(18) - 1.39e9*q(21) + 3.61e7*q(30) -
-  1.04e8*q(32) + 1.34e10*q(35)


 return
 end

 function eq36p(q,gi1,gi2,gi3,crot)
 IMPLICIT DOUBLE PRECISION (A-H,O-Z)
 dimension q(37)

 nxhat=0.d0

 eq36p=   -3.72e10*q(1)*q(2) - 5.55e10*q(2)*q(3) - 4.66e10*q(1)*q(4) + 6.94e10*q(3)*q(4) - 9.73e4*q(5) +
-  1.11e11*q(2)*q(6) + 7.45e10*q(4)*q(6) + 1.1e11*q(1)*q(7) + 6.27e10*q(3)*q(7) + 7.87e10*q(6)*q(7) -
-  1.36e9*q(8) + 1.77e6*q(9) + 1.68e9*q(5)*q(10) - 2.37e8*q(8)*q(10) + 4.47e9*q(9)*q(10) -
-  4.06e9*q(5)*q(11) + 4.22e8*q(8)*q(11) - 6.21e9*q(9)*q(11) + 2.23e9*q(5)*q(12) - 1.49e9*q(8)*q(12) -
-  3.55e9*q(9)*q(12) - 1.23e9*q(5)*q(13) + 2.89e9*q(8)*q(13) - 7.12e9*q(9)*q(13) + 1.02e9*q(5)*q(14) -
-  1.62e9*q(8)*q(14) + 1.28e10*q(9)*q(14) - 5.66e8*q(19) + 1.9e9*q(22) - 1.99e8*q(23) - 3.77e7*q(33) +
-  2.99e10*q(36) - 7.33e7*q(37)


 return
 end

 function eq37p(q,gi1,gi2,gi3,crot)
 IMPLICIT DOUBLE PRECISION (A-H,O-Z)
 dimension q(37)

 nxhat=0.d0

 eq37p=        4.6e9*q(1)*q(2) + 1.2e11*q(2)*q(3) + 1.16e11*q(1)*q(4) + 6.91e10*q(3)*q(4) + 3.48e5*q(5) -
-  6.63e10*q(2)*q(6) + 6.74e10*q(4)*q(6) - 6.83e10*q(1)*q(7) + 6.71e10*q(3)*q(7) + 6.81e10*q(6)*q(7) -
-  4.03e5*q(8) - 1.36e9*q(9) - 1.69e9*q(5)*q(10) - 4.49e9*q(8)*q(10) - 2.84e8*q(9)*q(10) +
-  7.62e9*q(5)*q(11) + 5.28e9*q(8)*q(11) + 7.2e8*q(9)*q(11) - 1.25e10*q(5)*q(12) + 4.96e9*q(8)*q(12) -
-  1.47e9*q(9)*q(12) + 8.77e9*q(5)*q(13) + 3.89e9*q(8)*q(13) + 4.89e8*q(9)*q(13) - 5.e9*q(5)*q(14) -
-  4.91e9*q(8)*q(14) - 2.39e9*q(9)*q(14) + 5.52e8*q(19) - 8.27e8*q(22) + 3.51e9*q(23) + 4.23e7*q(33) -
-  8.61e7*q(36) + 3.01e10*q(37)


 return
 end
```